SYNTHESIS AND PROPERTIES OF FULLY CONJUGATED PORPHYRIN ARRAYS FOR LIGHT HARVESTING

A thesis presented in partial fulfillment of the requirements for the degree of

Doctor of Philosophy

in

Chemistry

at Massey University, Palmerston North, New Zealand.

Fabio Lodato

August 2006

Abstract

This thesis presents the synthesis of porphyrin arrays for light-harvesting applications using Wittig chemistry, which allows the construction of covalently bound systems that are conjugated, stable and easy to characterize. This was achieved using a dendrimer strategy utilizing tetraarylporphyrins as building blocks, monofunctionalized with either aldehyde or phosphonium salt groups at the β-pyrrolic position, and benzenes, polyfunctionalized with either aldehyde or phosphonium salt groups; stepwise control of the addition of each porphyrin moiety was thus obtained. In this way, different porphyrins in different metallated states were arranged in a determinate geometrical relationship, which is of great importance in the investigations on electron/energy transfers. Arrays containing up to five metalloporphyrin units (two kinds of porphyrins coordinating two different metals) were synthesized and characterized.

The unexpected chromatography behaviour and ^{1}H-NMR spectra of a Zn porphyrin functionalized with a 1,3-bis(methyl(diethylphosphonate) benzene were the reason for an investigation, which uncovered, mainly with the use of NMR spectrometry, the first case of intramolecular coordination between the Zn centre and a phosphonate group of the same porphyrin. The dynamic nature of this coordination was characterized and chemical-physical parameters for Zn porphyrin/phosphonate binding were determined.

In order to establish the photophysical properties of our conjugated arrays, we synthesized a series of dyads containing Zn and free-base tetraphenylporphyrins (TPPs) connected through variable length phenylenevinylene-type bridges; along with this series, the preparation of the Zn and free-base homometallic homologue dyads and two series of monomers carrying the conjugated linker were realized. Collaboration with IFOS-CNR in Bologna, Italy was established in order to investigate the intramolecular photophysics of those systems, which involve efficient intramolecular energy transfer from the Zn to the free-base porphyrin.

Finally, dyads composed of Fe(III) and Zn porphyrin were prepared as part of a project in collaboration with the University of Pennsylvania for the investigation of new artificial photosynthetic systems. Two series of dimers were prepared in order to obtain incorporation in both the classes of hydrophobic and hydrophilic proteins. TPPs were used for the making of the hydrophobic dyads while hydrophilicity was achieved by employing tetraester porphyrin derivatives, which can be quantitatively hydrolyzed to afford the correspondent water soluble acids. A new monosubstituted porphyrin was also synthesized and incorporated in the arrays to minimize steric hindrance inside the protein binding sites.

Declaration

This is to certify that the work described in this thesis has not been submitted for a higher degree at any other university or institution.

Fabio Lodato

Acknowledgements

I'd like to thank the people who have had an influence on this experience, likely the most life-changing in my first 30 years.

First of all, all my family and friends from the other side of the world, their distance and support made me realize a lot of things, most of which I promise to improve.

My supervisor, David Officer, for the freedom of any kind on the work-place, the financial support and, most of the times, the understanding of my uses and moods.

My co-supervisor, Ken Jolley, who, without knowing it, made possible for me to complete this PhD.

My lab-mates Pawel Wagner and Sanjeev Gambhir for their great help with everything about synthetic chemistry, Wayne Campbell with porphyrins and Mark Vigneswaran with the Wittig-Horner chemistry. Thanks also to Adam Stephenson for the preparation of some starting material, to Klaudia Wagner for the attempts with electrochemistry and to everybody else in the NRC for every job I was spared to do and the attempts to make life more enjoyable.

Thanks to Pat Edwards (NMR), David Lun and Dave Harding (MALDI, electrospray) and to everybody else in Massey who has been too kind in helping me with anything.

I also want to thank our overseas collaborators, Les Dutton, Bohdana Discher and Ron Koder in Philadelphia (porphyrin/protein interactions) and Lucia Flamigni and Barbara Ventura in Bologna (photophysics) for making this thesis more interesting.

Finally, thanks to Massey University, Nanomaterials Research Centre, FRST MAUX0202 and the Marsden Fund for the financial support.

Table of Contents

4. Porphyrin photophysics

5. Porphyrin arrays for Maquette incorporation

6. References

Abbreviations

z	
anal.	analysis
aq.	aqueous
Ar	aryl
calc.	calculated
CV	cyclic voltammetry or cyclic voltammogram
DMF	dimethylformamide
DSSC	dye-sensitized solar cell
Et	ethyl
EtOH	ethanol
ε	extinction coefficient
ep	ethylphosphonate
eq.	equivalents
exc.	excitation
ext	extended
FAB-MS	fast atom bombardment mass spectroscopy
Fig.	Figure
HOMO	highest occupied molecular orbital
HRMS	high-resolution mass spectrometry
h	hour
ipp	isopropylphosphonate
IR	infrared
J	coupling constant
LUMO	lowest unoccupied molecular orbital
μL	microlitre
MALDI-MS	matrix assisted laser desorption of ions mass spectroscopy
max	maximum
Me	methyl
mep	meta-ethylphosphonate
min	minutes
M	molarity

mmol	millimole
mol	mole
NMR	nuclear magnetic resonance
pep	para-ethylphosphonate
Ph	phenyl
phos	phosphonate
Pr	propyl
ps	phosphonium salt
sat.	saturated
THF	tetrahydrofuran
TLC	thin layer chromatography
TPP	tetraphenylporphyrin
TXP	tetraxylylporphyrin
UV	ultraviolet

Index of Compounds

1	benzaldehyde
2	xylylaldehyde
3	TPP
4	TXP
5	TPP-CHO
6	TXP-CHO
7	TPP-CH_2-OH
8	TXP-CH_2-OH
9	TPP-CH_2-Cl
10	TXP-CH_2-Cl
11	TPP-ps
12	TXP-ps
13	terephthalaldehyde
14	TPP-Ph-CHO
15	TXP-Ph-CHO
16	1,3,5-tribromomethylbenzene
17	benzene-tricarboxaldehyde
18	$(TXP)_2$-Ph-CHO
19	mesitylenetris-(triphenylphosphonium bromide)
20	xylenebis-(triphenylphosphonium chloride)
21	1,3,5-mesitylenetris(diethylphosphonate)
22	TPP-Ph-$(ep)_2$
23	$(TPP)_2$-Ph-ep
24	$(TPP)_3$
25	$(TPP)_2$-Ph-CHO
27	$(TPP\text{-}Ph)_2$-Ph-ep
28	1,3,5-mesitylenetris(diisopropylphosphonate)
29	$(TPP\text{-}Ph)_2$-Ph-ipp
30	$(TXP\text{-}Ph)_2$-Ph-ipp
31	$((TPP)_2\text{-}Ph)_2$-Ph-ipp

32 $(NiTPP\text{-}Ph)_2\text{-}Ph\text{-}Ph\text{-}ZnTXP$

33 $(NiTPP\text{-}Ph)_2\text{-}Ph\text{-}Ph\text{-}(ZnTXP)_2$

34 $((NiTPP)_2\text{-}Ph)_2\text{-}Ph\text{-}Ph\text{-}ZnTXP$

35 1,3-xylenebis(diethylphosphonate)

36 TPP-Ph-mep

37 toluene(diethylphosphonate)

38 toluene(diisopropylphosphonate)

39 TPP-ext-COOMe

40 $TPP\text{-}ext\text{-}CH_2\text{-}OH$

41 TPP-ext-CHO

42 $TPP\text{-}ext\text{-}CH_2\text{-}Cl$

43 $TPP\text{-}ext\text{-}CH_2\text{-}ps$

44 1,4-xylenebis(diethylphosphonate)

45 TPP-Ph-pep

46 TPP-Ph-TPP

47 TPP-Ph-Ph-CHO

48 $TPP\text{-}CH{=}CH_2$

49 $TPP\text{-}ext\text{-}CH{=}CH_2$

50 $TPP\text{-}Ph\text{-}CH{=}CH_2$

51 $TPP\text{-}Ph\text{-}Ph\text{-}CH{=}CH_2$

52 ***trans***-4-stilbenecarboxaldehyde

53 ***trans***-4-vinylstilbene

54 $(TPP)_2$

55 TPP-ZnTPP

56 TPP-Ph-ZnTPP

57 TPP-ext-Ph-ZnTPP

58 TPP-ext-Ph-TPP

59 TPP-Ph-Ph-ZnTPP

60 TPP-Ph-Ph-TPP

61 FeTPP-Ph-TPP

62 FeTPP-ext-Ph-TPP

63 FeTPP-Ph-ZnTPP

64 FeTPP-ext-Ph-ZnTPP

65 FeTPP-Ph-Ph-ZnTPP

66 tetra(4-sulfonatophenyl)porphyrin, TSPP

67 tetra(4-pyridinyl)porphyrin, T4PyP

68 tetra(3-pyridinyl)porphyrin, T3PyP

69 tetra(4-methylpyridinium iodide)porphyrin, T4MPyP

70 tetra(3-methylpyridinium iodide)porphyrin, T3MPyP

71 TPyP-$(Br)_n$

72 3-bromomethyl benzoic acid

73 3-carboxaldehyde benzoic acid

74 3-carboxaldehyde-methylbenzoate

75 3-carboxaldehyde-ethylbenzoate

76 tetra(3'-(methylcarboxylate)phenyl)porphyrin, T3(M)EPP

77 tetra(3'-(ethylcarboxylate)phenyl)porphyrin, T3(E)EPP

78 T3(M)EPP-CHO

79 T3(E)EPP-CHO

80 T3(M)EPP-CH_2-OH

81 T3(E)EPP-CH_2-OH

82 T3(M)EPP-CH_2-Cl

83 T3(E)EPP-CH_2-Cl

84 T3(M)EPP-CH_2-ps

85 T3(E)EPP-CH_2-ps

86 4-bromobenzaldehyde acetal

87 terephthalaldehyde monoacetal

88 2-pyrrole methanol

89 dipyrrylmethane

90 dipyrrylthione

91 monoacetalporphyrin, MAP

92 para-diacetalporphyrin

93 porphine

94 monobenzylporphyrin, MBP

95 MBP-T3EPP

96 MBP-T3CPP

97 MBP-ZnT3EPP

98 FeMBP-ZnT3EPP

99 FeMBP-ZnT3CPP

100 T3(E)EPP-Ph-CHO

101 T3(E)EPP-Ph-ep

102 T3(E)EPP-Ph-Ph-ipp

103 FeMBP-Ph-ZnT3(E)EPP

104 FeMBP-Ph-Ph-ZnT3(E)EPP

105 FeMBP-Ph-ZnT3CPP

106 FeMBP-Ph-Ph-ZnT3CPP

107 FeTPP-Ph-ZnT3(E)EPP

108 FeTPP-Ph-ZnT3CPP

Index of Figures

Index of Synthetic Schemes

Index of Tables

1. INTRODUCTION

1.1. Porphyrins

Porphyrins are cyclic molecules in which four pyrrole rings are linked together to form a fully conjugated system. There is a tautomeric equilibrium in which the four nitrogen atoms exchange the two protons, making the four pyrrole rings equivalent (Figure 1-1). Porphyrin nitrogens can undergo single or double protonation or deprotonation in reasonably mild conditions and, when deprotonated, they form a square with ideal dimension to host a nucleus, typically a metal ion but also non-metallic elements of the groups XIII-XV (aluminium, silicon, phosphorous, etc.).

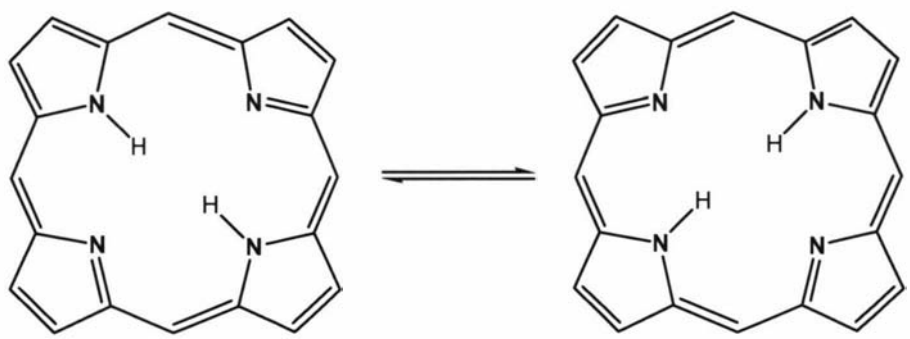

Figure 1-1 Porphine

A great variety of metalloporphyrins are known; almost every metal can be coordinated inside the macrocycle, different metallic oxidation states are possible and further coordination is possible at the axial positions.[1] As a result, an enormous variety of materials with very different properties have already been synthesized and studied.

Porphyrins have a highly aromatic character,[2,3] which is reflected in the planarity of the porphyrin core and which differs between free-base and metallated porphyrins[4] (Figure 1-2). In the free-base, it involves 18 of the 22 π–electrons leaving two localized double bonds on two opposing pyrroles; this, combined with the tautomery, makes the pyrrole rings less aromatic than the 'internal cross' represented by the

porphyrin without β-pyrrolic carbons. In fact, dianionic porphyrins have 18 π–electrons in the 'internal cross' and the β-pyrrolic positions are little involved in the overall aromatic system. In metalloporphyrin, instead, all electrons are delocalized all over the porphyrin ring.

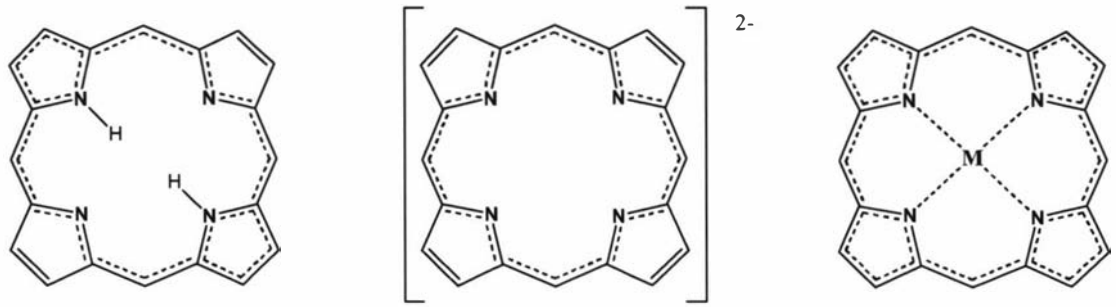

Figure 1-2 Aromaticity in free-base, dianionic and metallated porphyrins[4]

Aromaticity is probably the most important reason for which porphyrins have been utilized by nature in a wide range of processes; the possibility to delocalize electrons over such a large system gives porphyrin a good thermal stability and the ability to be oxidized and reduced with little destabilization of the overall system. Moreover, substituents and coordinated metals can have a strong effect on the electronic system, allowing chemical and physical properties to be finely tuned. Aromaticity is also responsible for very high molar extinction coefficient for the π–π^* transitions in the near-UV/visible part of the electromagnetic spectrum (Figure 1-3).

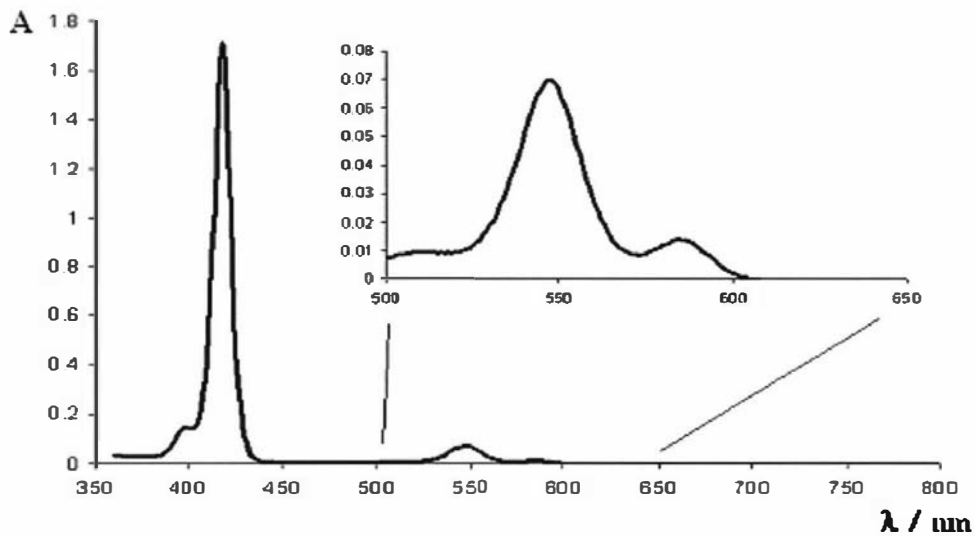

Figure 1-3 UV-visible absorption spectrum of ZnTPP (**Zn-3**) in dichloromethane (3.2×10^{-6}M) with the Q band region expanded

All porphyrins and metalloporphyrins show a very strong ($\varepsilon > 200{,}000$ $L \cdot mol^{-1} \cdot cm^{-1}$) Soret (or B) band at around 400 nm and weaker ($\varepsilon < 30{,}000$ $L \cdot mol^{-1} \cdot cm^{-1}$) Q bands (four in the free-base and two, named α and β, in metalloporphyrins) in the 500-700 nm region. The excited states produced by these transitions are usually characterized by long lifetimes (nanoseconds for free-base porphyrins) and often relax to the ground state by fluorescence. As a result of those physical and chemical properties, natural porphyrins play critical roles in biological activities like redox processes[5], oxygen transport and light harvesting.[5-7] Porphyrin chemistry has been intensively investigated over the last 50 years and synthetic porphyrins have been introduced into a variety of interesting applications such as in catalysis,[8,9] in medicine[10,11] and in optical devices.[12-14]

1.2. Porphyrin arrays

In some cases, both in natural and synthetic 'machines', porphyrins work in arrays, molecular and supramolecular structures, which allow an enhancement of a particular function and direct it to an active centre. This is made possible by the aromaticity and redox properties of metalloporphyrins which favour energy and electron transfer through large systems.[15-18] The interaction between porphyrins in an array is very sensitive to their relative position (both to distance and dihedral angle)[14,19] and to the atoms by which they are linked.[20,21] In particular, maximum electronic communication has been achieved when porphyrins are coplanar or face-to–face. In the first case, interactions happen 'through bonds' by orbital overlapping and distance plays a minor role compared to the nature of the linkers; Figure 1-4 shows an example of a "porphyrin tape", a chain of fused porphyrins which shows extended conjugation reflected in extremely low HOMO-LUMO gaps and very low oxidation potential

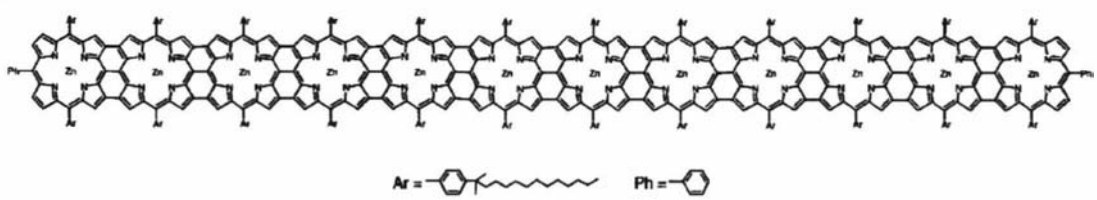

Figure 1-4 Fused porphyrin tapes by Tsuda and Osuka[22]

High electronic interactions can also be achieved by cofacial porphyrins but in this case the communication is 'through space', by pure electrostatic interactions; for this type of electronic interaction to be effective, the distance and the relative orientation of the porphyrin rings are critical. Extensive work on cofacial porphyrins has been realized by Collman *et al.*[23] (Figure 1-5a) and Fletcher and Therien[24] (Figure 1-5b).

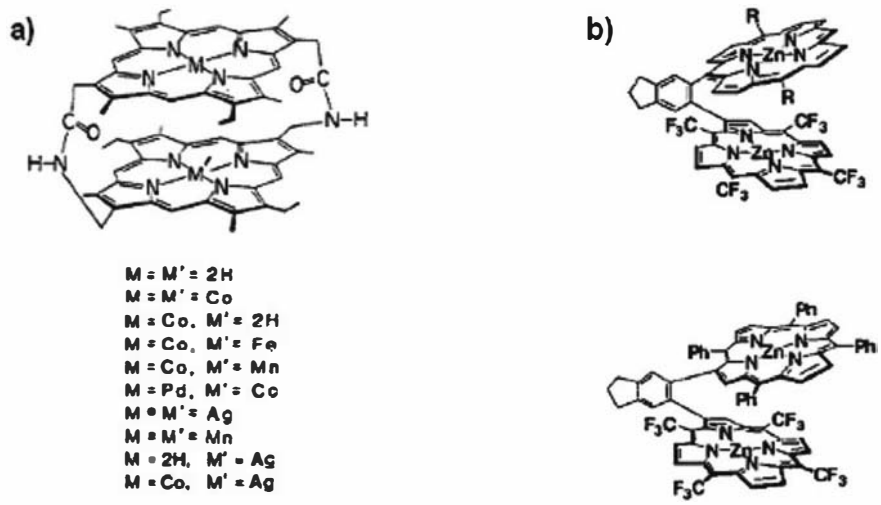

Figure 1-5 Cofacial dimers by a) Collman *et al.*[23] and b) Fletcher and Therien[24]

Porphyrin arrays are assembled in many ways depending upon the nature of the interactions required between single units. One way of building arrays is by complexation of the metal centres; metalloporphyrins in which the metal centre is able to further coordinate other atoms undergo self-assembly in the presence of appropriate ligands.[1,25] Porphyrin arrays can be assembled either using ligands attached to the porphyrin (Figure 1-6a)[26-29] or adding non-porphyrinic coordinating molecules to a porphyrin solution (Figure 1-6b).[30] Many examples have been described in which various metals (e.g. Zn, Fe, Ru, Co) as well as many ligands have been found to coordinate strongly enough to form stable supramolecular structures.[31] Zn and Ru porphyrins and pyridine- or imidazole-type ligands have been the most popular choices because of their typically high complexation constants of 10^4-10^{20} M^{-1}.[1] Ligands coordinating through oxygen atoms are also very common but the strength of the bond is typically not enough to produce stable supramolecular structures.[32]

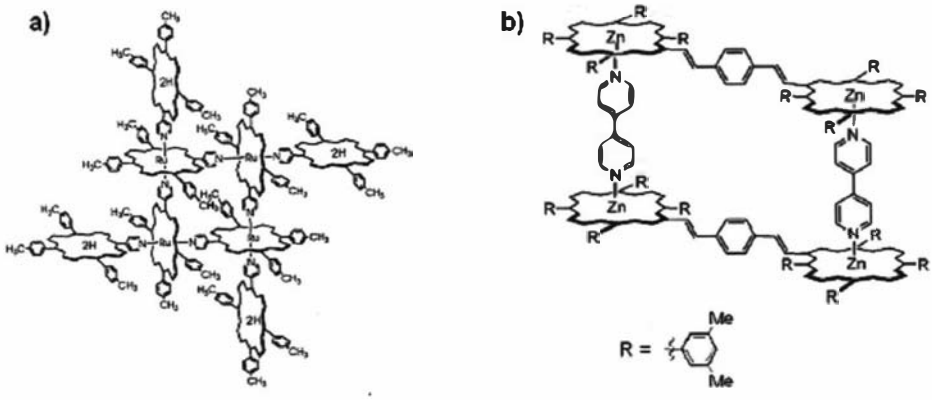

Figure 1-6 Coordinated porphyrin arrays by a) Okumura *et al.*[28] and b) Plieger *et al.*[30]

Interesting structures have been created in which arrays formed by self assembly have shown strong interactions and cooperative properties. An example is shown in Figure 1-7: this nine porphyrin array made by Mak *et al.*[33] is held together by Zn-pyrazine coordination and hydrogen bonding. Very strong electronic interactions have been registered between the cofacial Zn porphyrins while the expected energy transfer between the cofacial dyads and the central free base porphyrin was much less efficient because of the distance between the units and the absence of favourable pathways through bonds.

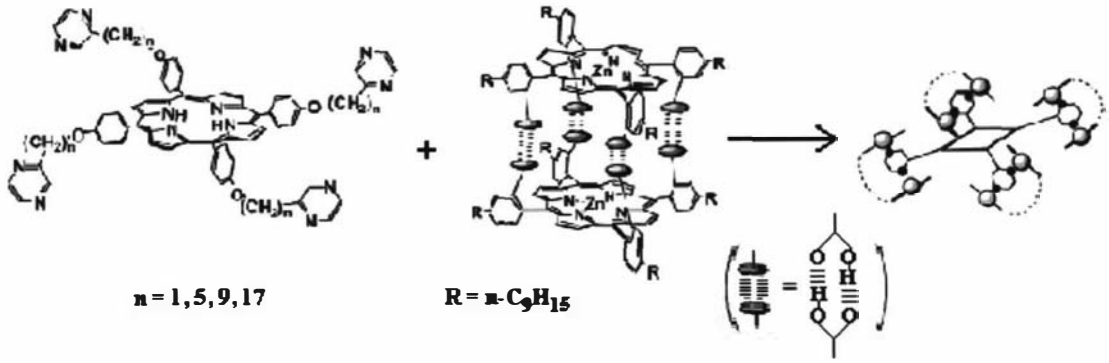

Figure 1-7 Coordinated nonaporphyrin array by Mak *et al.*[33]

In some cases, self-assembling reactions can also be designed to form well defined 'cages' for catalytic purposes, like the trimer shown in Figure 1-8. In this example, Slagt *et al.*[34] used Zn-porphyrins-pyridine coordination to create the desired geometrical environment around a Rh catalytic centre.

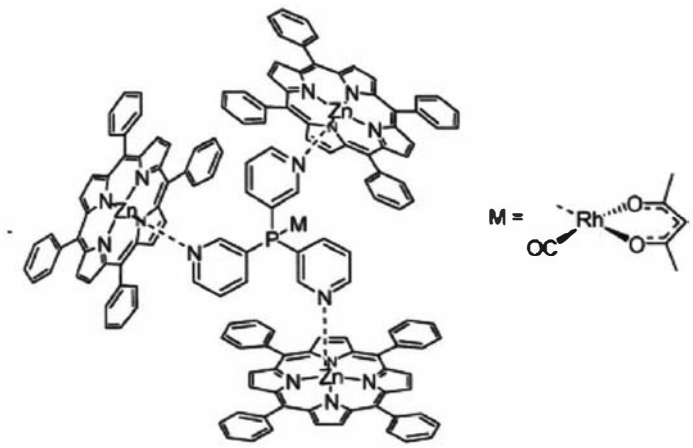

Figure 1-8 Coordinated triporphyrin array by Slagt *et al.*[34]

1.3. Covalently linked porphyrin arrays

While formation of coordinated arrays is achieved simply by self-assembly in solution, covalently linked arrays require a different approach. They can be made of porphyrins directly linked between the tetrapyrrolic rings (as in Figure 1-4) or connected through bridges (Figure 1-9).

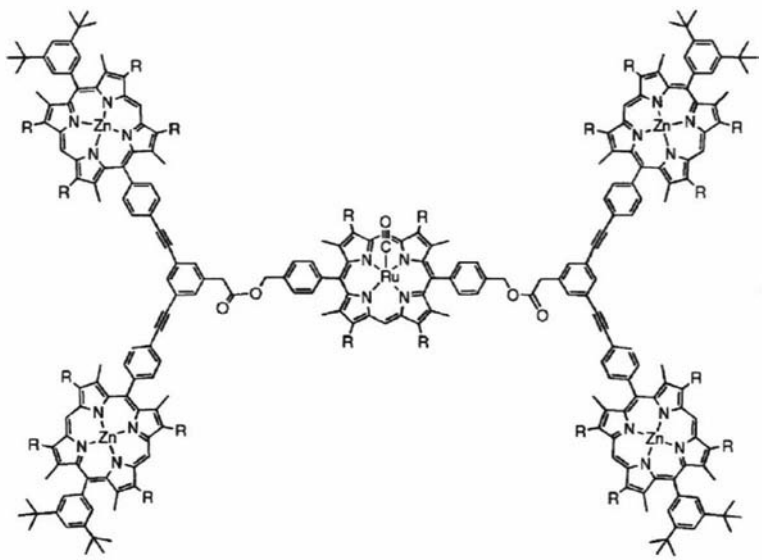

Figure 1-9 Covalently linked array by Sanders *et al.*[35]

Covalent arrays can be synthesised either in the course of the porphyrin formation or afterward, coupling appropriate functional groups of different porphyrins or by polymerization of a single porphyrin. A large number of covalently linked porphyrin arrays have already been created and porphyrin units have been connected through a variety of ways involving common linkages such as ether, amide, ester and single, double or triple C-C bonds.[21,29,35,36] Most of the literature is concerned with porphyrins connected through their meso-positions, because of a wider choice of available synthetic methods. The easy-to-synthesize tetra(meso)arylporphyrins can be prepared with functionalized aryl groups and these functionalities have been exploited to create arrays; similarly, octa(β-pyrrolic)alkylporphyrins can be functionalized in meso position and the newly introduced group can be used for the successive array formation. On the other hand, little work has so far been published about covalent arrays connected through their β-pyrrolic positions; this thesis work is aimed at developing the versatile strategy used in our laboratories to obtain such kind of arrays. A review of covalent porphyrin arrays along with their synthetic methods will be presented in Chapter 2.

1.4. Porphyrin and porphyrin array applications

Porphyrins, thanks to their ability to coordinate many metals and to carry many substituents, are amongst the most versatile molecules. These macrocycles, both as single units and in more complex structures, have been suggested for a large variety of applications. For example, porphyrins have been proposed as a tool in many medical treatments. The main application in this case has been in the well established photodynamic therapy of tumours where porphyrins can selectively bind cancer cells and destroy them by oxidation (typically, by singlet O_2 formation) after photoexcitation.[11,37] Similar results have also been achieved using ultrasound irradiation.[38] These methods have proved successful for many types of tumours and is very interesting because it does not cause the strong side-effects caused by classic methods (surgery, radiotherapy, chemotherapy). Porphyrins can also be useful in

other medical conditions such as spinal cord compression where antioxidant properties of low-valent metalloporphyrins (e.g. Mn(II)) can be exploited.[10]

Another major field of single porphyrin application is in catalysis. Metalloporphyrins have been found to be very efficient in catalyzing oxidations and reductions. For example, Fe(II) porphyrins have been employed to catalyze the reduction of highly polyhalogenated alkane pollutants[8] whereas Mn(III), Fe(III) and Rh(III) porphyrins have been successfully used in oxidations as O-O bond activators.[39,40] Moreover, chiral porphyrins can be used for asymmetric syntheses; Ru and Os porphyrins have shown high regioselectivity and enantioselectivity in oxidation of many substrates, particularly olefins.[41-43]

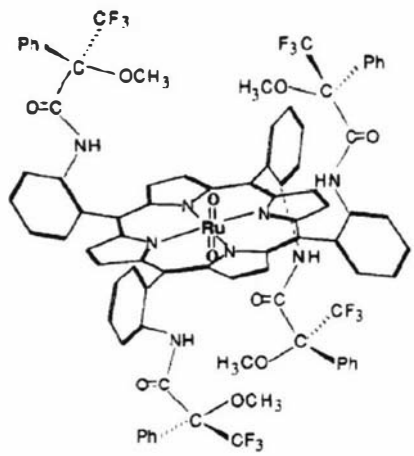

Figure 1-10 Chiral Ru(VI) porphyrin catalyst by Simonnaux and Le Maux[41]

The emission properties of metalloporphyrins make them suitable for applications in electroluminescent devices. The interest in OLEDs (organic light-emitting diodes) is rapidly growing thanks to the high efficiency, long lifetime and pure chromaticity of these new devices. Copper[44] and free-base[45] porphyrins have been found suitable for applications in this field.

Other applications include the use of porphyrin in new kinds of memory devices. The possibility to store information at the molecular level has become an object of great interest over the last few years. The ability of metalloporphyrins to switch through different oxidation states has led to the building of memory devices in which porphyrins oxidation states can be switched either by photoexcitation (by laser beam) for optical recording disks[12,48] or electrically.[49] A step forward can be achieved by

more complex structures in which assembled porphyrins can store multiple information as distinct oxidation states for the making of high-density recording devices; an elegant contribution on this field has been provided by the Lindsey group with the preparation of system such as the one represented in Figure 1-11.[50]

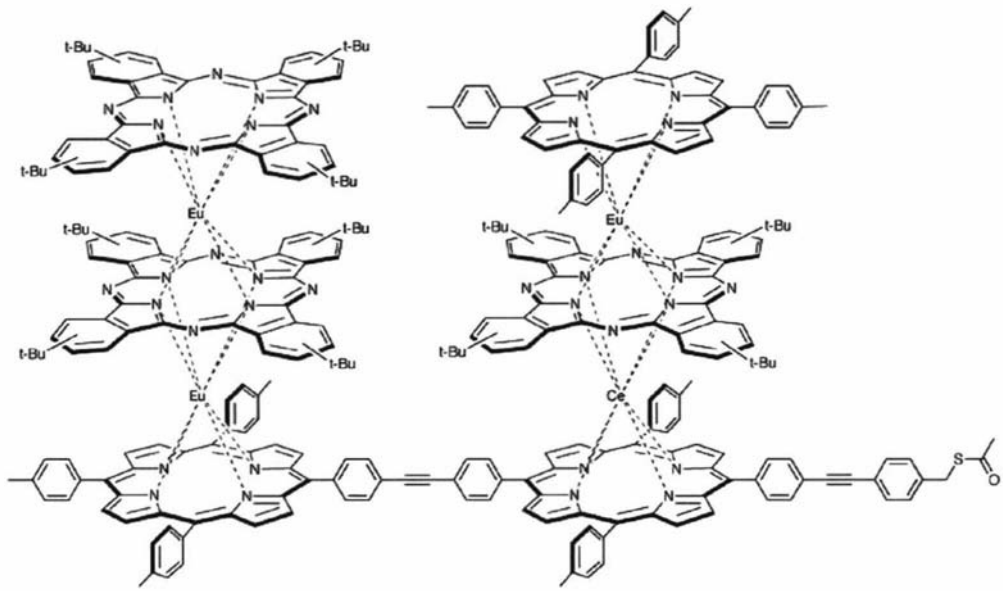

Figure 1-11 Triple-decker array by Schweikart *et al.*[50]

When porphyrins are put together in arrays, new properties can be achieved from the cooperation between the units. The possibility to tune system properties by using different porphyrin units or linkers makes them interesting molecular devices for photonics and optoelectronic applications.[51] Interesting work on this field has been presented by Holten *et al.*[52] with the investigation of series of arrays containing differently metallated porphyrins connected through diarylethyne linkers (Figure 1-12). In this way, there is little electronic coupling between the units (non-conjugated linker) but it is enough to allow well definite intramolecular energy transfers. In particular, they have found that a chain of Zn porphyrin is very efficient as energy conductive wire, whose output consists of an energy acceptor free-base porphyrin. Also, incorporation of a Mg porphyrin in the array produce the ability to switch the output; by oxidizing the Mg porphyrin, energy transfers to the free-base porphyrin and its emission are efficiently quenched. By arranging those units in various fashions it is possible to make molecular wires, linear or T-shaped gates.

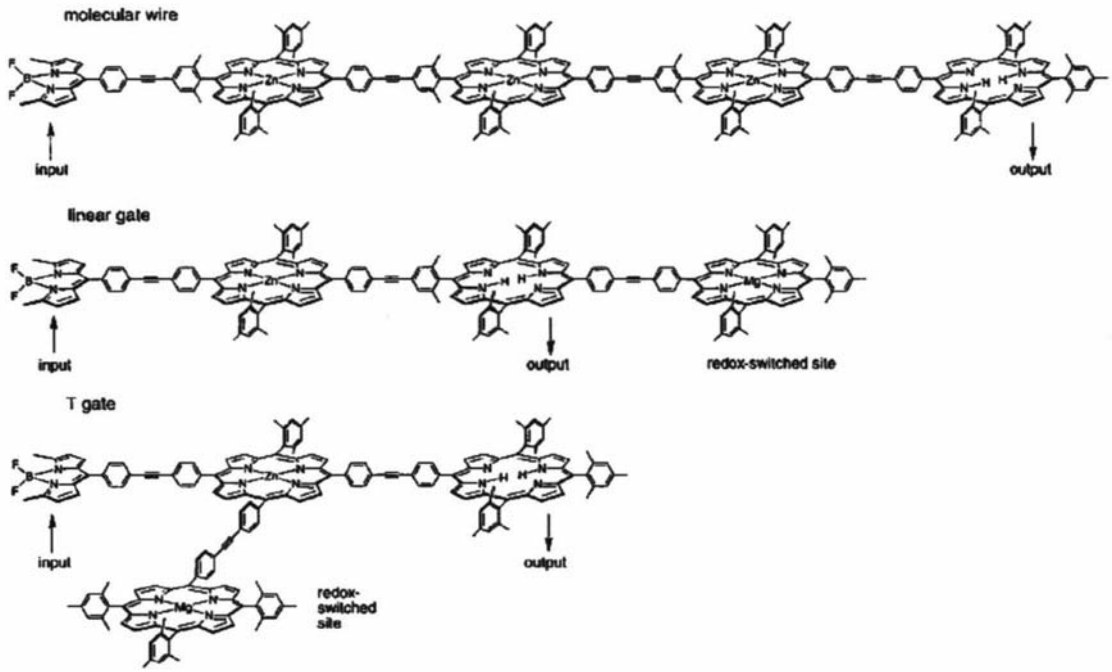

Figure 1-12 Arrays for optoelectronics by Holten *et al.*[52]

An impressive amount of work has also been undertaken by the Osuka group (examples in Figure 1-13 and Figure 1-14) in the syntheses and investigations of very large arrays in which directly linked porphyrins show strong electronic couplings; the strong dependence from linkage, dihedral angles and metallation state allows to tune the array properties, such as optical non-linearity, which are generally enhanced by increasing the size of the array. [14,19,21,53]

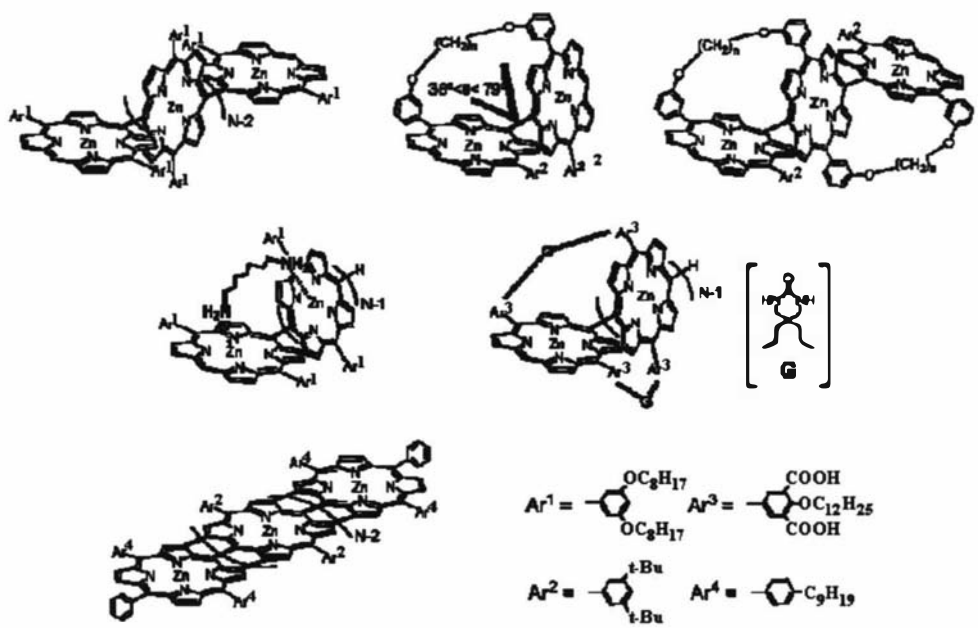

Figure 1-13 Linear arrays with controlled dihedral angles by Ahn *et al.*[19]

The ability to include those different arrangements in a three-dimensional structure is interesting because allows selective energy transfers which results in well definite oxidation states; large arrays of this kind would be ideal for the creation of molecular based multiple information storage systems (Figure 1-14).[54]

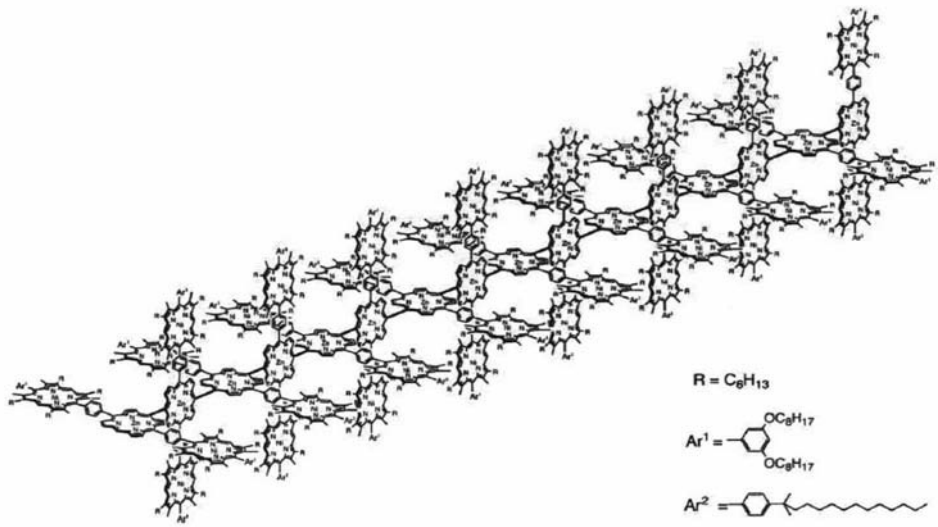

Figure 1-14 Three-dimensional grid array by Nakano *et al.*[54]

1.5. Porphyrins and porphyrin arrays for light harvesting

When we consider that the sun daily provides the same amount of energy we take from fossil fuels in a full year, it appears obvious to research a way to utilize such an enormous source. Nature, with photosynthesis, has found ways to employ sunlight to reduce CO_2 and oxidize H_2O so that we have life as we know it. It is no utopia to think that mankind should imitate such wonderful processes to help save this planet. Natural organisms, plants and bacteria, transform light into chemical energy in the first stage of photosynthesis; it is a large number of porphyrins that collect the sunlight and transfer the absorbed energy to a small number of central porphyrins which work as the active centre.[7,55] Figure 1-15 shows the model of the structure of the photosynthetic units LH2 (the outer one, shown on the left) and LH1 of purple bacteria: the two sets of porphyrins arranged in a 'circle' play the antenna role, catching the light and transferring the absorbed energy form LH2 to LH1 and then to the reaction centre that is in the middle of LH1 and contains a set of porphyrins which undergo redox reactions.

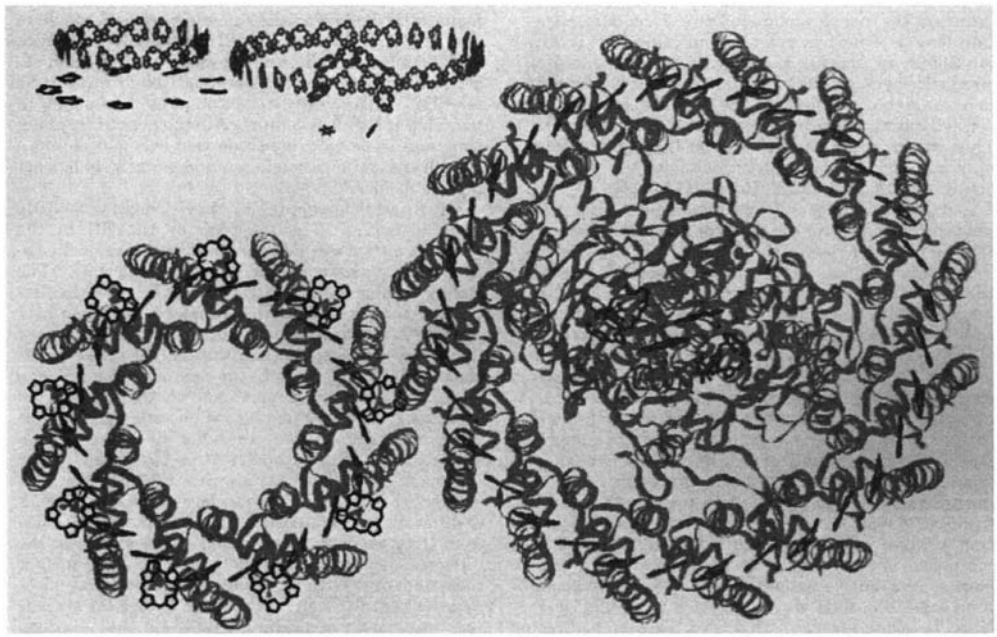

Figure 1-15 Model of the purple bacterial photosynthetic unit by Pullerits and Sundtröm[56]

It is not surprising, therefore, that there is great interest in creating porphyrin based devices able to exploit the sunlight energy.[57-61] Two possible approaches to reach this goal are photovoltaics and artificial photosynthesis. In both cases, porphyrins are required to use sunlight's energy to promote an electron to an excited state that then has to be 'utilized' before the porphyrin molecules relax to their state ground. In photovoltaics, the excited electron is injected into an electrode surface creating an electric current that can be either used by a device or stored. In photosynthesis, the 'excited state' of the porphyrin has to be transferred to an active center, where a chemical reaction will occur. Our first interest in porphyrin arrays comes from their potential use in photovoltaic devices. Dye-sensitized solar cells (DSSC) are currently the most promising devices of this kind, being able to obtain, using Ru complexes as light harvester, over 10% of efficiency (η) in solar energy conversion.[61] One variant of DSSC, known as the Grätzel cell (Figure 1-16),[62] has also been developed in our laboratories; devices of this kind, in which porphyrins are used as the light harvesting dye, have already been created in our group approaching 7% efficiency.[60]

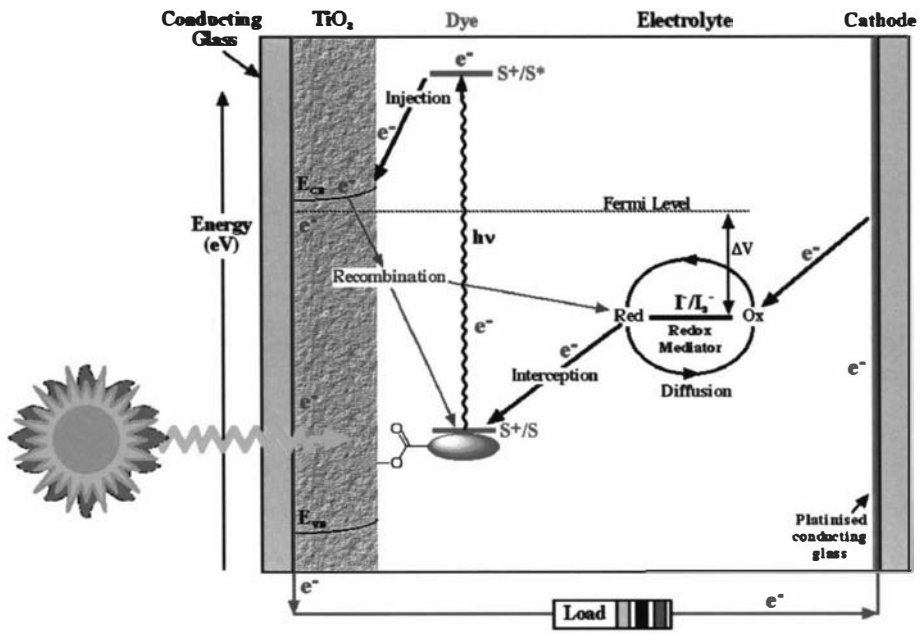

Figure 1-16 Schematic representation of a Grätzel cell by Campbell[63]

Figure 1-16 shows a Grätzel cell, in which porphyrins are immobilized on a TiO_2 semi-conductive support and sandwiched between two glass electrodes containing the I_2/I_3^- redox couple dissolved in a suitable electrolyte. Light excites an electron from the dye which is passed to an electrode through the TiO_2 layer; the counter electrode and the redox couple closes the circuit providing an electron to the ionized dye and re-establishing the original state. So far, the best results in our group have been obtained using single porphyrins as dye, adequately functionalized with acidic moieties for TiO_2 binding. Interestingly, it has been shown that porphyrins can also produce photocurrent in the opposite direction by extracting electron from the semi-conductive layer. Researchers have recently made a Grätzel-type cell that employs NiO instead of TiO_2 on which electron poor porphyrins as phosphorous(V) porphyrins are able to produce hole injection, instead of electron injection as is usual with Zn porphyrins, to the semi-conductive support (Figure 1-17).[64] However, in this case, the undesired recombination process between dye and semiconductive layer plays a much bigger role than in classic Grätzel cells, resulting in lower efficiency ($\eta < 0.1\%$).

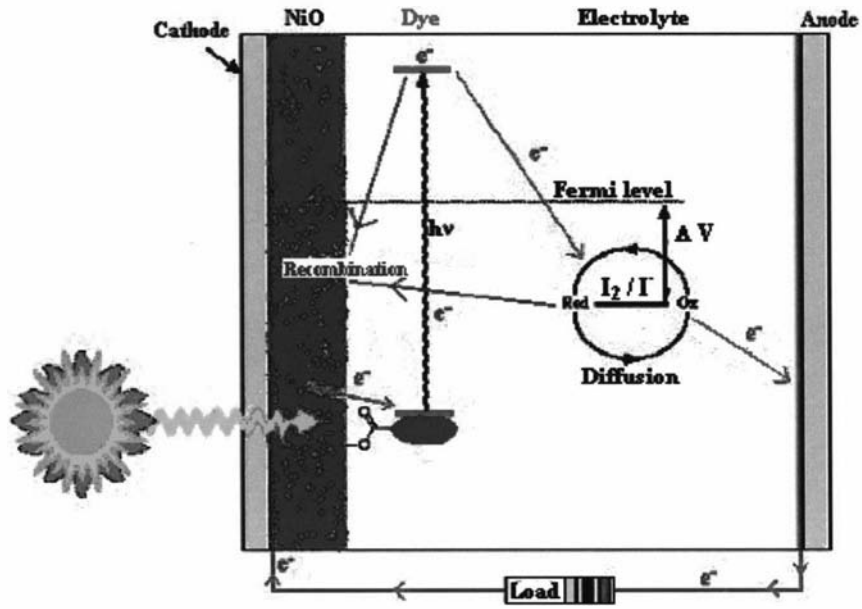

Figure 1-17 Schematic representation of an inverted photovoltaic device by Borgström *et al.*[64]

Research on alternative kind of porphyrin based photovoltaics is at early stages and other dye-sensitized devices are under investigations.[65-70] An elegant example involving the use of polypeptide backbone, porphyrins as electron donating dye and fullerene units as electron acceptors is shown in Figure 1-18.[70] Here, charge/hole separation is efficiently obtained by employing fullerene as charge acceptor while the polypeptide backbone controls the electron transfer from the electrode to the dye. Compared to Grätzel cells, this kind of more elaborate photovoltaic device has efficiency/cost ratios that are still much lower.

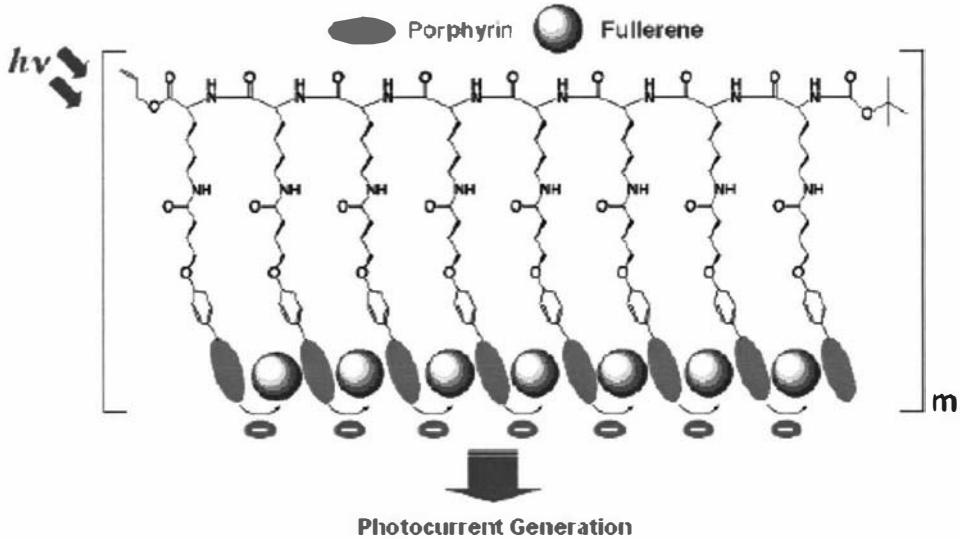

Figure 1-18 Polypeptide/porphyrin/fullerene photovoltaic device by Hasobe *et al.*[70]

The use of porphyrin arrays in such devices could produce an improvement in efficiency because of the possibility of an 'antenna effect'. Peripheral porphyrins, after excitation, can transfer either energy or electrons through the array to the porphyrin which is bound to the electrode (Figure 1-19); in this way, more porphyrin can be used per binding site (as long as the array size do not prevent binding because of its steric effects), increasing the amount of light collected.

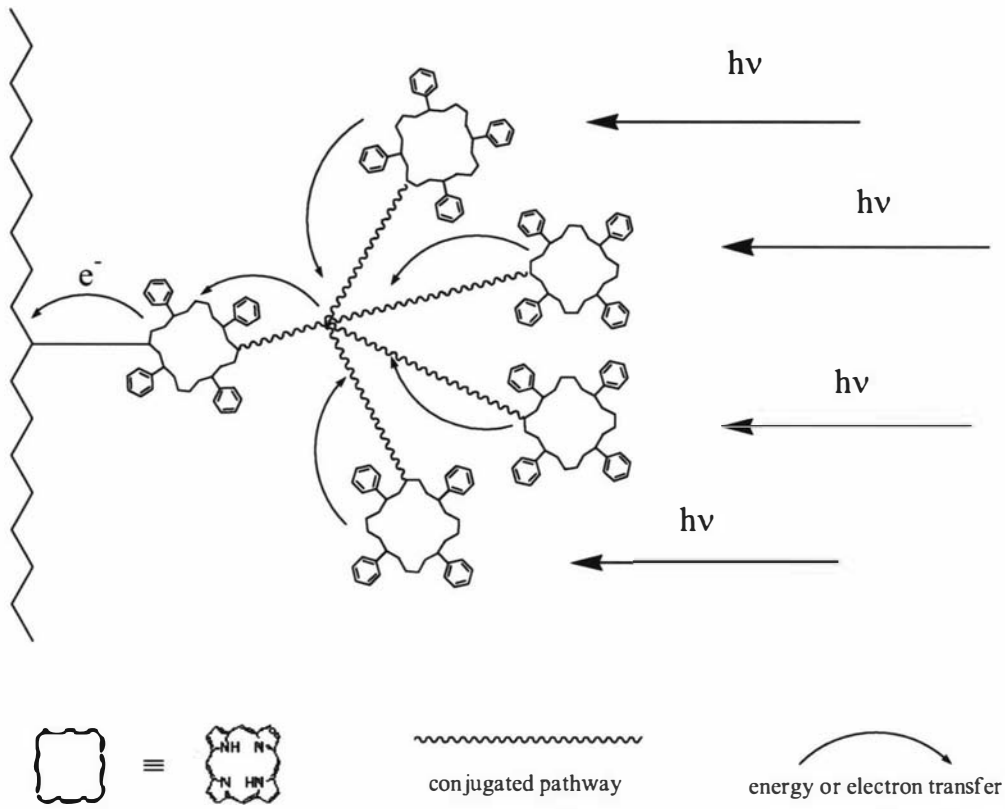

Figure 1-19 Schematic representation of antenna effect in porphyrin arrays

Antenna systems could be even more useful in artificial photosyntheses. It has been shown that in natural photosynthetic systems a large number of porphyrins work as antenna to collect large amount of lights and direct the energy to a small active centre.[7,55] To obtain high efficiency, artificial photosynthetic systems are likely to need a similar structure. The literature shows many attempts to reproduce antenna effect over large systems, mainly by assembling a large number of Zn porphyrins (as light-catching, energy donating part) around a free-base porphyrin which is the energy acceptor; many approaches have been utilized and many of them show the required properties (high light absorbance, efficient energy transfer) for their role in artificial photosynthesis.[21,33,71,72] The efficiencies of the energy transfer within these systems is

highly dependent on the geometrical distribution of the porphyrins. One of these model antenna made by Choi *et al.* [21] is represented in Figure 1-20.

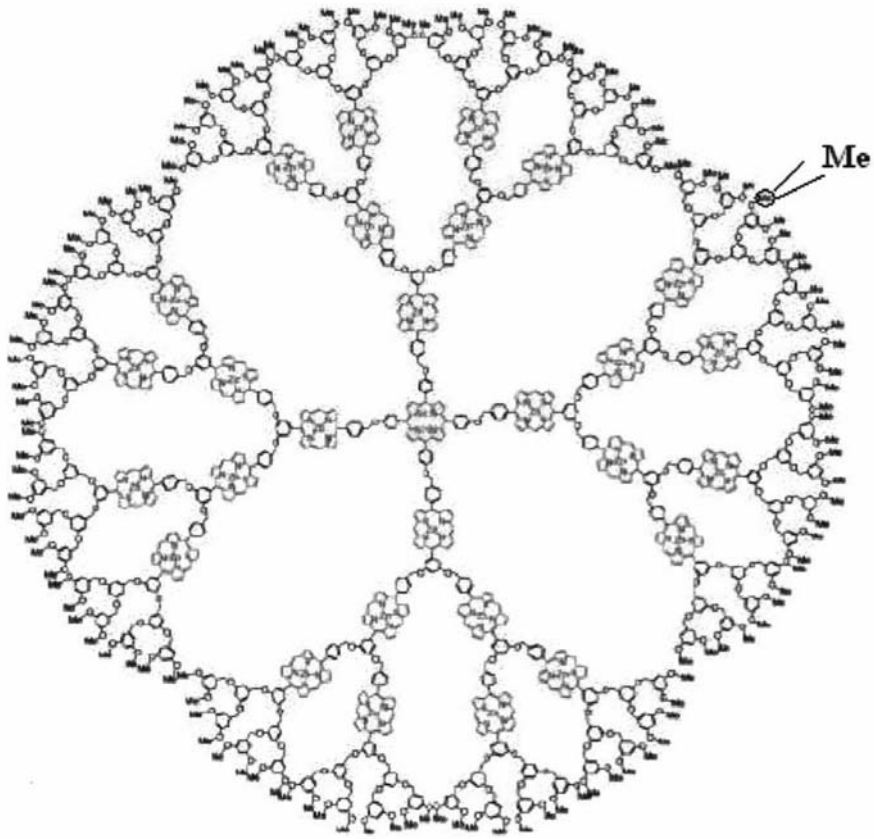

Figure 1-20 Dendritic multiporphyrin antenna by Choi *et al.*[21]

The main problems affecting the actual realization of efficient artificial photosynthetic systems are in the utilization of the absorbed energy before relaxation to the ground state occurs. To realize this, the end of the energy/electron chain transfer has to contain a catalytic centre for a reaction which would store that collected light as chemical energy. Although the understanding on natural photosyntheses is still far from being completely understood, some early attempts to imitate bacterial and plants abilities have already been created, even though low efficiencies have been obtained. One of the hardest obstacles for a sensible improvement lies in the choice of the photoactivated reaction; in fact, to be functional, reagents and products should be kept separated (or quickly separated after reaction) so that the inverse and undesired reactions will not occur. A simple example of artificial photosynthesis, reported by Miyatami and Amao,[58] is shown in Scheme 1-1. Here a Zn porphyrin works as light harvester and transfers an electron to an enzyme (L-lactate dehydrogenase, LDH)

through methyl viologen molecules (which work as electron carrier, in a similar way as I_2 in Grätzel cells); the enzyme catalyzes the reduction of pyruvic to lactic acid and the oxidized porphyrin is reduced to its ground state by the electron donor triethanolamine (TEOA).

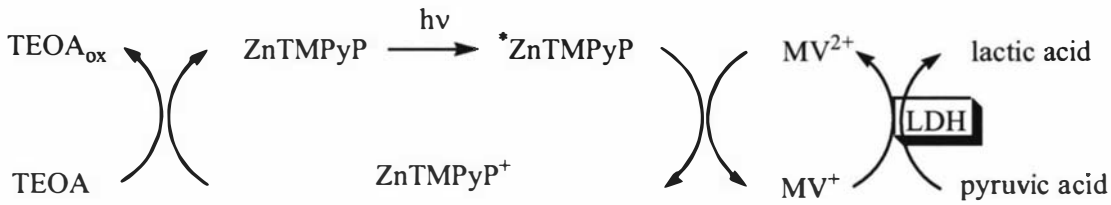

Scheme 1-1 Schematic representation of Miyatami and Amao photosynthetic system[58]

All the molecules involved in this system are in the same solution. In this way, charge separation and the electron funnelling from the porphyrin to the enzyme can not be very efficient; in fact, the efficiency of each step is dependent on the probability to have collisions between the desired molecules at the proper time and reverse reactions can occur. Furthermore, this system requires an electron donor (TEOA) which is not regenerated.

A similar system in which the porphyrin is directly linked to the viologen was successfully utilized with a hydrogenase enzyme for water reduction;[73] water splitting was completed by using grana (part of the chloroplasts rich in chlorophylls and photosynthetic systems)[74] as catalyst to photoreduce the NADP, which acts as renewable electron donor for the oxidized porphyrin (Figure 1-22).

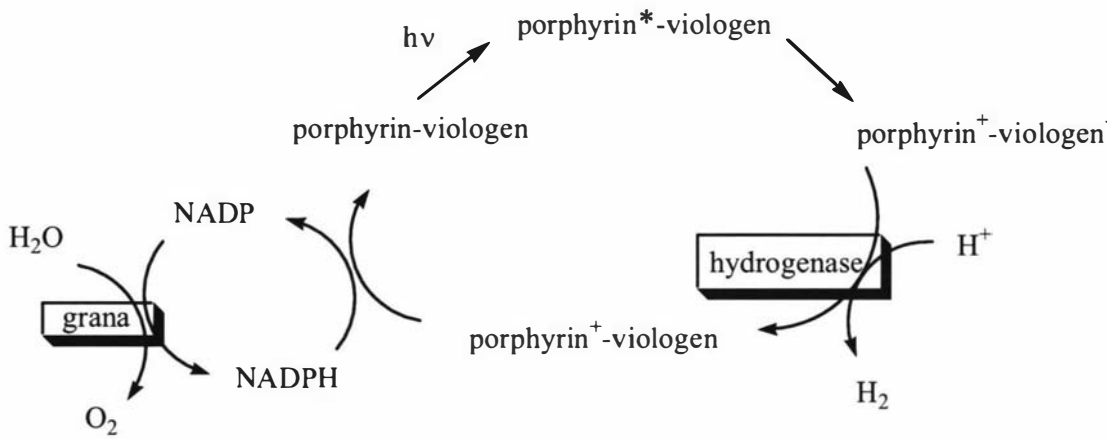

Scheme 1-2 Schematic representation of Amao and Okura photosynthetic system[73]

1.6. Object and structure of the thesis

As seen in the previous sections, porphyrins have very interesting properties that can be exploited in a number of applications; furthermore, when assembled in arrays, some porphyrin properties can be emphasized and new phenomena can be obtained. In the last years, some of the research in our laboratories has been dedicated to the development of photovoltaic cells in which porphyrins have been used as light harvesting dye. The work in this thesis is connected to this purpose and is aimed to the development of a flexible synthetic strategy for the preparation of porphyrin arrays; also, investigations on their ability to perform intramolecular energy/electron transfer for photovoltaics/photosynthesis applications were performed.

Among the different possibilities of creating arrays, we chose to focus our attention on discrete covalently bound arrays because they are more stable, easier to characterize and provide a larger range of synthetic options. Also, in order to favour the electronic communication through the entire array, and from the array to a binding site (within the photovoltaic or photosynthetic device), the research was directed towards systems in which porphyrins are covalently connected through conjugated systems. Furthermore, the 'rigidity' inherent in this kind of conjugated system allows a certain degree of control on the geometrical distribution of the single units in the array, which is very important in the investigations on electron and energy transfer.

Researchers in our laboratories have previously developed the syntheses of β-pyrrolic substituted tetraarylporphyrins,[75] which provide the building blocks for the making of the arrays described in this work. The development of a synthetic strategy to β-pyrrolic connected porphyrin arrays and the study of their photophysical properties is an almost unexplored subject[60,75-77,147] and allow us to describe the properties of novel systems and examine their suitability for photovoltaic and photosynthetic devices.

- Chapter 2 presents the making of fully conjugated porphyrin arrays through Wittig chemistry. The employment of a dendrimer strategy involving polyfunctionalized benzenes allowed stepwise control on the addition of further moieties so that different porphyrins in different metallated states were arranged in a determinate

geometrical relationship. Arrays containing up to five metalloporphyrin units (two kinds of porphyrins coordinating either zinc or nickel) were synthesized and characterized (Figure 1-21).

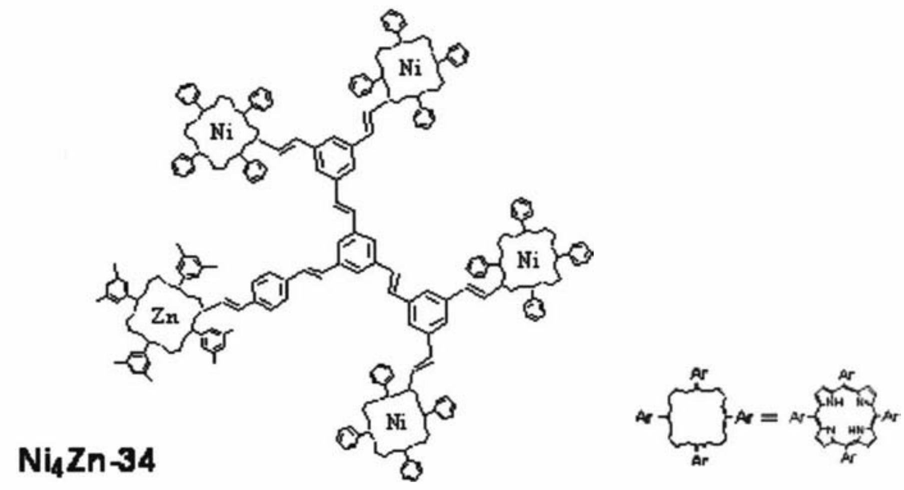

Figure 1-21 Mixed metal pentamer **Ni$_4$Zn-34**

- An unexpected co-product, obtained in the course of one the syntheses shown in Chapter 2, is the subject of investigation in Chapter 3. Here, the use of NMR spectrometry revealed an uncommon intramolecular coordination between the Zn ion and phosphonate groups of the same porphyrin (Figure 1-22). NMR spectrometry was also utilized for a characterization of the coordination equilibria between Zn porphyrins and phosphonates.

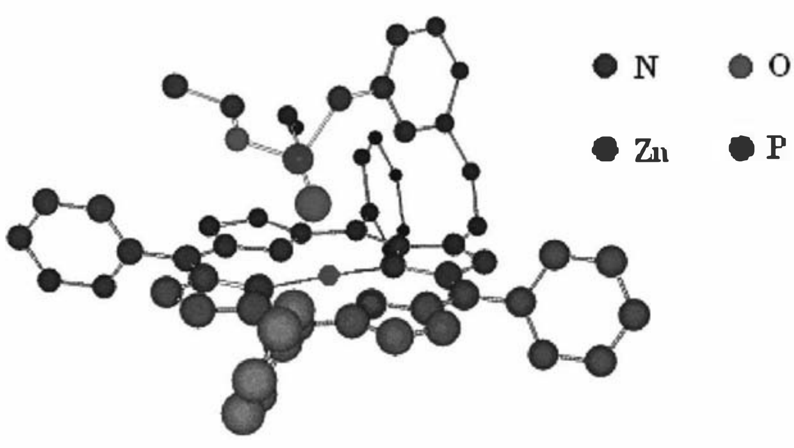

Figure 1-22 Simulated 3-dimensional structure of **Zn-22c** (the second phosphonate is not shown for clarity)

- Chapter 4 introduces the synthesis of a series of dyads containing Zn and free-base porphyrins connected through variously long phenylene-type bridges (Figure

1-23), along with two series of model molecules (the homometallic dyads and the monomers carrying the conjugated branch). Collaboration with IFOS-CNR in Bologna, Italy was established in order to investigate the intramolecular photophysics of those systems; spectroscopic characterizations and photophysical investigations were performed by Dr. L. Flamigni and Dr. B. Ventura at IFOS/CNR.

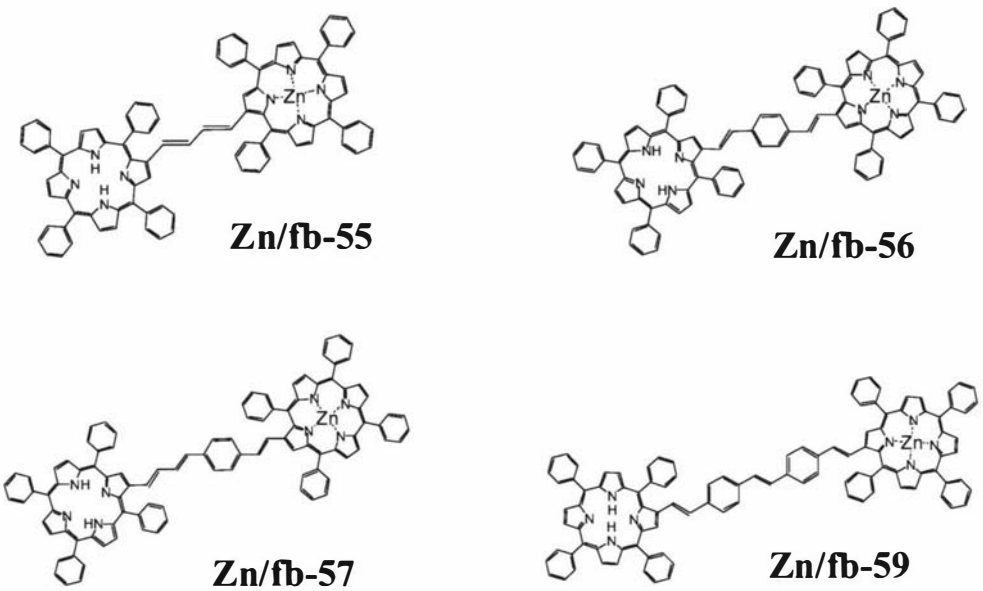

Figure 1-23 Series of Zn/free base porphyrin dyads

- Chapter 5, finally, presents the synthesis of dyads composed of Fe(III) and zinc porphyrin as part of a Marsden funded project in collaboration with the University of Pennsylvania for the investigation of new artificial photosynthetic systems. The syntheses of two sets of Fe(III)/Zn dimers, soluble either in organic solvents or in aqueous media, is described together with first attempts at their incorporation into synthetic proteins (Figure 1-24).

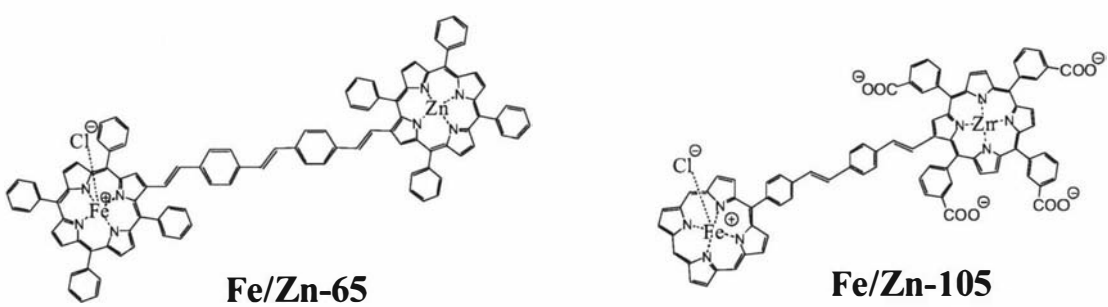

Figure 1-24 Fe(III)/Zn porphyrin dyads for protein binding

2. ARRAY SYNTHESES

2.1. Introduction to porphyrin array preparations

The use of porphyrins in complex structures has become of great interest because it allows the modulation and exploitation of the exceptional chemical and physical properties of these macrocycles. In particular, electronic communication between different moieties arranged in the same molecule is necessary for many interesting applications in light harvesting, artificial photosynthesis, photonics and optoelectronics. Most of the arrays reported in the literature are connected through the meso positions[29] and their chemical and physical properties have been extensively studied. For example, the Osuka group has prepared and investigated the properties of a series of octaalkylporphyrins connected through conjugated bridges (Figure 2-1).[78] On the other hand, very little is known about arrays connected through their β-pyrrolic positions; the core of this thesis describes the creation of such kind of arrays and the investigation of some of their properties.

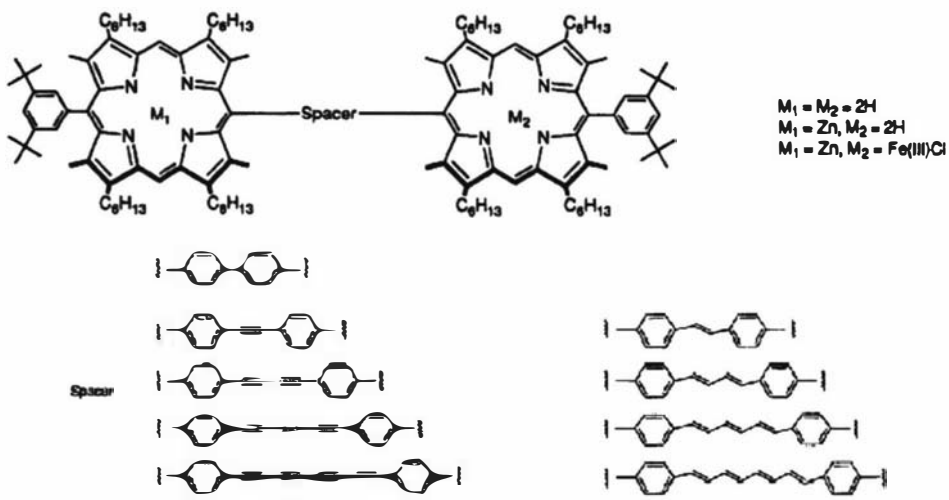

Figure 2-1 Meso-meso linked conjugated dimers by Osuka *et al.*[78]

In order to retain control over both the array formation and its geometrical structure, covalently linked systems have to be preferred. These arrays are generally prepared by exploiting the reactivity of some functional group on a single porphyrin. One of the most utilized in the literature is the aldehyde group, which can be used in

condensations with pyrrole derivatives to create arrays around newly synthesized porphyrins (Scheme 2-1).

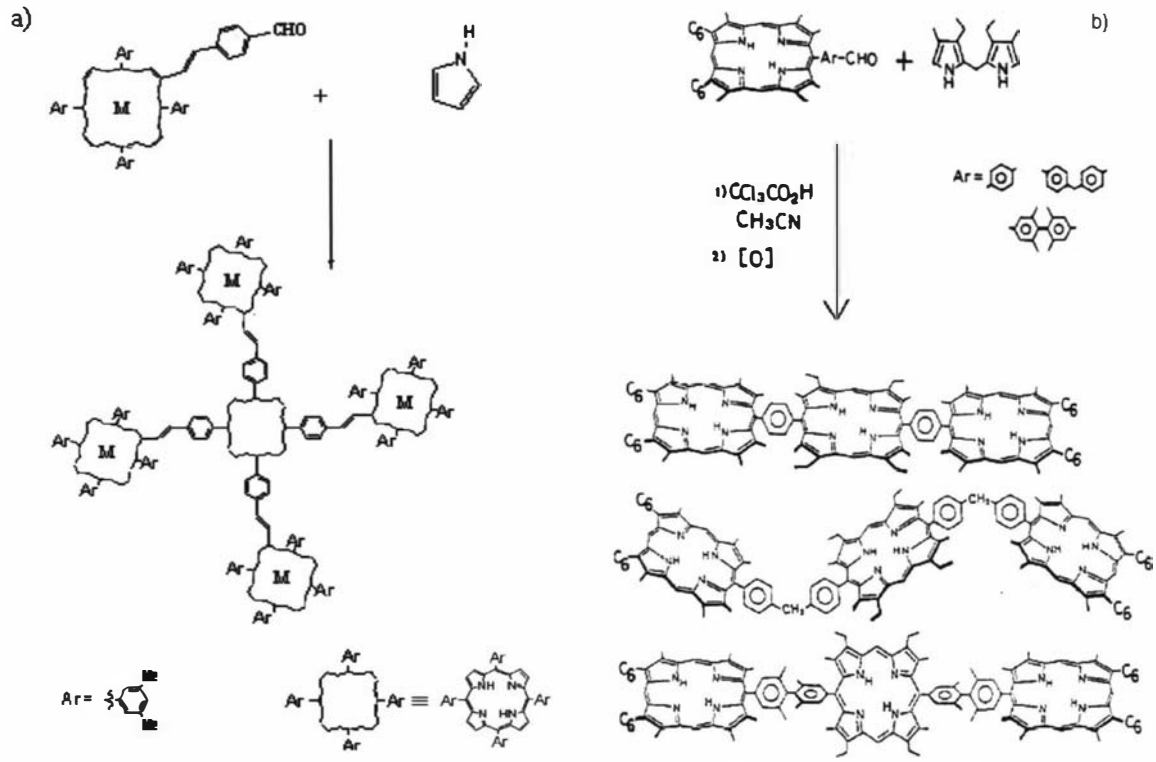

Scheme 2-1 Array syntheses by a) Burrell and Officer[75] and b) Nagata *et al.*[79]

Another very common way to create arrays is the reaction between two functional groups of two different porphyrins. Aldehydes and other functional groups can be introduced and modified to suit the synthetic requirements. Therefore, a large variety of organic reactions have been used to create porphyrin arrays, including ester (Scheme 2-2), amide, and imine formations.[21,29,35,36,80]

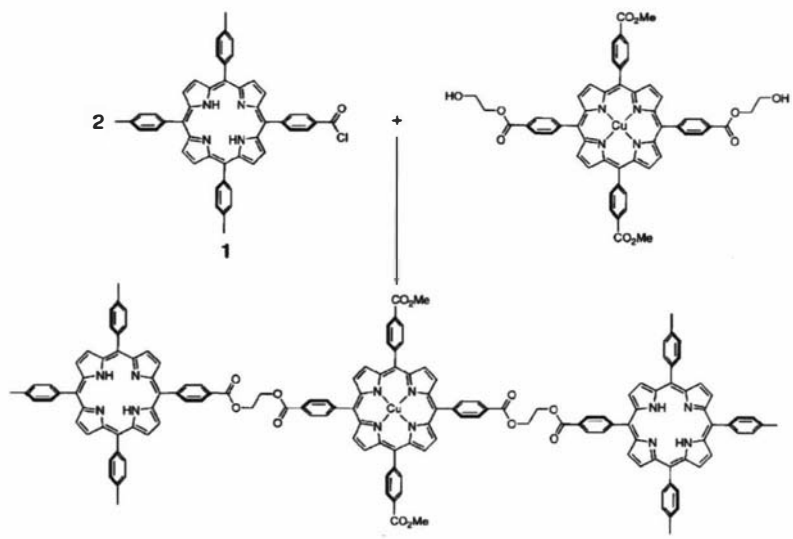

Scheme 2-2 Array syntheses by Anton *et al.*[80]

The use of aldehydes in couplings, either with other aldehydes (McMurray reactions) or with phosphorous ylides (Wittig reactions), represents a viable option for array preparation; the same array shown in Scheme 2-1a has also been prepared in our group by a Wittig reaction involving a tetrafunctionalized porphyrin (Scheme 2.3).

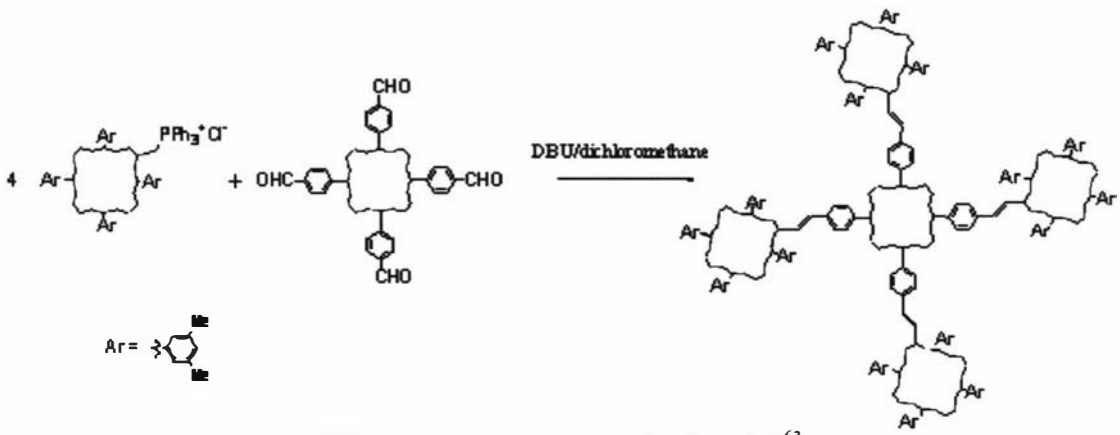

Scheme 2-3 Array syntheses by Campbell[63]

An interesting synthetic alternative is the use of metal-promoted couplings. Pd(0) complexes have been very extensively utilized by the Lindsay group for the preparation of alkyne-linked arrays. An example of this reaction is the synthesis of large and discrete arrays obtained using a central polyfunctionalized porphyrin (Scheme 2.4).[81] However, the formation of the monofunctionalized porphyrin acetylenes occurs in 5-12% yield and extensive purification of the arrays is required.

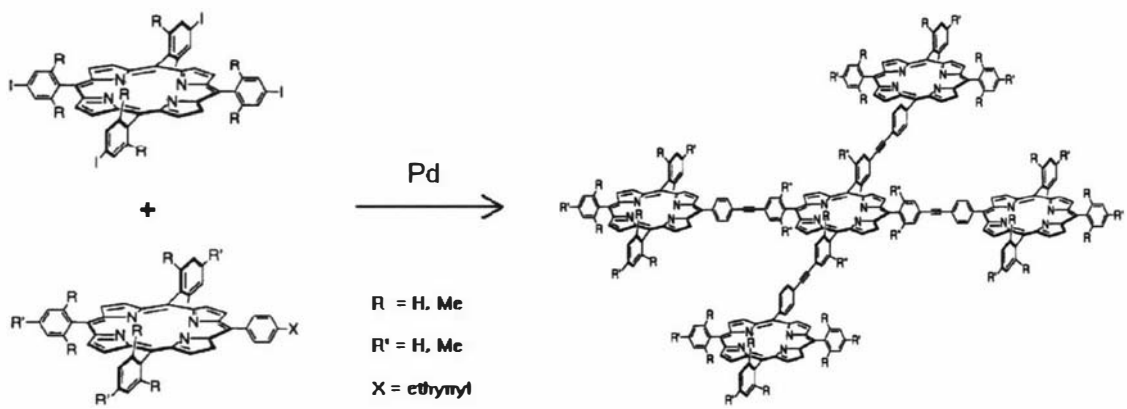

Scheme 2-4 Array syntheses by Prathaphan *et al.*[81]

Ag(I) salts have been shown to promote *meso-meso* coupling between two porphyrin units. By using porphyrins with two free meso-positions the Osuka group has obtained a great variety of large systems, including chain polymeric materials

(Scheme 2-5).[53] A certain degree of control over the formation of a desired structure has been obtained by optimization of the conditions (concentrations, solvents, amount of promoter); however, the presence of two equivalent reactive sites (the unsubstituted *meso* positions) makes very challenging to retain control over the length of such oligomers.

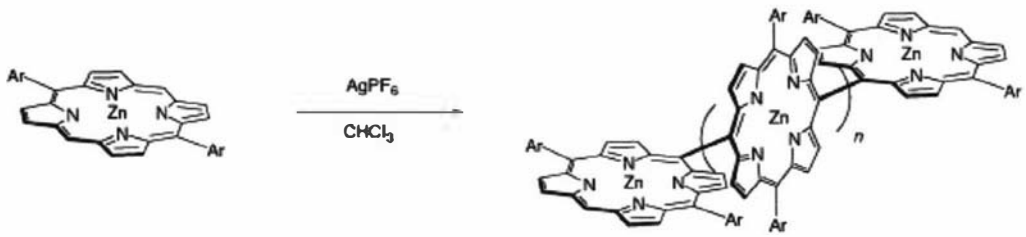

Scheme 2-5 Ag(I) promoted array syntheses by Park *et al.*[82]

All the synthetic methods described so far involve the use of only porphyrins and porphyrin precursors as reagents. In addition, an unlimited number of 'bridge molecules' can be used to connect the porphyrin monomers through their functional groups. As a result, a great variety of porphyrin arrays have already been prepared.[29] An example is shown in Scheme 2-6 where a phenylene group is used to connect two porphyrins.

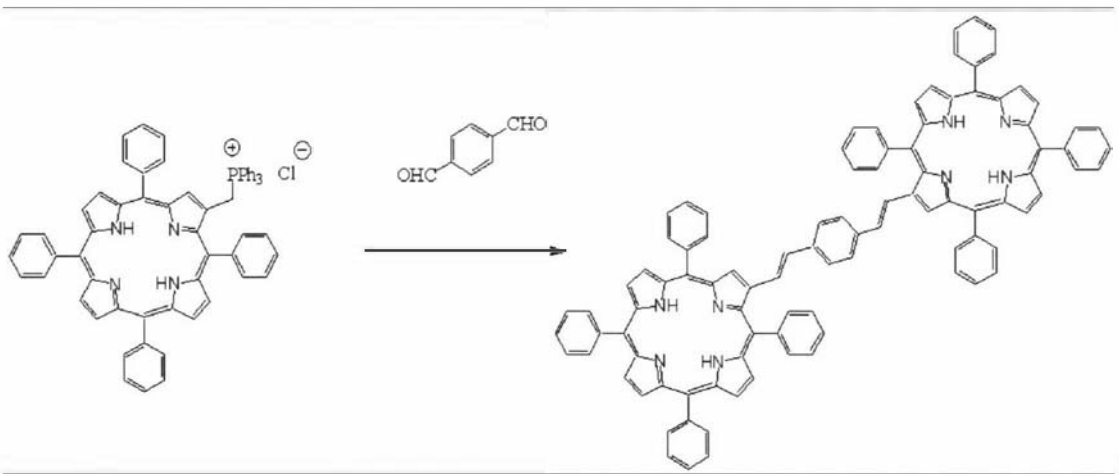

Scheme 2-6 Phenylene bridged dimer by Burrell and Officer[75]

The array syntheses described above highlight a number of problems associated with monofunctionalized porphyrins. From one point of view, they are necessary to avoid the statistical formation of multiple products, on the other hand they are usually quite difficult to prepare and isolate. In porphyrins, functional groups can either be present in the precursor to the porphyrin (usually in protected form) or be added later.[83] The

first way is useful for the creation of highly symmetric molecules, like porphyrins containing the same functional group in all four meso positions (Scheme 2-7).[84]

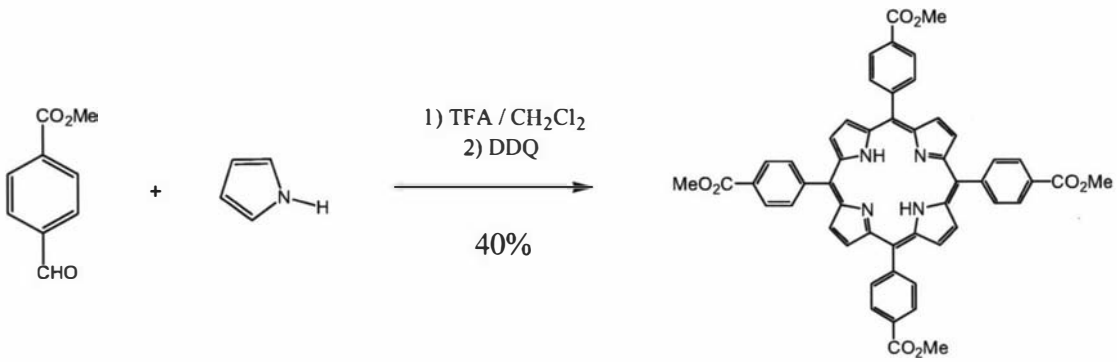

Scheme 2-7 Simmetrically functionalized porphyrin formation by Lindsey *et al.*[85]

The syntheses of porphyrins bearing only one functional group always results in overall low yields; in fact, in order to obtain unsymmetrical porphyrins, either the use of mixtures of reagents (Scheme 2-8a[86] and Scheme 2-9) or multi-step procedures (Scheme 2-8b)[87] are required for preparative scales.

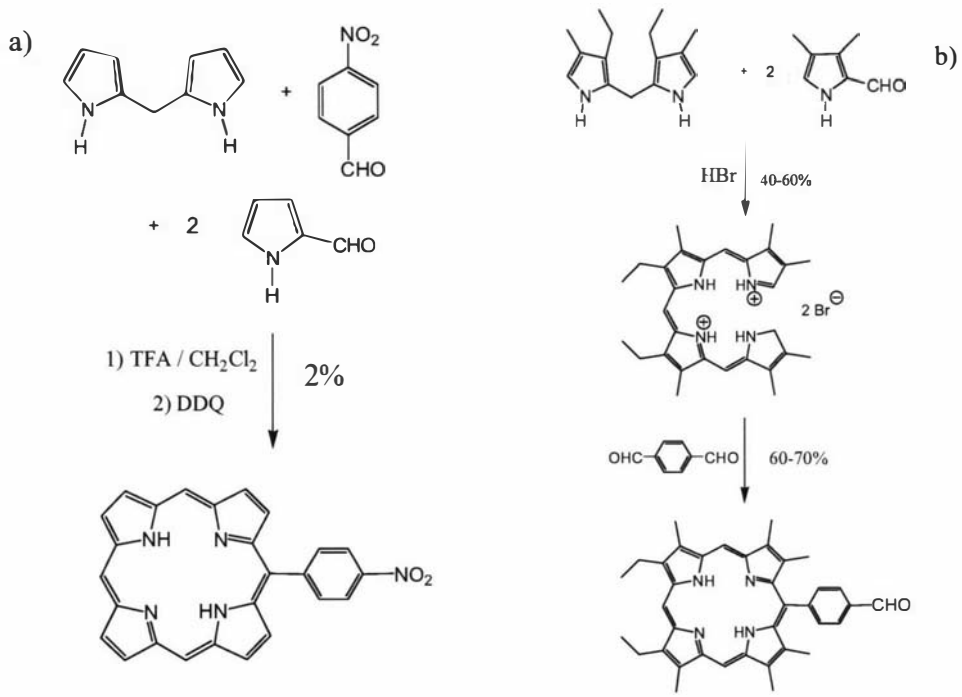

Scheme 2-8 Functionalized porphyrin formations by a) Wiehe *et al.*[86] and b) Kadish *et al.*[87]

In the first case, the reactions typically bring to the production of all the possible condensation products (Scheme 2-9), whose ratio will be determined by the relative reactivity between the different pyrroles and aldehydes and by the amount of each reagent utilized; furthermore, purification of the different isomers is typically

difficult. The multi-step reaction approach, on the other hand, allows a greater control but requires the synthesis of the desired synthons, which typically show low stability and whose purification can be challenging.

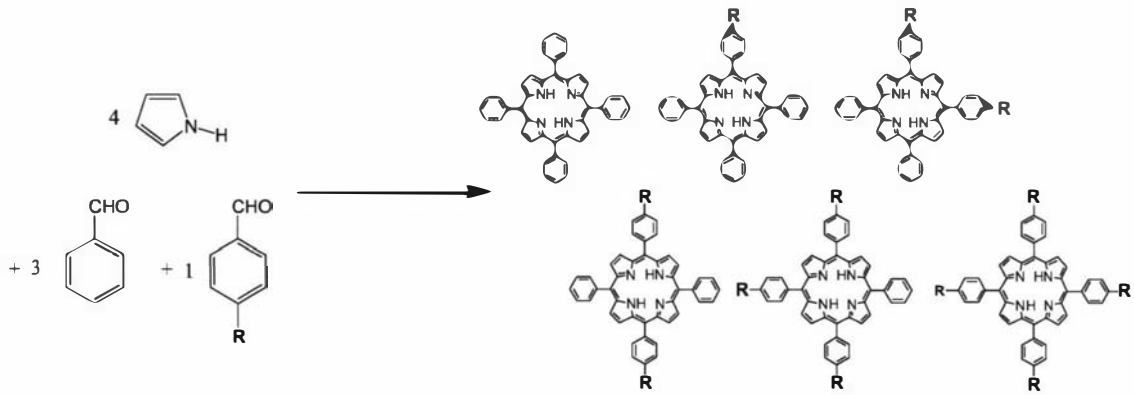

Scheme 2-9 Example of porphyrin preparation by mixed aldehyde condensation

Therefore, monofunctionalized porphyrins are most easily obtained by introducing a new group in a free and active position on the porphyrin core.[88] The best known reactions involve electrophilic substitutions either in the meso-position of β-pyrrolic substituted porphyrins or in the β-pyrrolic position of 5,10,15,20-tetraarylporphyrins (Scheme 2-10).[88,89] The Vilsmeier formylation is one of the most utilized reactions because it usually brings to the desired mono- or bis-formyl metalloporphyrin in good yield and these groups can be readily elaborated to a wide variety of other functionalities.

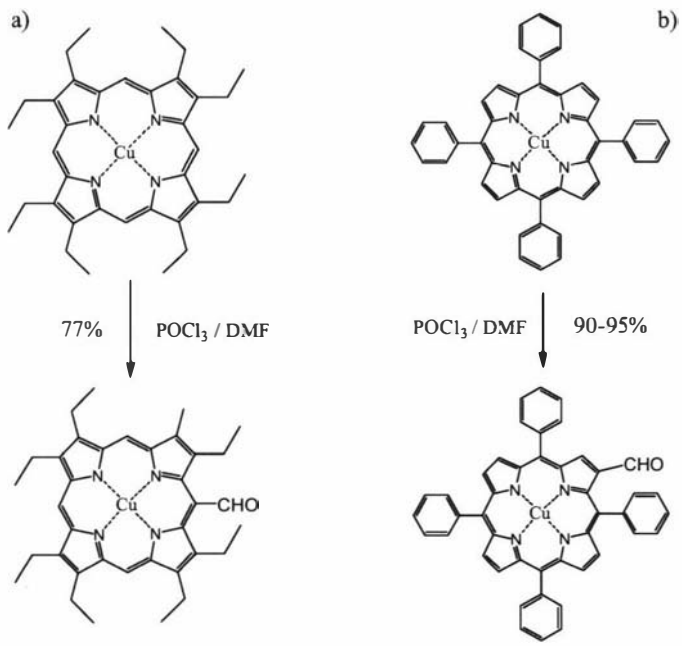

Scheme 2-10 Porphyrin Vilsmeier formylations by a) Inhoffen *et al.*[90] and b) Momenteau *et al.*[91]

2.2. Dendrimers

In order to both create large 'antenna' systems and retain control over the syntheses, a dendrimer strategy offers the simplest approach. 1,3,5-Trifunctionalized benzenes have been the most commonly exploited synthons so far; the accessibility of such compounds, together with the vast choice of functionalities available, have led to the preparation of many different large dendrimers. Two examples are described in Scheme 2-11. In the first case, the two benzene derivatives carry two carboxylic acid groups each while the third functionality is either an alcohol or a chloride; by using different basic conditions, Freeman and Frechet obtained selective esterifications (Scheme 2-11a).[92] The dendrimer in Scheme 2-11b was similarly obtained by Zeng and Zimmerman[93] by using esterification and iodide-acetylene coupling in alternate reactions.

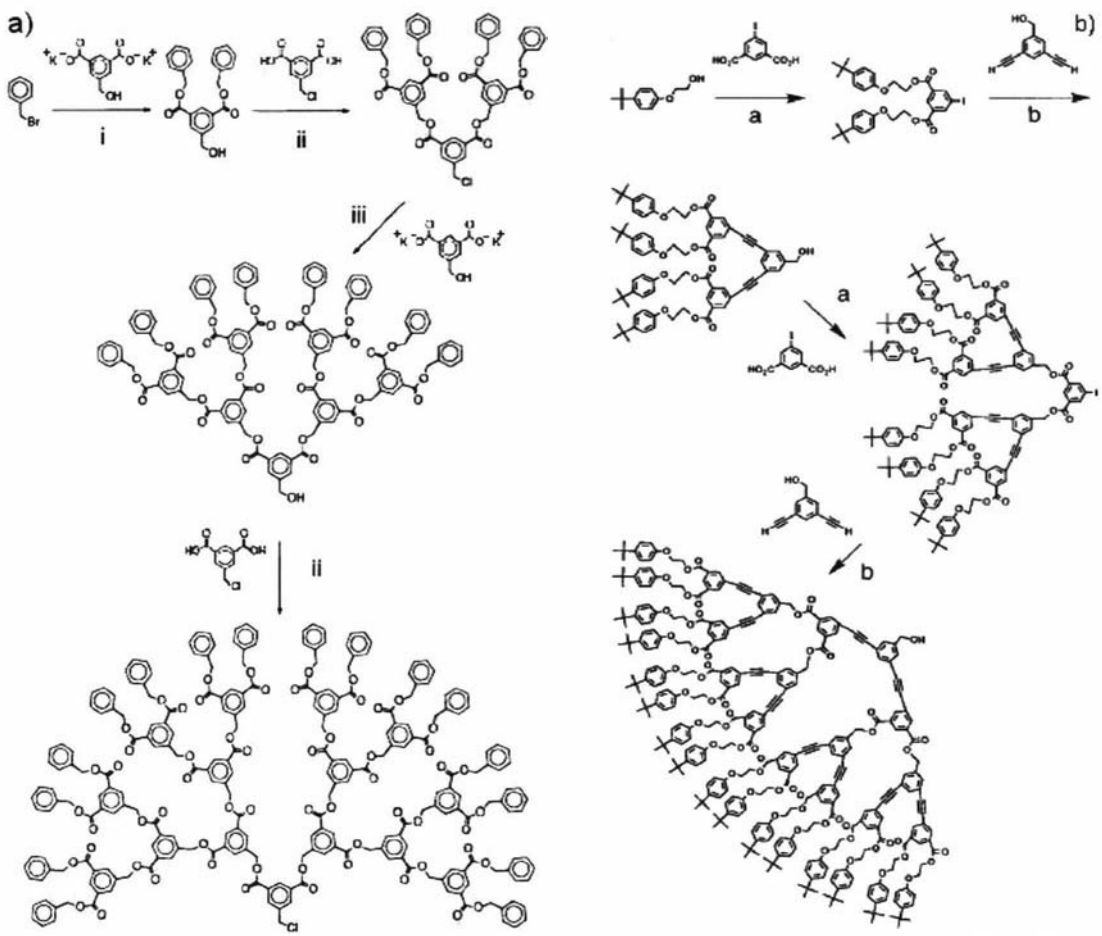

[a] (i) 18-crown-6, K_2CO_3, CH_3CN, Δ; (ii) DCC, DPTS, CH_2Cl_2, THF; (iii) KBr, DIPEA (1 drop), DMF, 80 °C.

(a) PPh_3, diethyl azodicarboxylate (DEAD), THF
(b) $Pd(PPh_3)_2Cl_2$, CuI,
or $Pd_2(dba)_3$, CuI, PPh_3, Et_3N, $PhCH_3$.

Scheme 2-11 Dendrimer preparations by a) Freeman and Fréchet[92] and b) Zeng and Zimmerman[93]

The ideal way to develop dendrimers is to use two different functional groups on the benzene moieties that can be coupled with functional groups both from the 'monomer' and from another trisubstituted benzene. By reiterating this process, each further step (or dendrimer generation) will give a molecule containing twice as many 'monomers' while still retaining a functional group for further reactions.

If a dendrimer has to work as an 'antenna', good communication within the structure is required. As already stated, long-distance energy/electron transfers are possible only when there is electronic interaction between the orbitals along the path, therefore conjugated systems are preferred.

Polyphenylene dendrimers have all these required characteristics and have been prepared using different strategies. Diez-Barra *et al.*[94] prepared trisubstituted benzenes that contained both aldehyde and phosphonate moieties (Figure 2-2), sometimes as precursors or protected versions. The preparation and purification of these benzenes, however, is not always trivial and, often, either protection/deprotection or functional group modifications were required.

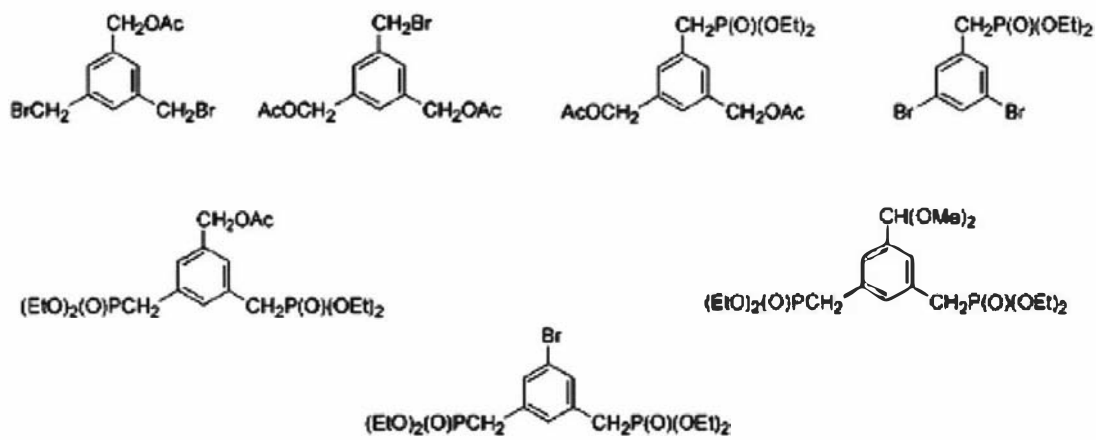

Figure 2-2 Precursor for polyphenylene dendrimers by Diez-Barra *et al.*[94]

Polyphenylene dendrimers were formed from these synthons using different routes, including the Wittig-Horner reaction. The resulting dendrimers (Figure 2-3) are characterized by full conjugation and high planarity, which make them ideal for applications where intersystem electronic communication is necessary.

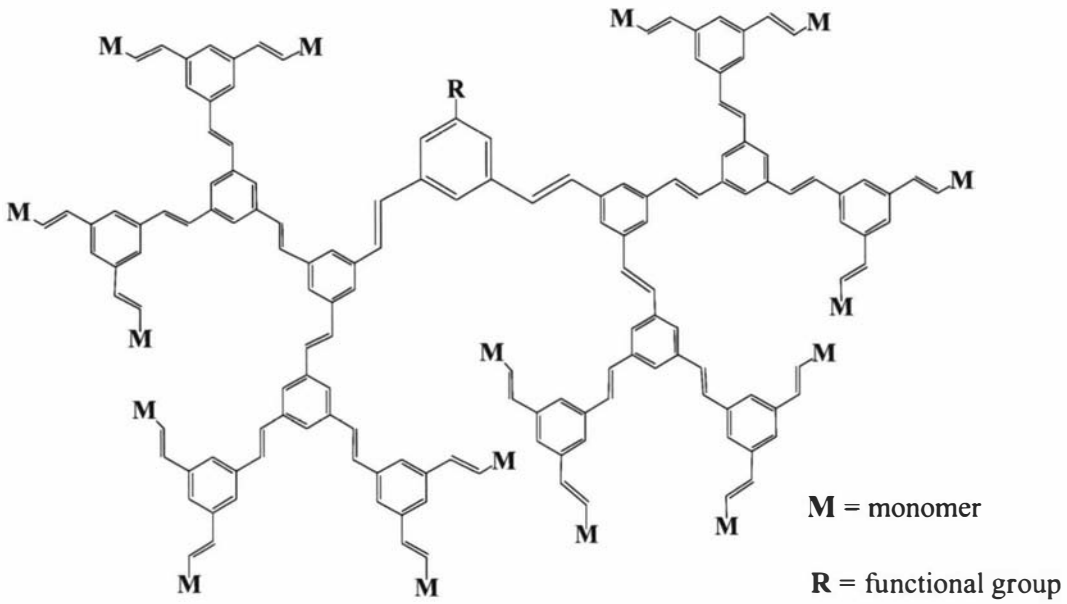

Figure 2-3 Polyphenylene dendrimer

The same structures could be obtained by using benzenes trifunctionalized with either aldehydes or phosphorous ylides but control over partial substitution (double and not triple) would be required to extend the dendrimer size (Scheme 2-12). Compared to the Diez-Barra strategy, this approach affords statistical mixtures but the difficult preparation of mixed trisubstituted benzenes is not required, nor is any protection/deprotection step. This idea has already allowed our group to create dendrimers containing up to 16 ferrocene units.[95]

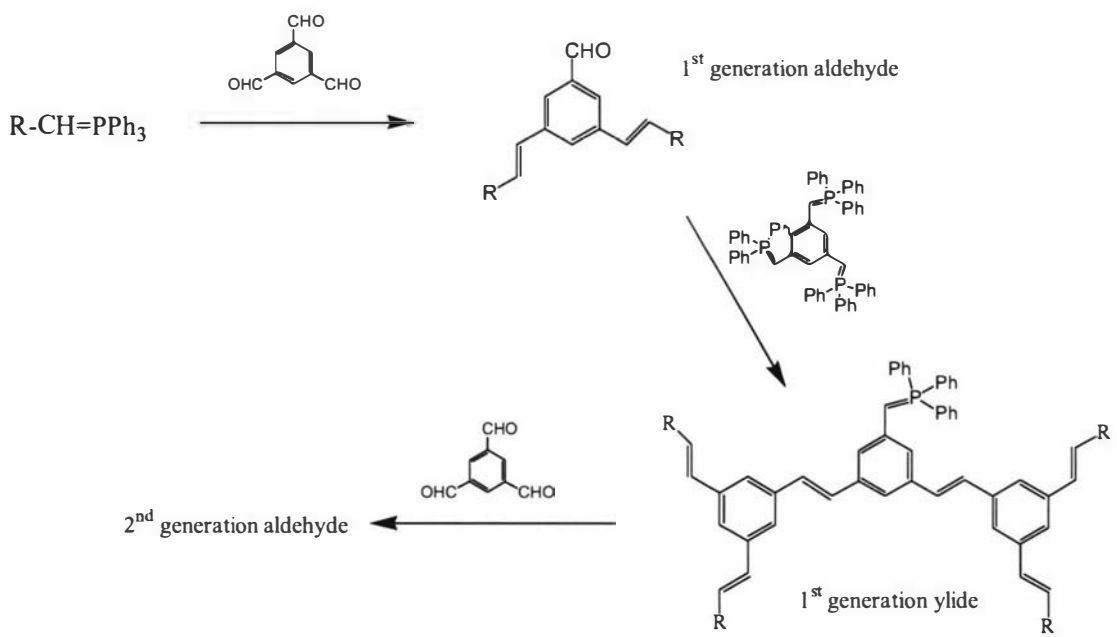

Scheme 2-12 Dendrimer formation through Wittig chemistry

Because it has been shown that a phenylene group attached in the β-pyrrolic position of a tetraarylporphyrin is coplanar to the porphyrin,[70] we choose to employ Wittig chemistry to attach phenylene derivatives (which are also planar, as long as steric hindrance does not prevent this) to the porphyrins. This approach was investigated in this chapter work for the making of rigid, planar multiporphyrin systems which allow high communication between the units of the array.

2.3. Porphyrin synthesis and functionalization

In this chapter, 5,10,15,20-tetraphenylporphyrin (TPP **3**) and 5,10,15,20-tetraxylylporphyrin (TXP **4**) were used as porphyrinic materials. Their syntheses were achieved according to the Adler method; equivalent amounts of pyrrole and the appropriate aromatic aldehyde were refluxed in propionic acid and the resulting porphyrin was precipitated in 15-20% yield by adding water (Scheme 2-13).

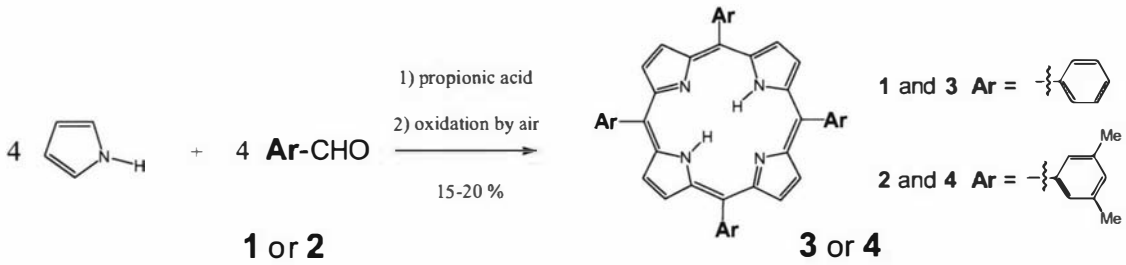

Scheme 2-13 Tetraarylporphyrins (TPP **3** and TXP **4**) synthesis by Adler *et al.*[96]

TPP and TXP were functionalized, according to methods developed in our laboratory,[75] by introducing an aldehyde group at the β-pyrrolic position by Vilsmeier formylation. Three further easy and high-yielding steps permitted the synthesis of the porphyrin phosphonium salts TPP-ps **11** and TXP-ps **12** (Scheme 2-14).

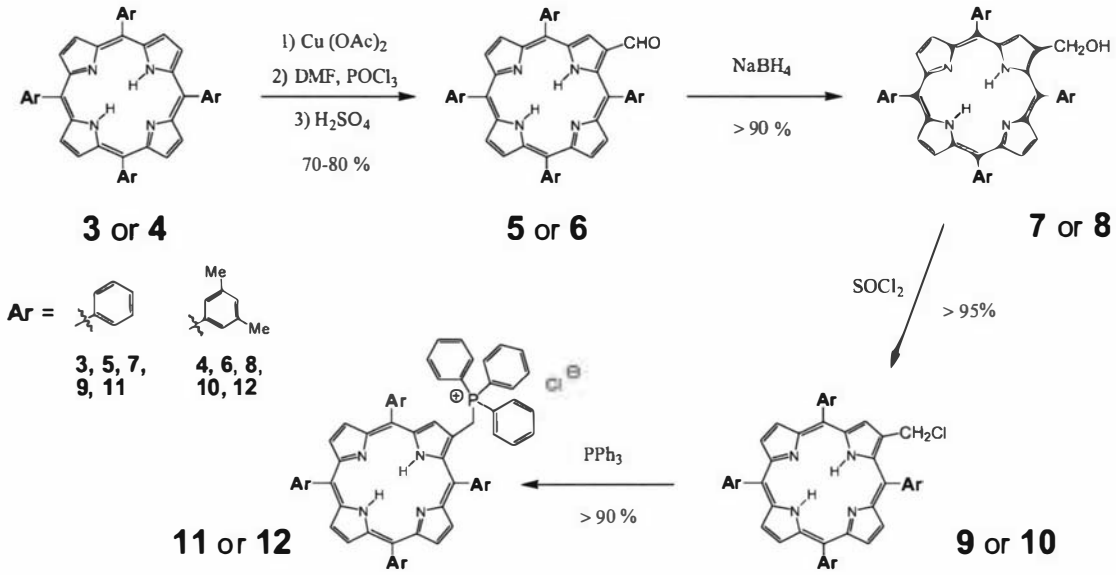

Scheme 2-14 Phosphonium salt TPP-ps **11** and TXP-ps **12** syntheses by Burrell and Officer[75]

Formylations were performed by adding the Vilsmeier complex ($POCl_3$/DMF) to a 1,2-dichloroethane solution of the porphyrin which was previously metallated with copper (using the acetate method).[97] The free-base 2-formyltetraarylporphyrins (**5** and **6**) were obtained by demetallation with sulphuric acid prior to the hydrolysis of the Vilsmeier complex. Large scale reactions (e.g. 8 g of porphyrin, 1 L of solvent) require intense mechanical stirring for the demetallation to occur in reasonable yields. Typically, the three steps of the formylation give 70-80% yield.

Aldehydes **5** and **6** were reduced to alcohols with $NaBH_4$ in THF in almost quantitative yield. Similarly, treatment of the alcohols with $SOCl_2$ in dichloromethane gave the chloromethyl derivatives **9** and **10** in high yield. Finally, the reaction of these chlorides with PPh_3 produced the porphyrin phosphonium salts **11** and **12** again with yields higher than 90%.

TPP was the first choice as dendrimer precursor because it was more cheaply and more easily prepared (depending on the use of commercial or synthesized xylylaldehyde **2** precursor) than TXP. The main difference between the two porphyrins is that the methyl groups in TXP derivatives increase the porphyrin solubility in common organic solvents as a result of decreased porphyrin aggregation. The syntheses of porphyrin aldehydes **5** and **6** and phosphonium salts **11** and **12** were

repeated many times during the course of this thesis and these molecules were used as the 'basic blocks' from which most of the arrays described in the next chapters were built from.

2.4. Wittig chemistry

The porphyrin phosphonium salts and aldehydes are the building blocks from which arrays can be built through Wittig reactions. These reactions involve coupling of a phosphorous ylide and an aldehyde to form a double bond between two carbon atoms. Phosphorous ylides, when not stable, can be created in situ from precursors, usually quaternary phosphonium salts, by treating them with strong base (Scheme 2-15).

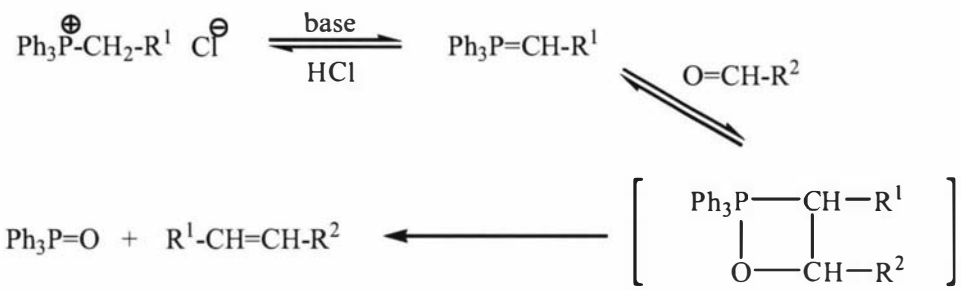

Scheme 2-15 Mechanism of the Wittig reaction

The ability of porphyrin phosphonium salts to undergo Wittig reaction is known from previous works; for example, TPP and TXP phosphonium salts (TPP-ps **11** and TXP-ps **12**) react in good yields with terephthalaldehyde **13** to give the useful porphyrin aldehydes **14** and **15** (Scheme 2-16).

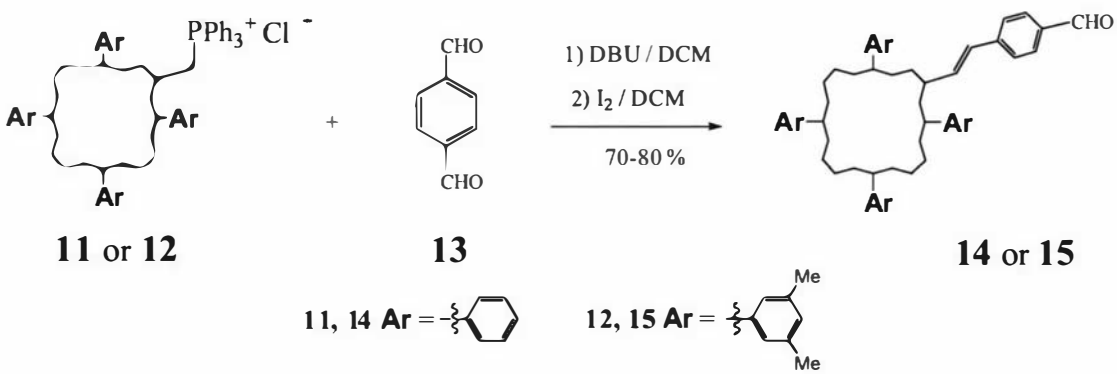

Scheme 2-16 Preparation of porphyrin aldehydes **14** and **15** by Burrell and Officer[75]

These reactions have been performed in dichloromethane using DBU as base and proceed with yields around 80% (the double Wittig reaction occurs to a minor extent giving the dimer as by-product). The products are a mixture of *trans/cis* isomers typically in a 6/4 ratio; pure *trans* configurations are obtained in a following step by I_2 treatment in chloroform. TXP-ps **12** has also been reacted with benzene tricarboxaldehyde **17** (Scheme 2-17), using the same conditions described for the syntheses of **14** and **15**. In this case, mono- bis- and tris-substituted products are obtained and the yield of the desired dimer is maximized (~70%) by using 2.2 equivalents of porphyrin phosphonium salt. Pure *trans* configurations are again obtained by I_2 isomerization.

As already stated about phosphonium salts **11** and **12**, the preparation of aldehydes **14**, **15** and **18** were repeated many times with little modification from the described procedures.

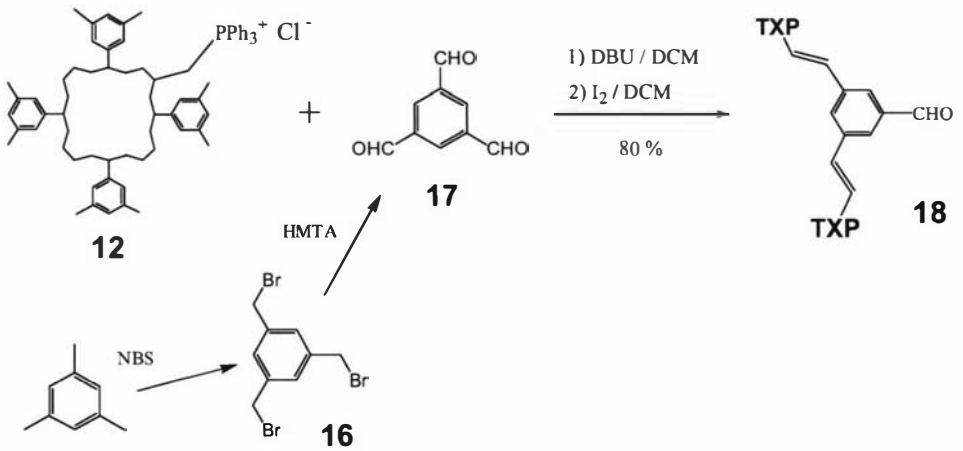

Scheme 2-17 Syntheses of trialdehyde **17** and porphyrin dimer **18** by Burrell and Officer[75]

The second synthon required for this dendrimer approach, benzene trisphosphonium salt **19**, was prepared in two easy steps from mesitylene as described by Stork and Maneke (Scheme 2-18).[98]

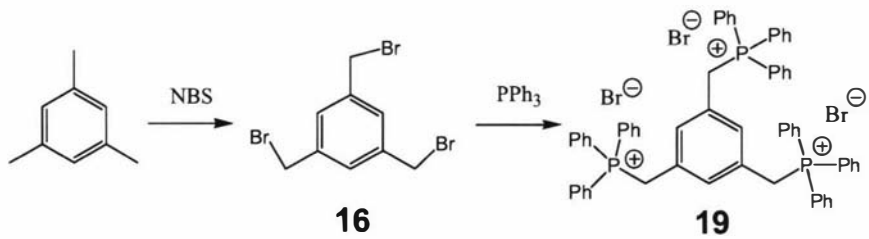

Scheme 2-18 Synthesis of mesitylenetris-(triphenylphosphonium bromide) **19** by Storck and Manecke[98]

In spite of previous reports on the successful Wittig condensation between triphosphonium salt **19** and porphyrin aldehydes,[99] all attempts to reproduce this chemistry were unsuccessful. In all cases, most of the porphyrin material was recovered while dark, highly polar, high molecular weight and phosphorous-rich material was quickly (few minutes) obtained, but not purified and fully characterized (Scheme 2-19). Changing the solvent (DCM, chloroform, THF, chloroform/water), base (DBU, BuLi, BuOK, NaOH), porphyrin metallation (free base, Zn, Ni) and reaction conditions (temperature, addition procedures) did not produce any of the expected products.

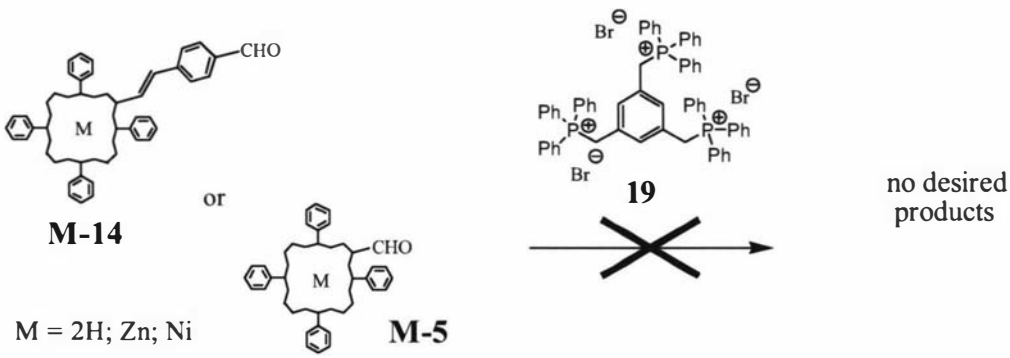

Scheme 2-19 Wittig chemistry attempts involving mesitylenetris-(triphenylphosphonium bromide) **19**

In order to simplify this kind chemistry, reactions involving bis-phosphonium salt **20** (previously prepared in our laboratories) were investigated (Scheme 2-20). Again, disappointing results were obtained with no production of the desired molecules.

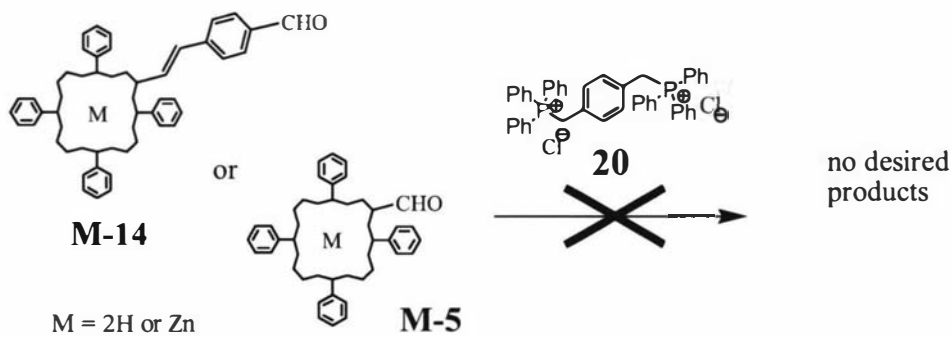

Scheme 2-20 Wittig chemistry attempts involving of xylenebis-(triphenylphosphonium chloride) **20**

Analyses of the tars typically obtained by reactions shown in Scheme 2-19 and 2-20, as well as the products obtained by treating **19** with DBU or other bases, revealed the formation of oligomers due to reaction between phosphonium salt groups; MALDI

spectrometry showed molecular weights corresponding to 8-10 benzene-phosphonium salt units and ^{31}P-NMR confirmed the presence of a large number of non-equivalent phosphorous signals. Portions of the product mixtures were soluble in highly polar solvents (water, MeOH), suggesting the presence of many ionic moieties.

To overcome those problems, our attention turned from phosphonium salts to phosphonates. The literature shows that phosphonates can undergo the same Wittig chemistry; although no ylide can be isolated, a carbanion can be formed and its nucleophilicity is higher than the corresponding phosphonium salt derivative.[100-101] Wittig reactions involving phosphonates are named after Horner, Wadsworth and Emmons. The most important difference between these Wittig reactions is the need for stronger bases (sodium hydride, amides, alkoxides) than those required for the equivalent phosphonium salts (sodium hydroxide, DBU). Phosphonate preparations are usually carried out by reacting a bromide or chloride in excess of tris-alkylphosphite, which also acts as solvent (Scheme 2-21). Yields are typically high (> 95%).

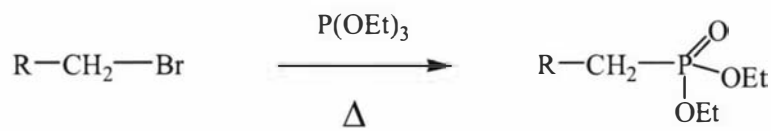

Scheme 2-21 Phosphonates syntheses by Michaelis and Haehne[102,107]

Following this procedure, 1,3,5-mesitylenetris(diethylphosphonate) **21** was prepared in almost quantitative yield by reaction of tribromobenzene **16** (previously prepared in our laboratories by NBS bromination of mesitylene) with commercial triethylphosphite (Scheme 2-22).

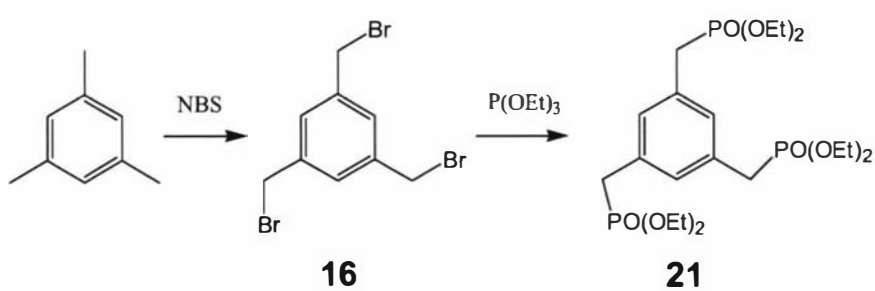

Scheme 2-22 1,3,5-mesitylenetris-(diethylphosphonate) **21** preparation

The suitability of this triphosphonate was demonstrated by a Wittig reaction with porphyrin aldehyde **Zn-5** (Scheme 2-23). The reaction was performed in dry THF, using ^{t}BuOK as base and two equivalents of porphyrin. The evolution of this reaction was monitored by TLC which showed no variation after 30 min. Products were separated by flash column chromatography (silica gel, gradient DCM/MeOH) and analyzed by MALDI mass spectrometry and ^{1}H-NMR spectrometry. Five main fractions were separated and characterized as the trisubsituted, disubstituted and monosubstituted (two bands, see Chapter 3) products. A good amount of unreacted aldehyde was also recovered. The MALDI spectra gave the right mass for each of the separated fractions and ^{1}H-NMR spectra clearly distinguished between the components (e.g. from the ratio between the integration of porphyrin and phosphonate signals).

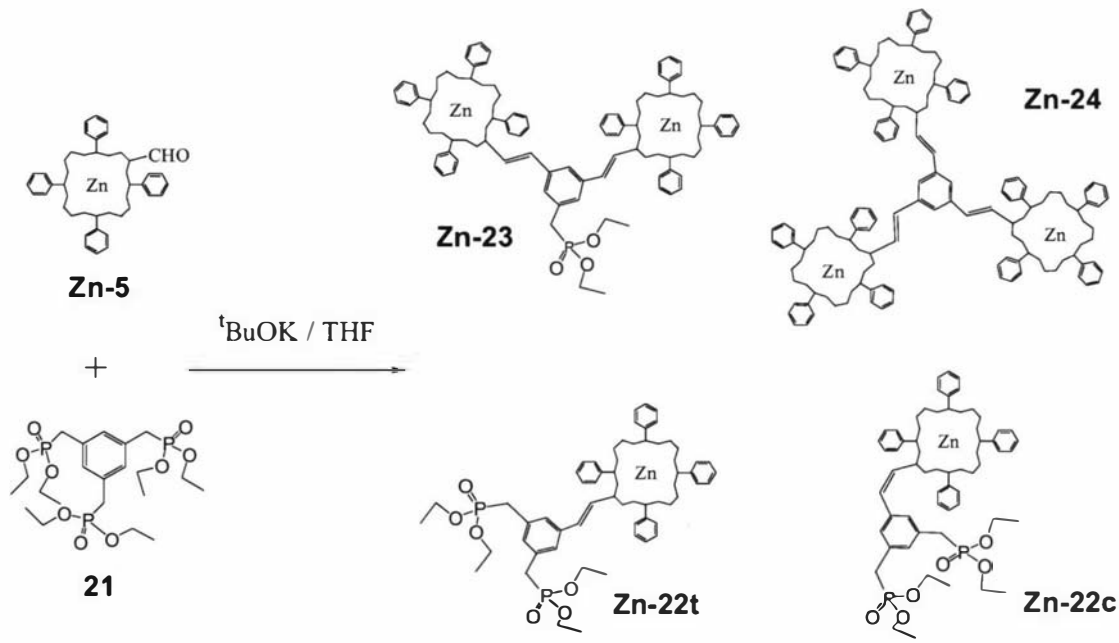

Scheme 2-23 Triphosphonate **21** Wittig reaction with **Zn-5**

Even though this reaction produced a complex mixture of products, the reactivity of phosphonate **21** represented a great improvement with respect to the use of polyphosphonium salts. As a consequence, phosphonate and Wittig-Horner-Emmons-Wadsworth reactions were used in the rest of this work for the making of most of the arrays presented.

2.5. Dendrimer syntheses

It has been shown that TXP-ps **12** reacts with benzenetricarboxaldehyde **17,** according to Scheme 2-17. The homologue dimer containing TPP as porphyrin was newly synthesized using the same procedure described for **18** (Scheme 2-24). In this case, product **25** is poorly soluble in many solvents but the reaction occurs in similar time and yield as for **18**. The purification of large amounts of **25** proved to be difficult because of its low solubility and was successfully performed by a series of recrystallizations from different solvents (DCM/hexane and DCM/MeOH).

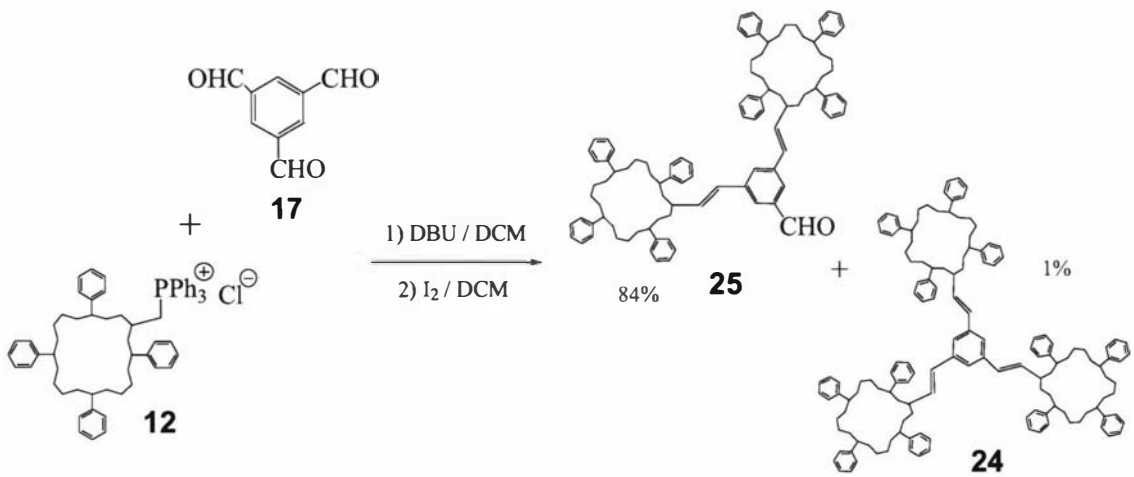

Scheme 2-24 Synthesis TPP dimer aldehyde **25**

Trimer **24** was obtained as co-product in yield lower than 1% and isolated (from hydrolysis side-products) through column chromatography from the solution discarded in the previously described recrystallizations. MALDI spectra confirmed the molecular weight of both **25** and **24** and ^{1}H-NMR spectra were consistent with the structures and similar to the data observed for **Zn-24** and reported for the TXP homologue **18**.[20] By modification of the reagent stoichiometric ratio (e.g. use of excess phosphonium salt **11**), this procedure could represent a viable way for the making of homometallic trimers, as well as the reaction shown in Scheme 2-23.

The formation of dimer aldehydes **18** and **25** is the first step of the dendrimer syntheses. The next step involves the reaction of porphyrin aldehydes with benzene phosphonates. Early attempts showed that free-base porphyrins were not ideal

reagents because their *N*-pyrrolic protons are more acidic than the methylphosphonate protons, requiring the use of excess base to form the desired carbanions. Unfortunately, these conditions produce side reactions, such as polymerization of the phosphonates. Experiments in which a solution of phosphonate **21** was treated with excess base (5 eq of ^{t}BuOK or NaH) showed a rapid formation of a brown oil which, from MALDI and NMR spectrometry, appeared similar to the tar obtained by using the triphosphonium salt **19** (high molecular weight, phosphorous rich material, high polarity). The solution to this problem was to metallate the porphyrins to remove pyrrolic acidic protons; in this way the formation of carbanions could be carried out using lower amounts of base (around 1.2 equivalents). For this work, the metals of choice were Zn and Ni. Zn is the ideal metal for two reasons: its low oxidation potential coupled with the long lifetime of its excited states produce the best performance in photovoltaic devices[103] and it can be easily inserted and removed in mild conditions (Scheme 2-25), allowing the introduction of a variety of other metals.

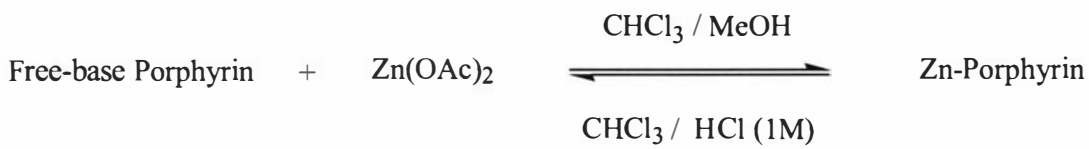

Scheme 2-25 Porphyrins Zn-metallation reversible reaction

The use of Ni is a useful alternative because, contrary to the Zn case, Ni porphyrins do not coordinate other ligands, making it easier to identify and purify the products. Reactions of triphosphonate **21** with porphyrin aldehydes **M-5** and **M-14** (M = Zn and Ni) produced the new arrays **M-23** and **M-27** containing two porphyrins and a phosphonate functional group (Scheme 2-26); these arrays can be considered as two versions of the first generation phosphonates of a dendrimer strategy. Characterization of the products was achieved by ^{1}H-NMR spectra that showed the typical dendrimer signals as in the previous arrays plus the characteristics phosphonate peaks (see Section 2.7). MALDI spectra confirmed the molecular weight of all the described products.

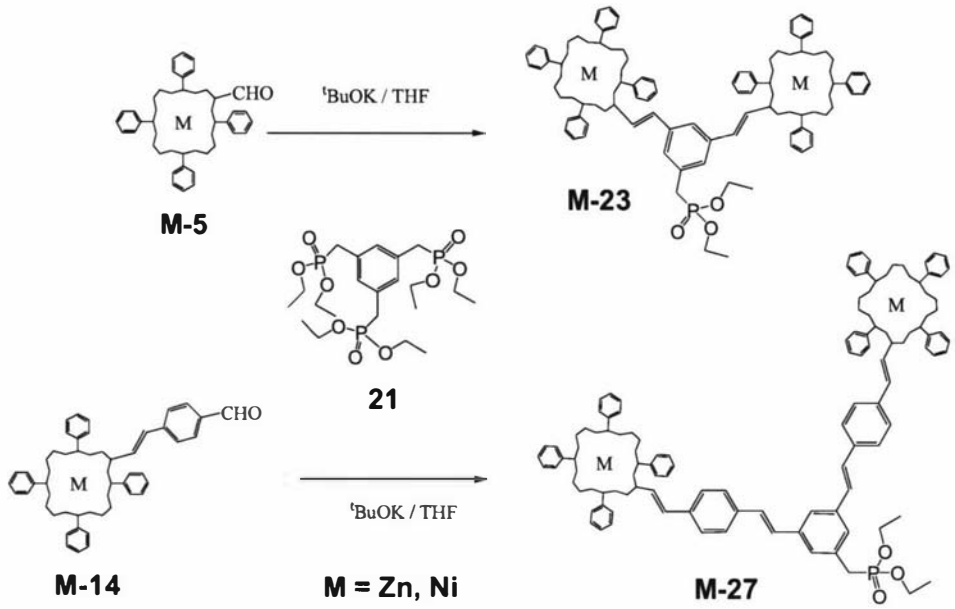

Scheme 2-26 Porphyrin dimer syntheses involving trisphosphonate **21**

The results of these reactions were always a mixture containing reagents, mono-, bis- and tris-substituted products and side-products that were isolated by careful column chromatography. Moreover, there usually is a *trans*/*cis* isomer ratio higher than 9/1; pure *trans* isomers can be obtained by treating the isomer mixture with iodine in chloroform (T = 20-60 °C) but were usually removed in the purification process (chromatography, recrystallizations). Interestingly, contrary to what was found in the reactions involving phosphonium salts (Scheme 2-17 and 2-24), measurable amounts of *cis* isomers have been found exclusively in monosubstituted products, suggesting a decreased reactivity of **Zn-22c** due to the *cis* configuration (Scheme 2-27).

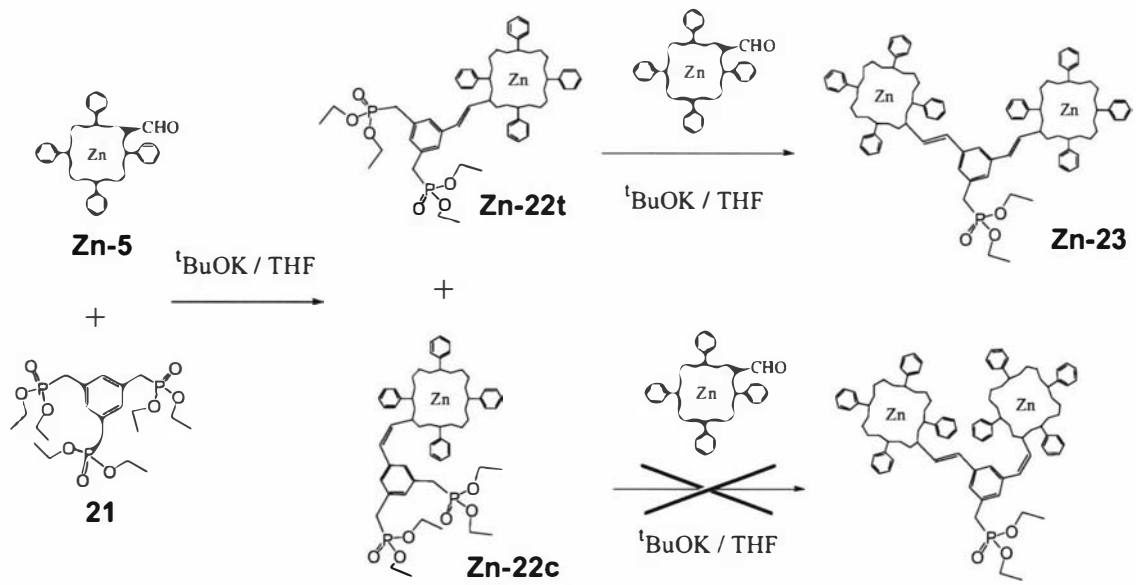

Scheme 2-27 Comparison between **Zn-22c** and **Zn-22t** reactivity

Yields in the desired disubstitution are listed in Table 2.1 and were maximized by using 2.2–2.5 equivalents of porphyrin aldehyde and ^{t}BuOK. Reactions were carried out under argon, using dry THF as solvent and at room temperature. Many variations were attempted to reduce the formation of undesired by-products; higher and lower temperatures (T = -80-60 °C), various ratios of reagents, different addition orders and different bases (NaH, ^{n}BuLi) were all examined but little or no improvements were achieved. The best results were obtained by dissolving phosphonate and porphyrin together (as is typical for Horner-Emmons reaction) and adding the base in 2-4 portions (to avoid too high base concentrations). Best reaction times were 30-60 minutes.

Aldehyde reagent	Phosphonate product	Yield
Zn-5	**Zn-23**	29%
Ni-5	**Ni-23**	33%
Zn-14	**Zn-27**	46%
Ni-14	**Ni-27**	54%

Table 2-1 Syntheses of porphyrin phosphonates **M-23** and **M-27**

Comparing the yields reported in Table 2-1, it can be observed that aldehydes **M-14** gave better results than **M-5;** in fact, the aldehyde group directly attached to the porphyrin was less reactive. Under the conditions just described, around half of the porphyrin reagent was recovered while increasing reaction time or base concentration resulted in higher amount of side-products. Moreover, Ni porphyrins gave higher yields than Zn ones. The main reason was that in the Zn case there was formation of side-products, which were more difficult to separate by chromatography, probably because of Zn-phosphonate coordination (see Chapter 3 for more details); Zn-phosphonate coordination could also be responsible for the variation in yield between the Zn and Ni porphyrins. However, regardless of the metal, the yields were not totally satisfactory. In spite of substantial effort in varying the conditions, side-reactions, possibly deriving from reactions between phosphonate groups, always occurred.

A way to improve these syntheses involved isopropyl phosphonates. It has been seen that triphosphonate **21** gave better results than triphosphonium salt **19**, probably

because of its improved stability in basic conditions. Phosphonate carbanions are not particularly stable and it has been shown that isopropyl groups (in place of ethyl ones) improve carbanion selectivity.[104] For this reason, isopropyl groups have been utilized for the preparation of otherwise unstable phosphonates.[150,151] Isopropyl phosphonates can be synthesized with the same procedure used for the ethyl homologues (Scheme 2-22). Thus, phosphonate **28** was prepared and compared to **21** in the reactions with **Zn-14** and **Ni-14** (Scheme 2-28).

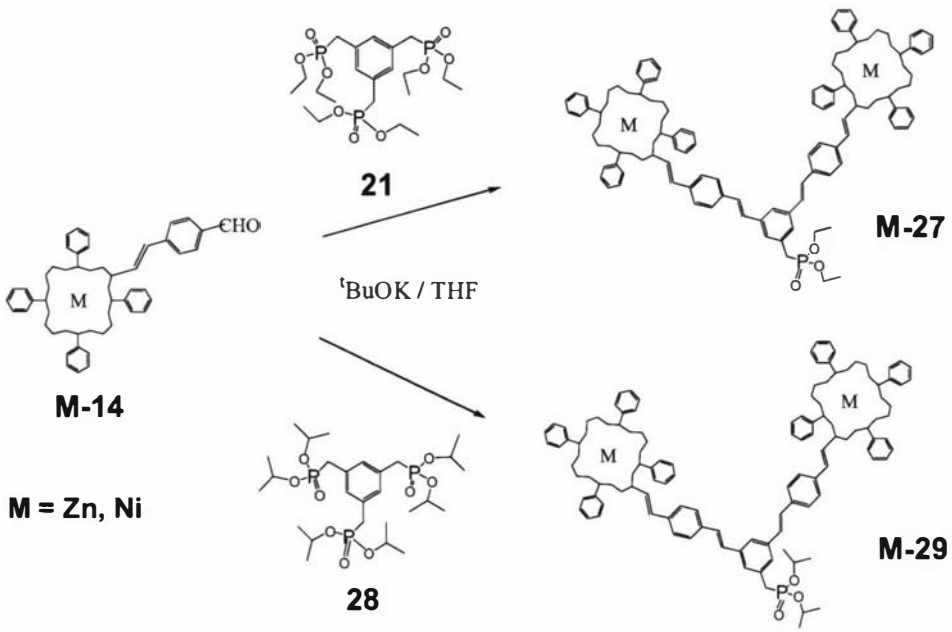

Scheme 2-28 Porphyrin dimer syntheses involving triphosphonates **21** and **28**

Reactions involving isopropylphosphonate **28** were performed in the same way as just described for ethylphosphonate **21.** The only difference was the use of slightly higher base concentrations and longer reaction times which were allowed by its higher stability. Also, isopropyl phosphonates do not produce any *cis* isomers, eliminating the need for an isomerization step, which usually gives some loss of product. As a result, we obtained higher yields, as shown in Table 2-2.

Trisphosphonate	Porhyrin reagent	Product	Yield
Ethyl **21**	**Zn-14**	**Zn-27**	46%
Isopropyl **28**	**Zn-14**	**Zn-29**	52%
Ethyl **21**	**Ni-14**	**Ni-27**	54%
Isopropyl **28**	**Ni-14**	**Ni-29**	68%

Table 2-2 Syntheses of phosphonates **M-27** and **M-29**

All the porphyrin dimers so far described show quite low solubility in most solvents, making it difficult to obtain pure compounds on a preparative scale (e.g. by flash column chromatography). TXP derivatives are always more soluble than TPP ones therefore the reactions of phosphonate **28** with aldehydes **Zn-14** and **Zn-15** were compared (Scheme 2-29).

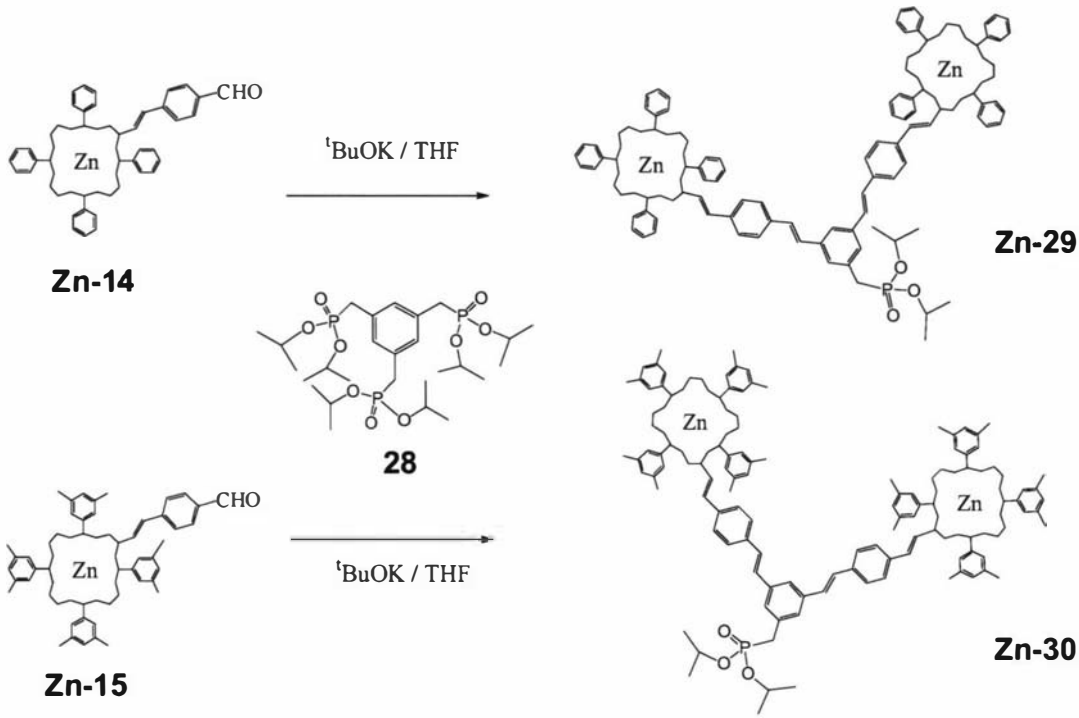

Scheme 2-29 Porphyrin dimer syntheses involving triisopropylphosphonate **28**

Phosphonate **Zn-30**, as predicted, showed improved solubility but as shown in Table 2-3, this did not result in a significant yield increase. Therefore, the use of TXP derivatives instead of TPP were not pursued as a general strategy, being that the disadvantages (longer preparation of starting materials) exceeded the advantages. However, their better solubility properties made the employment of TXP derivatives useful in some cases.

Aldehyde reagent	Phosphonate product	Yield
Zn-14	**Zn-29**	52%
Zn-15	**Zn-30**	54%

Table 2-3 Syntheses of phosphonates **Zn-29** and **Zn-30**

The reaction of porphyrin dimer aldehydes **M-25** with a triphosphonate led to the next generation of arrays, containing four porphyrins and a Wittig functional group (Scheme 2-30). The reaction was performed in similar fashion to all the previous ones which involve phosphonates and both Zn and Ni derivatives were examined. Contrary to all previous Wittig reactions, no trisubstitution was observed; it is probable that steric hindrance prevents the porphyrin dimer aldehyde **M-25** from reacting with the last phosphonate group in **M-31**.

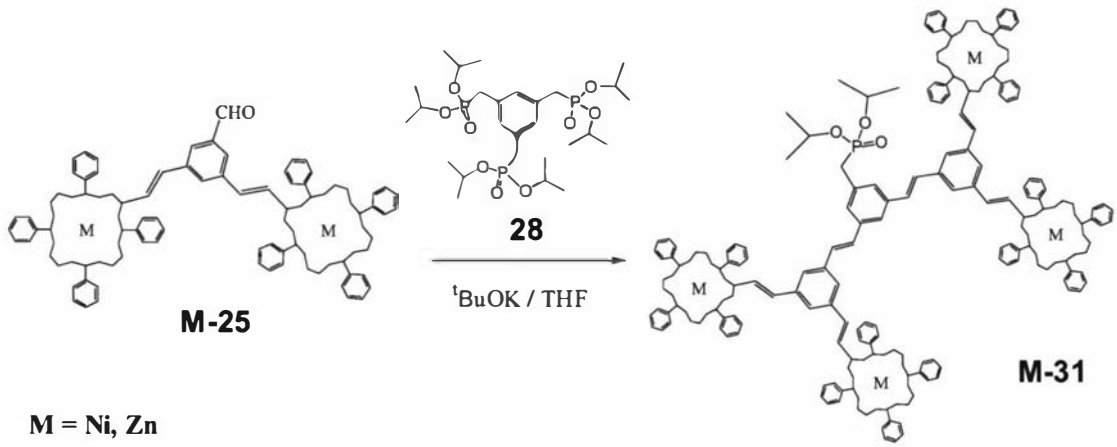

Scheme 2-30 Porphyrin tetramer **M-31** syntheses

Once again, we tried both Zn and Ni derivatives but in this case a poorer yield was obtained with the Ni porphyrin, probably due to the large scale preparation performed in the Ni case, which can be responsible for some lost of products during the purification steps.

Aldehyde reagent	Phosphonate product	Yield
Zn-25	**Zn-31**	52%
Ni-25	**Ni-31**	43%

Table 2-4 Syntheses of phosphonates **Zn-31** and **Ni-31**

The next step in the dendrimer strategy was the reaction between porphyrin phosphonate and benzenetricarboxaldehyde **14.** Unfortunately, early attempts involving Zn porphyrin phosphonates **Zn-29** and **Zn-31** were not successful (Scheme 2-31). In both cases, the appearance of new species was registered (TLC) only at high base concentrations or long reaction times; MALDI spectrometry on the chromatography separated fractions showed the presence of some high molecular

weight species, which were due to hydrolysis products of the Zn porphyrin phosphonates. Moreover, an array containing more than four porphyrins proved to be difficult to fully characterize (see Section 2.7), therefore the idea of extending the dendrimer syntheses to 8 or more porphyrins was not pursued at this stage, in favour of utilizing the prepared dendrimer components for the formation of mixed porphyrin arrays.

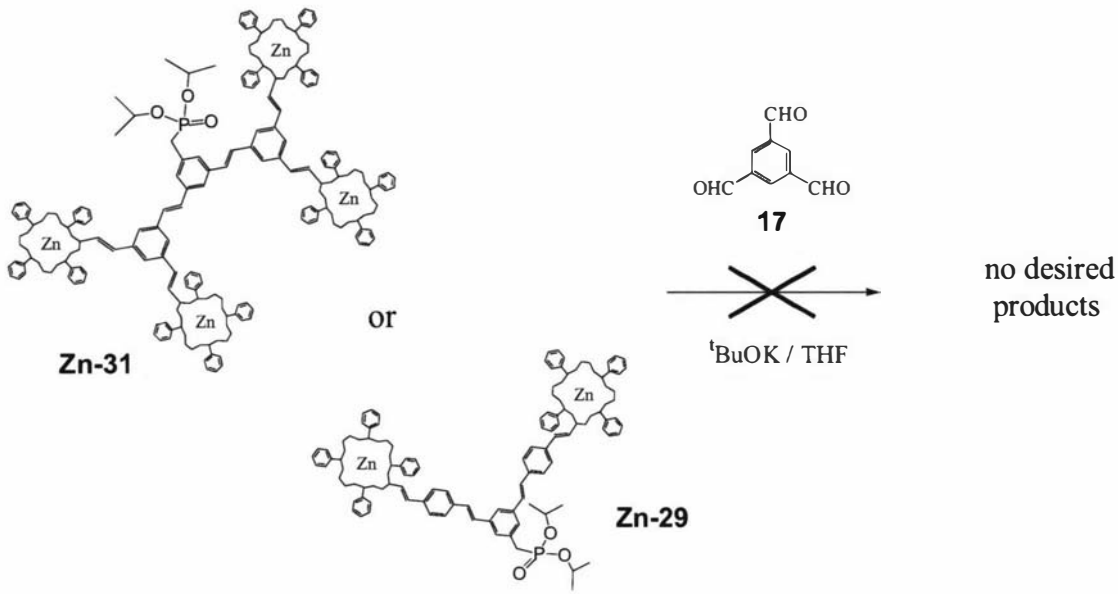

Scheme 2-31 Attempts to make 2nd generation aldehyde dendrimers

2.6. Mixed array preparations

Even though this dendrimer strategy did not seem ideal for creating very large arrays, it is very interesting because it presented the opportunity to create complex systems in which different porphyrins, coordinating different metals, could be arranged in the same molecule and connected by fully conjugated systems. In the previous section, syntheses involving two porphyrins derivatives (TPP and TXP) coordinating zinc or nickel were developed; by coupling those dendrimers it was possible to make arrays containing ZnTXP and NiTPP units with different porphyrin numbers and geometrical distribution.

Thus, the mixed porphyrin trimer **Ni_2Zn-32** was obtained by Wittig reaction between diporphyrin phosphonate **Ni-27** and porphyrin aldehyde **Zn-15** in very good yield as shown in Scheme 2-32. The reaction was performed using the same conditions previously described for the dendrimer syntheses which involve phosphonates. It can be noticed that this reaction occurred with a better yield, compared to previous reactions described in this chapter; the reason is that in this case there is only a single unhindered phosphonate group involved in the reaction. Purification and characterization of the product was straightforward; both MALDI and HRMS-FAB spectrometry provided the parent ion mass and ^{1}H-NMR clearly distinguished both ZnTXP and NiTPP resonances in the correct ratio.

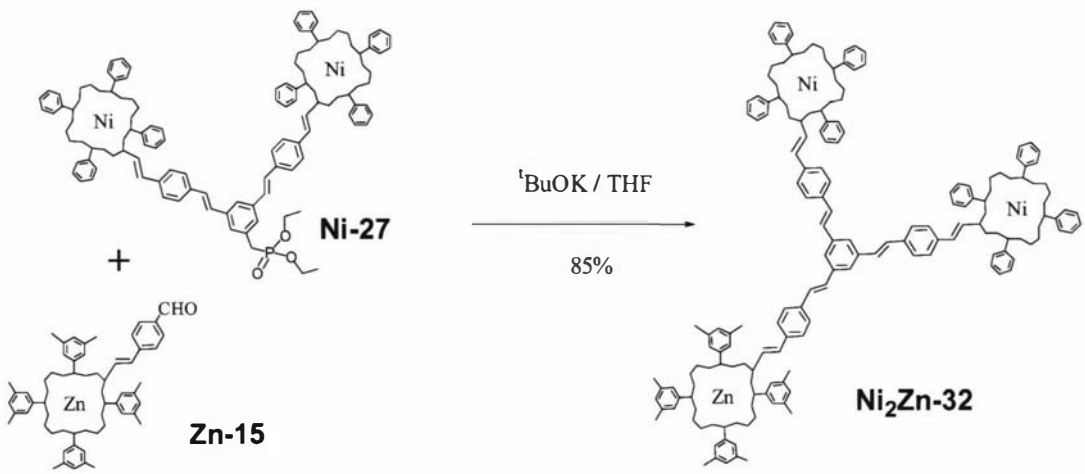

Scheme 2-32 Mixed trimer **Ni_2Zn-32** preparation

Similarly, by using the porphyrin dimer aldehyde **Zn-18** instead of **Zn-15,** the tetramer **Ni_2Zn_2-33** (Scheme 2-33) was obtained. The yield was again very good. As for the previous reaction, purification and characterization of the desired product did not present any particular problem, although full assignment of the proton resonance peaks were challenging because of superimposition of the signals due to the phenylene-vinylene linkers (see next section). Also, high resolution mass spectra were not obtained, because of unavailability of techniques able to successfully ionize porphyrin arrays with molecular weight higher than 2000.

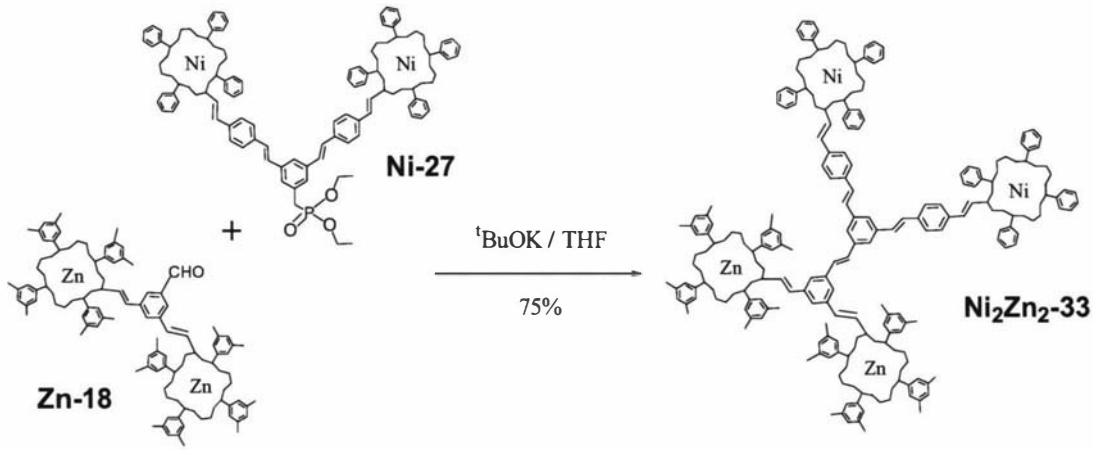

Scheme 2-33 Mixed tetramer **Ni_2Zn_2-33** preparation

Finally, pentamer **Ni_4Zn-34**, containing four NiTPP and one ZnTXP was made from **Ni-31** and **Zn-15** (Scheme 2-34). In this last case, a lower yield was obtained but a significant amount of starting material was recovered. It is likely that the yield could be improved by using higher base concentration and/or longer reaction time. The pentamer **Ni_4Zn-34** was characterized by ^{1}H-NMR and FAB spectrometry; as for the previous array, high-resolution mass measurements were not possible.

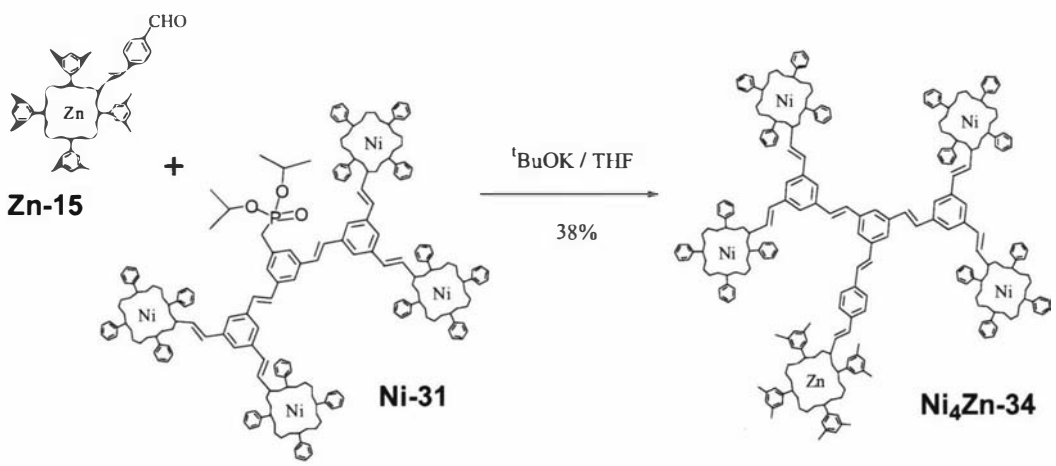

Scheme 2-34 Mixed pentamer **Ni_4Zn-34** preparation

These mixed array preparations showed that Horner-Emmons-Wadsworth reactions are a viable way to produce complex conjugated arrays containing different porphyrins; this method also allows a high control on the metallated state of the porphyrins and their geometrical distribution in the array, features which are of high value for possible applications of these molecules in various kinds of devices, particularly where long distance electronic interaction is required.

2.7. Array characterizations

The course of all reactions described in this chapter was monitored mainly by TLC and often, by MALDI-TOF spectrometry. UV-visible spectroscopy was only utilized in the cases in which major variation of the absorption were expected, such as in porphyrin formations or metallations/demetallations. First characterization (identification) of compounds was generally achieved by MALDI low resolution mass spectroscopy and one dimensional ^{1}H-NMR spectroscopy. Full characterization was obtained by NMR spectrometry, high resolution mass spectra (FAB) and UV-visible spectroscopy.

NMR spectrometry: the ^{1}H-NMR spectrometry of porphyrin arrays is a very useful tool for characterization but, while it is usually easy to identify the products from selected proton signals, the large number of non-equivalent protons makes a full correlation between signals and protons challenging. As an example of our porphyrin spectra, Figure 2-4 shows the ^{1}H-NMR spectrum of **25,** the simplest of the arrays introduced in this chapter. The lowest field resonance (10.15 ppm) is due to the aldehyde proton and generally is found as a sharp singlet. In rare cases (**Zn-41**), however, the aldehyde proton can be shielded by the anisotropic effect of some neighboring group and its resonance is superimposed on the porphyrin signals. Signals in the 7.5-9.5 ppm region are typical of TPP (see below), while resonances at slightly higher fields (6.5-8.0 ppm) are due to the conjugated phenylene-vinylene bridges. Finally, *N*-pyrrolic protons can be found at negative fields (-2 to -3 ppm), usually as broad singlet. The high field chemical shift of these *N*-pyrrolic, as well as the low field positions of most of the protons at the periphery of the porphyrin ring, are a consequence of the strong ring current that is characteristic of porphyrins (see next chapter for more details about porphyrin ring current).

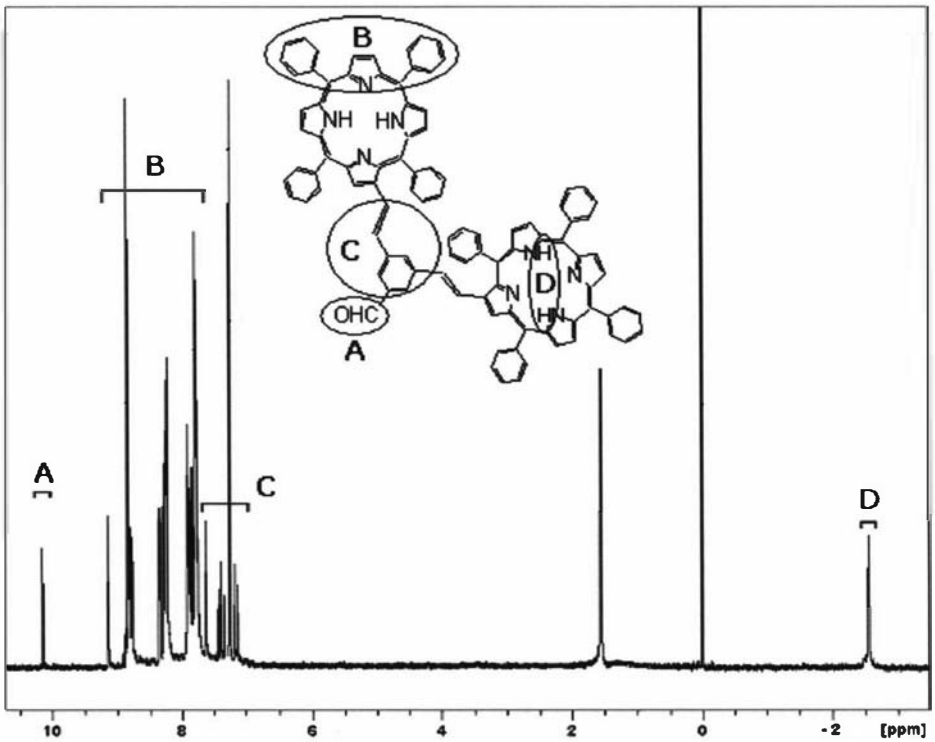

Figure 2-4 ^{1}H-NMR spectrum of **25**

An expanded view of the porphyrins ^{1}H-NMR aromatic region is shown in Figure 2-5. The signals at lower fields (typically 7.5-9.5 ppm) come from protons close to the porphyrin core; each *β*-pyrrolic substituted tetraphenylporphyrin produces three distinct multiplets, which originate from *β*-pyrrolic (7 protons), *ortho*-phenyl (8) and *meta*- and *para*-phenyl (12) protons. The *β*-pyrrolic protons are generally divided into two or three groups; the lowest field singlet is the proton ($\mathbf{H_A}$) close to the linker substituent and the increased shift is due to the anisotropic affect of the neighbouring vinyl group. In fact, when the double bond is in the *cis* configuration, steric hindrance prevents it from being coplanar and its anisotropy does not influence this proton in the same way (the signal is either in the same multiplet as the other *β*-pyrrolic protons or is at slight higher fields). In most cases, the other six *β*-pyrrolic signals ($\mathbf{H_B}$) form an overlapping groups of multiplets, but sometimes a doublet (J = 8 Hz) is distinguishable, at the high field extremity. The signals arising from the ortho-protons of the meso-phenyl groups ($\mathbf{H_C}$) are usually between 8.0 and 8.5 ppm; the lower field position, compared to the meta- and para-protons, is due to the ring current effect, which at the ortho positions is stronger than at the meta and para positions. The $\mathbf{H_C}$ signals form four doublets (typically with J = 8 Hz) which are usually superimposed but not equivalent (because of the unsymmetrical nature of *β*-substituted porphyrins).

The other phenyl protons, the meta- ($\mathbf{H_D}$) and the para- ($\mathbf{H_E}$) protons are generally found as a large multiplet in the 7.5-8 ppm region and can be superimposed on other proton resonances from the conjugated bridge.

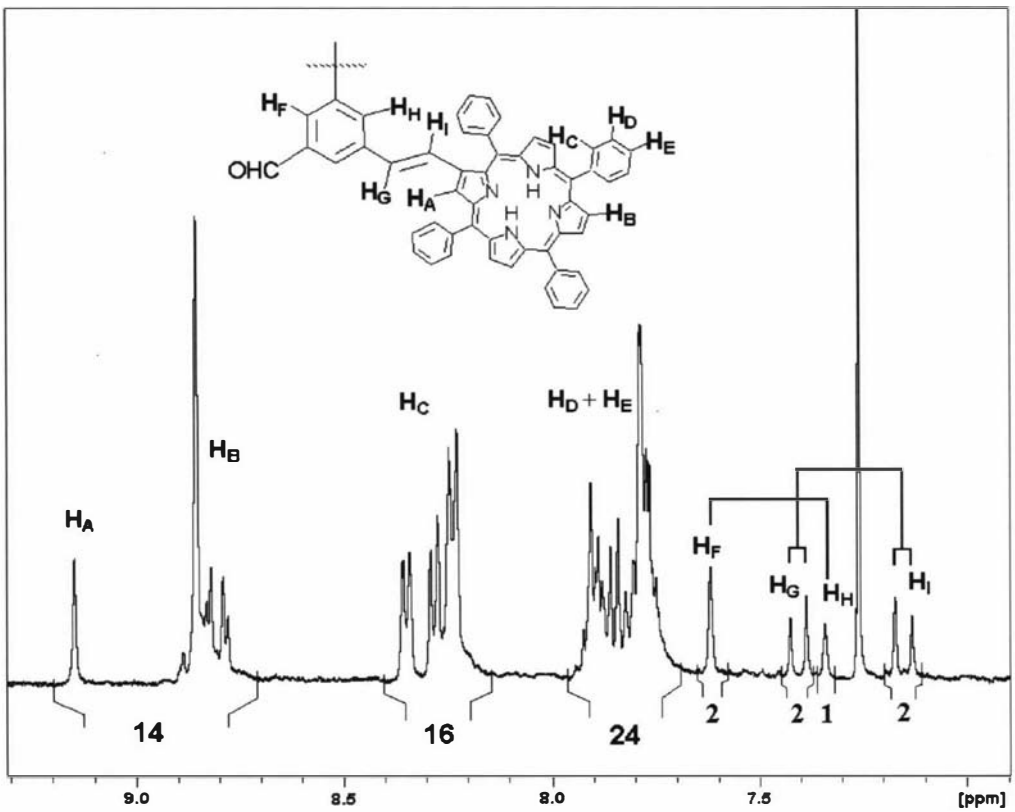

Figure 2-5 ^{1}H-NMR spectrum of the aromatic region of **25**
(the second porphyrin is not shown for clarity)

The highest field signals in Figure 2-5 are due to the phenylene-vinylene part. In this porphyrin dimer **25**, there are 7 protons in that region and the magnetic equivalence of some of them results in two singlets and two doublets. In particular, the phenyl signals $\mathbf{H_F}$ and $\mathbf{H_H}$ are easily recognizable as slightly broadened singlets (meta-coupling is usually too small to result in doublets) and integration of the peaks gives respectively two and one protons, making the attribution obvious. Less trivial is the assignment of the signals $\mathbf{H_G}$ and $\mathbf{H_I}$ from the double bond; both protons provide a doublet with the typical 16 Hz coupling but it is difficult to distinguish between the two. Previous reports[63] have assigned the highest field signal ($\mathbf{H_I}$ in the Figure 2-5) to the proton that is closer to the porphyrin, as a result of a small registered coupling (J = 0.6 Hz) to the closest β-pyrrolic proton ($\mathbf{H_A}$). However, in the course of this work, such couplings were hardly ever noticed (only in some of the metallated and none of the free base porphyrins) and the assignments were made with the aid of COSY (correlation

between proton-proton spin-coupling) and NOESY (proton-proton Overhauser interaction) spectra. ^{1}H-^{1}H correlations confirmed that the resonance of $\mathbf{H_G}$ is usually at lower fields than $\mathbf{H_I}$; in fact, long range COSY spectra show strong coupling between $\mathbf{H_I}$ and $\mathbf{H_A}$ while no coupling between $\mathbf{H_G}$ and $\mathbf{H_A}$ was ever registered; similarly, a large NOESY effect can be registered between $\mathbf{H_I}$ and $\mathbf{H_A}$ while there is no interaction between $\mathbf{H_G}$ and $\mathbf{H_A}$ (Figure 2-6).

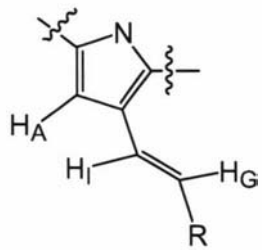

	H_A-H_G	H_A-H_I
COSY	No	Yes
NOESY	No	Yes

Figure 2-6 Signal assignments by ^{1}H-^{1}H NMR correlations

Interestingly, this behavior was only found when the β-pyrrolic substituent is in the *trans* configuration; in the next chapters it is shown that, both when the β-pyrrolic substituent is in the *cis* configuration (see Chapter 3) and when the substituent is simply a vinyl group (see Chapter 4), proton $\mathbf{H_G}$ always gives a higher field resonance than proton $\mathbf{H_I}$ (Figure 2-7). This fact has to be attributed to the planar (in the *trans* configuration) or out-of–plane conformation of the substituent which is affected differently by the porphyrin and the closest phenyl ring currents (see Chapter 3 for further discussion).

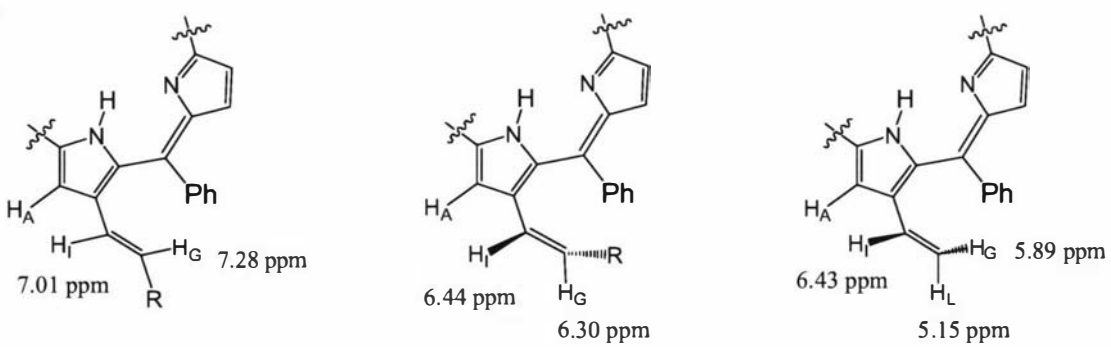

22t **22c** **48**

Figure 2-7 ^{1}H-NMR resonances of *trans*, *cis* and vinyl β-pyrrolic substituents indicating the rotation of the vinyl group out of the porphyrin plane

Figure 2-8 shows the ^{1}H-NMR spectrum of **Ni-31**, with the phosphonate region expanded. Here, signals originating from protons of porphyrins and phosphonate groups are easily recognized and, from the ratio between the integrals of these peaks, it is possible to confirm that there is one phosphonate per four porphyrins.

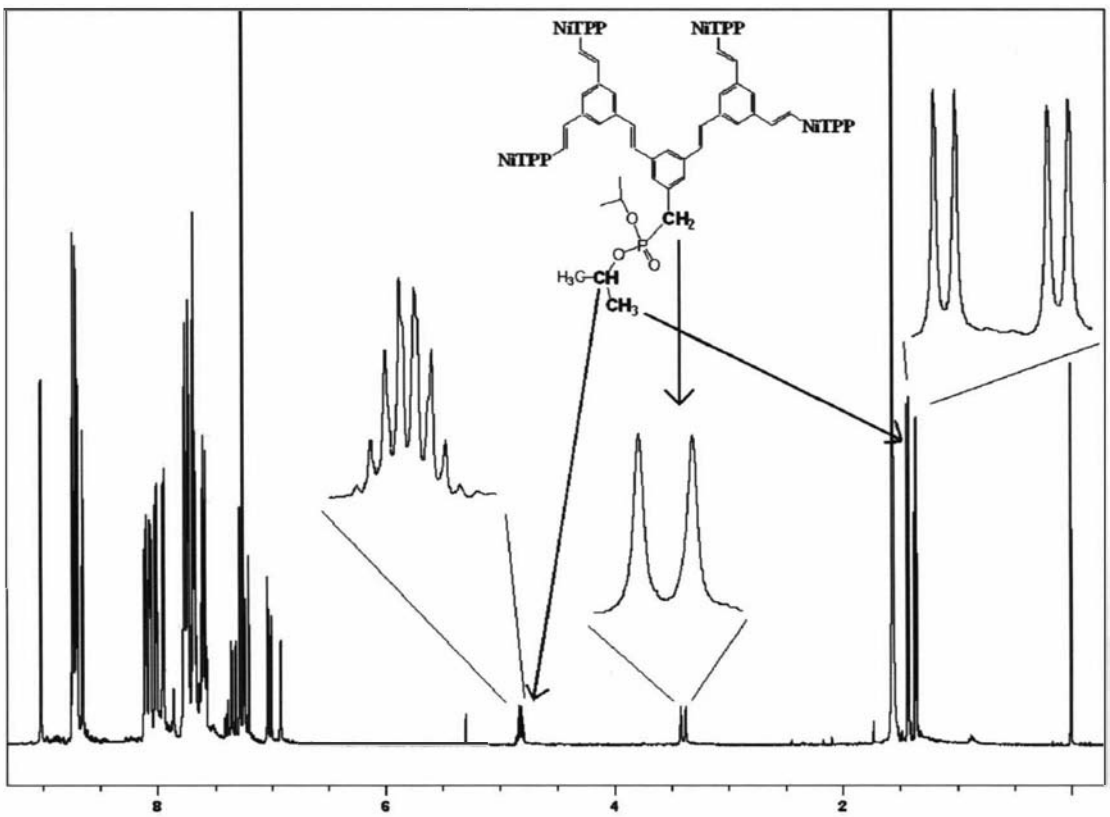

Figure 2-8 ^{1}H-NMR spectrum of **Ni-31**

The high multiplicity of the phosphonate group signals in Figure 2-8 is mainly due to ^{1}H-^{31}P short and long range couplings; as a result, CH protons produce an overlapping doublet of quartets (^3J_P = 26 Hz), the benzylic CH_2 group gives a doublet (^2J_P = 22 Hz) and the four equivalent CH_3 groups produce a double doublet; this particular multiplicity is typical of tetrahedral phosphorous derivatives of aromatic compounds.[105] The double doublet is due to the normal CH-CH_3 coupling (J_P = 6 Hz) and to the doubling caused by the closest phenyl ring current, which distinguish among two rotational conformers, producing shifts of 25-55 Hz. This factor is totally absent in ethylphosphonates, whose ^{1}H-NMR spectra show the expected triplet for the methyl protons. It can be noticed that in the case of **Ni-31**, the dendrimer symmetry results in a simple spectrum; however, this is not common because steric hindrance

and intermolecular coordination equilibria often produce loss of symmetry with broadening and/or shift of some signals.

Peak assignments in other regions proved to be challenging and required the use of COSY spectroscopy and the recourse to analogy with similar compounds. Figure 2-9 shows an expanded region of the ^{1}H-NMR spectrum of **Ni-31** and the ^{1}H-^{1}H coupling spectrum of the same compound. In this case, resonances are separated enough to be identified but, often, superimpositions made this process impossible.

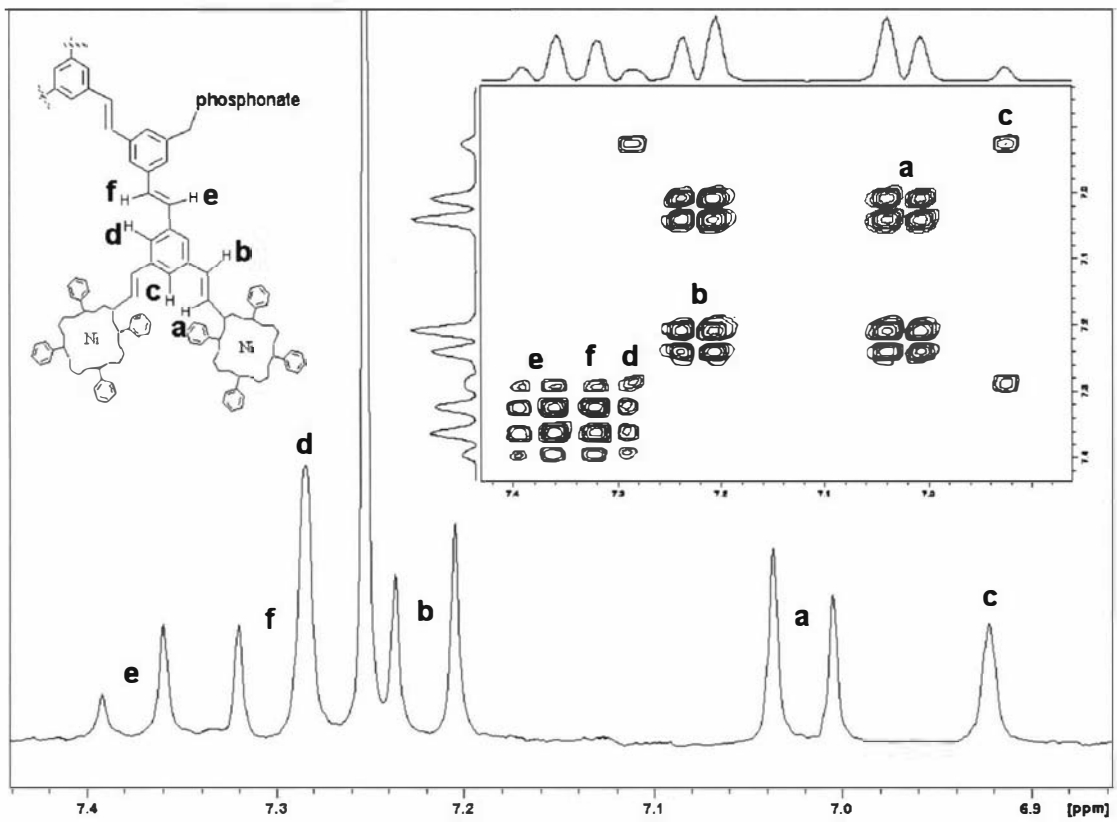

Figure 2-9 ^{1}H-NMR and COSY spectra of **Ni-31**

Even when the signals are separated it is still difficult to completely assign every peak. For example, the assignments of protons **e** and **f** in Figure 2-9 are arbitrary and there is no simple way to distinguish between them (COSY and NOESY spectra are inconclusive). Moreover, some of the molecules presented in this paragraph have non-equivalent porphyrins, which make the assignments even harder. In cases such as the mixed array **Ni_4Zn-34**, the ^{1}H-NMR spectrum of the pure compound (Figure 2-10) is not resolved enough to allow a complete characterization of the molecule by only their ^{1}H-NMR spectra at 500 MHZ.

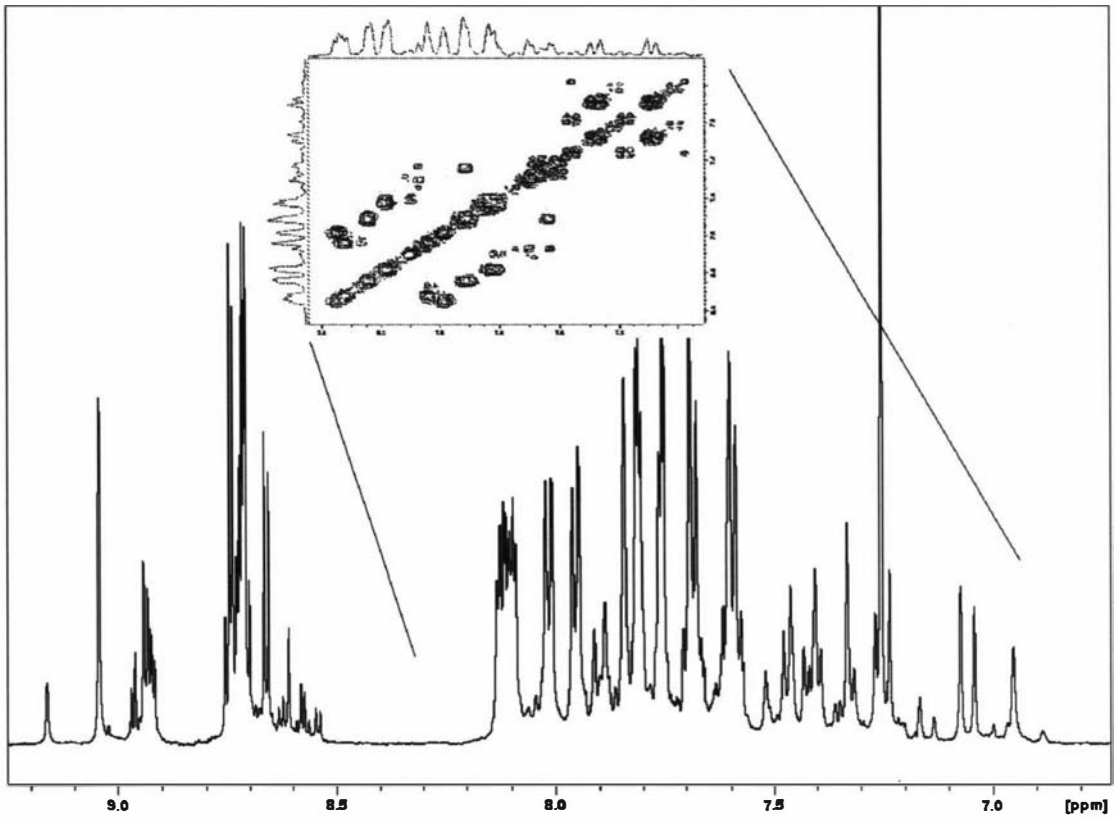

Figure 2-10 ^{1}H-NMR and COSY spectra of **Ni_4Zn-34**

Another complication arises from the fact that Zn porphyrins can weakly coordinate the phosphonates (and the aldehydes, to a minor degree) present in our molecules, resulting in concentration dependent chemical shifts which are particularly evident for the protons of the arylphosphonate groups. As a result, peak positions reported in this work for all Zn porphyrin phosphonates are relative to the solvent, concentration and temperature used in that experiment. The concentration effect, coupled with COSY spectroscopy, sometimes resulted in very useful information for assignments; in fact, when peaks were superimposed, a simple dilution of the sample would cause a different shift for different signals, allowing assignments. More information about Zn porphyrin phosphonates and their NMR spectrometry is discussed in Chapter 3.

Mass spectrometry: MALDI-TOF mass spectrometry was a fast and effective method of analysis; most of the reactions described in this paragraph were followed simply by taking a minimal amount of the reaction solution and depositing it on a MALDI plate, allowing the solvent evaporate before inserting it in the spectrometer. Typically, the use of a matrix was not required but some compounds, particularly

large molecules containing labile functionalities (such as phosphonates), do not produce parent ions and ^{1}H-NMR spectrometry had to be used for early identifications. MALDI spectrometry was particularly useful for following the course of the reactions for the production of mixed arrays. In the making of pentamer **Ni_4Zn-34** (Scheme 2-33), at least two low-polar products are expected (the desired array and the hydrolysis product of the phosphonate) and identification of the compounds by TLC and NMR spectroscopy was not easy; Figure 2-11 shows the MALDI spectrum of the first fraction eluted from the column chromatography after the reaction for the preparation of pentamer **Ni_4Zn-34**: the cluster created by the isotopic distribution of the various atoms in the molecule provides a very good indication about the mass and the actual ratio between the elements (C, N, H, Zn, Ni), even at low resolution. Moreover, the absence of peaks due to molecules containing more than one porphyrin show that there were no impurities coming for hydrolysis of **Ni-31.**

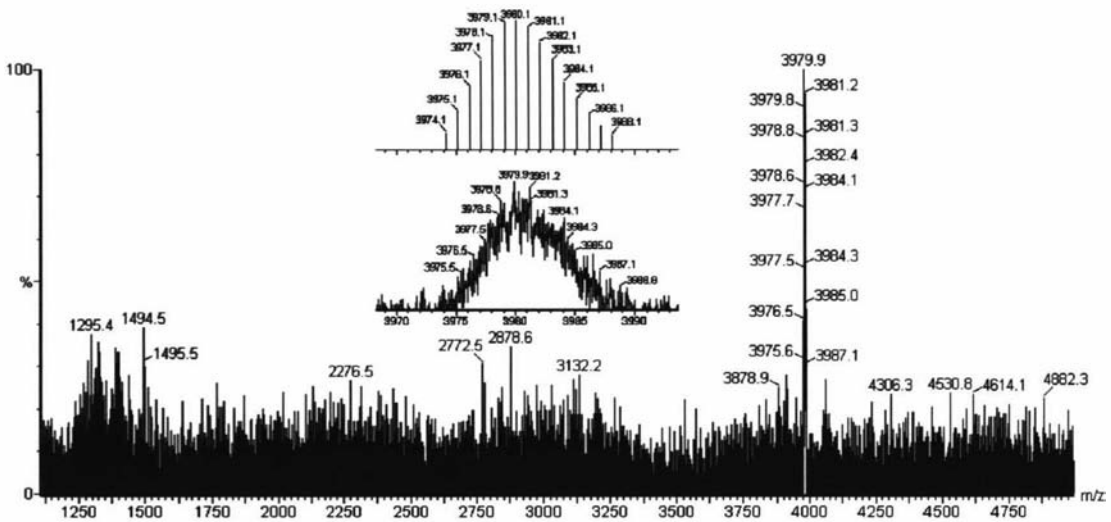

Figure 2-11 MALDI spectrum of **Ni_4Zn-34**

Although first analyses (identifications) of the products were obtained fairly easily by MALDI spectrometry, high resolution mass spectra of porphyrin arrays proved to be challenging to obtain. Samples were sent to three laboratories equipped with different spectrometers (see Section 2.8 for details) and all of them produced similar results. The only suitable ionization technique was found to be fast atom bombardment (FAB); FAB/HRMS have been obtained for all porphyrins with molecular weights lower than 2000 but larger molecules often did not produce molecular ions, giving only fragmentations.

UV-visible absorption spectroscopy: UV-visible spectroscopy of the compounds described in this chapter was performed as a characterization tool, although its utility for product identifications was not particularly high. This is because porphyrins of the same kind (e.g. variously substituted TPP) have quite similar absorbances, which are characteristic of $\pi-\pi^*$ transitions of the delocalized core electrons. Different metallation states (except for the free base) and substituents also have little influence on the absorption, producing only few nanometer band shifts and minor band shape changes. There is however some information that can be taken from these spectra and some patterns characteristic of particular groups of arrays. Figure 2-12 shows the absorption spectra of **25**, **Zn-25** and **Ni-25**.

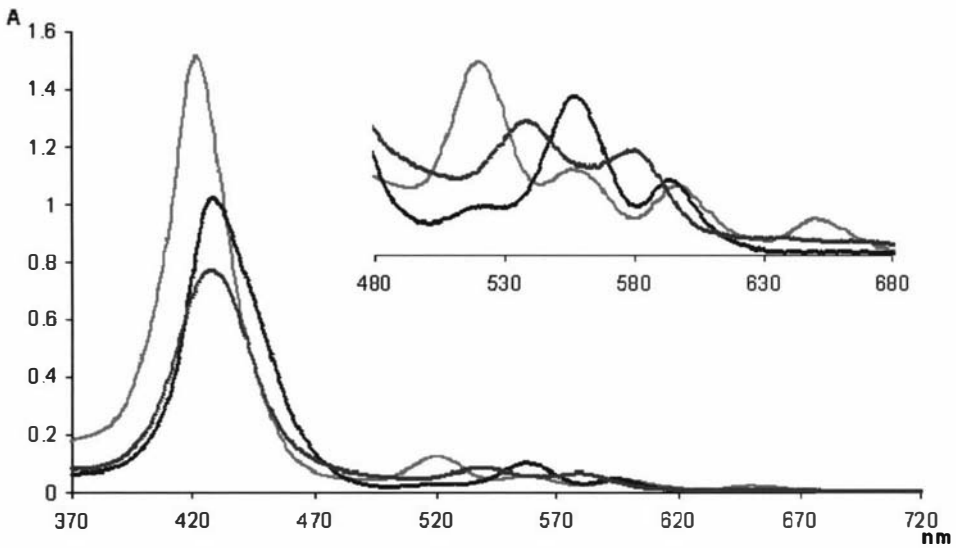

Figure 2-12 UV-vis absorption spectra of **25** (—), **Zn-25** (—) and **Ni-25** (—) in DCM (absorbance values are shown for equimolar concentrations of porphyrin)

Apart from the obvious statement that free-base **25** has four Q bands instead of the two of **Ni-25** and **Zn-25,** it can be noted that the size of the molar absorption coefficient ε follows the order fb > Zn > Ni. A similar trend in the ε has been observed in most of the other series of differently metallated porphyrin presented in this work. The effect of array size and the presence of functional groups have very little effect on the absorption spectra: Figure 2-13 shows that the spectra of dimer aldehyde **Ni-25** and tetramer phosphonate **Ni-31** are practically identical.

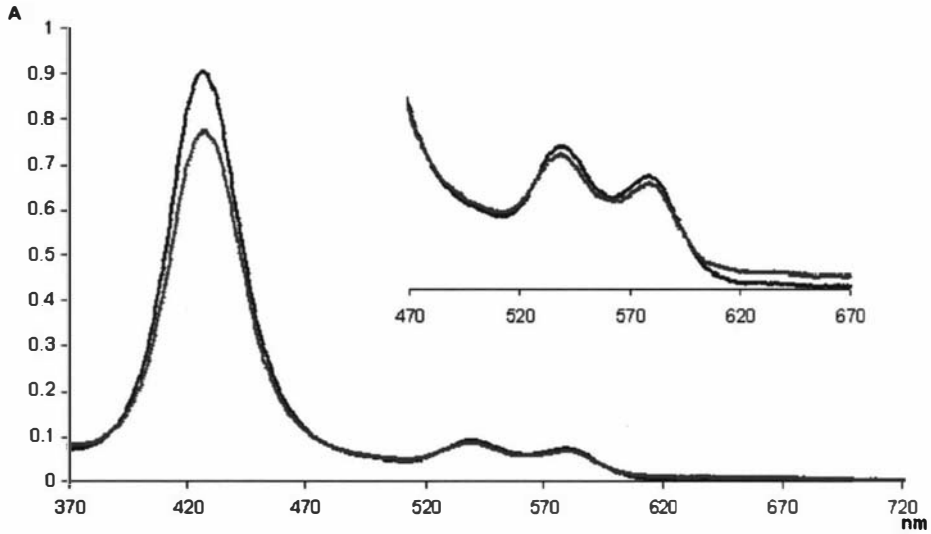

Figure 2-13 UV-vis absorption spectra of **Ni-25** ($3x10^{-6}$M, ▬) and **Ni-31** ($1.8x10^{-6}$M ▬) in DCM

2.8. Experimental procedures

General

Commercially available solvents and chemicals were purchased from different sources, as AR grade unless otherwise specified. Solvents for column chromatography (dichloromethane, hexane, methanol and toluene) were distilled lab grade. Water was purified by reverse osmosis. Dry THF and diethyl ether were obtained by passing commercially available argon degassed solvent through an activated alumina column. 1,2-Dichloroethane, pyridine and *N,N*-dimethylformamide were dried and purified according to standard lab procedures.[106]

UV-vis experiments were performed on a Shimadzu UV-3101PC scanning spectrophotometer. High resolution FAB mass spectra were recorded on a Varian VG-70SE instrument at the University of Auckland, on a VG70-250S at Hort Research, Palmerston North and on a VG ZAB 2 SEQ VG-Micromass at the Australian National University. MALDI-TOF mass spectra were carried out by the author and were performed on a Micromass ProteomWorks M@LDI-Reflectron mass spectrometer. ^{1}H-NMR spectrometry experiments were performed using 400 and 500 MHz Bruker Avance instruments running TOPSPIN 1.3 software. Proton chemical shifts in $CDCl_3$

are relative to TMS. Chemical shifts in other solvents are relative to residual protons (tetrahydrofurane-d_8, 3.58 ppm; dioxane-d_8, 3.53 ppm, dichloromethane-d_2, 5.32 ppm). Data are expressed as position (in ppm), multiplicity (s = singlet, d = doublet, t = triplet, q = quartet, m = multiplet, br = broad, app = apparent), relative integral, coupling constant (J_P indicating ^1H-^{31}P coupling) and assignment. Coupling constants were not reported when smaller than 1 Hz.

Precursor syntheses.

Porphyrins aldehydes **M-5** (M = 2H, Zn, Ni), **6**, **M-14** (M = 2H, Zn, Ni), **M-15** (M = 2H, Zn) and **M-18** (M = 2H, Zn), benzene-tricarboxaldehyde **17** and phosphonium salts **11** and **12** were prepared as previously published by our group.[75] 1,3,5-tribromomethylbenzene **16** was available in our laboratories and was prepared by NBS bromination of mesitylene in dichloromethane.

1,3,5-mesitylenetris(diethylphosphonate), 21.

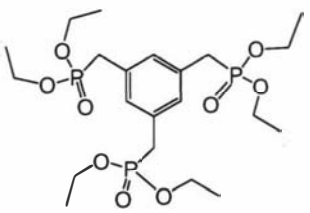

$C_{21}H_{39}O_9P_3$
Exact Mass: 528.18
Mol. Wt.: 528.45

Triphosphonate **35** was prepared according to the general method of Michaelis and Kaehne.[102,107]

1 g (2.8 mmol) of tribromomethylbenzene **16** was dissolved in 7 mL of commercial triethylphosphite under argon atmosphere. The solution was refluxed for 4 hours after which the excess phosphite and co-product EtBr were distilled off under high vacuum, yielding 1.4 g (98%) of pure **21** as pale yellow oil. ^1H-NMR (400 MHz, $CDCl_3$): δ 7.14 (q, J_P = 2.4 Hz, $3H_{Ph}$), 4.02 (quintet, J = 7.2 Hz, $12H_{CH2}$), 3.12 (d, J_P = 22 Hz, 6H), 1.26 (t, J = 7.1 Hz, $18H_{CH3}$). The ^1H-NMR spectrum is in agreement with the literature.[148]

$(ZnTPP)_2$-Ph-ep, Zn-23.

3,5-bis(*trans*-2'-(2"-(5",10",15",20"-tetraphenylporphyrinato zinc(II))yl)ethen-1'-yl)methyl(diethylphosphonate)benzene.

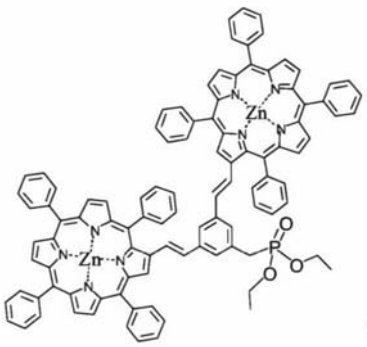

$C_{103}H_{73}N_8O_3PZn_2$
Exact Mass: 1628.41
Mol. Wt.: 1632.49

400 mg (568 μmol) of **Zn-5** and 136 mg (258 μmol) of **21** were dissolved in 120 mL of dry THF, under argon atmosphere. To the stirred solution, 70 mg (623 μmol) of ^{t}BuOK in dry THF were added at three intervals in 30 min. After further 30 min, the solution was evaporated to dryness, dissolved in DCM and precipitated by adding MeOH. The crude was purified through flash chromatography on silica gel: **Zn-5** and side-products were eluted with DCM after which the desired product was eluted with DCM/MeOH = 200/1. 82 mg (29%) of pure **Zn-23** were obtained by recrystallization from DCM/MeOH as purple crystals. ^{1}H-NMR (500 MHz, $CDCl_3$): δ 9.26 (s, 2H, $H_{\beta\text{-pyrrolic}}$), 8.97-8.83 (m, 12H, $H_{\beta\text{-pyrrolic}}$), 8.35-8.21 (m, 16H, $H_{o\text{-Ph}}$), 7.90-7.72 (m, 24H, $H_{m,p\text{-Ph}}$), 7.34 (d, J = 16 Hz, 2H, H_{alkene}), 7.11 (d, J = 16 Hz, 2H, H_{alkene}), 7.00 (br s, 1H, $H_{\text{Ph'}}$), 6.97 (br s, 2H, $H_{\text{Ph'}}$), 4.00-3.88 (m, 4H, $H_{\text{CH2-ethyl}}$), 3.08 (d, J_P = 22 Hz, 2H, $H_{\text{CH2-P}}$), 1.25 (t, J = 7 Hz, 6H, $H_{\text{CH3-ethyl}}$). *Assignments aided by variable concentration and COSY spectra.* UV-vis (CH_2Cl_2): λ_{max} [nm] (ε x 10^{-3}) 428.5 (222), 556 (17.9), 594 (9.3). FAB-HRMS for MH^+ ($C_{103}H_{74}N_8PO_3Zn_2$): 1629.4121, calculated: 1629.4204.

$(NiTPP)_2$-Ph-ep, Ni-23.

3,5-bis(*trans*-2'-(2"-(5",10",15",20"-tetraphenylporphyrinato zinc(II))yl)ethen-1'-yl)methyl(diethylphosphonate)benzene.

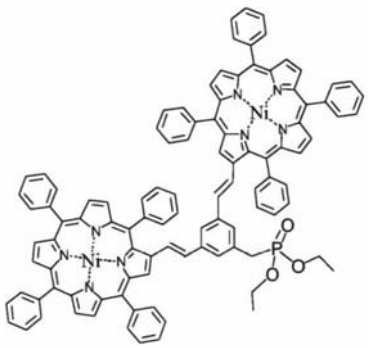

$C_{103}H_{73}N_8Ni_2O_3P$
Exact Mass: 1616.43
Mol. Wt.: 1619.09

54 mg (74.5 μmol) of **Ni-5** and 20 mg (37.8 μmol) of **21** were dissolved in 25 mL of dry THF, under argon atmosphere. To the stirred solution, 10 mg (89.1 μmol) of solid ^{t}BuOK were added in two portions in 20 min. After further 30 min, the solution was evaporated to dryness, dissolved in DCM and precipitated by adding MeOH. The crude was purified through flash chromatography on silica gel: **Ni-5** and side-products were eluted with DCM after which the desired product was eluted with DCM/MeOH = 100/1. 20 mg (33%) of pure **Ni-23** were obtained by recrystallization from DCM/MeOH as purple-red crystals. ^{1}H-NMR (400 MHz, $CDCl_3$): δ 8.98 (s, 2H, $H_{\beta\text{-pyrrolic}}$), 8.76-8.67 (m, 12H, $H_{\beta\text{-pyrrolic}}$), 8.14-7.98 (m, 16H, $H_{o\text{-Ph}}$), 7.80-7.65 (m, 24H, $H_{m,p\text{-Ph}}$), 7.15 (d, J = 16 Hz, 2H, H_{alkene}), 6.98 (s, 2H, $H_{Ph'}$), 6.91 (d, J = 16 Hz, 2H, H_{alkene}), 6.89 (s, 1H, $H_{Ph'}$), 4.16-4.04 (m, 4H, $H_{CH2\text{-ethyl}}$), 3.19 (d, J_P = 22 Hz, 2H, $H_{CH2\text{-P}}$), 1.29 (t, J = 7 Hz, 6H, $H_{CH3\text{-ethyl}}$). UV-vis (CH_2Cl_2): λ_{max} [nm] (ε x 10^{-3}) 426 (232), 538 (23), 574 (15.9). FAB-HRMS for M^+ ($C_{103}H_{73}N_8PO_3{}^{58}Ni_2$): 1616.4169, calculated: 1616.4250.

$(ZnTPP)_3$, Zn-24.

1,3,5-tris(*trans*-2'-(2"-(5",10",15",20"-tetraphenylporphyrin)yl)ethen-1'-yl)benzene.

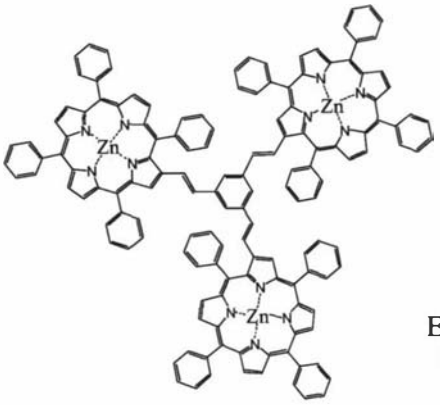

$C_{144}H_{90}N_{12}Zn_3$
Exact Mass: 2178.53
Mol. Wt.: 2184.51

Trimer **Zn-24** can be obtained by Zn metallation of the already described trimer **24.** In this case, it was obtained, as for **24**, as co-product in the preparation of the dendrimer dimer **Zn-23**. The trisubstituted product was the first fraction eluted from column chromatography (silica gel, DCM/hexane = 2/1) and was obtained in 5% yield. As for the synthesis of the free-base homologue **24**, the low yield is justified by the conditions set for disubstitution. ^{1}H-NMR (400 MHz, $CDCl_3$): δ 9.14 (s, 3H, $H_{\beta\text{-pyrrolic}}$), 9.02-8.83 (m, 18H, $H_{\beta\text{-pyrrolic}}$), 8.49-8.12 (m, 24H, $H_{o\text{-Ph}}$), 8.03-7.69 (m, 36H, $H_{m,p\text{-Ph}}$), 7.47 (d, J= 15.8 Hz, 3H, H_{alkene}), 7.21 (d, J= 16 Hz, 3H, H_{alkene}), 7.03 (s, 3H, $H_{Ph'}$). UV-vis (CH_2Cl_2): λ_{max} [nm] ($\varepsilon \times 10^{-3}$) 425 (346), 554 (36), 592.5 (14.5). MALDI-LRMS for M^+ ($C_{144}H_{90}N_{12}Zn_3$): cluster 2178.58-2191.57 (max 2183.59), calculated: cluster 2178.53-2191.53 (max 2184.53).

$(TPP)_2$-Ph-CHO, 25.

3,5-bis(*trans*-2'-(2"-(5",10",15",20"-tetraphenylporphyrin)yl)ethen-1'-yl)benzaldehyde.

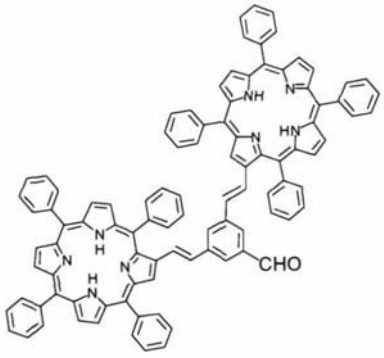

$C_{99}H_{66}N_8O$
Exact Mass: 1382.54
Mol. Wt.: 1383.64

700 mg (758 μmol) of TPP-ps **11** and 58 mg (358 μmol) of 1,3,5-tricarboxaldehyde **17** were dissolved in 120 mL of dichloromethane (AR grade) under argon. Excess of

DBU (0.5 mL) was added and the solution was stirred for 20 minutes. The solution was then washed with 0.3M HCl and precipitated by MeOH addition. The solid contained mainly the desired product as a mixture of cis/trans isomers; this mixture was dissolved in 150 mL of dichloromethane and 500 mg of I_2 were added. After 40 hours the solution was washed three times with a saturated solution of $Na_2S_2O_3$ and water and then precipitated with methanol. A second recrystallization from DCM/hexane provided 420 mg (84%) of pure **25** as purple crystals. ^{1}H-NMR (400 MHz, $CDCl_3$): δ 10.15 (s, 1H, $H_{aldehyde}$), 9.14 (s, 2H, $H_{\beta\text{-pyrrolic}}$), 8.93-8.77 (m, 12H, $H_{\beta\text{-pyrrolic}}$), 8.36-8.20 (m, 16H, $H_{o\text{-Ph}}$), 7.91-7.73 (m, 24H, $H_{m,p\text{-Ph}}$), 7.62 (s, 2H, $H_{Ph'}$), 7.40 (d, J = 16 Hz, 2H, H_{alkene}), 7.33 (s, 1H, $H_{Ph'}$), 7.15 (d, J = 16 Hz, 2H, H_{alkene}), -2.54 (br s, 4H, $H_{N\text{-pyrrolic}}$). *Assignments aided by COSY spectra.* UV-vis (CH_2Cl_2): λ_{max} [nm] (ε x 10^{-3}) 422 (839), 521 (70.4), 556 (31.6), 597 (25.3), 649 (13.3). FAB-HRMS for M^+ ($C_{99}H_{66}N_8O$): 1382.5279, calculated: 1382.5359.

(ZnTPP)$_2$-Ph-CHO, Zn-25.

3,5-bis(*trans*-2'-(2"-(5",10",15",20"-tetraphenylporphyrinato zinc(II))yl)ethen-1'-yl)benzaldehyde.

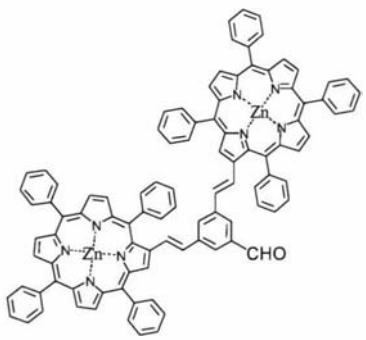

$C_{99}H_{62}N_8OZn_2$
Exact Mass: 1506.36
Mol. Wt.: 1510.38

450 mg (325 μmol) of aldehyde **25** were dissolved in 250 mL of dichloromethane (AR grade) and 1.2 eq. of $Zn(OAc)_2 \cdot H_2O$ (90 mg, 410 μmol), dissolved in the same amount of MeOH/water = 10/1, was added. The mixture was stirred for 2 hours and then washed with water and precipitate with MeOH. The solid collected was the pure desired porphyrin **Zn-25** (480 mg, 98%) as pale purple crystals. ^{1}H-NMR (400 MHz, $CDCl_3$): δ 10.16 (s, 1H, $H_{aldehyde}$), 9.27 (s, 2H, $H_{\beta\text{-pyrrolic}}$), 8.99-8.85 (m, 12H, $H_{\beta\text{-pyrrolic}}$), 8.36-8.22 (m, 16H, $H_{o\text{-Ph}}$), 7.92-7.73 (m, 24H, $H_{m,p\text{-Ph}}$), 7.63 (s, 2H, $H_{Ph'}$), 7.41-7.36 (m, 3H, $H_{Ph'}$ + $2H_{alkene}$), 7.33 (s, 1H, $H_{Ph'}$), 7.19 (d, J = 16 Hz, 2H, H_{alkene}). *Assignments aided by COSY spectra.* UV-vis (CH_2Cl_2): λ_{max} [nm] (ε x 10^{-3}) 429 (385),

522 (11.8), 557 (38.8). FAB-HRMS for M^+ ($C_{99}H_{62}N_8OZn_2$): 1506.3685, calculated: 1506.3630.

$(NiTPP)_2$-Ph-CHO, Ni-25.

3,5-bis(*trans*-2'-(2"-(5",10",15",20"-tetraphenylporphyrinato nickel(II))yl)ethen-1'-yl)benzaldehyde.

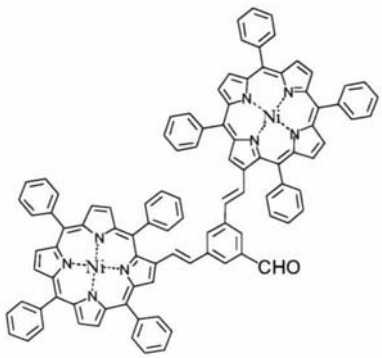

$C_{99}H_{62}N_8Ni_2O$
Exact Mass: 1494.38
Mol. Wt.: 1496.99

380 mg (274 μmol) of aldehyde **25** were dissolved in 200 mL of chloroform and the solution was heated to reflux. Excess $Ni(OAc)_2 \cdot 4H_2O$ (1 g, 15 eq) was dissolved in 15 mL of MeOH/water = 10/1 and added to the boiling porphyrin solution. Reflux was continued for 24 hours after which methanol was added and the precipitate was filtrated and washed with methanol. The crude was purified by three recrystallization from DCM/MeOH, yielding 278 mg (68%) of **Ni-25** as purple crystals. ^{1}H-NMR (400 MHz, $CDCl_3$): δ 10.09 (s, 1H, $H_{aldehyde}$), 9.00 (s, 2H, $H_{\beta\text{-pyrrolic}}$), 8.77-8.70 (m, 12H, $H_{\beta\text{-pyrrolic}}$), 8.12-7.99 (m, 16H, $H_{o\text{-Ph}}$), 7.81-7.66 (m, 24H, $H_{m,p\text{-Ph}}$), 7.52 (s, 2H, $H_{Ph'}$), 7.23 (d, J = 16 Hz, 2H, H_{alkene}), 7.22 (s, 1H, $H_{Ph'}$), 6.98 (d, J = 16 Hz, 2H, H_{alkene}). UV-vis (CH_2Cl_2): λ_{max} [nm] ($\varepsilon \times 10^{-3}$) 427.5 (254), 539 (28.8), 580 (22.6). FAB-HRMS for M^- ($C_{99}H_{62}N_8O^{58}Ni_2$): 1494.3826, calculated: 1494.3754.

$(TPP)_3$, 26.

1,3,5-tris(*trans*-2'-(2"-(5",10",15",20"-tetraphenylporphyrin)yl)ethen-1'-yl)benzene.

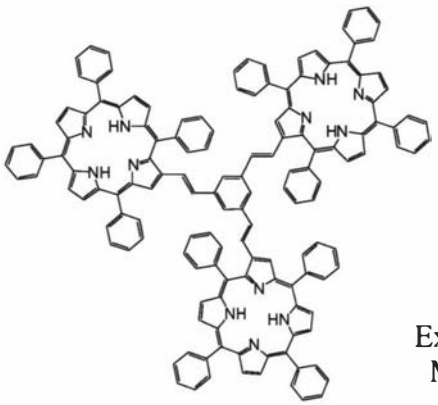

$C_{144}H_{96}N_{12}$
Exact Mass: 1992.79
Mol. Wt.: 1994.38

Trimer **26** was obtained as co-product in the syntheses of aldehyde **25**. It was recovered from the solution discarded during the recrystallization processes described above and isolated by column chromatography on silica gel (DCM/hexane = 1/1). The yield was around 1% but it has to be reminded that the conditions were chosen to optimize disubstitution (only 2 equivalents of porphyrin per trialdehyde). ^{1}H-NMR (400 MHz, $CDCl_3$): δ 9.31 (s, 3H, $H_{\beta\text{-pyrrolic}}$), 8.96-8.84 (m, 18H, $H_{\beta\text{-pyrrolic}}$), 8.51-8.46 (m, 6H, $H_{o\text{-Ph}}$), 8.38-8.33 (m, 6H, $H_{o\text{-Ph}}$), 8.30-8.25 (m, 12H, $H_{o\text{-Ph}}$), 8.05-8.01 (m, 6H, $H_{m,p\text{-Ph}}$), 7.90-7.65 (m, 30H, $H_{m,p\text{-Ph}}$), 7.49 (d, J = 16 Hz, 3H, H_{alkene}), 7.19 (d, J = 16 Hz, 3H, H_{alkene}), 7.02 (s, 3H, $H_{\text{Ph'}}$), -2.53 (br s, 6H, $H_{N\text{-pyrrolic}}$). FAB-HRMS for M^+ ($C_{144}H_{96}N_{12}$): 1992.7788, calculated: 1992.7881.

$(ZnTPP\text{-}Ph)_2$-Ph-ep, Zn-27.

3,5-bis(*trans*-2'-(4"-(*trans*-2'"-(5"",10"",15"",20""-tetraphenylporphyrinato zinc(II))yl)ethen-1'"-yl)phenyl)ethen-1'-yl)methyl(diethylphosphonate)benzene.

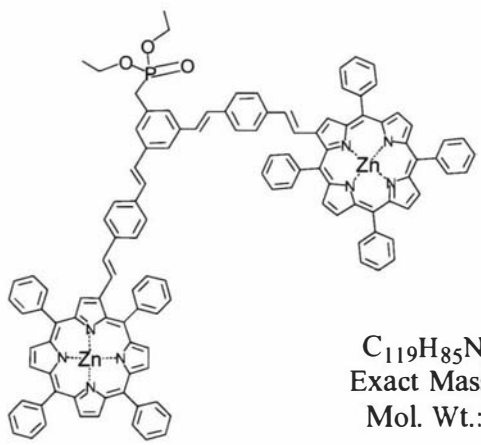

$C_{119}H_{85}N_8O_3PZn_2$
Exact Mass: 1832.51
Mol. Wt.: 1836.75

45 mg (56.5 μmol) of **Zn-14** and 14.2 mg (26.9 μmol) of **21** were dissolved in 25 mL of dry THF, under argon atmosphere. To the stirred solution, 8 mg (623 μmol) of

solid ^{t}BuOK were added. After 30 min, the solution was evaporated to dryness, dissolved in DCM and precipitated by adding MeOH. The crude was purified through flash chromatography on silica gel: **Zn-14** and side-products were eluted with DCM after which the desired product was eluted with DCM/MeOH = 200/1. 24 mg (46%) of pure **Zn-27** were obtained by recrystallization from DCM/MeOH as purple-green crystals. ^{1}H-NMR (400 MHz, $CDCl_3$): δ 9.12 (s, 2H, $H_{\beta\text{-pyrrolic}}$), 8.92-8.80 (m, 12H, $H_{\beta\text{-pyrrolic}}$), 8.22-8.12 (m, 16H, $H_{o\text{-Ph}}$), 7.90-7.70 (m, 24H, $H_{m,p\text{-Ph}}$), 7.37 (d, J = 8 Hz, 4H, $H_{Ph'}$), 7.35 (br s, 1H, $H_{Ph''}$), 7.21 (d, J = 16 Hz, 2H, H_{alkene}), 7.17 (d, J = 8 Hz, 4H, $H_{Ph'}$), 7.03 (d, J= 16 Hz, 2H, $H_{alkene'}$), 6.97 (d, J= 16 Hz, 2H, $H_{alkene''}$), 6.89 (d, J = 16 Hz, 2H, $H_{alkene''}$), 6.61 (br s, 2H, $H_{Ph''}$), 3.10-2.98 (m, 4H, $H_{CH2\text{-ethyl}}$), 1.82 (d, J_P = 22 Hz, 2H, $H_{CH2\text{-P}}$), 0.79 (t, J = 7 Hz, 6H, $H_{CH3\text{-ethyl}}$). *Assignments aided by variable concentration and COSY spectra.* UV-vis (CH_2Cl_2): λ_{max} [nm] (ε x 10^{-3}) 428 (370), 557.5 (43.7), 594.5 (26.3). FAB-HRMS for MH^+ ($C_{119}H_{86}N_8PO_3Zn_2$): 1832.5096, calculated: 1832.5065.

(NiTPP-Ph)$_2$-Ph-ep, Ni-27.

3,5-bis(*trans*-2'-(4"-(*trans*-2"'-(5"",10"",15"",20""-tetraphenylporphyrinato nickel(II))yl)ethen-1"'-yl)phenyl)ethen-1'-yl)methyl(diethylphosphonate)benzene.

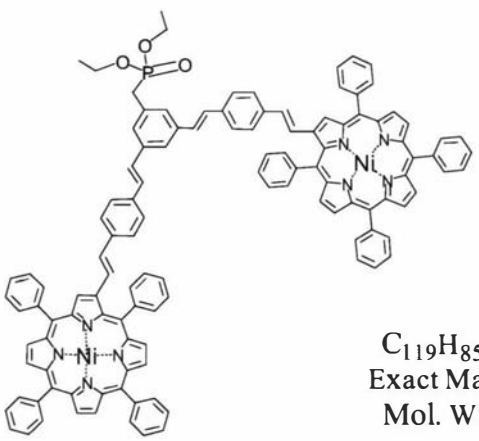

$C_{119}H_{85}N_8Ni_2O_3P$
Exact Mass: 1820.52
Mol. Wt.: 1823.36

54 mg (67.5 μmol) of **Ni-14** and 15 mg (28.4 μmol) of **21** were dissolved in 25 mL of dry THF, under argon atmosphere. To the stirred solution, 8 mg (62.3 μmol) of solid ^{t}BuOK were added. After 30 min, the solution was evaporated to dryness, dissolved in DCM and precipitated by adding MeOH. The crude was purified through flash chromatography on silica gel: **Ni-14** and side-products were eluted with DCM after which the desired product was eluted with DCM/MeOH = 200/1. 34 mg (54%) of pure **Ni-27** were obtained by recrystallization from DCM/MeOH as purple-red

crystals. ^{1}H-NMR (500 MHz, $CDCl_3$): δ 8.90 (s, 2H, $H_{\beta\text{-pyrrolic}}$), 8.72-8.67 (m, 12H, $H_{\beta\text{-pyrrolic}}$), 8.06-7.95 (m, 16H, $H_{o\text{-Ph}}$), 7.80-7.63 (m, 24H, $H_{m,p\text{-Ph}}$), 7.59 (br s, 1H, $H_{Ph''}$), 7.48 (d, J = 8 Hz, 4H, $H_{Ph'}$), 7.40 (br s, 2H, $H_{Ph''}$), 7.19 (d, J = 8 Hz, 4H, $H_{Ph'}$), 7.18-7.15 (d, J = 16 Hz, 4H, H_{alkene}), 7.14 (d, J = 16 Hz, 2H, $H_{alkene'}$), 6.89 (d, J = 16 Hz, 2H, $H_{alkene'}$), 4.16-4.04 (m, 4H, $H_{CH2\text{-ethyl}}$), 3.24 (d, J_P = 22 Hz, 2H, $H_{CH2\text{-P}}$), 1.32 (t, J = 7 Hz, 6H, $H_{CH3\text{-ethyl}}$). *Assignments aided by COSY spectra.* UV-vis (CH_2Cl_2): λ_{max} [nm] ($\varepsilon \times 10^{-3}$) 429 (331), 540.5 (38.2), 580 (33.9). FAB-HRMS for M^+ ($C_{119}H_{85}N_8PO_3{}^{58}Ni_2$): 1820.5168, calculated: 1820.5189.

1,3,5-mesitylenetris(diisopropylphosphonate), 28.

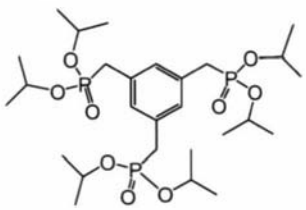

$C_{27}H_{51}O_9P_3$
Exact Mass: 612.27
Mol. Wt.: 612.61

Diphosphonate **35** was prepared according to the general method of Michaelis and Kaehne.[102,107]

2.4 g (6.8 mmol) of tribromomethylbenzene **16** was dissolved in 20 mL of commercial triisopropylphosphite under argon atmosphere. The solution was refluxed for 4 hours after which the excess phosphite and co-products were distilled off under high vacuum, yielding 4 g (96%) of pure **28** as colourless oil. ^{1}H-NMR (400 MHz, $CDCl_3$): δ 7.14 (q, J_P = 2.4 Hz, $3H_{Ph}$), 4.68-5.56 (m, $6H_{CH}$), 3.06 (d, J_P = 22.2 Hz, 6H), 1.23 (dd, *conformational doubling* = 35.5 Hz, J = 6.2 Hz, $36H_{CH3}$). HRMS for MH^+ ($C_{27}H_{52}O_9P_3$): 613.2823; calculated: 613.2824.

(ZnTPP-Ph)$_2$-Ph-ipp, Zn-29.

3,5-bis(*trans*-2'-(4"-(*trans*-2'''-(2''''-(5'''',10'''',15'''',20''''-tetraphenylporphyrinato zinc(II))yl)ethen-1'''-yl)phenyl)ethen-1'-yl)methyl(diisopropylphosphonate)benzene.

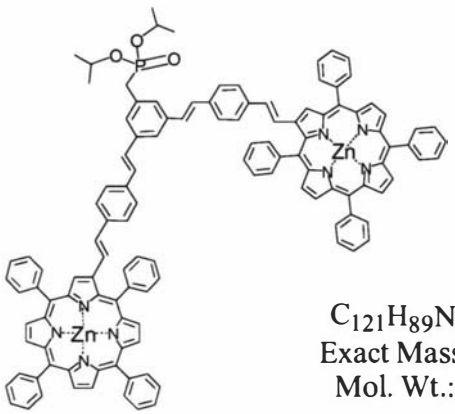

$C_{121}H_{89}N_8O_3PZn_2$
Exact Mass: 1860.54
Mol. Wt.: 1864.81

190 mg (235 μmol) of **Zn-14** and 67 mg (109 μmol) of **28** were dissolved in 50 mL of dry THF, under argon atmosphere. To the stirred solution, 33 mg (294 μmol) of ^{t}BuOK in dry THF were added in two portions in 30 min. After further 30 min, the solution was evaporated to dryness, dissolved in DCM and precipitated by adding MeOH. The crude was purified through flash chromatography on silica gel: **Zn-14** and side-products were eluted with DCM after which the desired product was eluted with DCM/MeOH = 100/1. 115 mg (52%) of pure **Zn-29** were obtained by recrystallization from DCM/MeOH as purple-green crystals. ^{1}H-NMR (500 MHz, $CDCl_3$): δ 9.12 (s, 2H, $H_{\beta\text{-pyrrolic}}$), 8.92-8.82 (m, 12H, $H_{\beta\text{-pyrrolic}}$), 8.32-8.18 (m, 16H, $H_{o\text{-Ph}}$), 7.92-7.70 (m, 24H, $H_{m,p\text{-Ph}}$), 7.39-7.32 (m, 6H, $4H_{Ph'}$ + $2H_{alkene}$), 7.27-7.15 (m, 8H, $4H_{Ph'}$ + $2H_{alkene}$ + $2H_{alkene'}$), 7.06 (d, J = 16 Hz, 2H, H_{alkene}), 7.17 (d, J = 8 Hz, 4H, $H_{Ph'}$), 7.03 (br s, 1H, $H_{Ph''}$), 6.94 (app d, J = 6 Hz, 4H, $H_{alkene'}$), 6.74 (br s, 2H, $H_{Ph''}$), 3.21-3.09 (m, 2H, $H_{CH\text{-propyl}}$), 2.33 (d, J_P = 22 Hz, 2H, $H_{CH2\text{-P}}$), 0.61 (dd, *conformational doubling* = 39 Hz, J = 6 Hz, 12H, $H_{CH3\text{-propyl}}$). *Assignments aided by variable concentration and COSY spectra.* UV-vis (CH_2Cl_2): λ_{max} [nm] (ε x 10^{-3}) 428 (358), 558 (42.7), 595 (25.1). FAB-HRMS for M^+ ($C_{121}H_{89}N_8PO_3Zn_2$): 1860.5360, calculated: 1860.5378.

(NiTPP-Ph)$_2$-Ph-ipp, Ni-29.

3,5-bis(*trans*-2'-(4"-(*trans*-2"'-(2""-(5"",10"",15"",20""-tetraphenylporphyrinato nickel(II))yl)ethen-1"'-yl)phenyl)ethen-1'-yl)methyl(diisopropylphosphonate)benzene.

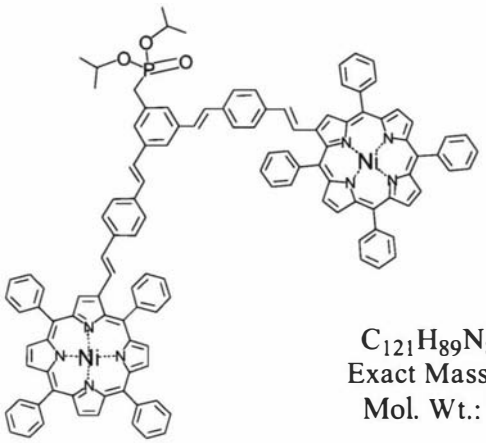

$C_{121}H_{89}N_8Ni_2O_3P$
Exact Mass: 1848.55
Mol. Wt.: 1851.41

380 mg (475 μmol) of **Ni-14** and 126 mg (206 μmol) of **28** were dissolved in 200 mL of dry THF, under argon atmosphere. To the stirred solution, 59 mg (527 μmol) of ^{t}BuOK in dry THF were added at three intervals in 50 min. After further 30 min, the solution was evaporated to dryness, dissolved in DCM and precipitated by adding MeOH. The crude was purified through flash chromatography on silica gel: **Ni-9** and side-products were eluted with DCM after which the desired product was eluted with DCM/MeOH = 200/1). 303 mg (68%) of pure **Ni-29** were obtained by recrystallization from DCM/MeOH as purple-red crystals. ^{1}H-NMR (500 MHz, $CDCl_3$): δ 8.90 (s, 2H, $H_{\beta\text{-pyrrolic}}$), 8.73-8.65 (m, 12H, $H_{\beta\text{-pyrrolic}}$), 8.06-7.92 (m, 16H, $H_{o\text{-Ph}}$), 7.80-7.62 (m, 24H, $H_{m,p\text{-Ph}}$), 7.54 (br s, 1H, $H_{Ph''}$), 7.46 (d, J = 8 Hz, 4H, $H_{Ph'}$), 7.40 (br s, 2H, $H_{Ph''}$), 7.17 (d, J = 8 Hz, 4H, $H_{Ph'}$), 7.18-7.13 (d, J = 16 Hz, 4H, H_{alkene}), 7.12 (d, J = 16 Hz, 2H, $H_{alkene'}$), 6.88 (d, J = 16 Hz, 2H, $H_{alkene'}$), 4.74-4.62 (m, 2H, $H_{CH\text{-propyl}}$), 3.20 (d, J_P = 21.5 Hz, 2H, $H_{CH2\text{-P}}$), 1.29 (dd, *conformational doubling* = 40 Hz, J = 6 Hz, 12H, $H_{CH3\text{-propyl}}$). *Assignments aided by COSY spectra.* - UV-vis (CH_2Cl_2): λ_{max} [nm] (ε x 10^{-3}) 428.5 (183), 540.5 (18.7), 580 (15.5). FAB-HRMS for M^- ($C_{121}H_{89}N_8PO_3{}^{58}Ni_2$): 1848.5461, calculated: 1848.5502.

(ZnTXP-Ph)$_2$-Ph-ipp, Zn-30.

3,5-bis(*trans*-2'-(4"-(*trans*-2"'-(2""-(5"",10"",15"",20""-tetra(3"",5""-dimethylphenyl)porphyrinato zinc(II))yl)ethen-1"'-yl)phenyl) ethen-1'-yl)methyl(diisopropylphosphonate)benzene.

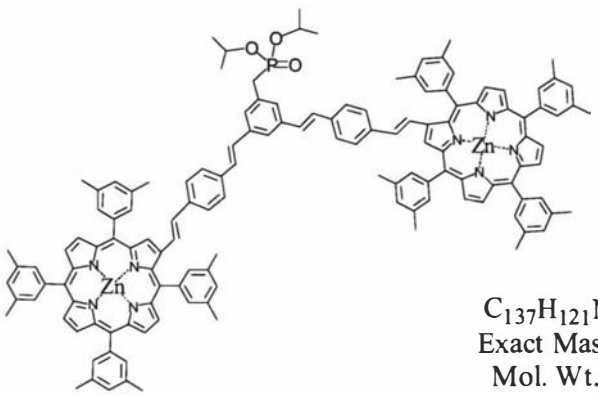

$C_{137}H_{121}N_8O_3PZn_2$
Exact Mass: 2084.79
Mol. Wt.: 2089.23

185 mg (201 μmol) of **Zn-15** and 50 mg (81.5 μmol) of **28** were dissolved in 100 mL of dry THF, under argon atmosphere. To the stirred solution, 30 mg (267 μmol) of ^{t}BuOK in dry THF were added in two portions in 30 min. After further 30 min, the solution was evaporated to dryness and the crude was purified through flash chromatography on silica gel: **Zn-15** and side-products were eluted with DCM after which the desired product was eluted with DCM/MeOH = 100/1. 115 mg (54%) of pure **Zn-30** were obtained by recrystallization from DCM/hexane as purple-green crystals. ^{1}H-NMR (500 MHz, $CDCl_3$): δ 9.14 (s, 2H, $H_{\beta\text{-pyrrolic}}$), 8.96-8.90 (m, 12H, $H_{\beta\text{-pyrrolic}}$), 7.88-7.83 (m, 16H, $H_{o\text{-xylene}}$), 7.58-7.38 (m, 14H, $8H_{p\text{-xylene}}$ + $4H_{Ph'}$ + $2H_{alkene}$), 7.34-7.22 (m, 8H, $4H_{Ph'}$ + $2H_{alkene}$ + $2H_{alkene'}$), 7.17-7.09 (m, 5H, $3H_{Ph''}$ + $2H_{alkene'}$), 4.29-4.17 (m, 2H, $H_{CH\text{-propyl}}$), 2.70-2.55 (m, 50H, $48H_{xylene}$ + $2H_{CH2\text{-}P}$), 1.09 (dd, *conformational doubling* = 55 Hz, J = 6 Hz, 12H, $H_{CH3\text{-propyl}}$). *Assignments aided by variable concentration and COSY spectra.* UV-vis (CH_2Cl_2): λ_{max} [nm] (ε x 10^{-3}) 430 (326), 559.5 (36.2), 595.5 (20.3). FAB-HRMS for MH^+ ($C_{137}H_{122}N_8PO_3Zn_2$): 2085.7888, calculated: 2085.7960.

((ZnTPP)$_2$-Ph)$_2$-Ph-ipp, Zn-31.

3,5-bis(*trans*-2'-(3",5"-bis(*trans*-2'''-(2''''-(5'''',10'''',15'''',20''''-tetraphenylporphyrinato zinc(II))yl)ethen-1'''-yl)phenyl) ethen-1'-yl)methyl(diisopropylphosphonate)benzene.

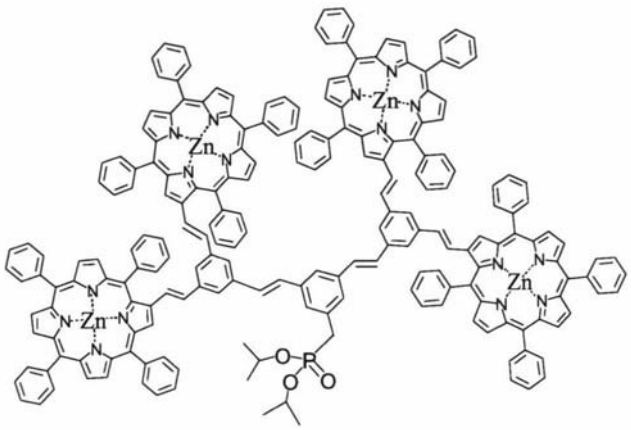

$C_{213}H_{145}N_{16}O_3PZn_4$
Exact Mass: 3260.86
Mol. Wt.: 3269.07

108 mg (71 μmol) of **Zn-25** and 17.6 mg (28.7 μmol) of **28** were dissolved in 50 mL of dry THF, under argon atmosphere. To the stirred solution, 12 mg (107 μmol) of solid ^{t}BuOK were added in two portions in 50 min. After further 10 min, the solution was evaporated to dryness, dissolved in DCM and precipitated by adding MeOH. The crude was purified through flash chromatography on silica gel: **Zn-25** and side-products were eluted with DCM after which the desired product was eluted with DCM/MeOH = 100/1. 60 mg (52%) of pure **Zn-31** were obtained by recrystallization from DCM/MeOH as purple-green crystals. ^{1}H-NMR (500 MHz, $CDCl_3$): δ 9.29 (s, 4H, $H_{\beta\text{-pyrrolic}}$), 8.98-8.80 (m, 24H, $H_{\beta\text{-pyrrolic}}$), 8.36-8.12 (m, 32H, $H_{o\text{-Ph}}$), 7.93-7.58 (m, 48H, $H_{m,p\text{-Ph}}$), 7.41-7.28 (m, 11H, $4H_{Ph'} + 3H_{Ph''} + 4H_{alkene'}$), 7.22 (d, J = 16 Hz, 4H, H_{alkene}), 7.02 (d, J = 16 Hz, 4H, H_{alkene}), 6.92 (br s, 2H, $H_{Ph'}$), 4.88-4.76 (m, 2H, $H_{CH\text{-propyl}}$), 3.40-2.43 (br s, 2H, $H_{CH2\text{-P}}$), 1.08 (dd, *conformational doubling* = 24 Hz, $J_{H\text{-}H}$ = 6 Hz, 12H, $H_{CH3\text{-propyl}}$). *Assignments aided by variable concentration and COSY spectra.* UV-vis (CH_2Cl_2): λ_{max} [nm] (ε x 10^{-3}) 428 (547), 557.5 (59.7), 592.5 (28.9). FAB-LRMS for M^+ ($C_{213}H_{145}N_{16}PO_3Zn_4$): cluster 3261.8-3275.8 (max 3269.8), calculated: cluster 3261.8-3276.8 (max 3268.8).

((NiTPP)$_2$-Ph)$_2$-Ph-ipp, Ni-31.

3,5-bis(*trans*-2'-(3",5"-bis(*trans*-2"'-(2""-(5"",10"",15"",20""-tetraphenylporphyrinato nickel(II))yl)ethen-1"'-yl)phenyl) ethen-1'-yl)methyl(diisopropylphosphonate)benzene.

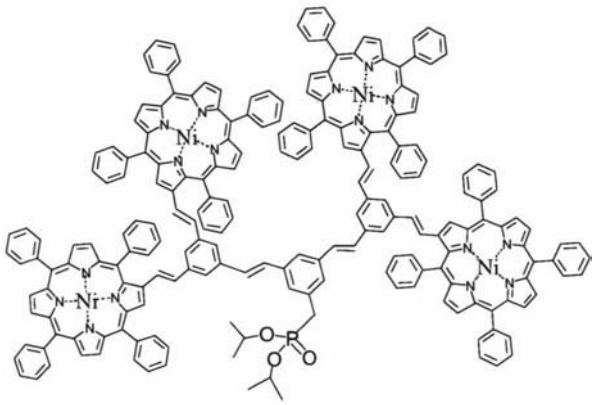

$C_{213}H_{145}N_{16}Ni_4O_3P$
Exact Mass: 3236.88
Mol. Wt.: 3242.28

500 mg (334 μmol) of **Ni-25** and 112 mg (183 μmol) of **28** were dissolved in 250 mL of dry THF, under argon atmosphere. To the stirred solution, 45 mg (401 μmol) of solid ^{t}BuOK were added in three portions in 60 min. After further 10 min, the solution was evaporated to dryness, dissolved in DCM and precipitated by adding MeOH. The crude was purified through flash chromatography on silica gel (DCM/MeOH = 200/1): **Ni-25** and side-products were eluted before the desired product was collected. 231 mg (43%) of pure **Ni-31** were obtained by recrystallization from DCM/MeOH as purple-red crystals. ^{1}H-NMR (400 MHz, $CDCl_3$): δ 9.02 (s, 4H, $H_{\beta\text{-pyrrolic}}$), 8.75-8.64 (m, 24H, $H_{\beta\text{-pyrrolic}}$), 8.12-7.93 (m, 32H, $H_{o\text{-Ph}}$), 7.78-7.56 (m, 51H, 48$H_{m,p\text{-Ph}}$ +3$H_{Ph''}$), 7.38 (d, J = 16.1 Hz, 2H, $H_{alkene'}$), 7.30 (d, J = 16.1 Hz, 2H, $H_{alkene'}$), 7.28 (br s, 2H, $H_{Ph''}$), 7.22 (d, J = 15.9 Hz, 4H, H_{alkene}), 7.02 (d, J = 15.9 Hz, 4H, H_{alkene}), 6.92 (br s, 2H, $H_{Ph'}$), 4.86-4.76 (m, 2H, $H_{CH\text{-propyl}}$), 3.40 (d, J_P = 22 Hz, 2H, $H_{CH2\text{-P}}$), 1.39 (dd, *conformational doubling* = 34 Hz, $J_{H\text{-}H}$ = 6.2 Hz, 12H, $H_{CH3\text{-propyl}}$). *Assignments aided by COSY spectra.* UV-vis (CH_2Cl_2): λ_{max} [nm] (ε x 10^{-3}) 427.5 (512), 539 (53.2), 580 (42.3). FAB-HRMS for M^+ ($C_{213}H_{145}N_{16}PO_3{}^{58}Ni_4$): 3236.8858, calculated: 3236.8837.

(NiTPP-Ph)$_2$-Ph-Ph-ZnTXP, Ni$_2$Zn-32.

1-(*trans*-2'-(4"-(*trans*-2"'-(2""-(5"",10"",15"",20""-tetra(3"",5""-dimethylphenyl)-porphyrinato zinc(II))yl)-ethen-1"'-yl)-phenyl) ethen-1'-yl)-3,5-bis(*trans*-2'-(4"-(*trans*-2"'-(2""-(5"",10"",15"",20""-tetraphenylporphyrinato zinc(II))yl)ethen-1"'-yl)phenyl)ethen-1'-yl)benzene.

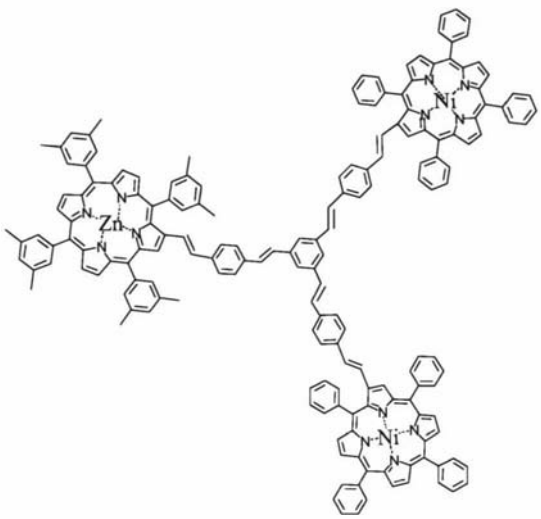

$C_{176}H_{124}N_{12}Ni_2Zn$
Exact Mass: 2584.81
Mol. Wt.: 2589.72

50 mg (54.4 μmol) of aldehyde **Zn-10** and 102 mg (71.9 μmol) of phosphonate **Ni-20** were dissolved in 100 mL of dry THF, under argon atmosphere. To the stirred solution, 15 mg (134 μmol) of solid ^{t}BuOK were added in two portions in 30 min. After further 10 min, the solution was evaporated to dryness and the crude was purified through flash chromatography on silica gel (DCM/toluene = 3/2): the first band was collected and recrystallized from DCM/hexane to yield 120 mg (85%) of pure **Ni$_2$Zn-32** as purple crystals. Excess **Ni-20** was recovered by elution with DCM/methanol = 100/1. ^{1}H-NMR (500 MHz, $CDCl_3$): δ 9.16 (s, 1H, $H_{\beta\text{-pyrrolic(Zn)}}$), 8.98-8.90 (m, 8H, $6H_{\beta\text{-pyrrolic(Zn)}}$ + $2H_{\beta\text{-pyrrolic(Ni)}}$), 8.74-8.67 (m, 12H, $H_{\beta\text{-pyrrolic(Ni)}}$), 8.08-7.96 (m, 16H, $H_{o\text{-Ph(Ni)}}$), 7.91-7.79 (m, 8H, $H_{o\text{-xylene(Zn)}}$), 7.77-7.65 (m, 24H, $H_{m,p\text{-Ph(Ni)}}$), 7.62-7.46 (m, 10H, $4H_{p\text{-xylene(Zn)}}$ + $6H_{Ph'}$), 7.41-7.10 (m, 19H, $6H_{Ph'}$ + $3H_{Ph''}$ + $6H_{alkene}$ + $4H_{alkene''}$), 6.91 (d, J = 16 Hz, 2H, $H_{alkene'(Ni)}$), 2.65-2.55 (m, 24H, H_{xylene}). *Assignments aided by COSY spectra.* UV-vis (CH_2Cl_2): λ_{max} [nm] (ε x 10^{-3}) 430 (305), 552.5 (40.8), 589 (33.3). FAB-HRMS for M^+ ($C_{176}H_{124}N_{12}{}^{58}Ni_2Zn$): 2584.8075, calculated: 2584.8070.

(NiTPP-Ph)$_2$-Ph-Ph-(ZnTXP)$_2$, Ni$_2$Zn$_2$-33.

1-(*trans*-2'-(3",5"-bis-(*trans*-2"'-(2""-(5"",10"",15"",20""-tetra(3"",5""-dimethylphenyl)-porphyrinato zinc(II))yl)ethen-1"'-yl)phenyl) ethen-1'-yl)-3,5-bis(*trans*-2'-(4"-(*trans*-2"'-(2""-(5"",10"",15"",20""-tetraphenylporphyrinato zinc(II))yl)ethen-1"'-yl)phenyl)ethen-1'-yl)benzene.

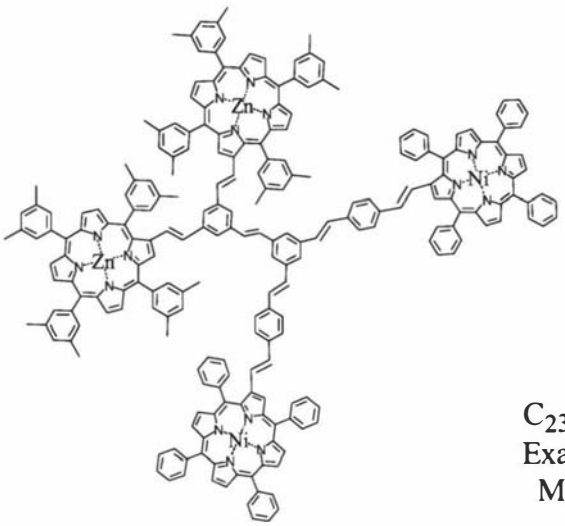

$C_{230}H_{168}N_{16}Ni_2Zn_2$
Exact Mass: 3397.09
Mol. Wt.: 3404.07

35 mg (20.2 μmol) of aldehyde **Zn-18** and 50 mg (27.0 μmol) of phosphonate **Ni-31** were dissolved in 50 mL of dry THF, under argon atmosphere. To the stirred solution, 8 mg (71.3 μmol) of solid ^{t}BuOK were added in two portions in 30 min. After further 30 min, the solution was evaporated to dryness and the crude was purified through flash chromatography on silica gel (DCM/toluene = 3/2): the first band was collected and recrystallized from DCM/hexane to yield 51 mg (75%) of pure **Ni$_2$Zn$_2$-33** as purple crystals. Excess **Ni-31** was recovered by elution with DCM/methanol = 100/1. ^{1}H-NMR (500 MHz, $CDCl_3$): δ 9.35 (s, 2H, $H_{\beta\text{-pyrrolic(Zn)}}$), 9.01-8.91 (m, 12H, $H_{\beta\text{-pyrrolic(Zn)}}$), 8.73-8.66 (m, 14H, $H_{\beta\text{-pyrrolic(Ni)}}$), 8.08-7.93 (m, 24H, $16H_{o\text{-Ph(Ni)}} + 8H_{o\text{-xylene(Zn)}}$), 7.88-7.62 (m, 36H, $24H_{m,p\text{-Ph(Ni)}} + 8H_{o\text{-xylene(Zn)}} + 4H_{p\text{-xylene(Zn)}}$), 7.58-7.38 (m, 15H, $4H_{p\text{-xylene(Zn)}} + 4H_{Ph'(Ni)} + 3H_{Ph'(Zn)} + 2H_{Ph''} + 2H_{alkene(Zn)}$), 7.36-7.31 (m, 6H, $4H_{alkene(Ni)} + 2H_{alkene(Zn)}$) 7.25-7.10 (m, 11H, $4H_{Ph'(Ni)} + 1H_{Ph''} + 2H_{alkene'(Ni)} + 1H_{alkene'(Zn)}$), 6.95-6.88 (m, 3H, $2H_{alkene'(Ni)} + 1H_{alkene'(Zn)}$), 2.66-2.53 (m, 48H, H_{xylene}). *Assignments aided by COSY spectra.* UV-vis (CH_2Cl_2): λ_{max} [nm] ($\varepsilon \times 10^{-3}$) 430.5 (585), 556.5 (53.9), 588(shoulder) (38.3). FAB-LRMS for M^- ($C_{230}H_{168}N_{16}{}^{58}Ni_2Zn_2$): cluster 3398.5-3411.5 (max 3404.1), calculated: cluster 3398.1-3411.1 (max 3404.1).

((NiTPP)$_2$-Ph)$_2$-Ph-Ph-ZnTXP, Ni$_4$Zn-34.

1-(*trans*-2'-(4"-(*trans*-2"'-(2""-(5"",10"",15"",20""-tetra(3"",5""-dimethylphenyl)-porphyrinato zinc(II))yl)ethen-1"'-yl)phenyl) ethen-1'-yl)-3,5-bis(*trans*-2'-(3",5"-bis(*trans*-2"'-(2""-(5"",10"",15"",20""-tetraphenylporphyrinato zinc(II))yl)ethen-1"'-yl)phenyl)ethen-1'-yl)benzene.

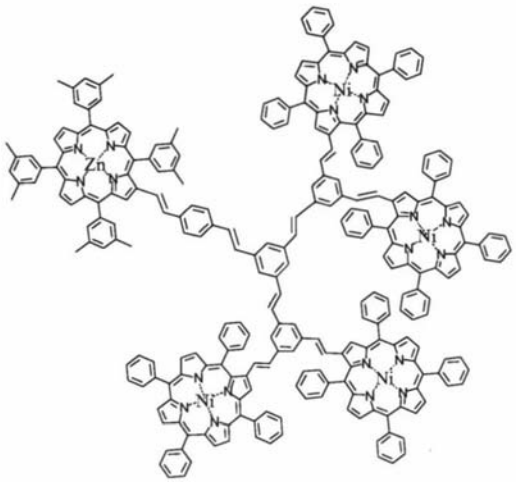

$C_{268}H_{180}N_{20}Ni_4Zn$
Exact Mass: 3973.14
Mol. Wt.: 3980.59

28.5 mg (31.0 μmol) of aldehyde **Zn-15** and 115 mg (35.5 μmol) of phosphonate **Ni-31** were dissolved in 50 mL of dry THF, under argon atmosphere. To the stirred solution, 8 mg (134 μmol) of solid ^{t}BuOK were added. After 45 min, the solution was evaporated to dryness and the crude was purified through flash chromatography on silica gel (DCM/toluene = 3/2): the first band was collected and recrystallized from DCM/hexane to yield 47 mg (38%) of pure **Ni$_4$Zn-34** as purple-red crystals. Unreacted **Zn-15** and **Ni-31** were eluted respectively with DCM and DCM/MeOH = 100/1. ^{1}H-NMR (500 MHz, $CDCl_3$): δ 9.16 (s, 1H, $H_{\beta\text{-pyrrolic(Zn)}}$), 9.04 (s, 4H, $H_{\beta\text{-pyrrolic(Ni)}}$), 8.97-8.91 (m, 6H, $6H_{\beta\text{-pyrrolic(Zn)}}$), 8.78-8.62 (m, 24H, $H_{\beta\text{-pyrrolic(Ni)}}$), 8.15-7.56 (m, 16H, $H_{o\text{-Ph(Ni)}}$), 7.91-7.79 (m, 8H, $H_{o\text{-xylene(Zn)}}$), 7.77-7.65 (m, 24H, $H_{m,p\text{-Ph(Ni)}}$), 7.62-7.46 (m, 10H, $4H_{p\text{-xylene(Zn)}} + 6H_{Ph'}$), 7.41-7.10 (m, 19H, $6H_{Ph'} + 3H_{Ph''} + 6H_{alkene} + 4H_{alkene''}$), 6.91 (d, J = 16 Hz, 2H, $H_{alkene'(Ni)}$), 2.65-2.55 (m, 24H, H_{xylene}). *Assignments aided by COSY spectra.* UV-vis (CH_2Cl_2): λ_{max} [nm] ($\varepsilon \times 10^{-3}$) 428.5 (1390), 542.5 (128), 575 (100). FAB-LRMS for M^- ($C_{268}H_{108}N_{20}{}^{58}Ni_4Zn$): cluster 3973-3988 (max 3980), calculated: cluster 3973.1-3988.1 (max 3980.1).

3. COORDINATION OF PENDANT PHOSPHONATE GROUPS IN Zn PORPHYRINS

3.1. Introduction

During the investigation of array syntheses that involved porphyrins and phosphonates, some unusual data were observed. The resonances in the NMR spectra of porphyrins, which contained one or two phosphonate groups, showed substantial shifts when metallated with Zn. We have seen that the reaction between Zn porphyrin aldehyde **Zn-5** and triphosphonate **21** is part of our strategy for dendrimer syntheses. This reaction, in appropriate conditions, produces a mixture of vinyl-substituted porphyrins as *cis/trans* isomers (Scheme 3-1).

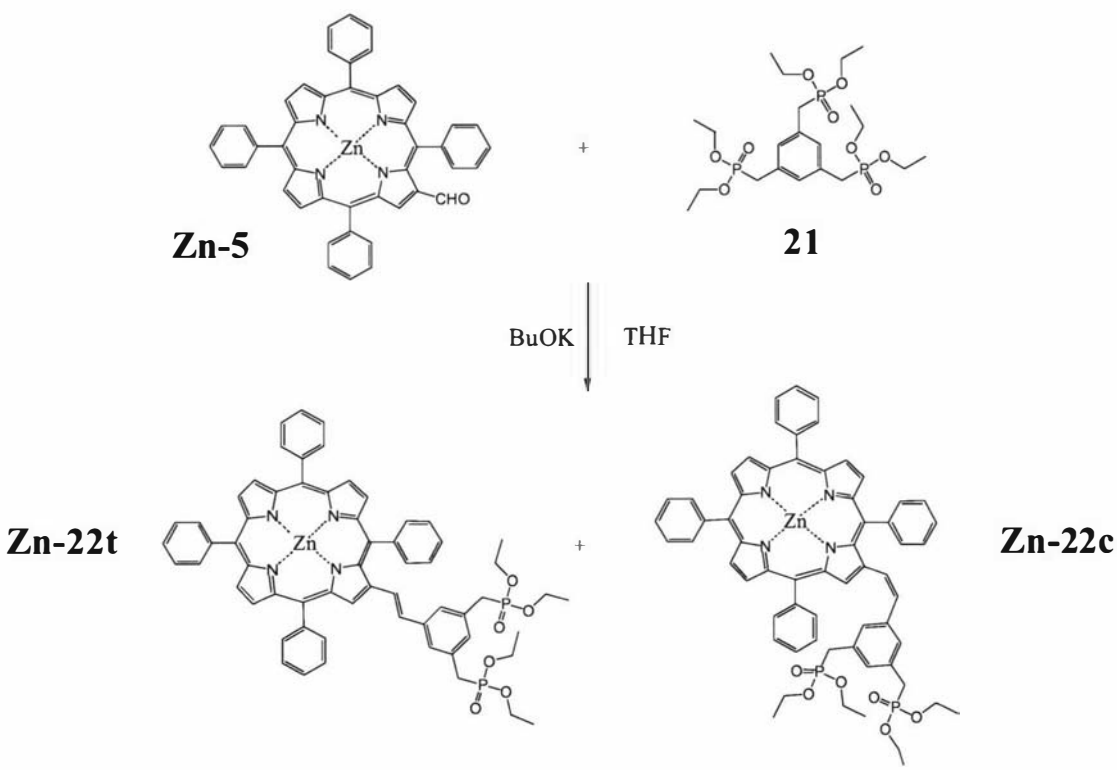

Scheme 3-1 Aldehyde **Zn-5** reaction with triphosphonate **21**

While similar reactions involving the Ni homologue or other Zn porphyrin aldehydes like **Zn-14, Zn-15, Zn-18** and **Zn-25** gave a ratio *trans/cis* > 20/1, in the case shown in Scheme 3-1 the ratio is < 7/3. Moreover, the two isomers showed a quite different

behaviour on chromatography; TLC (silica gel, DCM/MeOH = 100/1) of the mixture produced two separate bands with the *cis* isomer on the top (lower polarity) and, unlike all other *cis/trans* isomer mixtures described in this thesis, it was possible to separate the isomers by careful column chromatography.

In addition, the position of non-porphyrinic ^{1}H-NMR resonances in **Zn-22c** were quite different from all the other described porphyrins; in particular, most of the protons belonging to the *β*-pyrrolic substituent (vinyl, phenyl and phosphonate protons) showed resonances at higher field then expected (by comparison to other Zn porphyrins and other *cis* products). Therefore, the nature of the unexpected shifts was investigated.

3.2. ^{1}H-NMR investigation of Zn coordination in Zn-22 isomers

Figure 3-1 shows the ^{1}H-NMR spectra of the isomers **Zn-22c** and **Zn-22t**: it can be seen that the resonance of the vinyl, phenyl and phosphonate groups are quite different, and at particularly high fields in the case of the *cis* isomer.

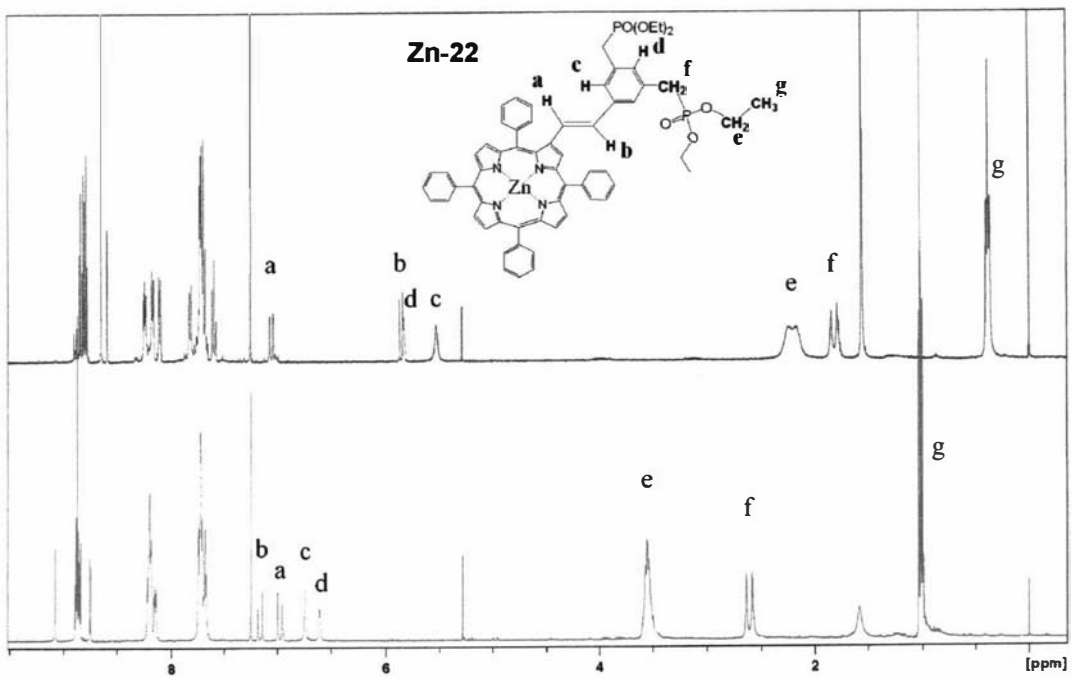

Figure 3-1 ^{1}H-NMR (500 MHz) spectra of **Zn-22t** (bottom) and **Zn-22c** (top)

A comparison of these spectra with those obtained for the Ni and free base homologues is necessary to provide some indication about the cause of the shifts. **Ni-22** (Scheme 3-2) was obtained as a mixture of *cis/trans* isomers with the same procedure described for **Zn-22** in Scheme 3-1. Free-base porphyrins **22c** and **22t** were prepared by demetallation from **Zn-22c** and **Zn-22t**. First attempts to demetallate **Zn-22c** only produced **22t**, presumably due to acid catalyzed isomerization; to avoid this, the treatment with the acid solution was reduced to just 30 seconds.

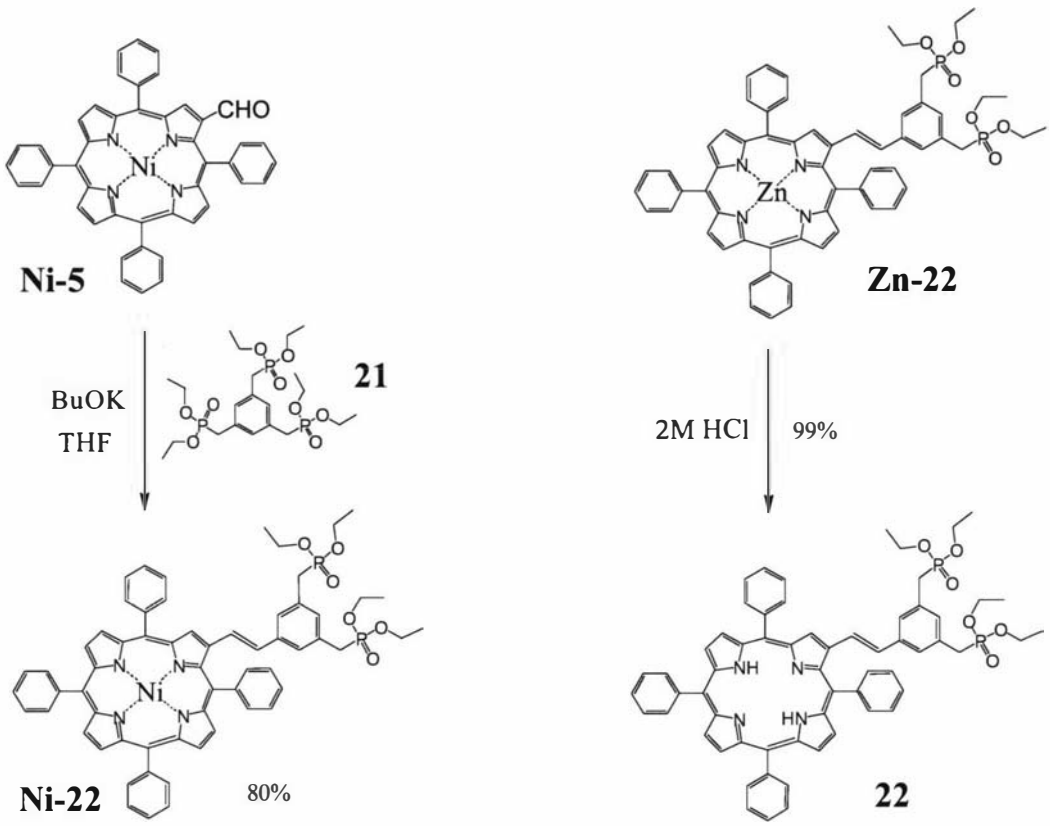

Scheme 3-2 Preparations of **Ni-22** and free base **22**

The ^{1}H-NMR spectra of **Ni-22** and free-base **22** are very similar. In both the cases, the *cis* isomers show large (0.5-1 ppm) high field shifts for the vinyl signals and smaller (0.2-0.5 ppm) shifts for the phosphonate protons (Table 3-1). Compared to **Zn-22c**, however, the *cis/trans* effects on the chemical shifts are very different; the shifts are smaller, there is no inversion of the positions of the resonances attributed to the aryl ring (peaks **c** and **d** in Figure 3-1 and Table 3-1) and the vinyl proton **a** is shifted in the opposite direction. It is evident that the *cis* configuration in **Zn-22c** is responsible for only a part of these anomalies.

	a [a]	b [a]	c [a]	d [a]	e [a]	f [a]	g [a]	c.d. [b]
Zn-3t	6.98	7.16	6.74	6.60	3.55	2.61	1.02	large
Zn-3c	7.05	5.86	5.53	5.83	2.21	1.81	0.38	small
Ni-3t	6.86	7.10	6.98	7.11	4.06	3.15	1.30	no
Ni-3c	6.33	6.16	7.14	7.06	3.70	2.89	0.93	no
H_2-3t	7.01	7.28	7.07	7.16	4.08	3.19	1.30	no
H_2-3c	6.44	6.30	7.10	7.03	3.65	2.81	0.87	no

a. Refers to labels in Fig.1
b. concentration dependence

Table 3-1 ^{1}H-NMR (400 MHz) chemical shifts of variously metallated *cis* and *trans* **M-22**

The large shifts observed in this series of similar molecules can only be explained by a variation in the effect of the porphyrin ring (and, to a minor degree, the meso phenyl rings) anisotropy on the corresponding protons of the different porphyrins. As is well known, the large magnetic field-induced ring current in aromatic systems such as porphyrins cause a significant local anisotropy field that shields or deshields all close nuclei.[108,109] A clear example is shown in Figure 3-2a: [18]annulene contains two kind of protons, both of them linked to the same type of carbon and they would be expected to have chemical shifts around $\delta = 5.5$ ppm (relative to TMS). Because of the ring current that deshields the external protons and shields the internal ones, the two set of protons show signals respectively at $\delta = 9.3$ ppm and at $\delta = -3.0$ ppm.[109]

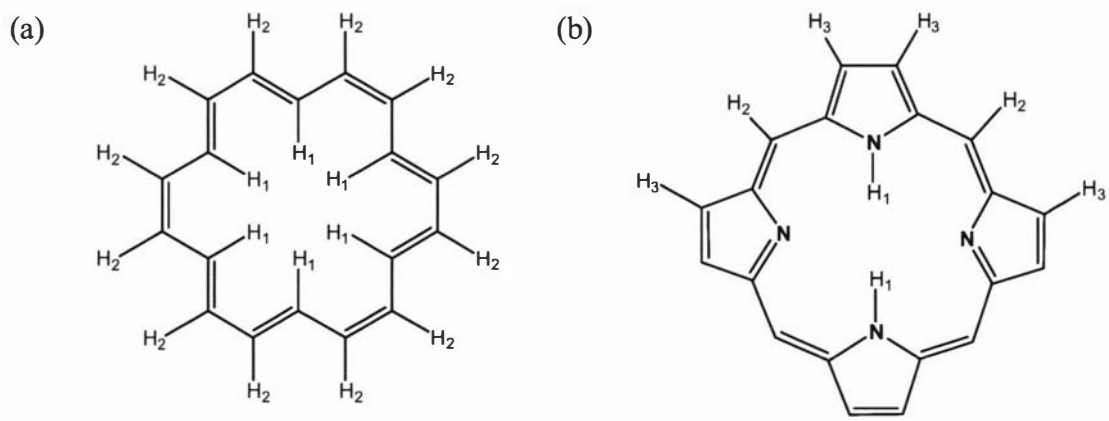

Figure 3-2 Ring current effect on proton chemical shifts in annulene (a) and a general porphyrin (b)

The analogous structure of porphyrins produces very similar shielding effects and this has been particularly useful for the study of axial coordination of metalloporphyrins. Theoretical calculations[110] and empirical studies[111] allow the correlation of the shielding effect on the position of nuclei; to a good approximation, Figure 3-3 shows how to estimate the actual shifts due to the ring-current magnetic field knowing radial (ρ) and axial (z) distances from the porphyrin centre. As a result, coordination equilibria can be studied by measuring NMR chemical shifts.

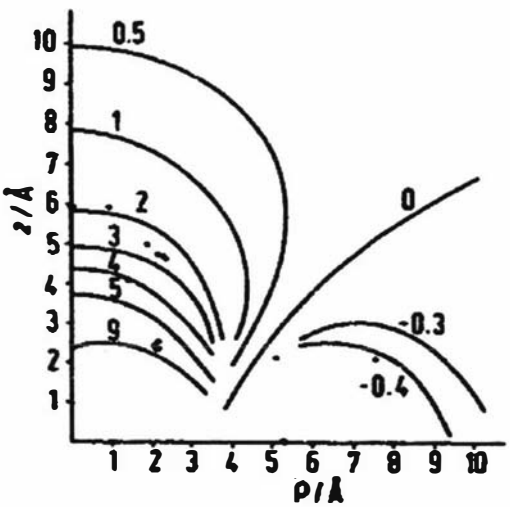

Figure 3-3 Empirical estimate of ring current shield (in ppm) in porphyrins by Riche *et al.*[111]

With regard to **M-22c** and **M-22t**, the difference in the vinyl resonance of the *cis* and *trans* isomers is largely due to the different geometry of the two molecules. In the *trans* case, the double bond lies in the same plane as the porphyrin[112] while in the *cis* case, because of the steric hinderance caused by the phenyl rings, the double bond has to lie out of the porphyrin plane where the protons are less deshielded (Figure 3-4). Also, all the benzene phosphonate substituent lies in a less deshielded region, explaining the general high field shifts recorded for all the *cis* isomers. Finally, the different geometry of the double bond produces a similar effect on the β-pyrrolic proton α to the linker (proton **a**, Figure 3-1), which in the *cis* case does not show the further deshielding due to the double bond anisotropy ($\delta = 9.08$ ppm in **Zn-22t** and $\delta = 8.60$ ppm in **Zn-22c,** Figure 3-1). Regardless of all of this, the described proton shifts of the Zn homologues (including the concentration dependence of some chemical shifts) have to be explained by some other factor.

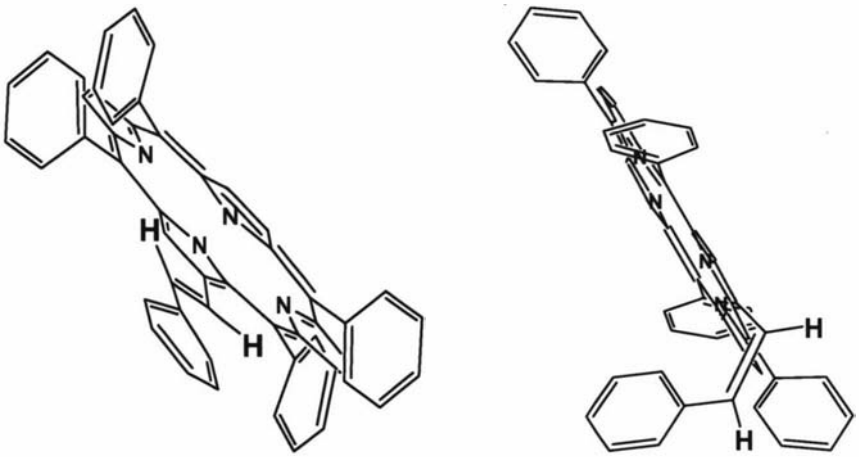

Figure 3-4 Computer-generated models of the conformations in *trans* and *cis* isomers of **M-22** (the phosphonate groups are not shown for clarity)

3.3. Phosphonate coordination to Zn porphyrins

It is known that phosphonates can coordinate to a Zn centre[113] (usually tetrahedrally) but, to the best of our knowledge, there are no reports in which a phosphonate coordinates to a Zn atom that is already strongly coordinated such as in Zn porphyrins. However, it is well known that Zn porphyrins undergo further coordination to other O-ligands (e.g. water, alcohols, ketones, ethers) or N-ligands.[114-118]

When a ligand binds to a Zn porphyrin, the coordinating atom must approach the porphyrin centre where the ring current produces the strongest shielding effect. Therefore, the larger shifts in **Zn-22** can be explained by coordination of a phosphonate group which brings this part of the molecule inside the shielding zone of the porphyrin core (Figure 3-5). This could occur by oxygen coordination either inter- or intra-molecularly, although the absence of similar effects on the NMR spectra of the *trans* isomer (in which intramolecular coordination could not occur) suggested that this was an intramolecular phenomenon.

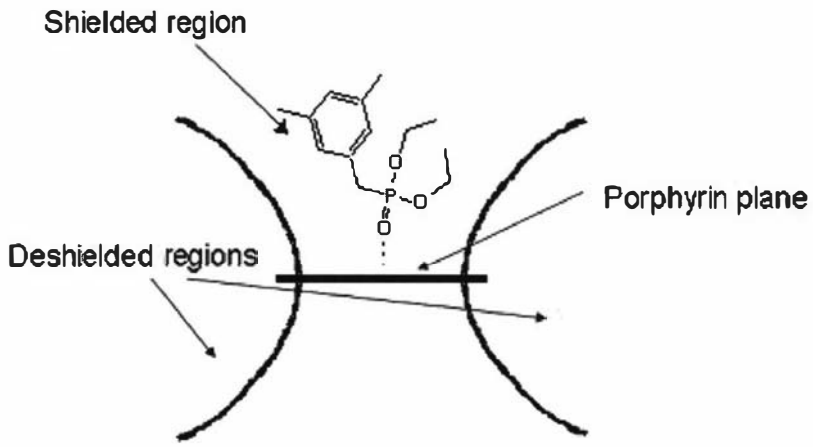

Figure 3-5 Phosphonate coordination to a Zn porphyrin

To investigate how the coordination was occuring, ZnTPP **Zn-3** was used to titrate solutions of a phosphonate, a phosphoxide and a phosphite and the titrations were were followed by ^{31}P-NMR spectroscopy. The resulting high-field shifts, reported in Figure 3-6, indicate the presence of coordination equilibria, as is the case with **Zn-22**. Furthermore, the similarity between phosphonate and phosphoxide behaviour strongly suggests that the coordination occurs through the P=O bond.

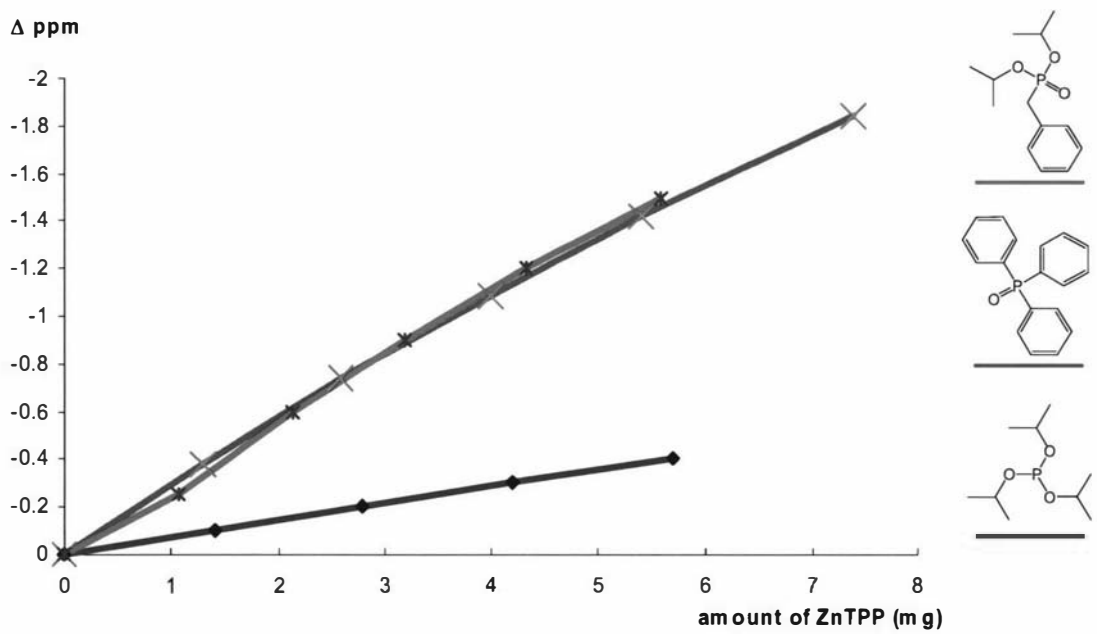

Figure 3-6 ZnTPP titration of ligands containing P-O bonds using ^{31}P-NMR

Another indication of coordination equilibria obtained by NMR is the concentration dependence of the **Zn-22** proton peak positions. Unlike their free-base and Ni-

metallated homologues, the resonance peaks of these molecules, especially in the non-porphyrin region, move to higher fields as the solution concentration increases; this is consistent with a coordination equilibrium in which a higher concentration increases the ratio of coordinated/uncoordinated phosphonate groups. The concentration dependence also helps explain the difference between the *cis/trans* isomers. When a solution of **Zn-22t** was diluted ten times, a 0.21 ppm low-field shift of the methyl group signals occurred while, under the same conditions, **Zn-22c** showed a shift of only 0.02 ppm (Figure 3-7); the other protons of the phosphonate group also showed similar shifts. Similarly, ^{31}P-NMR resonances were shifted by 0.70 ppm for **Zn-22t** and just 0.04 for **Zn-22c**. Clearly, the two isomers coordinate in a different way.

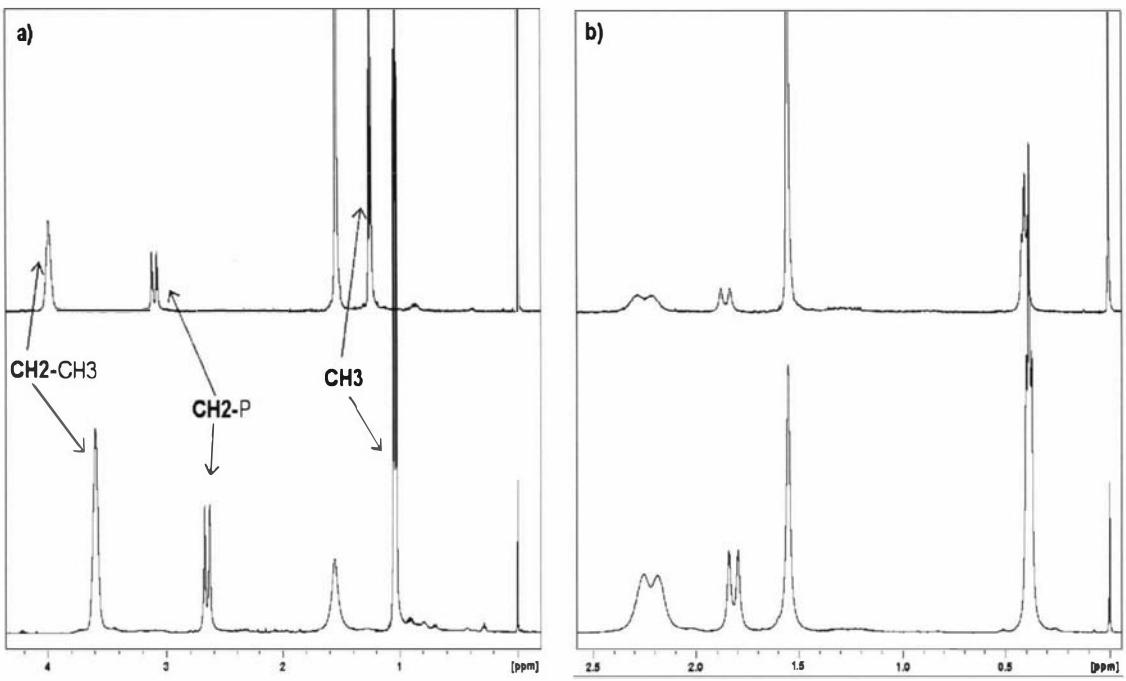

Figure 3-7 ^{1}H-NMR (500 MHz) spectra of **Zn-22t** (a) and **Zn-22c** (b) at concentrations of 10^{-2}M (bottom) and 10^{-3}M (top)

Figure 3-8 shows a computer generated model of the **Zn-22c** structure; here, one phosphonate group can be arranged in a position in which it is very close to the Zn of the same molecule. Therefore, it is possible to have intramolecular coordination.

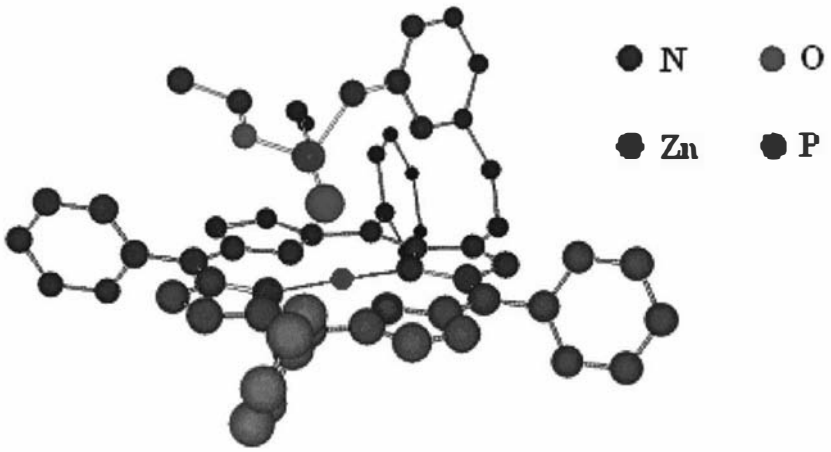

Figure 3-8 Simulated 3-dimensional structure of **Zn-22c** (the second phosphonate is not shown for clarity)

The intramolecular coordination could also explain the low field position of one of the vinyl protons in **Zn-22c** (proton **a** in Figure 3-1 and Table 3-1). To bring the coordinating phosphonate at bonding distance, a slight distortion of the β-pyrrolic substituent may be required; by moving the Zn porphyrin–vinyl bond slightly out-of-plane, as shown in Figure 3-9, one of the vinyl protons gets closer to the porphyrin plane (more deshielded region) while the other one moves in the opposite direction. These observed chemical shift differences are consistent with the ring current effects.

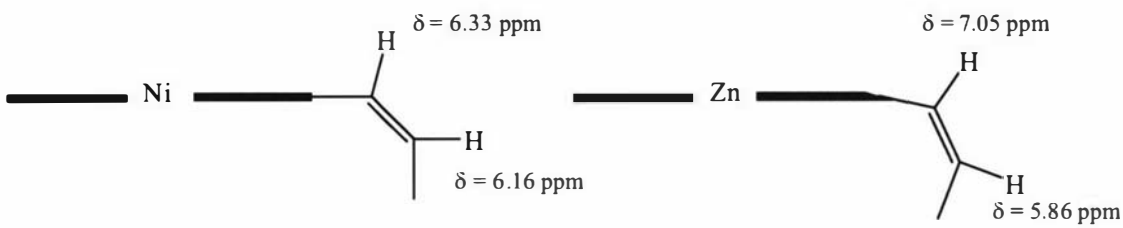

Figure 3-9 Bond distortion effect on vinyl NMR resonances of **Ni-22c** and **Zn 22c**

Although we can not fully understand the complex equilibria of all the species in solution, it can be observed that the barely noticeable concentration effect on **Zn-22c** NMR chemical shifts, compared to the **Zn-22t** is consistent with the hypothesis in which the zinc is mainly coordinated intramolecularly to one of the phosphonate groups.

Evidence for intramolecular coordination could be obtained from the examination of **Zn-36c,** the parent molecule carrying just one phosphonate. Diphosphonate **35** was

prepared according to general procedures[102,107] from the commercial dibromo homologue and reacted with aldehyde **Zn-5** (Scheme 3-3). Unfortunately, less then 5% of the *cis* isomer was obtained, and it was not possible to isolate it from the *trans* homologue.

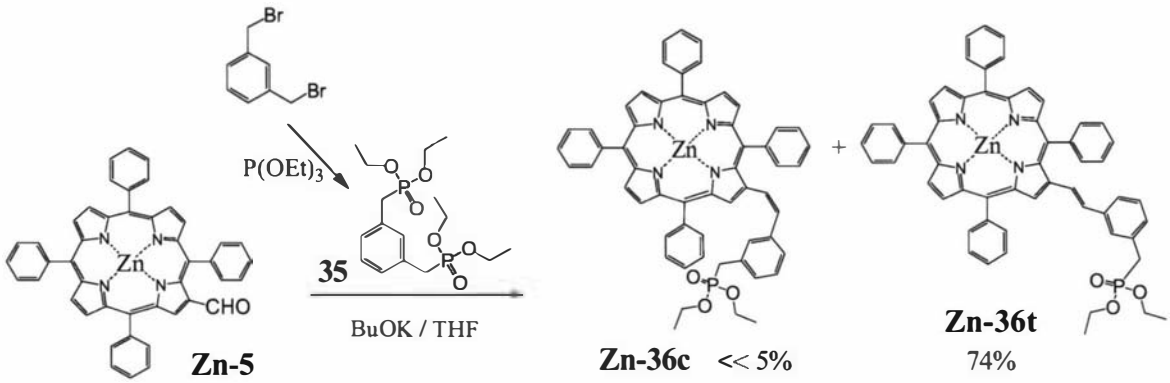

Scheme 3-3 Porphyrin phosphonate **Zn-36** synthesis

Nonetheless, the NMR spectrum of the mixture (Figure 3-10) shows a methyl group resonance that is significantly shifted to negative fields and which is a well defined sharp triplet whose chemical shift is not concentration dependent. This is consistent with intramolecular coordination in the *cis* isomer that is not subject to equilibrium.

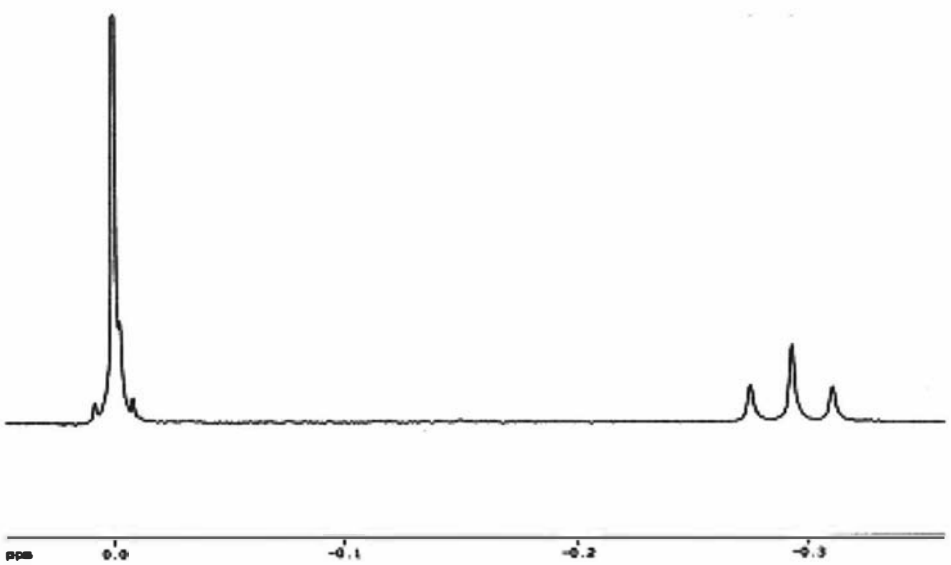

Figure 3-10 ^{1}H-NMR (400 MHz) resonance of methyl groups in **Zn-36c**

3.4. Low temperature NMR experiments

By comparing the spectra of **Zn-22c** and **Zn-36c** (Figure 3-7b and Figure 3-10) it can be noticed that in the case in which only one phosphonate group is present, the resonance of the methyl group is at even higher field and the triplet is better resolved; the explanation for this could be that the two phosphonates in **Zn-22c** interchange their position giving a single signal, an average of the coordinated and non-coordinated phosphonate groups.

In order to prove that the unexpected high field shift in **Zn-22c** is the result of this intramolecular phosphonate interchange, variable temperature NMR experiments were carried out. At low temperatures, it is possible to 'freeze' the exchange equilibria and to separate the different resonance shifts. Figure 3-11a shows the peaks attributed to the methyl groups at different temperatures; on cooling down, the peak at δ = 0.35 ppm (average of four methyl groups) splits into two, well separated resonances attributed to the coordinated ($\delta \doteqdot$ -0.40 ppm) and uncoordinated (δ = 1.20 ppm) phosphonates. The same behaviour was observed using the ^{31}P resonances of the phosphonate group (Figure 3-11b).

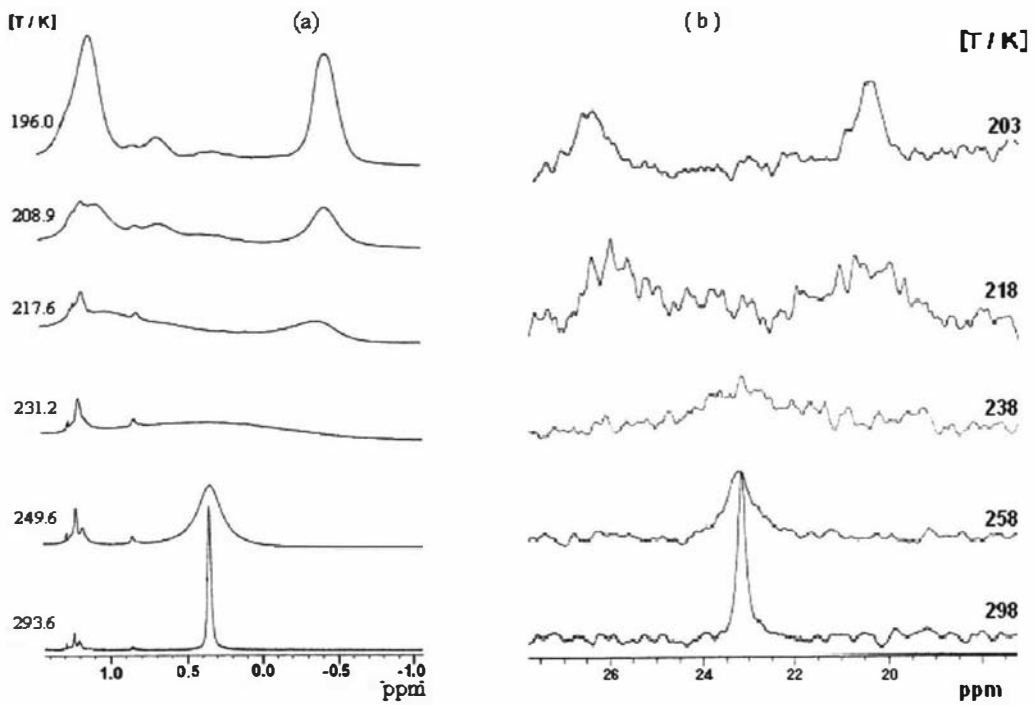

Figure 3-11 (a) ^{1}H-NMR (700 MHz) and (b) ^{31}P-NMR (400 MHz) spectra of **Zn-22c** at various temperatures

From a comparison of Figures 3-10 and 3-11a (T = 196 K), it is clear that the two resonances attributed to the intramolecularly coordinated phosphonate methyl groups are at similar positions in both the *cis* compounds (-0.3 and -0.4 ppm respectively for **Zn-36c** and **Zn-22c**). This fact is consistent with the freezing of the intramolecular interchange in **Zn-22c** at such low temperatures, giving two different signals for coordinated and non-coordinated groups.

Quantitative data about the exchange rate and the energy involved in this process can be obtained from the analysis of the line-shape of the NMR spectra. In the absence of spin-spin coupling between the two sites, Gutowsky and Holm[119] derived an equation which permits a determination of the lifetime of the exchange process ($\tau = {}^{\tau_A}/_{2} = {}^{\tau_B}/_{2}$), providing that the separation between the two signals under slow exchange conditions ($\delta\nu = \nu_A - \nu_B$), the spin-spin relaxation time T_2 and the population of the two sites (in this case, $p_A = p_B = 0.5$) are known (Equation 3-1).

According to the theory, the intensity of the absorption is represented by the imaginary part (n) of the total magnetization of the nuclei involved

(Eq. 3-1)
$$n = \frac{\omega_i M_0 \left[\left(1 + \tau T_2^{-1}\right) P + QR \right]}{P^2 + R^2}$$

where ω_i is a constant for any given lineshape that depends on the equilibrium magnetization and M_0 is the magnitude of the magnetic field. In our case (two sites with same population),

$$P = \tau \left\{ T_2^{-2} - \left[2\pi \left(\frac{\delta\nu}{2} - \nu \right) \right]^2 + \left[\pi \delta\nu \right]^2 \right\} - T_2^{-1}$$

$$Q = 2\pi\tau \left(\frac{\delta\nu}{2} - \nu \right)$$

$$R = 2\pi \left(\frac{\delta\nu}{2} - \nu \right) \left(1 - \frac{2\tau}{T_2} \right)$$

with ν being the registered resonance in Hz. T_2, or more accurately T_2^*, was obtained from the linewidth at half height (linewidth = $1/\pi T_2^*$) of the average peak in

fast exchange conditions (T = 332 K); T_2 also contains a contribution from magnetic field inhomogeneity and is temperature dependent but confining the line-fitting procedure to exchange dominated spectra, this temperature dependence is not significant. $\delta\nu$ was measured from the NMR spectrum in slow exchange conditions (1090 Hz, obtained at T = 196 K).

The Microsoft Excel software was used to generate the lineshapes from the set of input parameters $\delta\nu$, T_2 and τ; for convenience, the experimental frequencies were transposed such that $\nu_A = -\nu_B$ and the generated spectra would be symmetric about the $\nu = 0$ midpoint. The maxima of the generated spectra was normalized to that of the observed spectra and the sum of the square of the intensity differences between the two spectra (SS = $\sum_{\nu}(I_{calc} - I_{obs})^2$) were calculated. The values for τ were obtained by the software as best fitting values (minimum SS) for Equation 3.1. Figure 3-12 shows the good fit obtained for some of the variable temperature spectra.

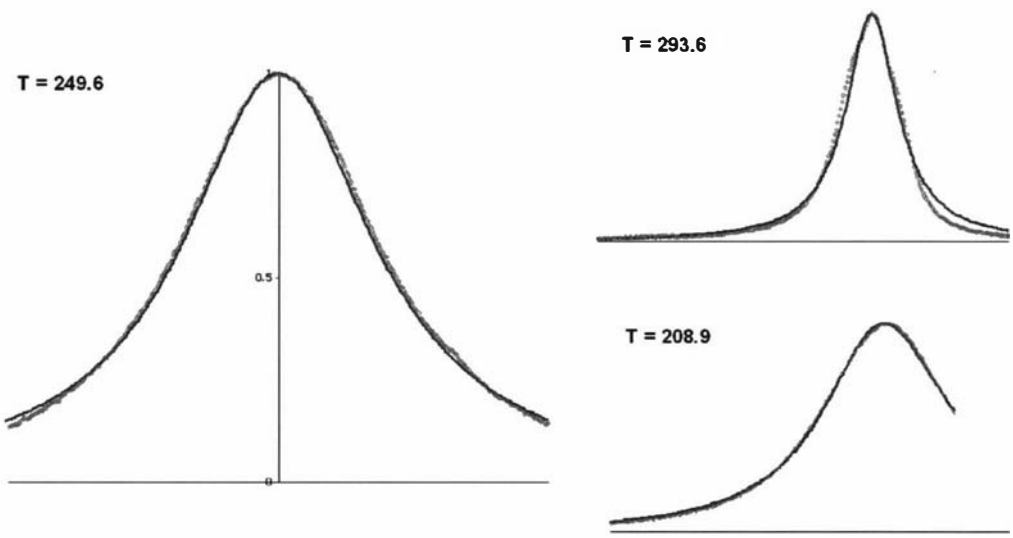

Figure 3-12 Observed (—) and calculated (—) lineshapes for ^{1}H-NMR spectra of **Zn-22c** at various temperatures

The large frequency difference between the two sites enabled a wide temperature range to be sampled and in this range exchange effects dominated. Data in Table 3-2 show that rate exchange (τ^{-1}) is around 10^3 s at low temperatures (slow exchange) and increases to 10^6 s (faster than NMR times) only around 300 K. The accuracy of

this method is confirmed by the insensitivity of the obtained lifetimes to changes in $\delta\nu$ and T_2.

T / K	208.9	217.6	231.2	249.6	293.6
τ^{-1} / s	$8.3\text{x}10^2$	$1.59\text{x}10^3$	$5.99\text{x}10^3$	$3.32\text{x}10^4$	$8.29\text{x}10^5$

Table 3-2 Temperature dependence of exchange rate τ^{-1} between coordinated and uncoordinated phosphonate ligands in **Zn-22c**

The exchange rates obtained with the Gutowsky-Holm equation were useful to estimate the energy involved in such exchange and, therefore, the strength of the Zn-phosphonate coordination. According to the Arrhenius equation,

(Eq. 3-2) $$\frac{1}{\tau} = k = A \cdot e^{\frac{E_a}{RT}}$$

which can also be written as

(Eq. 3-3) $$\ln\left(1/\tau\right) = \ln A - \frac{E_a}{RT}$$

By plotting the data reported in Table 3-2, we can obtain the activation energy E_a from the slope and the pre-exponential factor A from the intercept (Figure 3-13). The obtained values of E_a = 42.2 kJ/mol and A = $2.5\text{x}10^{13}$ s^{-1} are consistent with a labile coordination bond (E_a is an order of magnitude smaller than that of typical covalent bond energies and roughly twice that of hydrogen-bond energies).

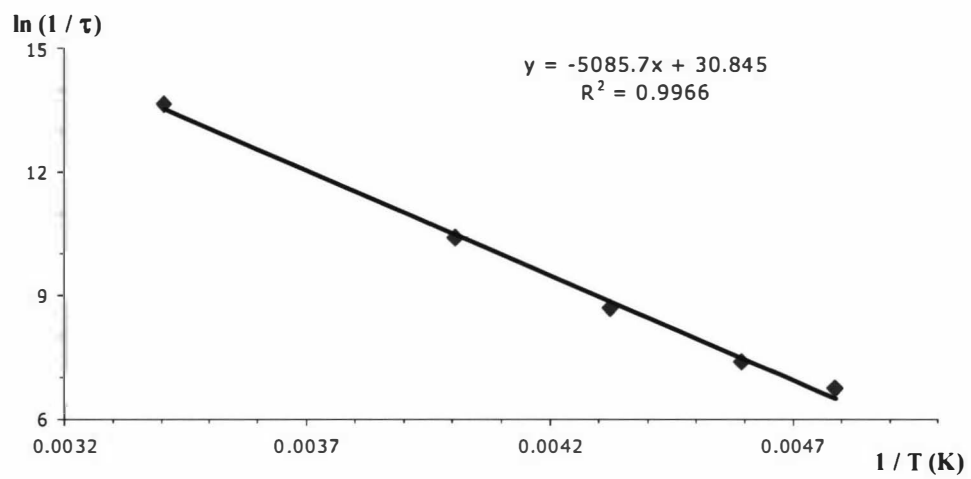

Figure 3-13 Arrhenius plot for phosphonate exchange in **Zn-22c**

3.5. Identification of the coordination around the metal in Zn porphyrins

There are a number of literature reports that show that Zn porphyrins can coordinate other molecules increasing their coordination number to five (C.N. = 5) or six (C.N. = 6). Although in solution C.N. = 5 seems to be preferred,[32,120] there are comparable numbers of solid state structures with C.N. = 6.[121,122] In order to determine if the Zn porphyrins bind either one or two phosphonates, the concentration dependence in the **Zn-22c** NMR spectra was examined. Since the Zn atom is already intramolecularly coordinated, a concentration dependence of chemical shifts might imply further coordination, resulting in a C.N. = 6 species. However, the results of such experiments (Figure 3-7b) showed minor shifts that could be attributed to other phenomena, such as porphyrin-porphyrin π-π stacking, which has been observed at concentrations as low as 10^{-18} M.[123]

An indirect answer can be obtained by studying the thermodynamic constants of the complexation. NMR is again a useful tool in this regard because it allows a correlation of the peak frequencies to the relative concentrations of coordinated and uncoordinated species. In order to probe this, the coordination of ZnTPP (**Zn-3**) and benzene monophosphonates **37** and **38** (Scheme 3-4) was investigated.

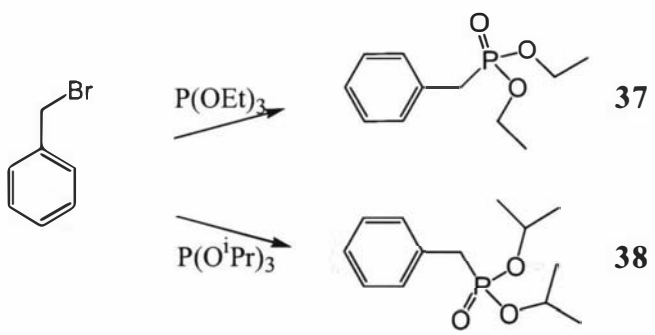

Scheme 3-4 Synthesis of monophosphonates **37** and **38**

In solution,

$$M \underset{-L}{\overset{L}{\rightleftharpoons}} ML \underset{-L}{\overset{L}{\rightleftharpoons}} ML_2$$

where **M** represents the metalloporphyrin, **L** is the phosphonate ligand, **ML** and **ML_2** are the complexes. Considering only the first complexation, the relative concentration between **L** and **ML** can be calculated from NMR chemical shifts by:

(Eq. 3-4) $$\delta_x = \frac{\delta_L \cdot [L] + \delta_{ML} \cdot [ML]}{L_x} \qquad \text{with} \qquad L_x = [L] + [ML]$$

where δ_x indicates the actual position of any resonance in the solution **x,** and δ_L and δ_{ML} are the signal positions for the two pure species. In a solution of ZnTPP (**Zn-3**) and phosphonate, in which the porphyrin is more than one hundred times in excess, **ML_2** it is unlikely to exist and the concentration of **M** can be considered to be constant. In this condition, a linear correlation is obtained that permits an estimation of the equilibrium constant and the resonances of **ML**. From the expression of mass balance and the equilibrium constant the peak frequencies can be correlated to the equilibrium constant:

$$K_1 = \frac{[ML]}{[M] \cdot [L]}; \qquad L_x = [L] + [ML]; \qquad M_x = [M]$$

.

$$K_1 = \frac{L_x - [L]}{M_x \cdot [L]} \quad \Longrightarrow \quad [L] = \frac{L_x}{K_1 \cdot M_x + 1} \quad \text{and} \quad [ML] = \frac{L_x \cdot K_1 \cdot M_x}{K_1 \cdot M_x + 1}$$

Substitution of these expressions in Equation 3-4 gives

$$\delta_x = \frac{\delta_L + \delta_{ML} \cdot K_1 \cdot M_x}{K_1 \cdot M_x + 1}$$

that can be rearranged to give a linear expression

(Eq. 3-5) $$\delta_x = \frac{\delta_L - \delta_x}{M_x} \cdot {}^{1}\!/_{K_1} + \delta_{ML}$$

in which the slope = $1/\mathbf{K_1}$ and the intercept = δ_{ML}.

An ^{1}H-NMR titration experiment (Figure 3-14) using phosphonate **38** in non-ideal conditions ($\mathbf{M_x/L_x} \cong 40$) gave a value of $\mathbf{K_1} \cong 80\ M^{-1}$ and a δ_{ML} = 0.07 ppm for the phosphonate methyl signals.

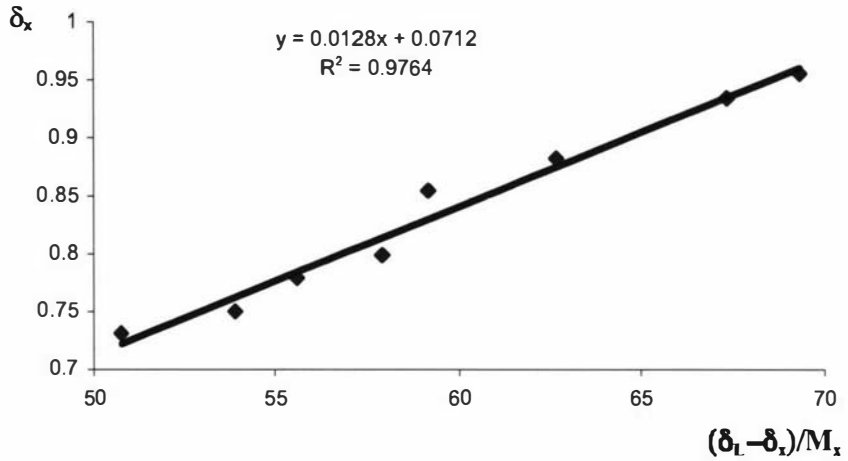

Figure 3-14 Zn-3 ^{1}H-NMR titrations of phosphonate **38**

Unfortunately, the low solubility of **Zn-3** made it very difficult to obtain solutions in which the porphyrin is more than one hundred times in excess and at the same time the phosphonate is concentrated enough to be detected by NMR spectroscopy. A way to sensibly improve the sensitivity involved the use of ^{31}P-NMR and the use of a different NMR probe, which is able to load and analyze samples in larger NMR tubes (diameter = 10 mm). Under these conditions, phosphonate **37** and **Zn-3** gave $\mathbf{K_1} \cong 50\ M^{-1}$ and δ_{ML} = 23.8 ppm (Figure 3-15). This means that in concentrated solutions ($\cong 0.05$ M) there are comparable amounts of coordinated and uncoordinated species.

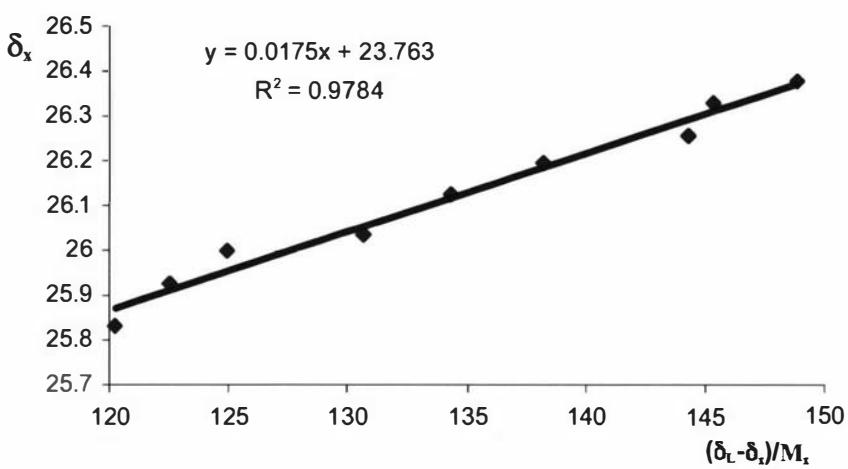

Figure 3-15 Zn-3 ^{31}P-NMR titration of phosphonate **37**

For the case of two phosphonates binding to a Zn porphyrin at the same time, forming **ML_2**, the chemical shifts for any resonance δ_x is given by:

$$\delta_x = \frac{\delta_L \cdot [L] + \delta_{ML} \cdot [ML] + 2 \cdot \delta_{ML_2} \cdot [ML_2]}{L_x} \qquad \text{(Eq. 3-6)}$$

The terms δ_{ML} and δ_{ML2} represent the phosphonate chemical shifts in the two possible complexes. The distances between the phosphonate and the porphyrin centre in the two complexes with C.N. = 5 (d_1) and C.N. = 6 (d_2) are not supposed to be equal because of the crystal field theory (CFT), which predict longer distances for higher coordination numbers (Figure 3-16) due to the repulsion between ligands; furthermore, when C.N. = 5, the Zn ion can be displaced from the porphyrin ring plane in the direction of the new ligand because of a similar electrostatic phenomenon. Crystallographic data also show that equivalent coordination bonds (i.e. Zn/water) are 0.2-0.4 Å longer when C.N. = 6.[121,122,152-155] As a consequence, the ring current will affect the phosphonates in the two complexes to a different degree and δ_{ML} and δ_{ML2} will not be equal, making the solution of Equation 3-6 difficult.

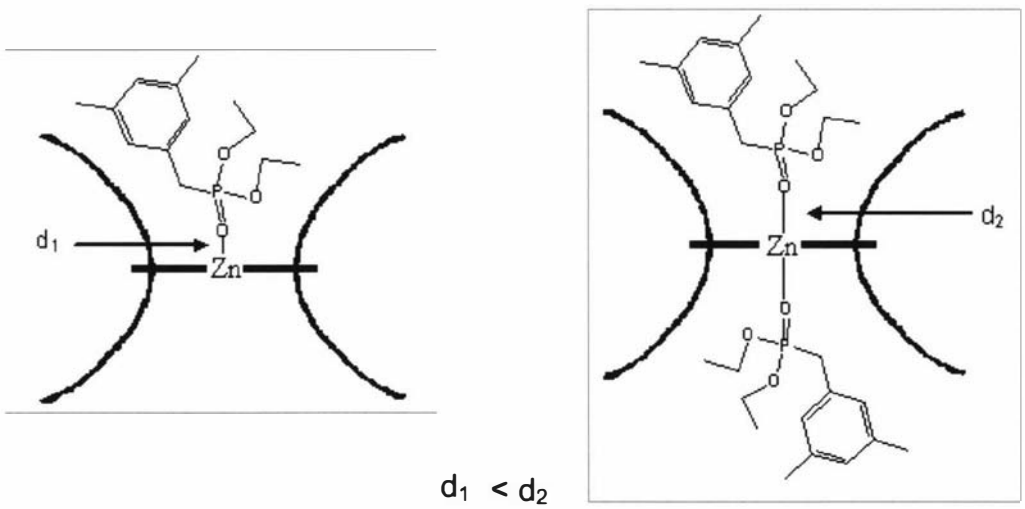

Figure 3-16 Zn-O distances in complexes with C.N. = 5 and C.N. = 6

The results for titrations with phosphonates **37** and **38**, in Figure 3-14 and 3-15 respectively, are reasonably linear. The calculated δ_{ML} in both cases (δ_{ML} = 0.07 ppm for the methyl signal of **38** and δ_{ML} = 23.8 ppm for the phosphorous shift of **37**), show the predicted large high-field shift to the ring current effect; however, the calculated

δ_{ML} value for the bound phosphonate **38** do not perfectly correspond to the experimental values recorded at low temperature for **Zn-22c** (δ_{ML} = -0.40 for methyl groups and δ_{ML} = 20.5 ppm for phosphorous). It can be reasonably supposed that in **Zn-22c**, the intramolecular coordination has to occur with a different geometry, which could account for the discrepancy (Figure 3-17); however, this difference may also be due to some contribution either from the coordination of a second phosphonate or from porphyrin-porphyrin π-π stacking.

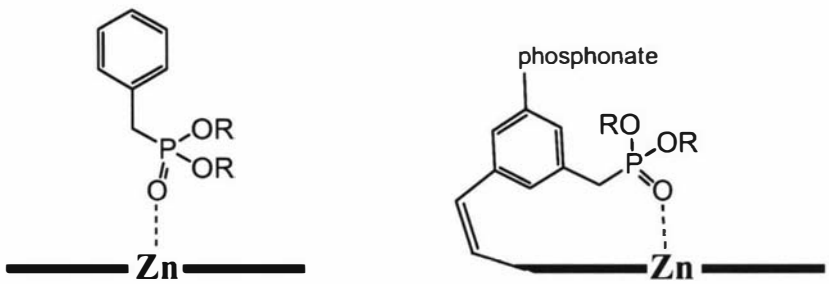

ZnTPP + phosphonate **Zn-22c**

Figure 3-17 Possible difference in the coordination geometry between ZnTPP + phosphonate and **Zn-22c**

3.6. Conclusions

An unexpected amount of *cis* isomer was obtained in a typical Wittig-Horner reaction of a porphyrin aldehyde and benzyl phosphonate and its unusual ^{1}H-NMR spectrum provided the impetus to investigate it further. Zn-porphyrin/phosphonate coordination through the phosphoryl oxygen was demonstrated and, to the best of our knowledge, the first case of an intramolecularly coordinated porphyrin phosphonate complex was uncovered.[124] Low temperature NMR spectroscopy demonstrated that the intramolecular coordination is actually a dynamic phenomenon in which the two phosphonate groups present in the same molecule switch between the coordinating/non-coordinating positions. The same experiments also gave us an estimate of the rate of the exchange process and the activation energy involved. Titrations of phosphonates with ZnTPP showed that coordination can also occur intermolecularly and the complexation constant was estimated. Low-temperature experiments and titrations provided independent values for the activation energy (E_a =

42.2 kJ/mol) and complexation constant ($K \approx 50\ M^{-1}$); both those values are consistent with a coordination that is too labile to be employed for the making of stable supramolecular structures such as coordination arrays. However, the described Zn porphyrin/phosphonate coordination could find applications where a fast ligand turnover is required, such as sensors or catalysis.

3.7. Experimental procedures

Dry THF was obtained by passing commercially available solvent through an activated alumina column. Other solvent and chemicals were AR grade and used without further purification. NMR spectrometry experiments were performed using 400, 500 and 700 MHz Bruker Avance instruments. Low temperature experiments were carried out by using liquid nitrogen flushes regulated by temperature controllers connected to the spectrometers and with the assistance of Dr. Pat J. Edwards. Proton chemical shifts in $CDCl_3$ are relative to TMS; phosphorous chemical shifts are relative to 90% D_3PO_4 (external standard). Chemical shifts in dichloromethane-d_2 are relative to residual protons (δ = 5.32 ppm). Data are expressed as position (in ppm), multiplicity (s = singlet, d = doublet, t = triplet, q = quartet, m = multiplet, br = broad, app = apparent), relative integral, coupling constant (J_P indicating ^1H-^{31}P coupling) and assignment. Coupling constants were not reported when smaller than 1 Hz. UV-visible absorption experiments were performed on a Shimadzu UV-3101PC scanning spectrophotometer. High resolution FAB mass spectra were recorded on a Varian VG-70SE at the University of Auckland.

Precursor syntheses.

Porphyrins aldehydes **M-5** (M = 2H, Zn, Ni), were prepared as previously published by our group.[75]

ZnTPP-Ph-(ep)$_2$, Zn-22.

In a 100 mL round bottom flask, 200 mg (284 μmol) of **Zn-5** and 159 mg (301 μmol) of triphosphonate **21** were dissolved in 40 mL of dry THF, under argon atmosphere. To the stirred solution, 40 mg (356 μmol) of ^{t}BuOK in dry THF were added at three

intervals in 30 min. After a further 30 min, 5 mL of water were added and the solution was concentrated. The concentrated solution was diluted with 100 mL of DCM and washed with 200 mL of water. The organic layer was dried over $MgSO_4$, filtered, evaporated to dryness and the crude mixture purified by flash chromatography on silica gel (DCM/MeOH = 100/1). After the elution of side-products and unreacted **Zn-5**, two separate bands yielded respectively 67 mg (22%) of **Zn-22c** and 153 mg (51%) of **Zn-22t** as purple solids.

***trans*-ZnTPP-Ph-(ep)$_2$, Zn-22t.**

5-(*trans*-2'-(2"-(5",10",15",20"-tetraphenylporphyrinato zinc(II))yl)ethen-1'-yl)-1,3-bis(methyl(diethylphosphonate))benzene.

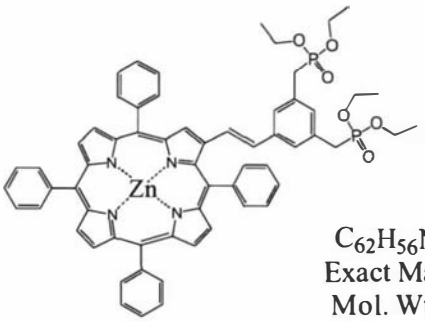

$C_{62}H_{56}N_4O_6P_2Zn$
Exact Mass: 1078.3
Mol. Wt.: 1080.47

^{1}H-NMR (400 MHz, $CDCl_3$): δ 9.08 (s, 1H, H_{pyrr}), 8.84-8.90 (m, 5H, H_{pyrr}), 8.65 (d, J = 4.5 Hz, 1H, H_{pyrr}), 8.13-8.24 (m, 8H, $H_{o\text{-}Ph}$), 7.65-7.77 (m, 12H, $H_{m,p\text{-}Ph}$), 7.16 (d, J = 16 Hz, 1H, H_{alkene}), 6.98 (d, J = 16 Hz, 1H, H_{alkene}), 6.74 (br s, 2H, H_{Ph}), 6.60 (br s, 1H, H_{Ph}), 3.50-3.60 (m, 8H, H_{ethyl}), 2.61 (d, J_P = 22 Hz, 4H, $H_{CH2\text{-}P}$), 1.02 (t, J = 7 Hz, 12H, H_{ethyl}). UV-vis (CH_2Cl_2): λ_{max} [nm] (ε x 10^{-3}) 428.5 (162), 557 (13), 591 (5.5). FAB-HRMS for M^+ ($C_{62}H_{56}N_4O_6P_2Zn$): 1078.2944, calculated: 1078.2967.

***cis*-ZnTPP-Ph-(ep)$_2$, Zn-22c.**

5-(*cis*-2'-(2"-(5",10",15",20"-tetraphenylporphyrinato zinc(II))yl)ethen-1'-yl)-1,3-bis(methyl(diethylphosphonate))benzene.

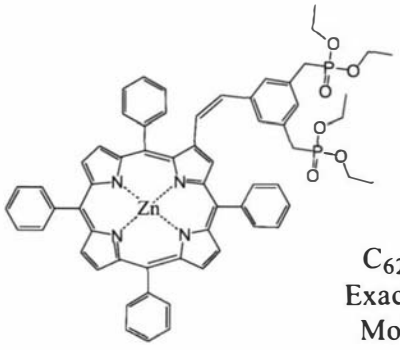

$C_{62}H_{56}N_4O_6P_2Zn$
Exact Mass: 1078.30
Mol. Wt.: 1080.47

^{1}H-NMR (400 MHz, $CDCl_3$): δ 8.78-8.86 (m, 4H, H_{pyrr}), 8.65 (s, 2H, H_{pyrr}), 8.60 (d, J = 1.3 Hz 1H, H_{pyrr}), 8.09-8.27 (m, 8H, $H_{o\text{-}Ph}$), 7.57-7.85 (m, 12H, $H_{m,p\text{-}Ph}$), 7.05 (dd, J = 12 Hz, J = 1.3 Hz 1H, H_{alkene}), 5.86 (d, J = 12 Hz, 1H, H_{alkene}), 5.83 (br s, 1H, H_{Ph}), 5.53 (br s, 2H, H_{Ph}), 2.10-2.32 (m, 8H, H_{ethyl}), 1.81 (br d, J_P = 22 Hz, 4H, $H_{CH2\text{-}P}$), 0.38 (br t, J = 7 Hz, 12H, H_{ethyl}). UV-vis (CH_2Cl_2): λ_{max} [nm] (ε x 10^{-3}) 431.5 (294), 562.5 (13.8), 603.5 (5.7). FAB-HRMS for M^- ($C_{62}H_{56}N_4O_6P_2Zn$): 1078.2963, calculated: 1078.2967.

NiTPP-Ph-(ep)$_2$, Ni-22.

The synthesis of this compound was carried out using the same procedure described for **Zn-22**. In a 100 mL round bottom flask, 200 mg (287 μmol) of **Ni-5** and 162 mg (307 μmol) of triphosphonate **21** were dissolved in 40 mL of dry THF, under argon atmosphere. To the stirred solution, 40 mg (356 μmol) of ^{t}BuOK were added. After 45 min, 5 mL of water were added and the solution was concentrated. The solution was diluted with 100 mL of DCM and washed with 200 mL of water. The organic layer was dried on $MgSO_4$, evaporated to dryness and the mixture was purified through flash chromatography on silica gel DCM/MeOH = 100/1) to give 245 mg (80% yield) of **Ni-22** as mixture of *cis* (**Ni-22c**) and *trans* (**Ni-22t**) isomers. NMR assignments were made comparing spectra of mixtures containing different *cis/trans* ratio.

***trans*-NiTPP-Ph-(ep)$_2$, Ni-22t.**

5-(*trans*-2'-(2"-(5",10",15",20"-tetraphenylporphyrinato nickel(II))yl)ethen-1'-yl)-1,3-bis(methyl(diethylphosphonate))benzene.

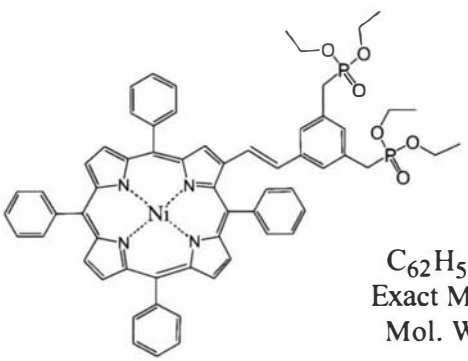

$C_{62}H_{56}N_4NiO_6P_2$
Exact Mass: 1072.30
Mol. Wt.: 1073.77

^{1}H-NMR (400 MHz, $CDCl_3$): δ 8.88 (s, 1H, H_{pyrr}), 8.65-8.76 (m, 6H, H_{pyrr}), 7.94-8.04 (m, 8H, $H_{o\text{-}Ph}$), 7.63-7.81 (m, 12H, $H_{m,p\text{-}Ph}$), 7.11 (d, J = 1.6 Hz, 1H, H_{Ph}), 7.10 (d, J =

16 Hz, 1H, H_{alkene}), 6.86 (d, J = 16 Hz, 1H, H_{alkene}), 6.98 (d, J = 1.6 Hz, 2H, H_{Ph}), 4.01-4.11 (m, 8H, H_{ethyl}), 3.15 (d, J_P = 22 Hz, 4H, H_{CH2-P}), 1.30 (t, J = 7 Hz, 12H, H_{ethyl}). UV-vis (CH_2Cl_2): λ_{max} [nm] (ε x 10^{-3}) 425.5 (131), 536 (10), 575 (5.6). FAB-HRMS for M^+ ($C_{62}H_{56}N_4O_6P_2{}^{58}Ni$): 1072.2994, calculated: 1072.3029.

cis-NiTPP-Ph-(ep)$_2$, Ni-22c.

5-(*cis*-2'-(2"-(5",10",15",20"-tetraphenylporphyrinato nickel(II))yl)ethen-1'-yl)-1,3-bis(methyl(diethylphosphonate))benzene.

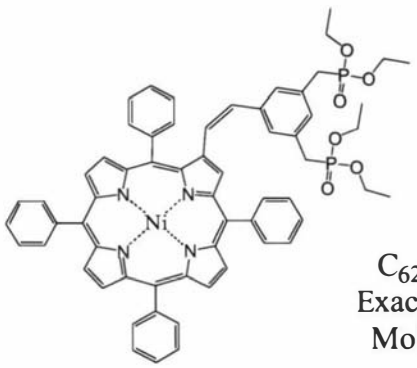

$C_{62}H_{56}N_4NiO_6P_2$
Exact Mass: 1072.30
Mol. Wt.: 1073.77

^{1}H-NMR (400 MHz, $CDCl_3$): δ 8.65-8.76 (m, 6H, H_{pyrr}), 8.43 (d, J = 1.1 Hz 1H, H_{pyrr}), 7.97-8.26 (m, 8H, $H_{o\text{-}Ph}$), 7.48-7.88 (m, 12H, $H_{m,p\text{-}Ph}$), 7.14 (br s, 2H, H_{Ph}), 7.06 (br s, 1H, H_{Ph}), 6.33 (dd, J = 12 Hz, J = 1.1 Hz, 1H, H_{alkene}), 6.16 (d, J = 12 Hz, 1H, H_{alkene}), 3.63-3.77 (m, 8H, H_{ethyl}), 2.89 (d, J_P = 22 Hz, 4H, H_{CH2-P}), 0.93 (t, J = 7 Hz, 12H, H_{ethyl}).

trans-TPP-Ph-(ep)$_2$, 22t.

5-(*trans*-2'-(2"-(5",10",15",20"-tetraphenylporphyrin)yl)ethen-1'-yl)-1,3-bis(methyl(diethylphosphonate))benzene.

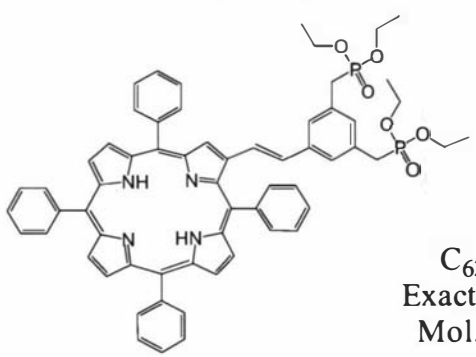

$C_{62}H_{58}N_4O_6P_2$
Exact Mass: 1016.38
Mol. Wt.: 1017.09

Free base porphyrin **22t** was obtained from homologue **Zn-22t**. Demetallation was performed by dissolving 50 mg (46.3 μmol) **Zn-22t** in 20 mL of dichloromethane and

stirring this solution with the same volume of 3M HCl in water. After 2 hours the organic layer was separated, washed with a solution of sodium bicarbonate and dried on $MgSO_4$. The solution was then evaporated to dryness, affording 46 mg (98%) of **22t**. ^{1}H-NMR (400 MHz, $CDCl_3$): δ 9.00 (s, 1H, H_{pyrr}), 8.69-8.81 (m, 6H, H_{pyrr}), 8.18-8.27 (m, 8H, $H_{o\text{-}Ph}$), 7.70-7.92 (m, 12H, $H_{m,p\text{-}Ph}$), 7.28 (d, J = 16 Hz, 1H, H_{alkene}), 7.16 (br s, 1H, H_{Ph}), 7.07 (br s, 2H, H_{Ph}), 7.01 (d, J = 16 Hz, 1H, H_{alkene}), 4.03-4.13 (m, 8H, H_{ethyl}), 3.19 (d, J_P = 22 Hz, 4H, $H_{CH2\text{-}P}$), 1.30 (t, J = 7 Hz, 12H, H_{ethyl}), -2.59 (s, 2H, $H_{N\text{-}pyrr}$). UV-vis (CH_2Cl_2): λ_{max} [nm] (ε x 10^{-3}) 428.5 (159), 516 (sh, 2.5), 557 (12.9), 591.5 (5.4), 627 (sh, 1.7). FAB-HRMS for M^+ ($C_{62}H_{58}N_4O_6P_2$): 1016.3863, calculated: 1016.3832.

***cis*-TPP-Ph-(ep)$_2$, 22c.**

5-(*cis*-2'-(2"-(5",10",15",20"-tetraphenylporphyrin)yl)ethen-1'-yl)-1,3-bis(methyl(diethylphosphonate))benzene.

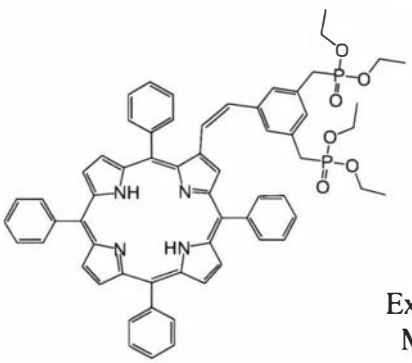

$C_{62}H_{58}N_4O_6P_2$
Exact Mass: 1016.38
Mol. Wt.: 1017.09

Free base porphyrin **22c** was obtained from homologue **Zn-22c**. Demetallation was quickly performed (to avoid isomerization) by dissolving 20 mg (23 μmol) of **Zn-22c** in 20 mL of dichloromethane and shaking this solution with 20 mL of 2M HCl in a separation funnel. After 30 seconds the organic layer was separated, washed with a solution of sodium bicarbonate and precipitated by methanol addition, affording 18 mg of **22c**. ^{1}H-NMR (400 MHz, $CDCl_3$): δ 8.73-8.86 (m, 6H, H_{pyrr}), 8.54 (br s, 1H, H_{pyrr}), 8.18-8.24 (m, 4H, $H_{o\text{-}Ph}$), 8.07 (d, J = 7 Hz, 2H, $H_{o\text{-}Ph}$), 8.01 (d, J = 7 Hz, 2H, $H_{o\text{-}Ph}$), 7.55-7.81 (m, 12H, $H_{m,p\text{-}Ph}$), 7.10 (br s, 2H, H_{Ph}), 7.03 (br s, 1H, H_{Ph}), 6.44 (d, J = 12 Hz, 1H, H_{alkene}), 6.30 (d, J = 12 Hz, 1H, H_{alkene}), 3.71-3.59 (m, 8H, H_{ethyl}), 2.81 (d, J_P = 22 Hz, 4H, $H_{CH2\text{-}P}$), 0.87 (t, J = 7 Hz, 12H, H_{ethyl}), -2.72 (s, 2H, $H_{N\text{-}pyrr}$). MALDI-LRMS for $(M+H)^+$ ($C_{62}H_{58}N_4O_6P_2$): cluster 1017.5-1020.5 (max 1017.5), calculated: cluster 1017.4-1020.4 (max 1017.4).

1,3-xylenebis(diethylphosphonate), 35.

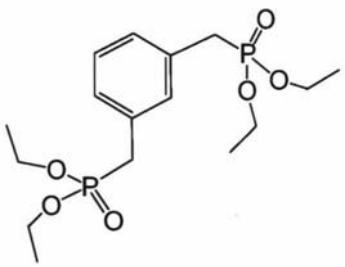

$C_{16}H_{28}O_6P_2$
Exact Mass: 378.14
Mol. Wt.: 378.34

Diphosphonate **35** was prepared according to the general method of Michaelis and Kaehne.[10,107]

264 mg (1 mmol) of commercial m-dibromoxylene were dissolved in 3 mL of commercial triethylphosphite under argon atmosphere. The solution was refluxed for 4 hours after which the excess phosphite and co-product EtBr were distilled off, yielding 330 mg (87%) of pure **35** as pale yellow oil. ^{1}H-NMR (400 MHz, $CDCl_3$): δ 7.32-7.29 (m, 4H, H_{Ph}), 4.06-3.95 (m, 4H, $H_{CH2\text{-}ethyl}$), 3.16 (d, J = 21.6 Hz, 2H, $H_{CH2\text{-}P}$), 1.24 (t, J = 7 Hz, 6H, $H_{CH3\text{-}ethyl}$). The ^{1}H-NMR spectrum is in agreement with the literature.[148]

ZnTPP-Ph-mep, Zn-36.

3-(*trans*-2'-(2"-(5",10",15",20"-tetraphenylporphyrinato zinc(II))yl)ethen-1'-yl)methyl(diethylphosphonate)benzene.

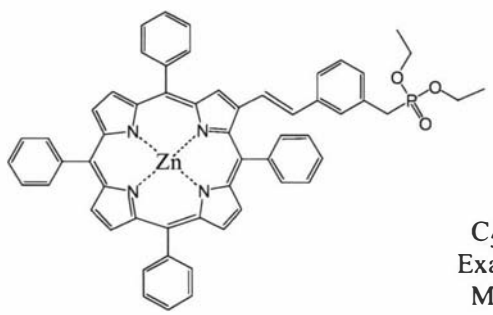

$C_{57}H_{45}N_4O_3PZn$
Exact Mass: 928.25
Mol. Wt.: 930.36

195 mg (277 μmol) of **Zn-5** and 106 mg (280 μmol) of diphosphonate **35** were dissolved in 30 mL of dry THF under argon atmosphere. 40 mg (356 μmol) of ^{t}BuOK were added and the solution was stirred for 1 hour. The solution was extracted with 100 mL of DCM and 100 mL of water and the organic phase was dried over $MgSO_4$ and evaporated to dryness. Flash chromatography on silica gel (DCM/MeOH = 200/1) afforded 190 mg (74%) of purple solid **Zn-36t** containing less than 5% of **Zn-36c.**

Zn-36t: ^{1}H-NMR (400 MHz, $CDCl_3$): δ 9.07 (s, 1H, H_{pyr}), 8.85-8.92 (m, 5H, H_{pyr}), 8.77 (d, J = 5 Hz 1H, H_{pyr}), 8.13-8.24 (m, 8H, $H_{o\text{-}Ph}$), 7.68-7.80 (m, 12H, $H_{m,p\text{-}Ph}$),

7.14-7.21 (m, 2H, $1H_{alkene}$+$1H_{Ph}$), 7.08 (br d, J = 7 Hz, 1H, H_{Ph}), 6.98 (d, J = 16 Hz, 1H, H_{alkene}), 6.92 (br s, 1H, H_{Ph}), 6.70 (br d, J = 7 Hz, 1H, H_{Ph}), 3.42-3.60 (m, 4H, H_{ethyl}), 2.72 (d, J_P = 22 Hz, 2H, $H_{CH2\text{-}P}$), 1.03 (t, J = 7 Hz, 6H, H_{ethyl}). UV-vis (CH_2Cl_2): λ_{max} [nm] (ε x 10^{-3}) 428 (163), 556 (13), 591 (5.3). FAB-HRMS for M^+ ($C_{57}H_{46}N_4O_3PZn$): 929.2587, calculated: 929.2599.

toluene(diethylphosphonate), 37.

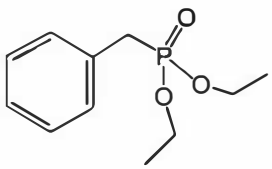

$C_{11}H_{17}O_3P$
Exact Mass: 228.09
Mol. Wt.: 228.22

Phosphonate **37** was prepared according to the general method of Michaelis and Kaehne.[102,107]

1 mL (8.4 mmol) of benzyl bromide and 2 mL of triethylphosphite were refluxed under argon for 4h. The solution was refluxed for 4 hours after which the excess phosphite and co-products were distilled off under high vacuum, yielding 1.8 g (95%) of the desired phosphonate **37** as a colourless oil. ^{1}H-NMR (400 MHz, $CDCl_3$): δ 7.32-7.29 (m, 5H, H_{Ph}), 4.06-3.95 (m, 4H, $H_{CH2\text{-}ethyl}$), 3.16 (d, J_P = 21.7 Hz, 2H, $H_{CH2\text{-}P}$), 1.24 (t, J = 7 Hz, 6H, $H_{CH3\text{-}ethyl}$). The ^{1}H-NMR spectrum is in agreement with the literature.[149]

toluene(diisopropylphosphonate), 38.

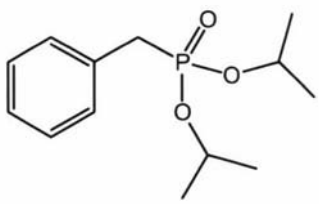

$C_{13}H_{21}O_3P$
Exact Mass: 256.12
Mol. Wt.: 256.28

Phosphonate **38** was prepared according to the general method of Michaelis and Kaehne.[102,107]

1 mL (8.4 mmol) of benzyl bromide and 2 mL of triisopropylphosphite were refluxed under argon for 4h. The solution was refluxed for 4 hours after which the excess phosphite and co-products were distilled off under high vacuum, yielding 2.1 g (97%) of the desired phosphonate **38** as a colourless oil. ^{1}H-NMR (400 MHz, $CDCl_3$): δ 7.31-7.29 (m, 5H, H_{Ph}), 4.65-4.54 (m, 2H, $H_{CH\text{-}propyl}$), 3.11 (d, *conformational doubling* = 21.7 Hz, 2H, $H_{CH2\text{-}P}$), 1.22 (dd, J_P = 46.4 Hz, J = 6.2 Hz, 12H, $H_{CH3\text{-}propyl}$).

4. PORPHYRIN PHOTOPHYSICS

4.1. Introduction

The photophysics of porphyrins has been widely investigated, mainly in an attempt to rationalize the mechanisms involved in photosynthesis. Even though different photosystems exist in nature, the presence of porphyrins cooperating in complex structures is a constant feature, as a result of their unique chemical and physical properties. In particular, porphyrins show strong light absorbance in the near UV-visible spectrum, can have long excited state lifetimes and can easily undergo energy and electron transfer. In addition, a great variety of synthetic porphyrins are now accessible and it is possible to 'tune' their properties by metal coordination and modification of the functional groups. As a result, porphyrins are the ideal molecules for photophysical studies, especially in relation to understanding and mimicking photosynthesis.

The typical porphyrin absorption spectrum shows a very intense band at 390-430 nm called the Soret or B band and a group of weaker Q bands in the 450-700 nm region. Both of these groups of absorptions lead to a singlet excited state as shown in Figure 4-1. The different Q bands represent different vibrational energy levels and their number depends on the symmetry; free base porphyrins typically show four Q bands while the increased symmetry in metallated porphyrins (D_{4h} vs. D_{2h}) results in degeneration and therefore in just two Q bands.

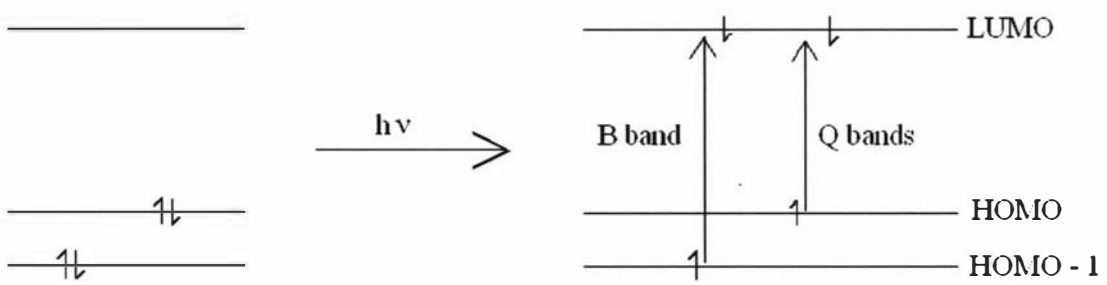

Figure 4-1 Porphyrin electronic transitions after excitation in the UV-visible region

After photoexcitation to any excited state, the system relaxes radiationlessly to the lowest singlet excited state (equivalent to the lowest energy Q band absorption) in a few picoseconds; from this point, the pathway to the ground state involves mainly (>99%) fluorescence and intersystem crossing to the lowest triplet excited state. In free-base porphyrins, fluorescence decay times are of the order of a few nanoseconds while metallation typically enhances spin-orbit couplings, which favour intersystem crossing and result in faster fluorescence decays (e.g. 10 ns for free-base, 1 ns for Zn porphyrins, no fluorescence for Fe(III) porphyrins).[125] When intersystem crossing is the favoured pathway, phosphorescence from the lowest excited triplet state can happen; usually, phosphorescence in porphyrins is observable only at low temperatures.[126,127] Porphyrin ring substituents, as well as metallation, can strongly influence the electronic states of the porphyrins; in particular, metallation and meso substituents have effects mainly on the orbitals involved in the Q band transitions while β-pyrrolic substituents also affect the Soret band transitions.

The chemical and physical properties of porphyrins are influenced by their substituents; in particular, porphyrin systems linked by conjugated bridges are receiving increasing attention in view of their potential application in the design of molecular wires for electronic and photonic applications (see Section 1-4). In this context, the analysis of the effect of the kind of conjugated substituents presented in this thesis becomes of great relevance. Several studies on multi-porphyrinic arrays[128,129] have demonstrated that when the spacer is a phenyl group directly connected to the ring (usually in the *meso* position), the orbital interaction between the porphyrin and the bridge is strongly reduced by the close-to-perpendicular position preferentially assumed by the two components in order to minimize steric hindrance. In these systems, the through-bond electronic communication between the units is negligible and their spectral properties are usually characterized by exciton coupling originating from the Coulombic interactions between the dipole moments of the adjacent porphyrin units, which results in a split Soret band (Figure 4-2).

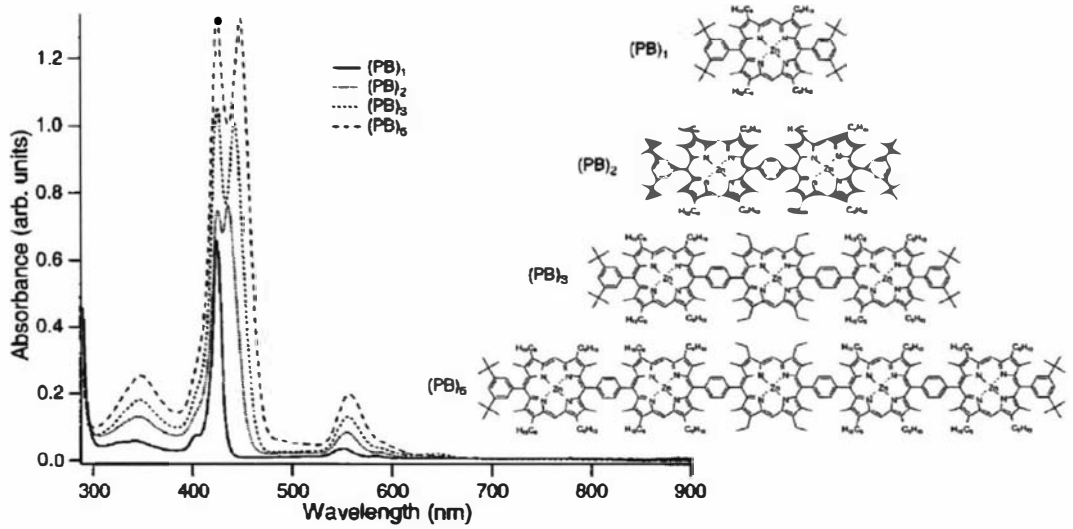

Figure 4-2 Exciton coupling in non-conjugated linear porphyrin arrays by Piet *et al.* [128]

However, when the porphyrins are connected in a manner that the rings can be assumed to be coplanar, an extension of the π-conjugation over the bridge, with the consequent formation of highly delocalized excited states, is possible. The spectral characteristics of these arrays, compared to those of the single porphyrins, are a red-shifting of all absorption bands, a pronounced broadening and/or splitting of the Soret band, and an enhancement of the Q bands. For example, in a fused porphyrin array, wherein the individual porphyrins are triply linked to form a long tape, the extensive π-conjugation results in extremely red-shifted (up to 3000 cm^{-1}) and intensified Q bands (Figure 4-3).[14,22]

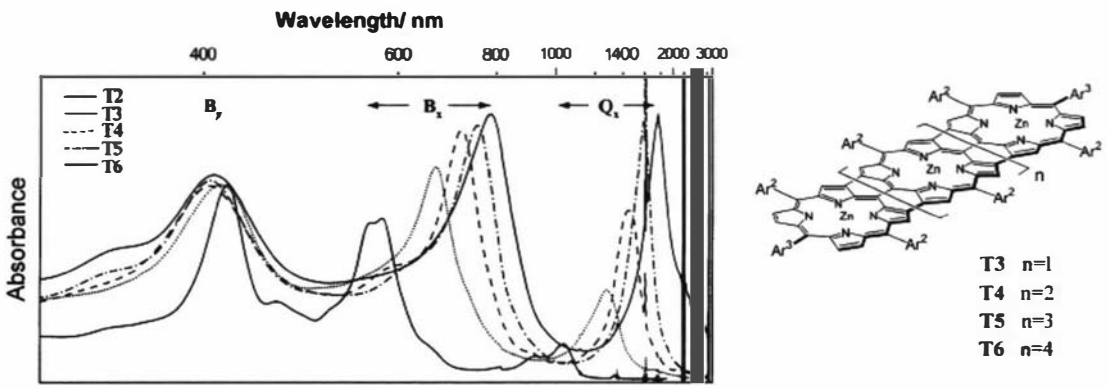

Figure 4-3 UV-visible-near IR absorption spectra of a series of porphyrin 'tapes' by Kim and Osuka[14]

Since the electronic properties of the frontier orbitals of porphyrins depend on both the nature and the position of the substituents,[125,130,131] it is important to understand the effect of varying the point of substituent attachment. While the electronic properties

of meso-substituted conjugated porphyrins have been well studied,[52,132] the effect of conjugated β-substituents on the photochemical and electrochemical properties of porphyrins has not been explored in detail, and only a small number of papers report the spectral properties of porphyrins β-substituted with conjugated substituents.[60,76,132,159-162] In order to understand the effect of phenylenevinylene substituents on the electronic communication between the units of multi-porphyrin arrays, a detailed photophysical study of a series of β-pyrrolic substituted porphyrins was undertaken.

This chapter introduces the syntheses of a series of four Zn/free-base porphyrin dyads and two series of homometallic homologues (Section 4-7) for the investigation of intramolecular energy transfer in our type of porphyrin array (Figure 4-4); it also presents the syntheses of a series of four free-base and four Zn porphyrins with either vinyl groups or *p*-phenylenevinylene groups in the β-pyrrolic position (Section 4-5), which are necessary as models for the characterization of the dyads photophysics.

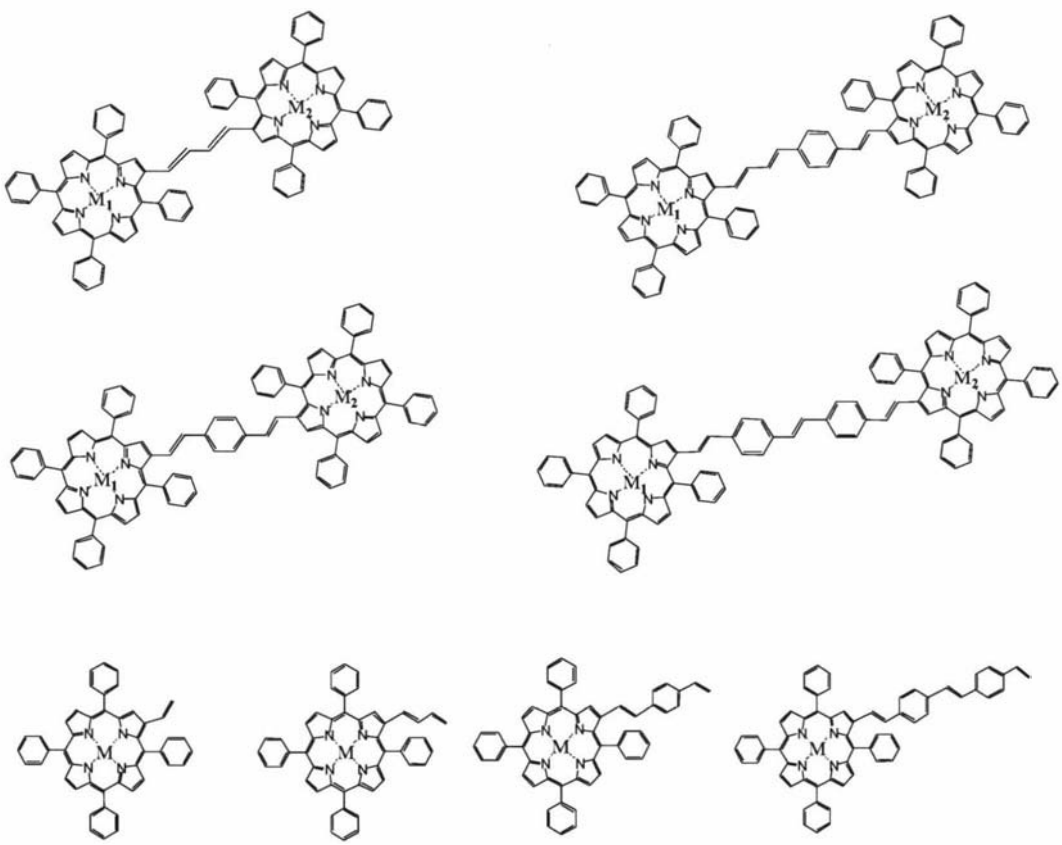

M, M_1 and M_2 = Zn or 2H

Figure 4-4 Zn and free-base dyads and monomers for photophysical investigation

The full spectroscopic and photophysical characterization of the two series of monomer models (Section 4-6) has been performed in collaboration with Dr. L. Flamigni and Dr. B. Ventura at ISOF/CNR, Bologna, Italy. The photophysical investigation of the dyads (Section 4-8) is currently in progress at the same institute.

4.2. Intramolecular photophysics

Over the last two decades, as a result of improved analytical techniques, there have been an increasing number of studies on porphyrin photophysics. When a porphyrin undergoes light excitation, the excited state can be 'transferred' to a nearby acceptor through non-radiative mechanisms. Mg, Zn, Fe Au, Ru and free-base porphyrins have been included in systems that undergo energy and electron transfer, often with a quantum yield close to one.[133,134] Examples where porphyrins play the donating role and the acceptors are either perylene derivatives or fullerene are common (Figure 4-5).[135-137,158]

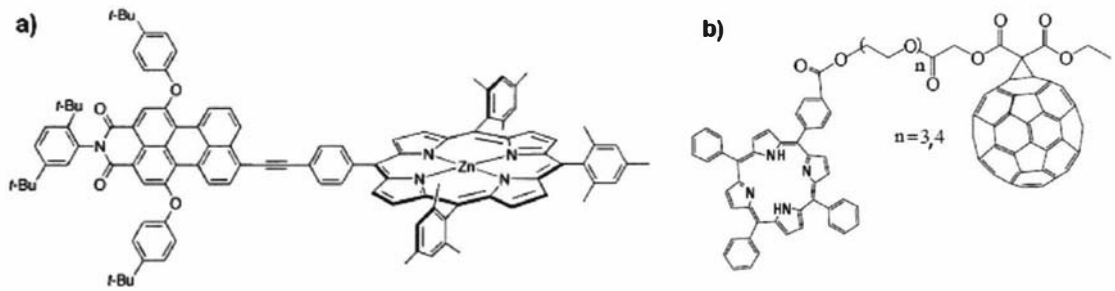

Figure 4-5 (a) Porphyrin-perylene dyad by Tomizaki *et al.*[136] and (b) porphyrin-fullerene dyad by Schuster *et al.*[135]

As previously discussed, the nature of the coordinated metal is critical for the photophysical properties of porphyrins. Mg(II)[137] and Zn(II) porphyrins, for example, are typically electron rich, therefore they have been shown to be very effective as energy/electron donors; on the contrary, Au(III)[138] and Fe(III) porphyrins can use easily available lower oxidation states and are ideal as electron acceptors. When multielectron transfers are required, non-metallic porphyrins show the best chemical and physical properties ($Sn^{II} \rightarrow Sn^{IV}$, $Sb^{III} \rightarrow Sb^{V}$).[139] By connecting electron-rich and electron-poor porphyrins, it has been possible to make dyads in which the excitation

energy of one porphyrin (donor) is efficiently transferred to the other one (acceptor). The transfer must be between isoenergetic states, therefore the emission spectrum of the donor and the absorption spectrum of the acceptor have to overlap; when this condition is fulfilled, excited state transfer can occur by one of two possible mechanisms. The first involves the formation of a resonant oscillating dipole in the acceptor produced by the electric field of the excited donor dipole. This pathway, known as the Förster or Coulomb mechanism, does not involve any orbital overlap, being a pure electrostatic interaction. The second type of transfer is known as the Dexter or exchange mechanism; in this case, there is an exchange of electrons between donor and acceptor, which leads to an excited state localized on the acceptor. When the excited state transfer does not involve oxidation/reduction (e.g. energy transfer vs. electron transfer), the Dexter mechanism can be seen as a synchronized electron transfer between the two species (Figure 4-6).

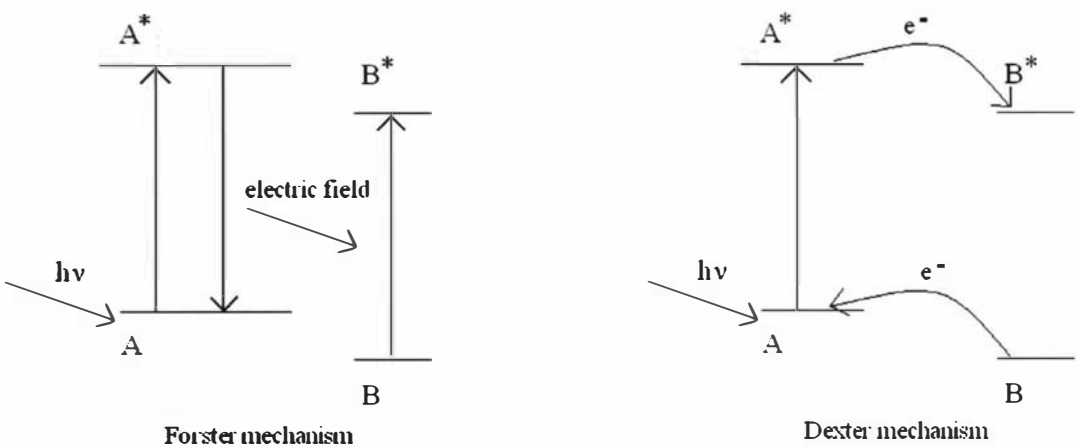

Figure 4-6 Förster vs. Dexter energy transfer mechanisms

Many systems have already been created in which both electron and energy transfers have been observed; both Dexter and Förster processes have been obtained by choosing the nature of the connecting bridge between the porphyrin units and their relative distance/orientation. For example, Kadish *et al.*[87] prepared a series of Zn/Zn and fb/fb dyads in which the porphyrins are very close but have little electronic interaction (Figure 4-7); when the two porphyrin were the same (e.g. TPP), partial fluorescence quenching was observed while, with different porphyrins, only fluorescence from TPP was noted. In both cases, energy transfer through the Forster mechanism was found to be the reason for the emission quenching.

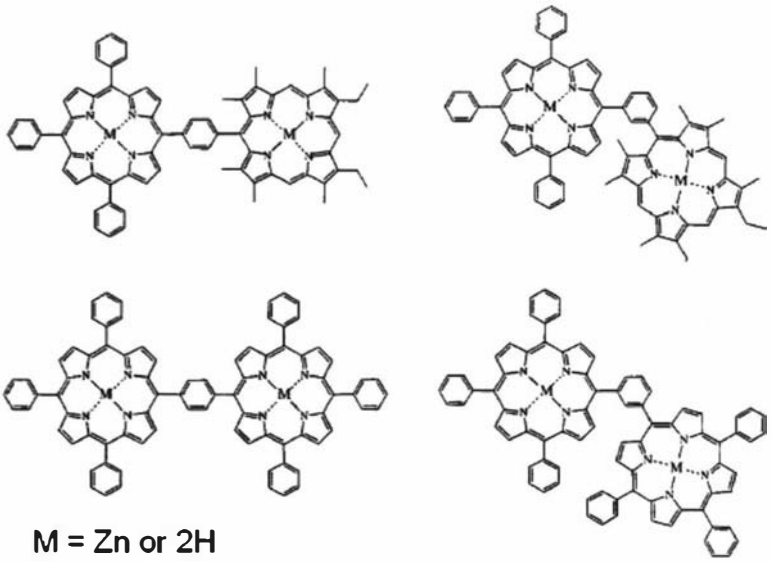

Figure 4-7 Homometallic dyads by Kadish *et al.*[87]

The Lindsey group examined a series of ethyne-linked porphyrin arrays and obtained fast and efficient energy transfer from photoexcited Zn to free-base porphyrins; the Dexter mechanism in such systems prevails and is supported by the fact that the electron transfer rate and efficiency is dependent on the ability of the bridges to adopt conformations which are favourable for electronic communication (Figure 4-8a).[16] Similar results were obtained by Osuka *et al.*[78] in the study of polyene and polyyne linked Zn/free base dyads (Figure 4-8b).

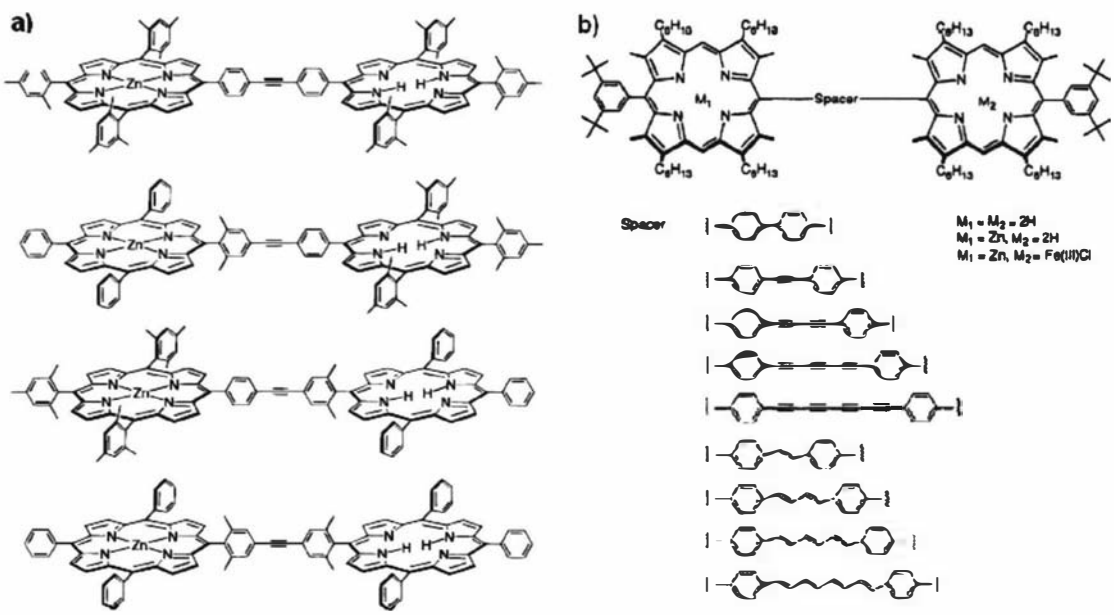

Figure 4-8 Zn/free base dyads by (a) Hsiao *et al.*[16] and (b) Osuka *et al.*[78]

In arrays containing Fe(III) porphyrins, electron transfer becomes the favoured relaxation pathway and many reports have been published in which such electron transfer occurs efficiently. For example, the homologues of molecules in Figure 4-8b containing a Fe(III) in place of a free base porphyrin showed practically the same 'transfer' efficiency and bridge dependence as for the Zn/fb homologue;[78] in fact, in both cases, a Dexter (through bond) mechanism is involved. Similar work has been done by Helms *et al.* (Figure 4-9).[140] Here, the porphyrin units are connected through phenyl ring chains, which do not allow the electrons to flow as easily from one porphyrin to the other. It was found that the efficiency of the electron transfer is dependent on the number of conjugation interruptions (the transfer rate drop was 6-fold per phenyl ring).

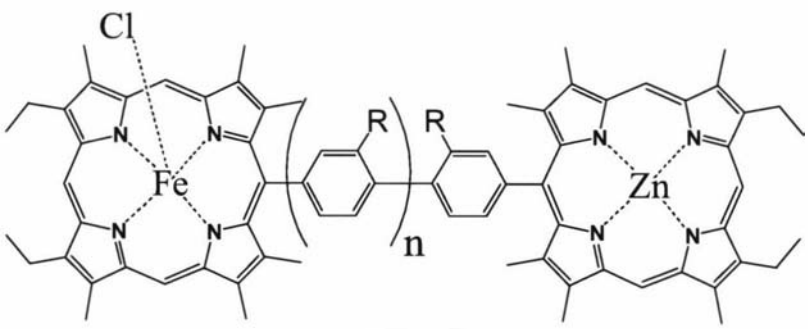

n = 0, 1, 2

Figure 4-9 Zn/Fe(III) dyads by Helms *et al.*[140]

It is worth making a comment about the nature of the bridges utilized in the last examples. The Osuka group[78] compared polyene to polyyne bridges and realized that energy/electron transfer is more efficient through the double bonds than through alkyne linkers; in both cases, however, efficiency was higher than what was obtained by the Helms group (polyphenyl chains). It seems clear that the loss of coplanarity, along with the consequent interruption of the conjugation, is responsible for the drop in the electron transfer quantum yield.

As for energy transfer, conjugation is important only for long distance processes. Fujita *et al.*[141] showed that efficient electron transfer from Zn to Fe(III) porphyrins can be achieved by cofacial disposition, with the condition that the distance between the porphyrin units is not too long (Figure 4-10).

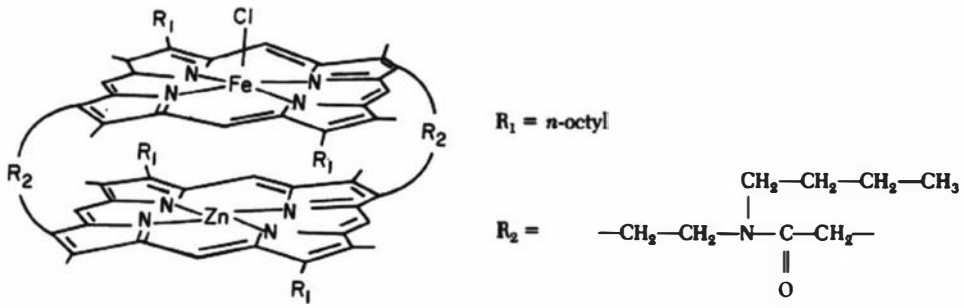

Figure 4-10 Zn/Fe(III) dyad by Fujita *et al.*[141]

Interestingly, in the great majority of the reported work, the porphyrins are connected through their meso positions and it is likely that substitution at β-pyrrolic carbon would produce different photophysical properties. To the best of our knowledge, the only extensive investigation on the photophysics of β-pyrrolic connected porphyrin arrays is due to the Therien group.[159-161] A series of monomers, dimers and trimers featuring alkynyl substitution at β-pyrrolic position were prepared as intermediate for the preparation of face-to-face arrays (Figure 4-11). Interestingly, even though the alkynyl bridges should allow conjugation and high electronic communication between the units, the photophysical and EPR investigations on such systems showed that very little electronic communication is possible along the arrays; UV-visible spectra showed that exciton coupling was the only new feature deriving from the intramolecular interactions[159] and EPR showed that excited triplet states are completely localized on one porphyrin.[160] All these data are consistent with weak electronic interactions due to electrostatic perturbation between close but perpendicular porphyrin rings; therefore, the possibility of conjugation deriving from alkynyl linkage is not sufficient to 'force' the porphyrin into assuming a planar conformation, which would allow efficient electronic delocalization over the array.

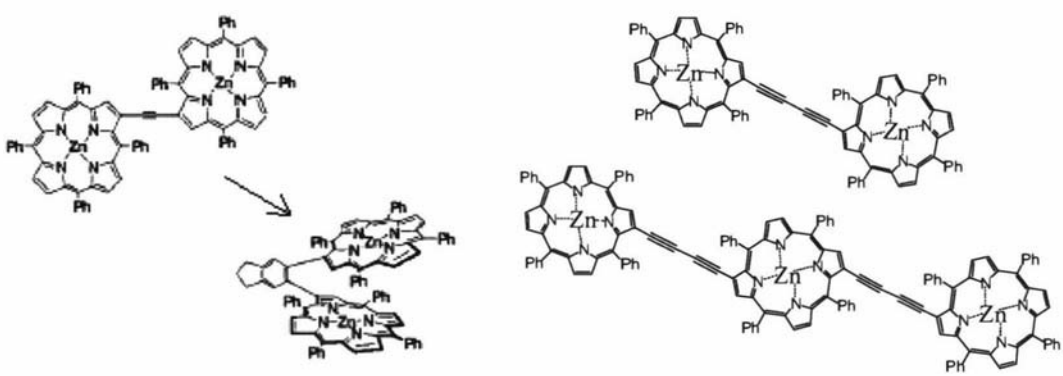

Figure 4-11 β-Pyrrolic alkynyl linked porphyrin arrays by Therien *et al.*[159,160]

The synthetic route to porphyrin arrays described in the course of this thesis allows the creation of structures with different porphyrins connected through their β-pyrrolic positions; moreover, contrarily to the just described alkynyl linkages, the nature of the phenylene-vinylene bridges should constrain the array in the planar conformation, allowing long range energy/electron transfer *via* the Dexter mechanism through the conjugated system.

4.3. Time-resolved spectroscopy

Investigation of the phenomena that take place in excited states requires the ability to follow some measurable physical properties of the system from its excitation to its relaxation to the ground state. The time scale of these processes varies from microseconds to a few picoseconds. Today, there are different techniques that can be employed in the study of such fast phenomena. The most exploited techniques involve the measurement of either absorbance or emission from a sample that is excited by a short laser pulse (pulse time has to be shorter than the excited state lifetime). Many variations are possible, depending on the time-scale of the process under investigation.

The simplest time-resolved technique is based on transient absorption measurements. Here, a strong laser pulse is used to excite a portion of the sample. Perpendicular to the laser is a Xe arc lamp, which produces the analyzing light whose transmittance is recorded at different times after the pulsed excitation; the instrumentation is synchronized by a trigger system, which connects the laser source to the receiver/analyzer (Figure 4-12). Absorption (at one selected wavelength) is recorded at different times after irradiation and the resulting A(t) provides information about lifetimes of the excited states. It is also possible to obtain spectra of the excited states but because of the shortness of the time available for each acquisition, a very long time (thousands of acquisitions) is required to obtain accurate data and the power of the laser can cause decomposition of the compounds under examination. In order to increase the amount of light that can be collected by the receiver/analyzer system, a few modifications to the base instrumentation are required. The continuous source is

modified by a short time high voltage application; in this way the intensity of the source can be increased up to 30 times for 1 ms. Similarly, the use of photomultipliers between the monochromator and the detector can result in more accurate data.

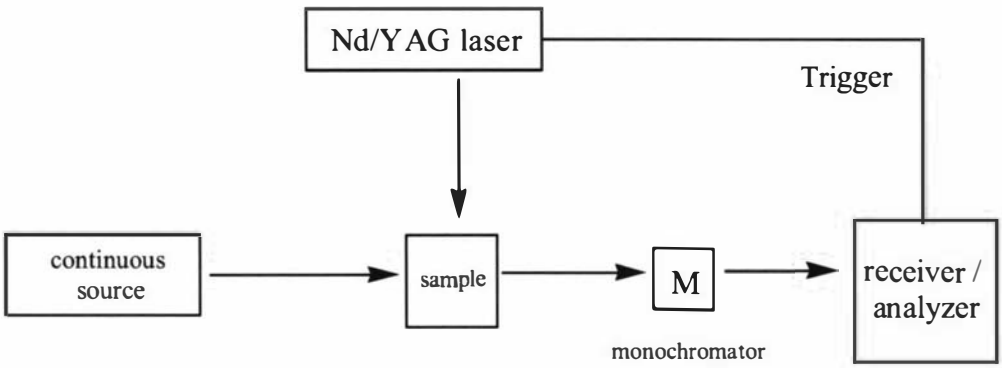

Figure 4-12 Schematic representation of a ns time-resolved absorbance spectrometer

The faster the process under investigation, the more difficult it is to create short pulses and fast analysis techniques. For phenomena slower then 10 ns, a Nd-YAG laser is typically used to excite the sample. This laser produces a very intense beam at 1064 nm which can be transformed to its harmonics at 532, 355 and 266 nm, useful for UV-vis spectroscopy. When investigations of faster processes (lifetime < 1 ns) are required, more complicated instrumentation has to be employed; in particular, the laser source has to be able to produce shorter pulses. Pulses of 18-35 ps can be achieved by modifying the Nd/YAG laser source with a mode-locked, cavity dumped system. In this adaptation of UV-vis absorption spectroscopy (Figure 4-13), the laser beam is split in two parts, which works as both the exciting and analyzing beam; this second beam is then transformed into 'white light' by passing it through a cell containing D_2O/D_3PO_4 and splitting it to two different portions of the sample. The exciting beam is delayed by a computer-controlled optical path and is directed to one of the two portions irradiated with the analyzing light. Finally, the two analyzing beams are recorded by two sets of diode arrays which provide two sets of A(t), from which the time-resolved spectra derive. Accurate data usually requires the average of hundreds of acquisitions.

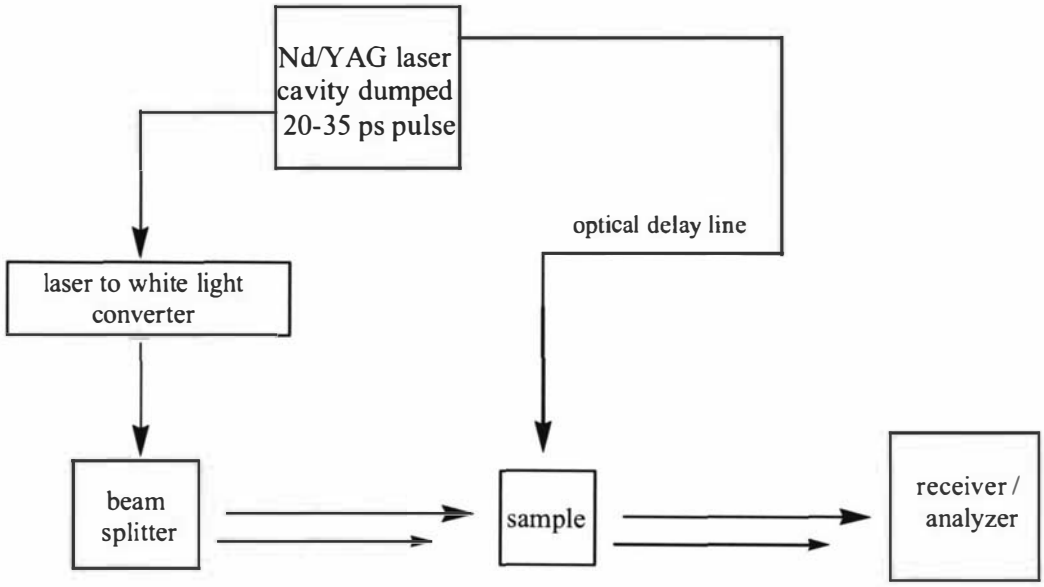

Figure 4-13 Schematic representation of a ps time-resolved absorbance spectrometer

Similar information about excited states can be obtained by emission spectroscopy. For processes in the nanosecond time domain, a modified Nd-YAG laser source (similar to the source described for absorption spectroscopy) is generally used to excite the sample. The other essential part of this kind of apparatus (Figure 4-14) is a digital oscilloscope in the receiver/analyzer apparatus, which is triggered by the laser pulse to correlate emission vs. time. While this method is very useful for qualitative data, it is not very accurate and the powerful Nd/YAG laser source can cause decomposition of the sample.

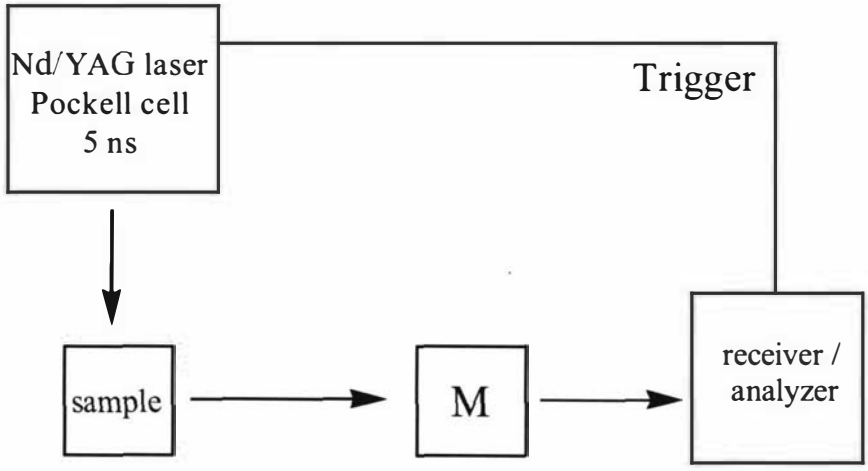

Figure 4-14 Schematic representation of a ns time-resolved emission spectrometer

The most accurate data on lifetimes can be obtained by time-correlated single photon counting (TCSPC). This technique utilizes the apparatus shown in Figure 4-15, a less powerful N_2 or Ar lamp is the source which provides 1 ns long pulses and a time-to-amplitude converter (TAC) is the core of the instrument. The TAC creates an increasing ΔV between two electrodes when it is triggered by the first photon emitted by the lamp. By using a multichannel analyzer, in which every channel records at one specific ΔV_C, a correlation between time (from ΔV) and number of photons emitted can be obtained. This technique allows 1000 measurement per second to be made and, therefore, data can be easily obtained as the average of millions of exponential decays producing very accurate measurements of lifetimes of excited states.

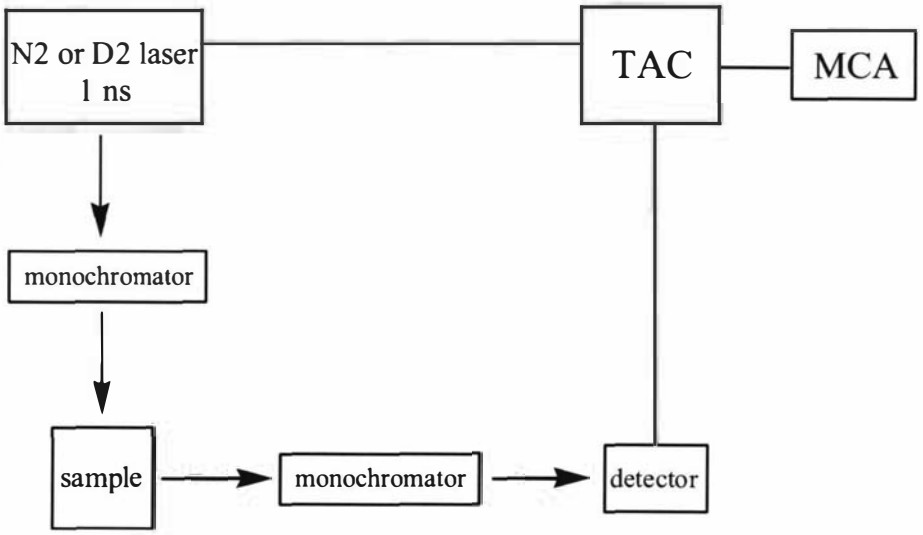

Figure 4-15 Schematic representation of single photon counting apparatus

The investigation of emissions in the picosecond time domain requires more sophisticated equipment. An example of one of the instruments used in the course of this collaboration with researchers at IFOS-CNR is shown in Figure 4-16. The laser source is the same as already described for picosecond absorption spectroscopy (Nd/YAG modified with a mode-locked, cavity dumped unit) and the trigger system and the optical delay path are also the same. The main modification in this apparatus is the use of a streak camera to record the time-resolved emissions. The emitted light is passed through a spectrograph in which a grating disperses this beam horizontally. The second step involves the use of the streak camera in which a photocathode transforms this light into electrons. Finally, the horizontal electron flow is deflected vertically by the triggered increasing ΔV and ends up exciting a phosphorous screen.

The result is a two-dimensional image where the axes represent the wavelength of the radiation and the delay from the excitation, and the intensity of the image is related to the intensity of the emission; this image is then elaborated by a computer. Accurate measurements usually require thousands of acquisitions and the resolution is around 20 ps.

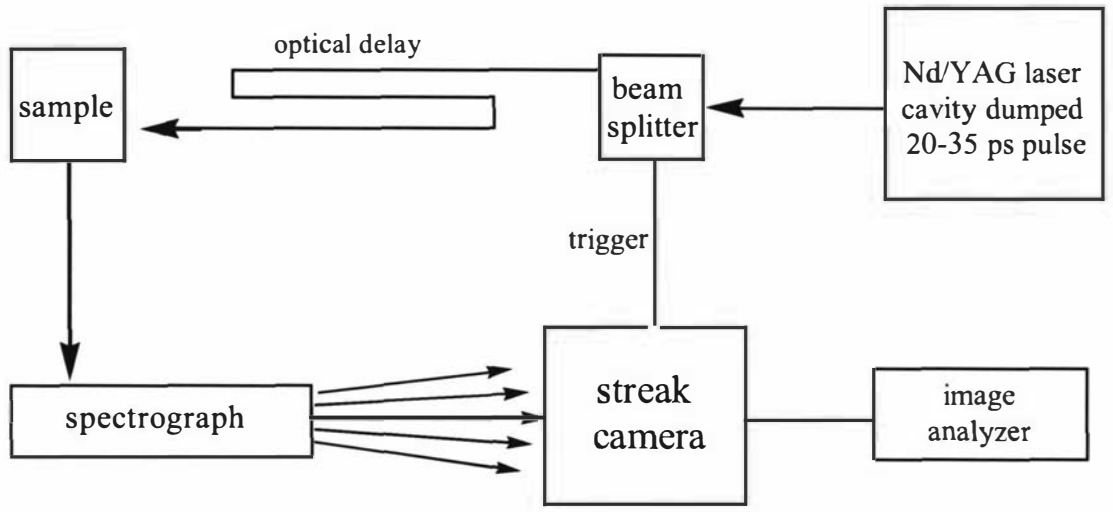

Figure 4-16 Schematic representation of a ps time-resolved emission spectrometer

4.4. Zn/fb and Zn/Fe^{III} porphyrin dyads photophysics

In Chapter 2, it was shown that our synthetic strategy using Wittig chemistry allowed the preparation of arrays in which different porphyrins could be connected through highly conjugated bridges. In order to assess the effectiveness of electron/energy transfers throughout these kinds of systems and to evaluate their possible application in photovoltaic/photosynthetic systems, a collaboration with researchers at the IFOS-CNR in Bologna, Italy, was set up to take advantage of their instrumentation and expertise. The most commonly studied systems are Zn/fb and Zn/Fe(III) porphyrin dyads. In both cases, the Zn porphyrin is the effective 'excited state donor' but, in the first case, there is an energy transfer while, when the acceptor is a Fe(III) porphyrin, an electron is transferred to the ferric centre (Figure 4-17).

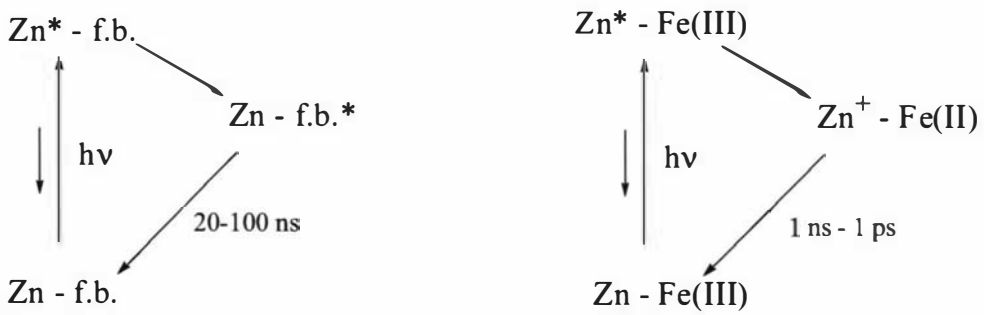

Figure 4-17 Photophysics of Zn/free base and Zn/Fe(III) porphyrin dyads

In Chapter 5, we describe the synthesis of conjugated Zn/Fe(III) dyads for artificial photosynthetic systems. Unfortunately, the absence of fluorescence in Fe(III) porphyrin limits the number of techniques that can be utilized to study them and the appropriate instrumentation is not currently available at IFOS-CNR; in fact, many works in literature that describe this kind of electron transfer are not necessarily correct: assumptions have been made without an actual observation of the short-life excited states, underestimating alternative possibilities such as enhanced intersystem crossing caused by high-spin paramagnetic Fe(III).[183,184] The investigation of homologue Zn/fb dimers is made simpler by the slower rate that is characteristic of such energy transfers and by the distinct fluorescence of free-base porphyrins (which always happens at lower energy than in Zn homologues). It is plausible to think that similar photophysical properties will occur in the homologue Zn/Fe(III) dyads; in fact, the relative position (both distance and angles) of the porphyrin units makes energy transfer *via* a Förster (through space) mechanism highly unlikely and the effectiveness of intramolecular transfers, in both cases, is dependent on the porphyrin/bridge/porphyrin orbital overlapping.

4.5. Monomer models syntheses

Because of the lack of literature on phenylenevinylene β-pyrrolic substituted porphyrins, the syntheses and the photophysical study of a series of monomers functionalized with this kind of conjugated 'branches' was performed. All ideal models were designed to contain a terminal methylene group so that the extension of the conjugation is maximized.

Okuma *et al.*[142] have shown that phosphonium salt CH_3-$PPh_3^+Br^-$ (Me-ps) undergoes Wittig reactions with activated aromatic aldehydes in very good yields, using DBU as base. Less activated aldehydes required longer reaction times and higher temperatures (higher boiling solvents). This seemed ideally suited to the preparation of our target compounds. This Wittig reaction employs the same chemistry that has been introduced so far and requires the use of porphyrin aldehydes as reagents, the syntheses of which have mostly been described in Chapter 2. It is possible to make a series of porphyrins carrying variously long substituents in which the conjugation is maximized by this route (Scheme 4-1).

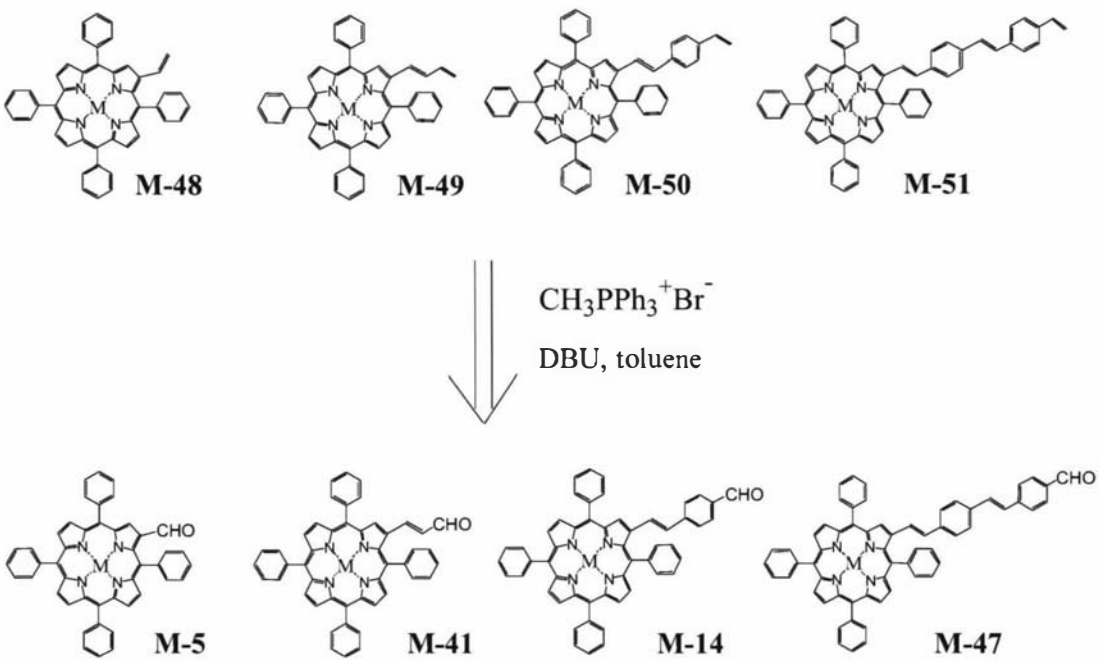

Scheme 4-1 Retrosynthetic scheme for the synthesis of porphyrins **M-48-M-51**

In order to make both free-base and Zn metallated porphyrin models, Wittig reactions can either be performed on free-base or on Zn porphyrin aldehydes and the homologue obtained by standard metallation/demetallation. First attempts showed that there is no substantial difference in yields therefore we decided to use the most readily available reagents (i.e. the ones we had already prepared in a large amount).

The syntheses of aldehydes **5** and **14** have already been described in Chapter 2. 'Extended' aldehyde **41** (along with the Zn homologue **Zn-41**) was prepared from the 'extended alcohol' **40** according to the procedure described by Wang *et al.*[60] (Scheme 4-2). **Zn-41** was obtained by standard metallation of **41**. Alcohol **40** was also utilized

as precursor for the synthesis of the 'extended' phosphonium salt **43**, according to the procedure developed in our laboratories by Dr. W. Campbell.[143]

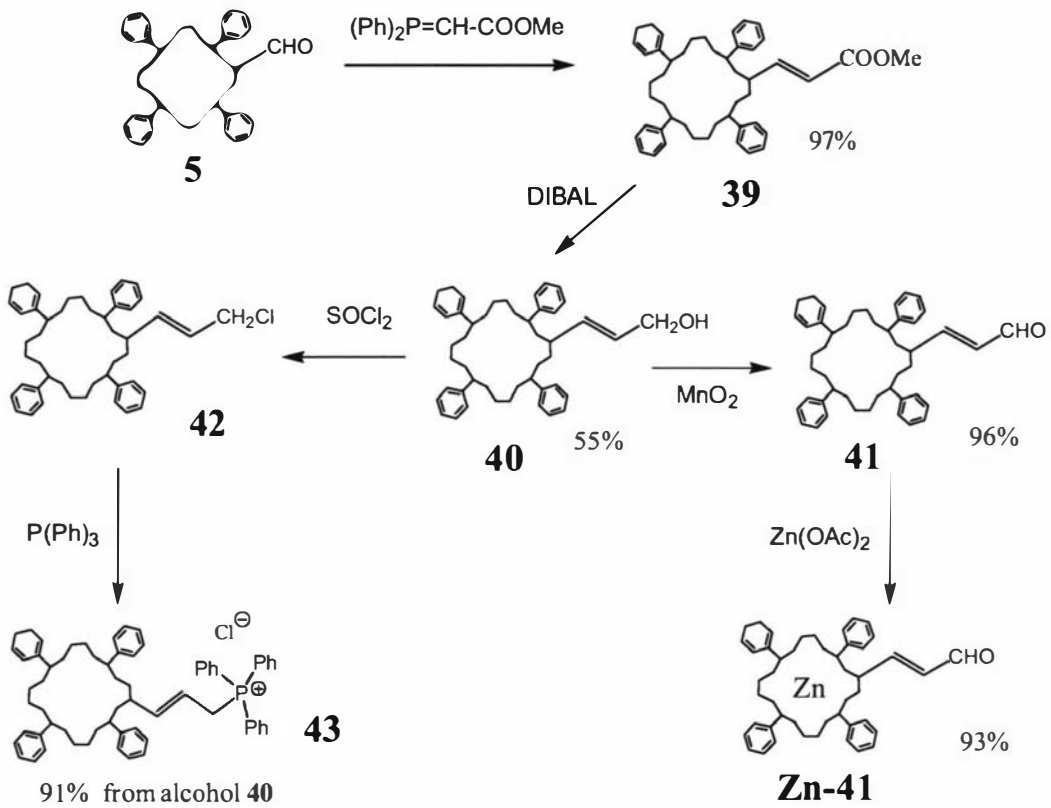

Scheme 4-2 Syntheses of "extended" aldehyde[60] **41** and phosphonium salt[143] **43**

The synthesis of porphyrin aldehyde **Zn-47** containing two phenylene groups was realized in two steps from the **Zn-5**: this aldehyde was first reacted with excess diphosphonate **44** (prepared according to the general procedure from commercial *p*-dibromoxylene) to give Zn porphyrin phosphonate **Zn-45** as major product (47%). Under our standard Wittig-Horner conditions, the disubstituted product **Zn-46** was also obtained and characterized by ^{1}H-NMR and mass spectrometry (Scheme 4-3). The yield in the dimer **Zn-46** can be dramatically increased (up to 80%) by using an excess of the porphyrin aldehyde. The ^{1}H-NMR spectra also showed that these products had pure *trans* configurations.

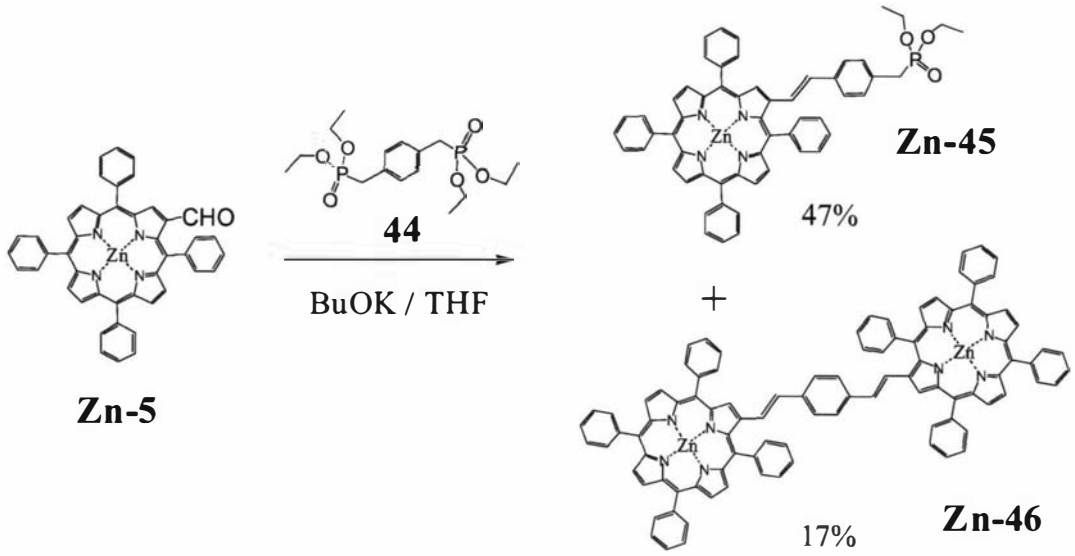

Scheme 4-3 Wittig reaction of aldehyde **Zn-5** with diphosphonate **44**

The successive reaction of phosphonate **Zn-45** with excess *p*-terephthalaldehyde produced the desired porphyrin aldehyde **Zn-47** in good yield (Scheme 4-4).

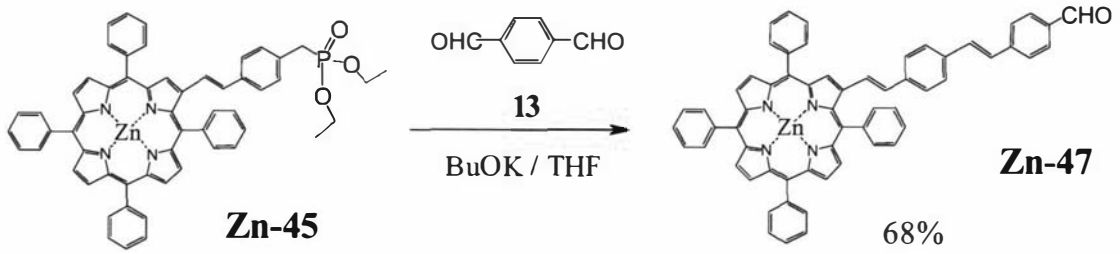

Scheme 4-4 Wittig reaction of phosphonate **Zn-45** with dialdehyde **13**

The free-base and Zn porphyrin aldehydes **M-5**, **M-41**, **M-14** and **M-47** were converted to the homologue 'terminal methylene' porphyrins according to the retrosynthetic method shown in Scheme 4-1. Although the synthesis of 2-vinylTPP **48** has already been described,[144] it was prepared in the same way as all four members of the series in order to compare the reactivity of the different aldehydes. For the first three members of the series (**M-5**, **M-41** and **M-14**), both Zn and free-base aldehydes were reacted with methylphosphonium salt to add the terminal methylene group. Because those aldehydes are not particularly activated, the first attempts using either dichloromethane or chloroform as solvents were not successful; all reactions of this type were therefore performed in refluxing dry toluene. Yields were independent of the metallation state (Table 4-1), except for **Zn-5** which produced a very low yield of

Zn-48 (experiment not repeated). Reactions were optimized by dissolving/suspending the porphyrin aldehyde and three equivalents of the phosphonium salt, and adding DBU in excess (more than 10 equivalents) at reflux. Reaction times varied from 16 to 48 hours. The lower yields obtained for the 'shorter' aldehydes **48** and **49** were not surprising and confirmed their lower reactivity versus Wittig reactions, as already observed for **48** in Chapter 2.

Aldehyde reagent	Product	Yield
5	**48**	26%
Zn-41	**Zn-49**	28%
Zn-14	**Zn-50**	64%
Zn-47	**Zn-51**	79%

Table 4-1 Syntheses of the series of terminal methylene porphyrins **48-51**

For spectroscopic comparison purposes, the preparation of vinylstilbene **53** (Scheme 4-5) was undertaken. The synthesis of this molecule has been described in the literature using different methods.[145] In this work, however, the preparation was performed in two steps using Wittig chemistry.

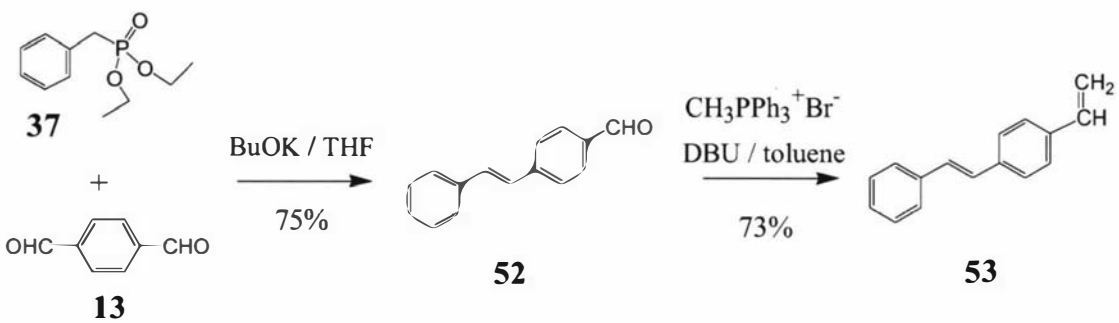

Scheme 4-5 Synthesis of vinylstilbene **53** via Wittig chemistry

The characterization of all the porphyrin monomers presented in this section was straightforward. The ^{1}H-NMR spectra of all the compounds displayed proton magnetic resonances typical of β-substituted tetraphenylporphyrins (see Section 2-7). The spectra of the vinylporphyrins **M-48**, **M-51** and **53** showed the normal AMX coupling pattern for a terminal vinyl grouping in which the geminal protons are not

chemical shift equivalent and the coupling of the terminal protons typically in the order of 1-2 Hz (Figure 4-18)

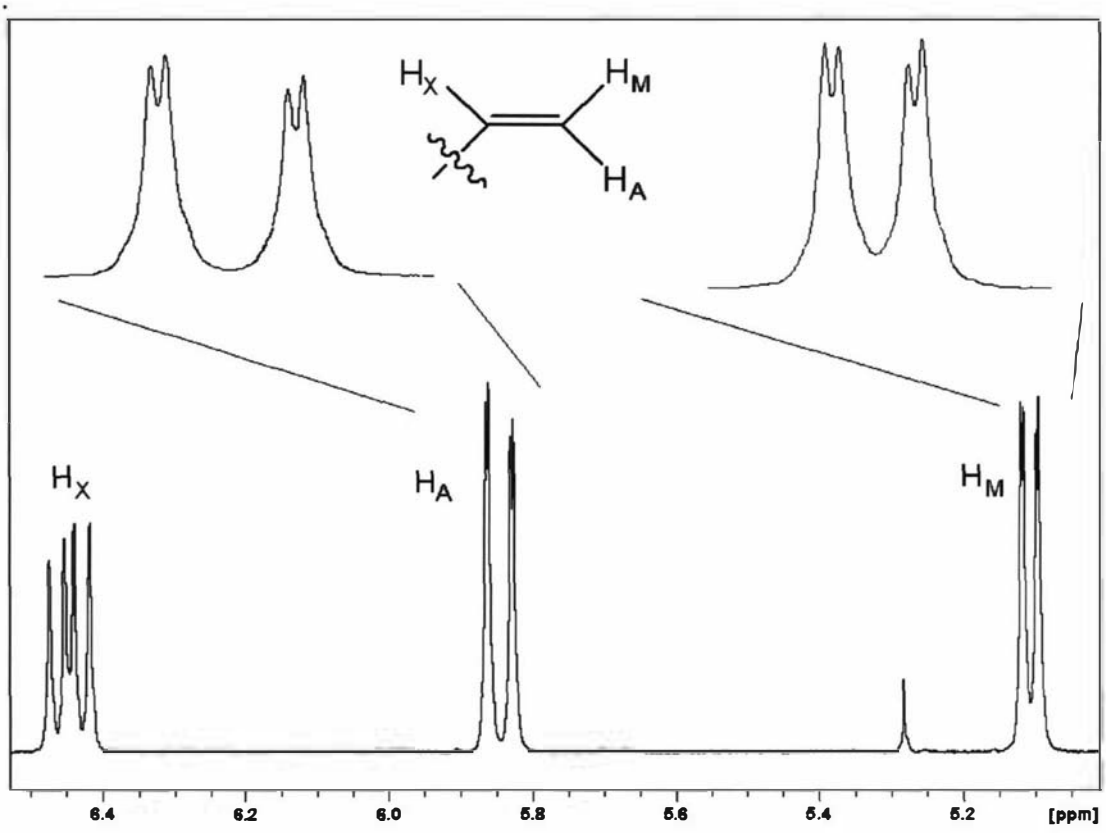

Figure 4-18 ^{1}H-NMR spectrum of the vinyl region in **Zn-45**

LR-MALDI and HR-FAB mass spectra were also used for the characterization of the compounds presented in this section; either molecular ions (M^+) or protonated ions ($M + H^+$) were measured for all the compounds described.

4.6. Monomer models spectroscopy and photophysics

All spectroscopic investigations presented in this chapter were performed by Dr. L. Flamigni and Dr. B. Ventura at ISOF/CNR, Bologna, Italy.

Absorption spectroscopy

In order to demonstrate the effect of the conjugation on the spectral properties of free-base and Zn porphyrins, the absorption spectrum of the free-base porphyrin **51,** that carries the longest arm, is reported in Figure 4-19 where it is compared with the

absorption spectra of **TPP** and the vinylstilbene unit **53**, which can be considered as a good model for the *β*-pyrrolic substituent in **51**. Very similar pictures can be obtained for all others members of the series **M-48-M-51** (M = Zn, 2H). From this picture, it is clear that in passing from TPP to **51,** the conjugation between the porphyrin and the *β*-pyrrolic substituent is reflected in a dramatic decrease in ε_{max} and a red-shift and a broadening of the absorption bands, the Soret band in particular.

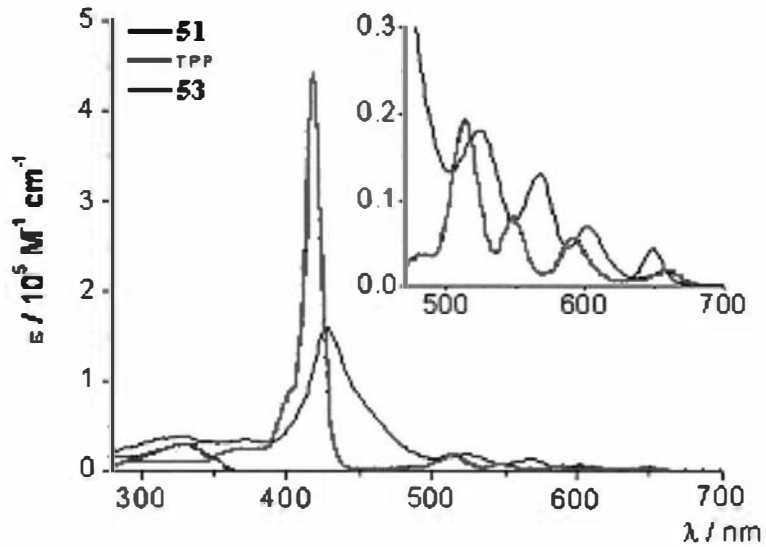

Figure 4-19 Comparison between UV-visible absorbtion spectra of **51** and the sum of TPP and the conjugated substituent **53**

The absorption spectra of free-base porphyrins **48-50** are displayed in Figure 4-20. From inspection of the spectra of the free-base series it is clear that in passing from TPP to **51,** the increased degree of conjugation of the *β*-pyrrolic substituent is reflected in a proportional decrease in ε_{max} and a red-shift and a broadening of the absorptions (Table 4-2). In particular, the decrease in the absorbance is large for **48**, **49** and **50** where one vinyl group, two vinyl groups and a phenylene group, respectively, are attached to the tetrapyrrolic ring. For fb porphyrin **51**, whose substituent has a further phenylene group, the Soret ε_{max} remains unchanged compared to **50** but a further broadening of the band is observed. The red-shift of the Soret band is more pronounced in passing from TPP to the first member of the series **48** (from 419 nm to 424 nm) than to the other porphyrins in the series. A similar trend is observed for the Q bands where a general red-shift of all bands along the series occurs with increasing conjugation.

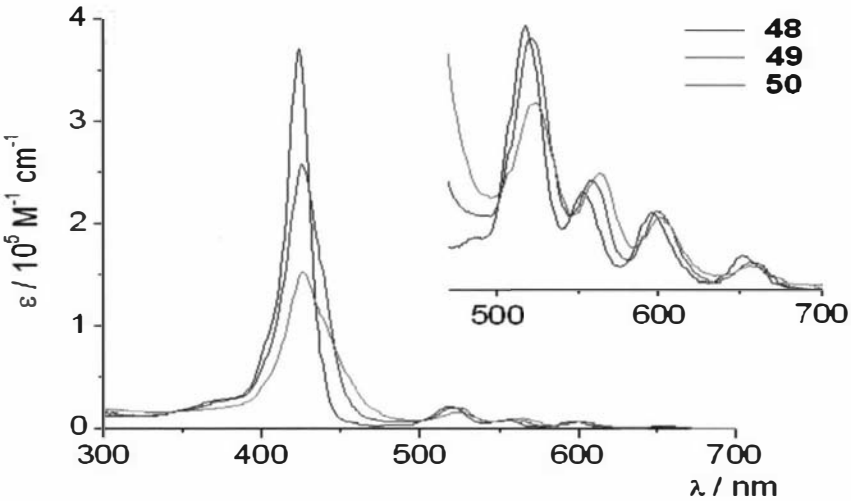

Figure 4-20 UV-visible absorbtion spectra of free-base porphyrins **48-50**

In the spectra of the Zn porphyrins (Figure 4-21 and Table 4-2), the Soret bands present a trend similar to that observed in the free-base series; the decrease in the maximum of the absorbance is evident for **Zn-49** and **Zn-50** compared to ZnTPP whereas **Zn-50** and **Zn-51** mainly show a broadening of the band around 470 nm. The Q bands, on the other hand, in addition to exhibiting the trend in the bathochromic shifts, also show a variation in the relative intensities: the lowest energy band increases its intensity while the highest energy band is almost unaffected.

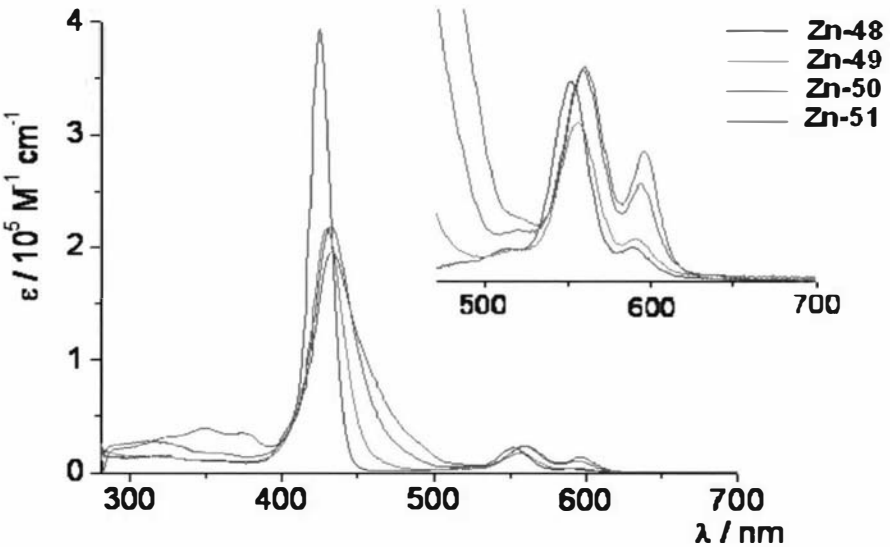

Figure 4-21 UV-visible absorbtion spectra of Zn porphyrins **Zn-48**-**Zn-51**

	λ_{max}/nm	ε / 10^3 $M^{-1}cm^{-1}$		λ_{max}/nm	ε / 10^3 $M^{-1}cm^{-1}$
TPP	419 514 548 592 648	443 19 8 5 4	**ZnTPP**	423 550 589	537 24 5
48	424 519 554 596 653	369 22 8 6 3	**Zn-48**	425 552 590	393 22 4
49	426 522 560 600 659	257 21 9 7 2	**Zn-49**	430 556 591	216 18 5
50	427 524 564 602 659	167 17 1 6 1	**Zn-50**	433 559 594	218 23 11
51	344 (sh) 373 (sh) 428 524 568 602 659	32 34 159 18 13 7 2	**Zn-51**	350 (sh) 375 (sh) 433 560 597	40 35 196 24 14

Table 4-2 Absorption data for TPP, ZnTPP and porphyrin series **48-51** and **Zn-48-Zn-51** in toluene and at room temperature

These first experiments have shown that a conjugated β-pyrrolic substituent has a strong influence on the electronic states of the porphyrin core. In particular, the extensive broadening of the Soret band and the red-shift of the entire spectrum are consistent with the electronic transitions that involve new molecular orbitals deriving from the mixing of orbitals from the porphyrin and from the conjugated substituent. The presence of a uniform trend passing from the unsubstituted porphyrin to the longest arm models (**M-51**) indicates that orbital interactions occur over relatively long distances. The observed bathochromic shift can be explained by considering that conjugation generally reduces the HOMO-LUMO gap. In the examined β-substituted porphyrins, the decrease of the HOMO-LUMO gap along the series could be due both to the stabilization of the LUMO orbitals as a consequence of the increased delocalization and to the destabilization of the filled HOMO orbitals as a result of mixing with the substituent π-orbitals that lie at lower energies.[162]

Emission spectroscopy

The emission spectra of the free-base porphyrins series **48-50** (in toluene) at room temperature upon excitation at 520 nm are displayed in Figure 4-22 and the data is reported in Table 4-3. It is evident that the emission of the free-base porphyrins shifts slightly to lower energy with respect to the emission of **TPP** when the conjugation of the β-substituent increases, with a trend that follows the behavior of the absorption spectra. Those red shifts are consistent with the extension of the π-conjugation of the porphyrin ring over the substituent.

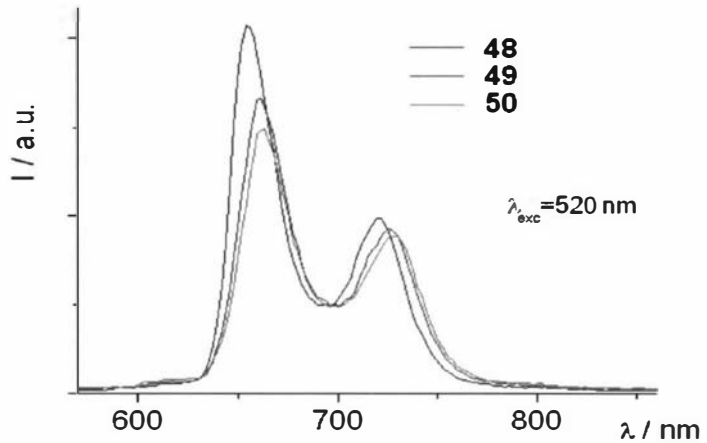

Figure 4-22 Emission spectra (at 295 K) of the series **48-50** in toluene

The emission spectra and data for the Zn porphyrin series **Zn-49-Zn-51** (upon excitation at 560 nm) are displayed in Figure 4-23 and Table 4-3, respectively, and are similar to that of the homologue free-base series, except that, as for the absorption (Figure 4-21), the effect of the conjugation on the various vibrational states is different and results in the inversion of the relative intensities of the two emission bands in Zn porphyrins.

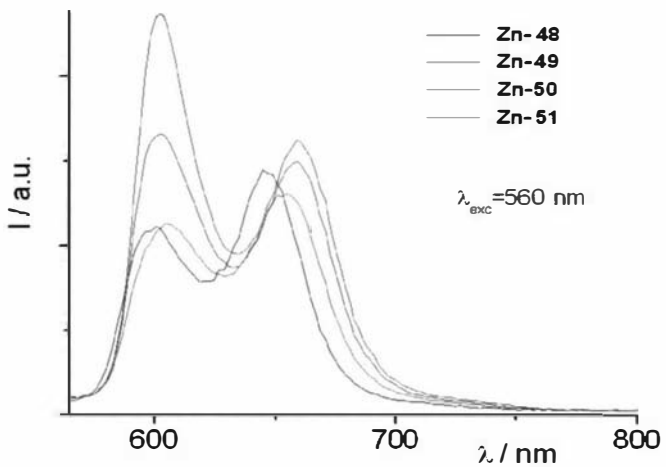

Figure 4-23 Emission spectra (at 295 K) of the series **Zn-48-Zn-51** in toluene

The spectra obtained in a glassy matrix at 77 K allowed the detection of the phosphorescence of all the examined Zn porphyrins that occurs between 780-790 nm, as can be observed in Figure 4-24 (data in brackets in Table 4-3). In the free-base series, phosphorescence was not observed, but triplet states (with lifetimes in the order of 100 μs) were identified in both free-base and Zn porphyrins by their transient absorption spectra, which show the typical absorption in the 700-900 nm region.[47] The measured energies of the Zn porphyrin triplet states show a modest but continuous decrease in energy, indicating that, in addition to stabilizing the singlet excited states of porphyrins, an enhanced delocalization of the molecular orbitals also stabilizes the triplet states.

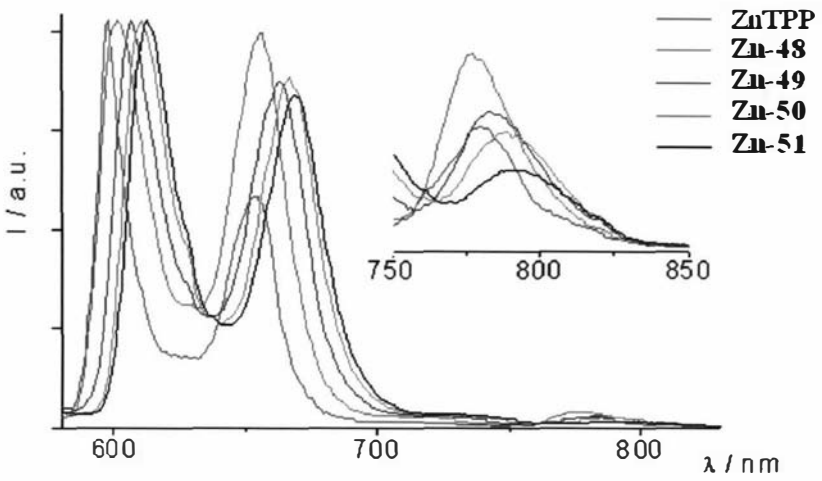

Figure 4-24 Emission spectra at 77 K of the series **Zn-48-Zn-51** (phosphorescence shown in the expanded region)

The quantum yields (intensity) of the emissions were referenced to standard TPP emission (Φ_{fl} = 0.11)[158] and measured using optically matched solutions. The fluorescence quantum yields appear uniform within the free-base series **48-51** (Φ_{fl} = 0.090-0.091) and are smaller than that of TPP. In contrast to the free-base series, the fluorescence quantum yields of the Zn porphyrins **Zn-48** and **Zn-49** remain almost unchanged compared to ZnTPP (Φ_{fl} = 0.047) and only **Zn-50** (Φ_{fl} = 0.063) and **Zn-51** (Φ_{fl} = 0.073) show a significant increase.

	295 K				77 K		
	λ_{max}[a]/nm	Φ_{fl}[a]	τ[b]/ ns	k_r / s^{-1}	λ_{max}[a]/nm	τ[b]/ ns	E[c]/eV
TPP	650 715	0.11 0	9.3	1.2×10^7	643 712	13.4	1.92
48	655 721	0.091	8.5	1.1×10^7	648 718	12.3	1.91
49	662 726	0.091	8.5	1.1×10^7	652 721	12.4	1.90
50	663 729	0.090	8.1	1.1×10^7	655 724	12.2	1.89
51	662 730	0.091	9.0	1.0×10^7	657 726	13.7	1.89
ZnTPP	594 642	0.047	1.9	2.5×10^7	598 654 (780)	2.7	2.07 (1.59)
Zn-48	599 645	0.044	1.7	2.6×10^7	602 656 (777)	2.5	2.06 (1.59)
Zn-49	605 654	0.050	1.8	2.8×10^7	607 663 (785)	2.6	2.04 (1.58)
Zn-50	603 659	0.063	1.9	3.3×10^7	611 667 (789)	2.6	2.03 (1.57)
Zn-51	603 660	0.073	1.8	4.1×10^7	613 669 (792)	2.4	2.02 (1.57)
13	355 375 391(sh)	0.35	0.72	4.9×10^8	357 376 398	2.07	3.47

[a] Emission maxima derived from non-corrected emission spectra. Absolute quantum yields were determined by comparing corrected emission spectra, using **TPP** in aerated toluene as a standard (Φ_{fl} = 0.11).[155] Excitation at 520 nm for the free-base porphyrin series, at 560 nm for the Zn porphyrin series and at 329 nm for model **13**. [b] Excitation at 560 nm for the porphyrin series and at 331 nm for model **13**. [c] Derived from the emission maxima at 77 K

Table 4-3 Luminescence properties of series **48-51** and **Zn-48-Zn-51** in toluene

Another important parameter to be investigated is the lifetime (τ) of the excited states. Time-correlated single photon counting was used for the determination of the τ of the two series of monomers. As for the quantum yields, lifetimes also remain almost uniform along the free-base series and are similar to that of TPP, with a value that ranges from 8.1 ns to 9.0 ns at room temperature and from 12.2 ns to 13.7 ns at 77 K. As for the free-base series, the measured lifetimes remain almost unchanged for all the Zn porphyrins, varying from 1.7 ns to 1.9 ns at room temperature and from 2.4 ns to 2.7 ns at 77 K.

The analysis of the data just described allows some interesting conclusions to be drawn. The relationship between the fluorescence quantum yield and the lifetime of the excited state is

(Eq. 4-1) $$\Phi_{fl} = k_r \bullet \tau$$

allowing the radiative rate constant (k_r) of both series of porphyrin to be calculated. In the free-base porphyrins, the registered reduction in both quantum yield and lifetimes (compared to TPP) and the little variation of those parameters along the series, produce values of k_r which are constant and very similar to that of unsubstituted **TPP** (1.2×10^7 s^{-1}). As a result, it appears that the nature of the substituent has very little influence on the emitting properties of the series of free-base porphyrins **48-51.** In contrast, in the Zn series, the increase in fluorescence quantum yield going from ZnTPP to **Zn-51** is reflected in an increment of the calculated radiative rate constant which increases from 2.5×10^7 s^{-1} to 4.1×10^7 s^{-1}. The presence of the phenylene units, therefore, has a major effect on the emitting properties of the Zn porphyrins, increasing the efficiency of the radiative pathway by ca. 70%. Confirmation of this was obtained from calculations of the oscillator strengths going from the unsubstituted ZnTPP to **Zn-51**.[47]

Vinyl-substituted porphyrins have been used in photodynamic therapy[152,153] therefore, in order to get information on the capability of our conjugated porphyrins to generate singlet oxygen, their photosensitizing ability was explored by measuring the quantum yield of singlet oxygen production, *via* detection of its characteristic luminescence at

1270 nm.[47] In comparison to TPP and ZnTPP, both series showed a high reactivity with ground state molecular oxygen. In particular, the free-base porphyrins show yields that are uniform within the series and greater than that of TPP. For the Zn series, a more inhomogeneous behavior is observed but the values are similar to that of ZnTPP. However, the high values obtained in both series, confirm the strong reactivity of these β-substituted porphyrins with molecular oxygen and their possible use as photosensitizers.

4.7. Zn/Zn, fb/fb, and Zn/fb dyad syntheses

In order to investigate the potential for intramolecular energy/electron transfer along our conjugated arrays, a series of dimers was synthesized and their photophysical characterization is currently being undertaken at the IFOS-CNR in Bologna, Italy. A series of four Zn/fb dyads, connected by the same kind of conjugated linkers investigated in the monomer models, was prepared utilizing Wittig chemistry (Figure 4-25). The homometallic homologues were also prepared and investigated in order to better understand the photophysics of such systems, producing four groups (**A-D** series) of three dyads.

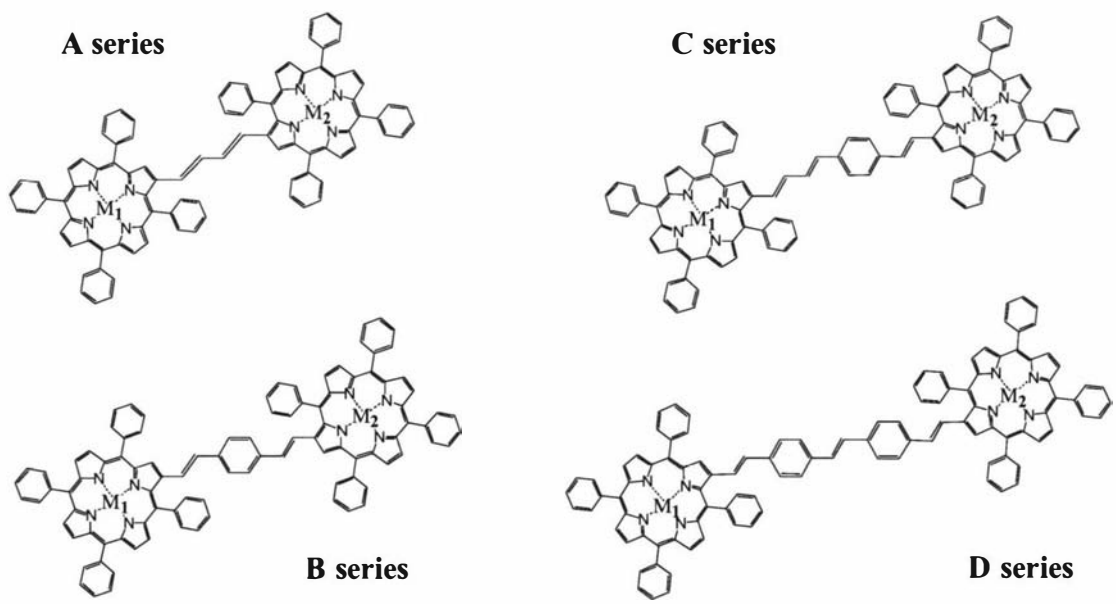

M_1 and M_2 = Zn or 2H

Figure 4-25 Series of homometallic and heterometallic (M = Zn or 2H) porphyrin dyads

The syntheses of the homometallic dyads were simpler than the heterometallic homologues. The easy Zn insertion/removal allowed the preparation of either the Zn/Zn or the fb/fb homologue, obtaining the other one in almost quantitative yield. Moreover, in many cases phosphonate chemistry was employed for the syntheses of Zn/Zn dimers, avoiding isomerization steps and in one case (C series), the symmetry led to the synthesis of the product in one step from the simple aldehyde **Zn-5**.

A series: The synthesis of these dimers with different combinations of M_1 and M_2 has been described by Bonfantini and Officer.[146] In this biphasic Wittig reaction, the porphyrin is dissolved in dichloromethane and the base is dissolved in water. The preparations of **54** and **Zn/fb-55** in the course of this work were performed according to this method. The homologue **Zn-54** was obtained by standard Zn metallation of **Zn/fb-55,** as shown in Scheme 4-6.

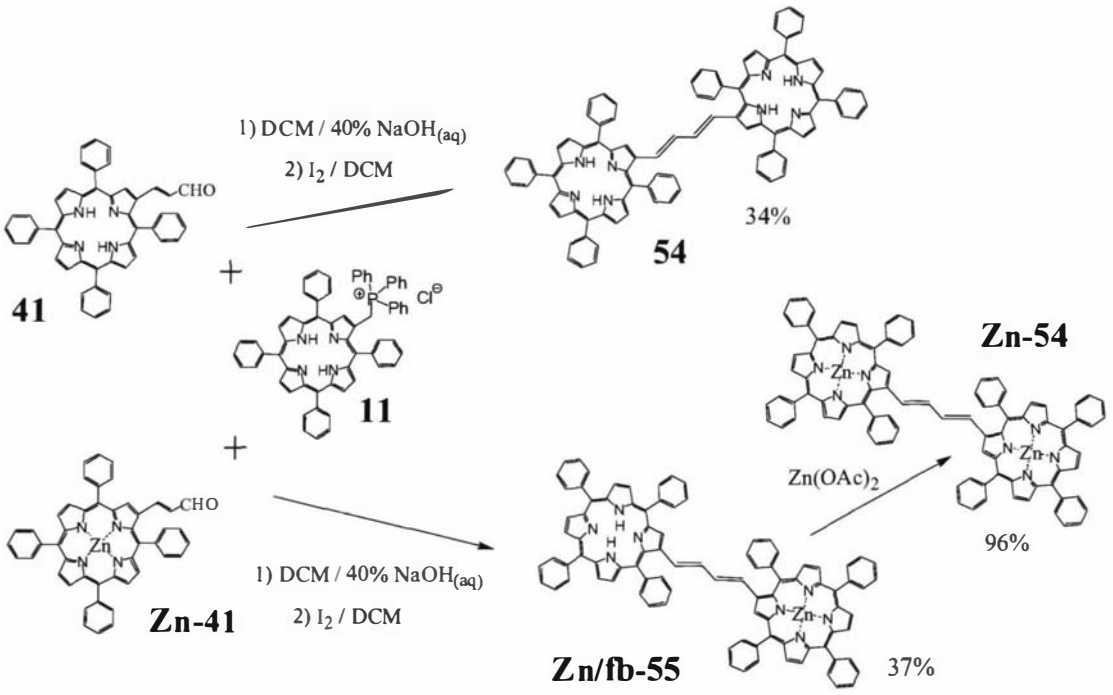

Scheme 4-6 Syntheses of A series dyads **54**, **Zn-54** and **Zn/fb-55**

The slightly lower yield in the case of the homometallic homologue **54** may be due to the reduced 'electrophilicity' of the free-base porphyrin aldehyde. An isomerization step (by I_2 treatment) was required to convert all the butadiene linkers to the *trans/trans* configuration.

B series: The Zn/Zn dyad of this series, **Zn-46,** has been already described as a co-product in the syntheses of phosphonate **Zn-45** (Scheme 4-3). The yield of this disubstituted product can be easily increased to 80% using a deficiency of the phosphonate reagent. The free-base homologue **46** was obtained by standard demetallation with dilute HCl of **Zn-46** in almost quantitative yield. Finally, the synthesis of the heterometallic version **Zn/fb-56** was obtained by Wittig reaction between TPP phosphonium salt **11** and aldehyde **Zn-14** according to Scheme 4-7. Once again, I_2 catalyzed isomerization was required to obtain all double bonds in a *trans* configuration.

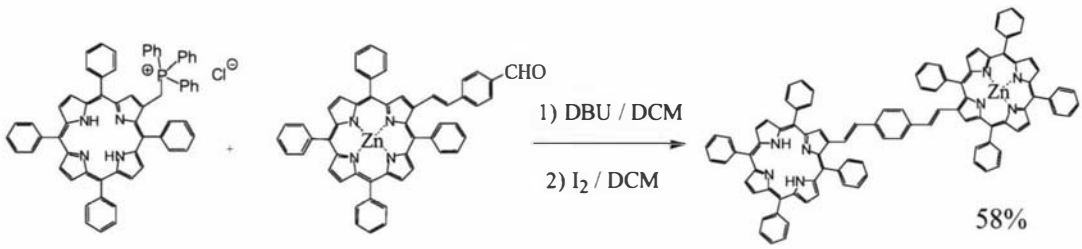

11 **Zn-14** **Zn/fb-56**

Scheme 4-7 Synthesis of heterometallic dyad **Zn/fb-56**

C series: The synthesis of the heterometallic member of this series was achieved in similar fashion as for **Zn/fb-56,** using phosphonium salt **43** in place of **11**. Similarly, an isomerization step was needed to obtain all the double bonds in the *trans* configuration (Scheme 4-8).

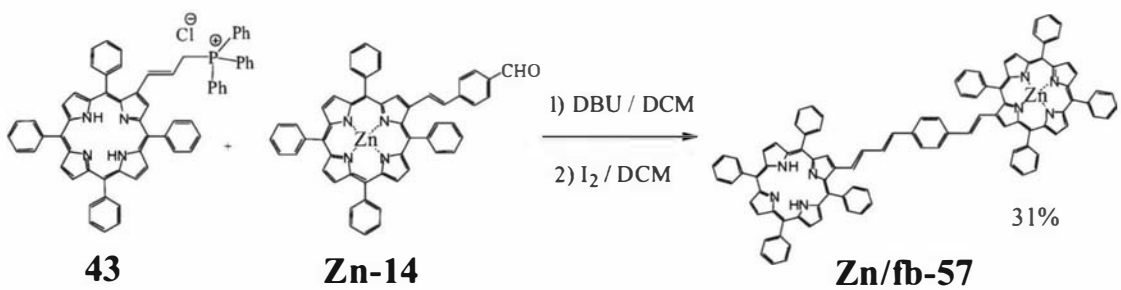

43 **Zn-14** **Zn/fb-57**

Scheme 4-8 Synthesis of heterometallic dyad **Zn/fb-57**

The Zn/Zn dimer of this series, **Zn-58,** was synthesized by the reaction in Wittig-Horner conditions between the previously described porphyrin aldehyde **Zn-41** and phosphonate **Zn-45** (Scheme 4-9). This reaction was preferred to the Zn metallation of the homologue heterometallic dyad **Zn/fb-56** because of the higher yield expected by using phosphonate reagents in place of phosphonium salt (no isomerization is

required, lower amounts of hydrolysis side-products). Standard demetallation of this **Zn-58** provided the free base homologue **58**.

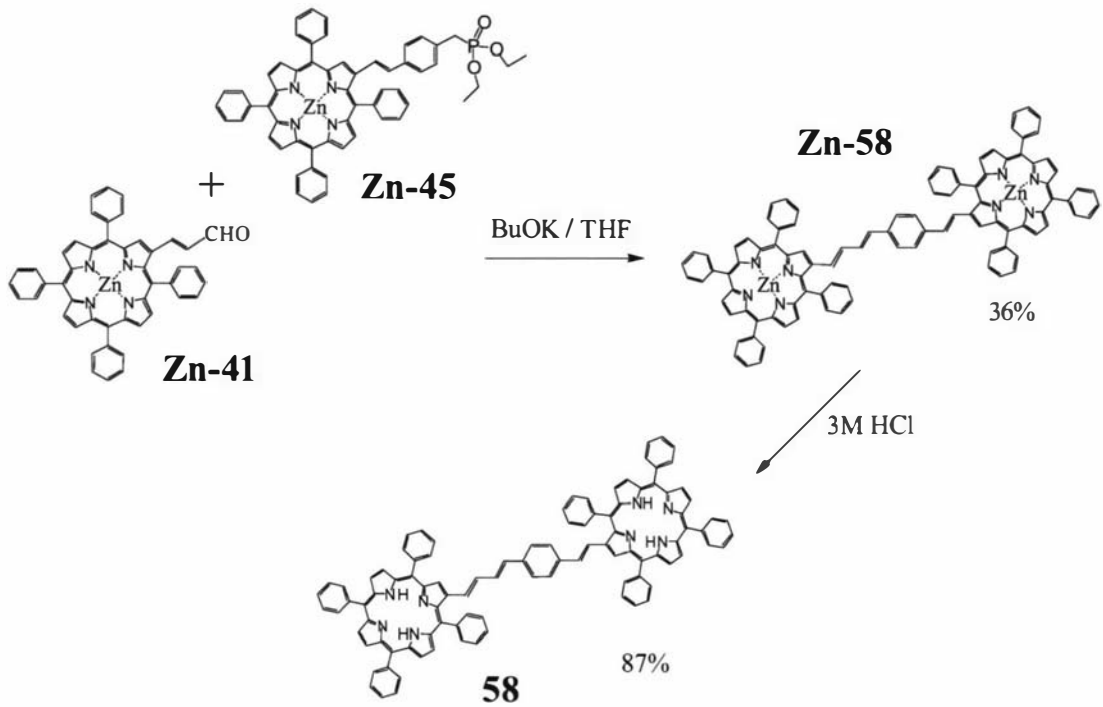

Scheme 4-9 Synthesis of homometallic dyads **58** and **Zn-58**

D series: As for the C Series, the syntheses of the heterometallic dyad was achieved by a reaction involving a porphyrin phosphonium salt while the absence of *N*-pyrrolic protons permitted the use of phosphonate (with BuOK as base) for the preparation of the Zn/Zn homologue. Reaction in dichloromethane of the previously prepared phosphonium salt **14** and aldehyde **Zn-47** afforded the heterometallic dyad **Zn/fb-59** in reasonable yield (Scheme 4-10).

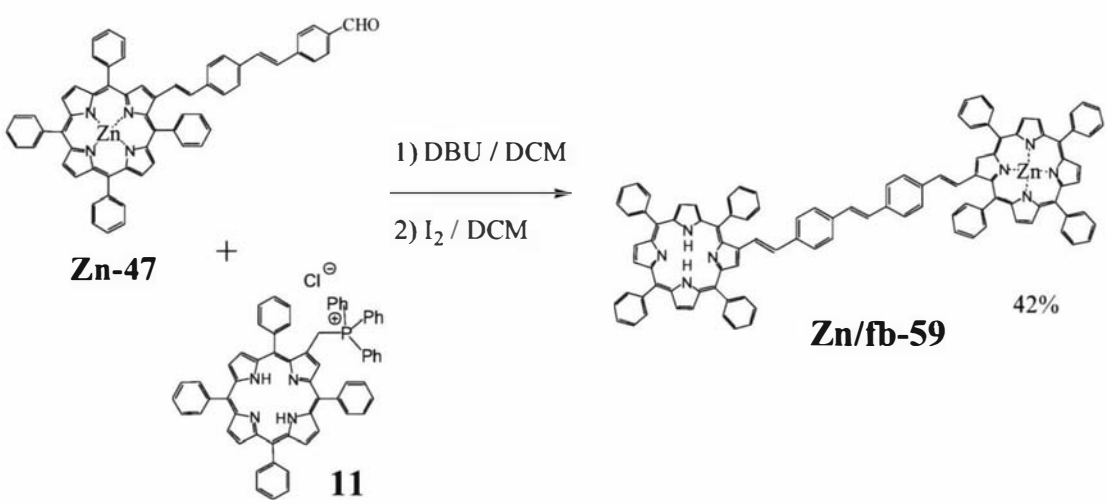

Scheme 4-10 Synthesis of heterometallic dyad **Zn/fb-59**

Reaction of phosphonate **Zn-45** with aldehyde **Zn-14** gave the desired homometallic homologue **Zn-60**. As for the previous two series, the free base array **60** was obtained by demetallation of the Zn homologue **Zn-60** (Scheme 4-11).

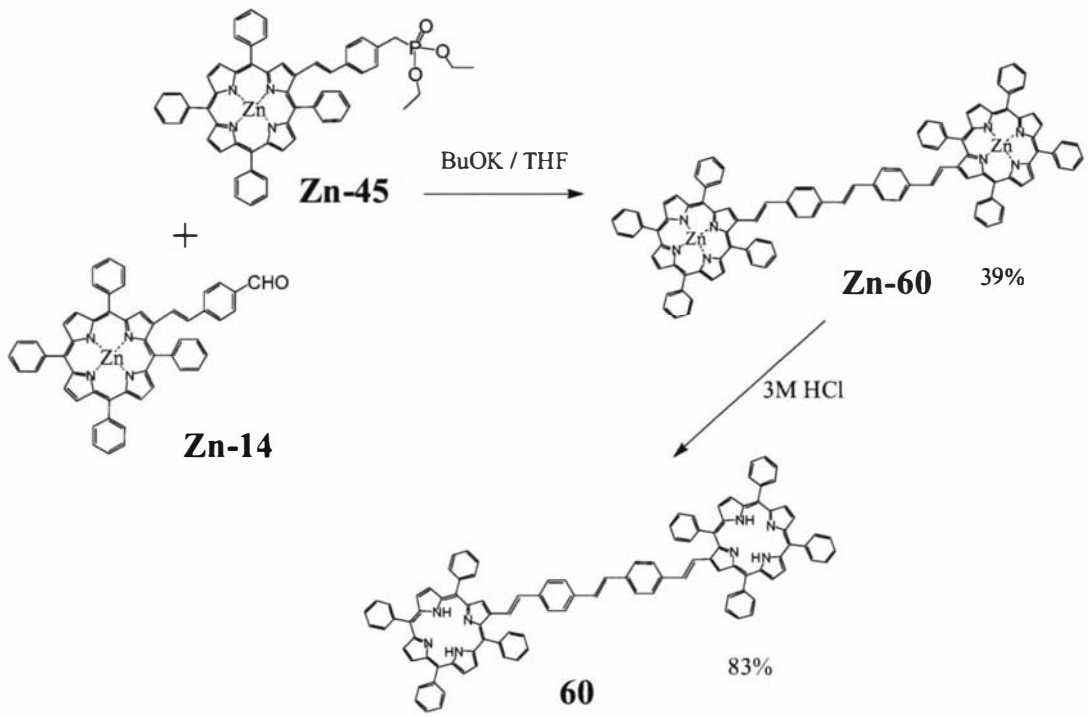

Scheme 4-11 Synthesis of homometallic dyads **60** and **Zn-60**

Purification and characterization

The purification and characterization processes for the dyad series were more challenging than for the monomer models presented in the previous sections. This was mainly due to the generally lower solubility of this kind of array in any typical organic solvent. In particular, the series containing the longest linkers (the **D series** and, to a minor degree, the **C series**) showed a strong tendency to aggregation, resulting in difficulties in performing efficient column chromatography and recrystallizations. Along the series, the solubility followed the order Zn/fb > Zn/Zn > fb/fb, suggesting that high symmetry plays an important role and that free-base

porphyrin arrays form less soluble aggregates.[163] In these cases, quick flash chromatography (through few cm of silica gel) followed by a series of recrystallizations from different solvent mixtures was the optimal purification procedure. Low solubility was also responsible for problems in obtaining well resolved NMR spectra; typically, deuterated ethers (dioxane or THF) had to be used either as solvents or as a co-solvent to improve the solubility in $CDCl_3$.

Characterizations, besides the spectroscopic investigations so far described, were performed by ^{1}H-NMR spectrometry and mass spectrometry. LR-MALDI and HR-FAB mass spectra were obtained for all the dyads presented in this section; either molecular ions (M^+) or protonated ions ($M + H^+$) were measured for the majority of compounds, although some of the members of the **C** and **D series** only produced molecular oxygen adduct ions ($M + O_2 + H^+$).

The ^{1}H-NMR spectra of all dyad series show all the typical resonances of β-substituted tetraphenylporphyrins. In the symmetric cases (all the homometallic dimers, except for the **C series**) a slight broadening of the equivalent signals was often observed. Similarly, the resonances of the linkers showed not perfect symmetry, suggesting some degree of conformational freedom. As an example, the ^{1}H-NMR spectra of the **A series** show two kinds of alkene protons for the butadiene linkers; Figure 4-26 shows the typical multiplets (in place of the expected doublets) from the protons of the butadiene linker in **Zn-54**.

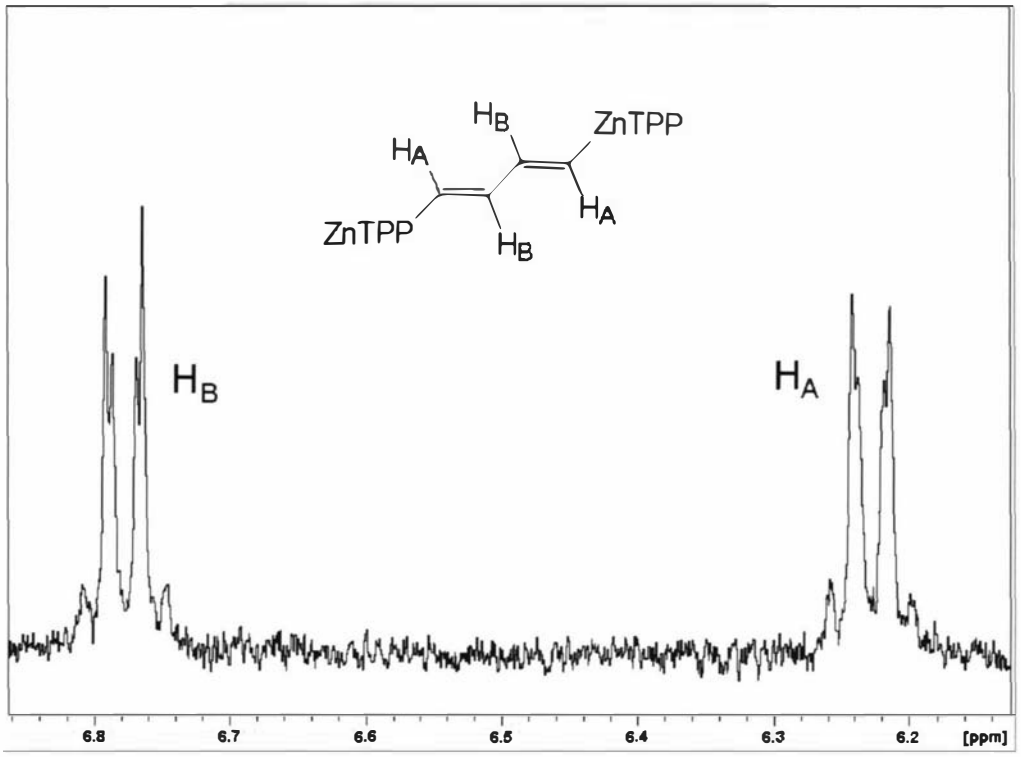

Figure 4-26 ^{1}H-NMR resonances of the butadiene linker in **Zn-54**

4.8. Dyad spectroscopy and photophysics

As for the monomer models, all spectroscopic investigations presented in this section are being performed by Dr. L. Flamigni and Dr. B. Ventura at ISOF/CNR, Bologna, Italy. Unfortunately, to date, the investigation is still in progress and there is not enough data for a complete discussion of the phenomena involved in the intramolecular photophysics of these compounds. However, first results allow us to make some comments.

Figure 4-27 shows the absorption spectra of the series of free-base homometallic dyads. Comparing these spectra with the ones in Figure 4-20 (free-base monomers) it is evident that the electronic interactions are increased by the presence of another porphyrin at the end of the conjugated linker. Compared to the spectra of homologue monomers, all the absorptions in Figure 4-27 and Table 4-5 show a slight further red-shift and, most of all, increased absorbances in the region between Soret and Q bands (450-500 nm). Those absorbances are not characteristic either of porphyrins or of

phenylene-vinylene linkers, and can be seen as indication of high electronic delocalization over the entire array. Very similar spectra have also been obtained for the homologue Zn homometallic series.

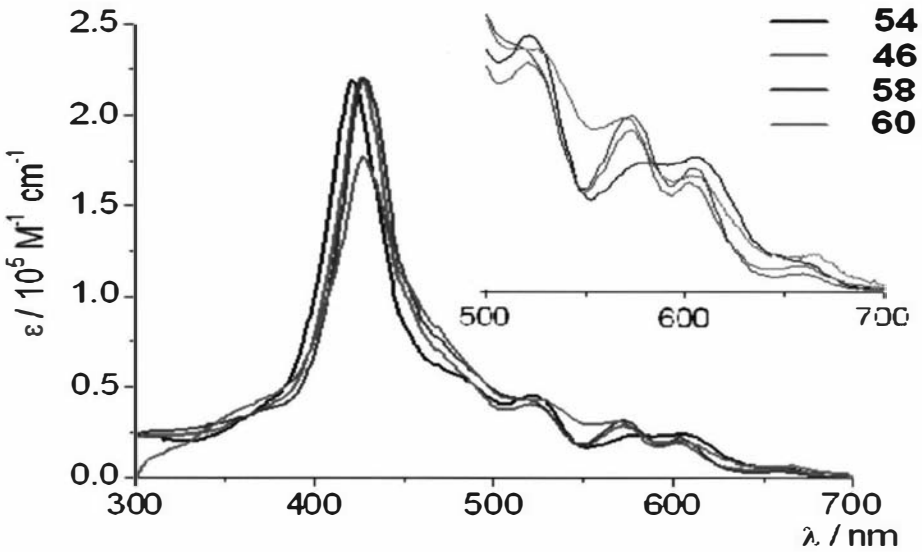

Figure 4-27 UV-visible absorbtion spectra of the series of free-base homometallic dyads **54**, **46**, **58** and **60** in toluene

An inspection of the UV-vis absorbances of the heterometallic dyads (Figure 4-28 and Table 4-4) shows identical behaviour to that of the homometallic dyads. Electronic delocalization appears to be very effective in this series as well.

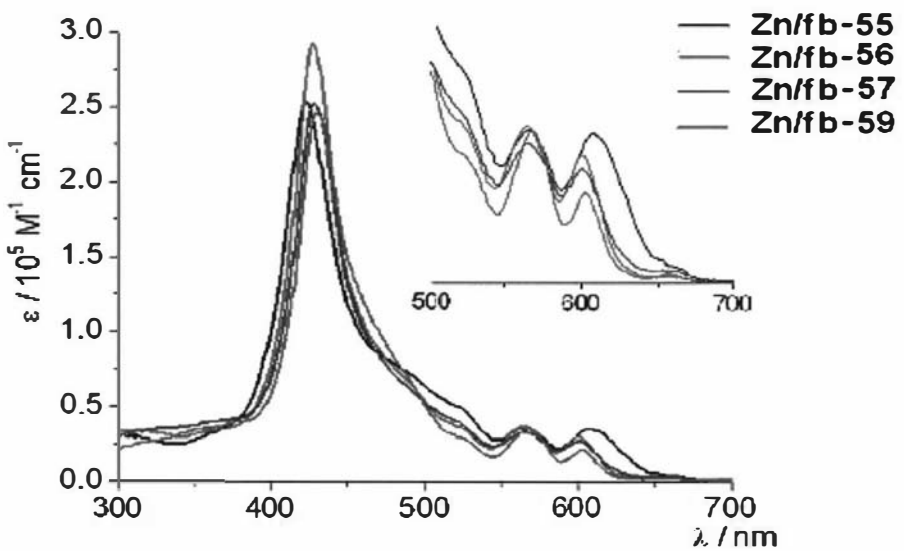

Figure 4-28 UV-visible absorbtion spectra of the series of heterometallic dyads **Zn/fb-55**, **Zn/fb-56**, **Zn/fb-57** and **Zn/fb-59** in toluene

	λ_{max}/nm	ε / 10^3 $M^{-1}cm^{-1}$
Zn/fb-55	424	253
	493 (sh)	70
	522 (sh)	50
	566	36
	609	35
	661 (sh)	4
Zn/fb-56	429	92
	492 (sh)	65
	523 (sh)	37
	566	37
	601	30
	659	2
Zn/fb-57	430	252
	518 (sh)	42
	566	33
	602	27
	659	3
Zn/fb-59	432	246
	525 (sh)	29
	569	36
	603	21
	659	2

Table 4-4 Absorption data for the series of heterometallic dyads **Zn/fb-55**, **Zn/fb-56**, **Zn/fb-57** and **Zn/fb-59** in toluene and at room temperature

	λ_{max}/nm	ε / 10^3 $M^{-1}cm^{-1}$		λ_{max}/nm	ε / 10^3 $M^{-1}cm^{-1}$
54	422	219	**Zn-54**	427	319
	483 (sh)	55		505 (sh)	75
	522	45		566	49
	581	23		614	40
	607	24			
	661 (sh)	5			
46	427	20	**Zn-46**	434	336
	484 (sh)	57		498 (sh)	74
	522	40		568	49
	573	29		607	37
	603	19			
	658	5			
58	429	221	**Zn-58**	434	359
	519 (sh)	43		498 (sh)	96
	574	31		568	57
	605	22		607	47
	660	3			
60	428	176	**Zn-60**	435	356
	526	43		495 (sh)	89
	571	30		566	52
	606	20		603	34
	665	7			

Table 4-5 Absorption data for the series of Zn and free-base homometallic dyads **M-54**, **M-46**, **M-58** and **M-60** in toluene and at room temperature

In order to investigate intramolecular processes, a first analysis of the emission properties of the heterometallic series was performed. Figure 4-29 shows the emission of the 'longest' dyad **Zn/fb-59** compared to the model **Zn-51**, which are identical except for the presence of a free-base porphyrin at the end of the conjugated linker in the dyad. It is clear that the typical emission of the Zn porphyrin (600 nm) almost disappears while the typical free-base emission (730 nm) is well recognizable. The most likely explanation for these phenomena lies in the expected energy transfer from the excited Zn porphyrin to the free-base porphyrin at the opposite end of the molecule. Similar behaviour has also been registered for the other members of the heterometallic series.

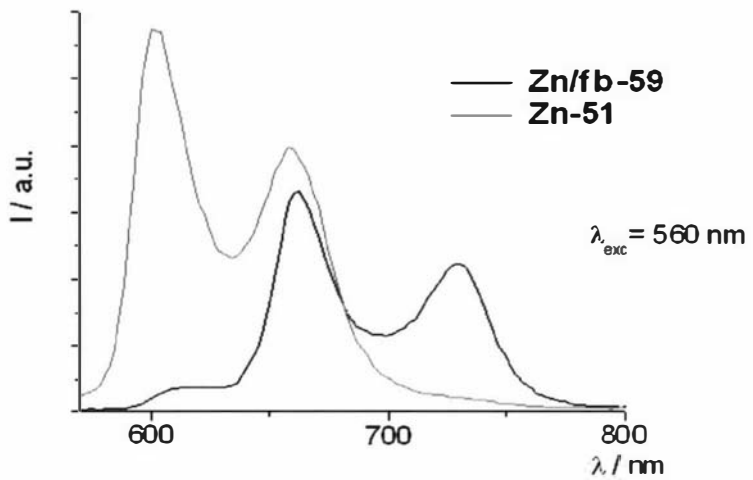

Figure 4-29 Emission spectra of the of heterometallic dyad **Zn/fb-59** and monomer model **Zn-51** in toluene

Time-resolved spectroscopy, as stated in the previous section, is the most powerful tool for the investigation of such processes. In particular, Figure 4-30 shows the picosecond time-resolved emission of **Zn/fb-59** at the moment of excitation and 200 ps later. It can be readily seen that there is an initial emission in the typical Zn porphyrin region, which disappears after 200 ps when an increase in the emission at 720-740 nm is also observed. All the data is in good agreement with the theorized system in which intramolecular energy transfer quickly and effectively occurs between Zn porphyrin (donor) and free-base porphyrin (acceptor). Moreover, the fact that this behaviour is similar for the entire heterometallic series, strongly suggest that the intramolecular energy transfer occurs through a Dexter/through-bond mechanism.

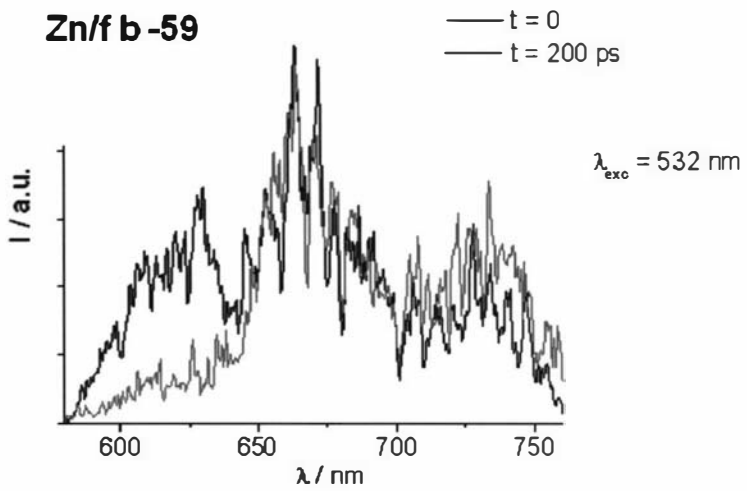

Figure 4-30 Picosecond time-resolved emission spectra of **Zn/fb-59** in toluene

4.9 Conclusions

In order to assess the suitability of β-pyrrolic phenylene-vinylene bridges towards intramolecular energy/electron transfer, a photophysical investigation of conjugated porphyrin arrays was undertaken. Three series of dyads (free-base/free-base, Zn/Zn and free-base/Zn) connected by various linker lengths were prepared and characterized. Zn and free-base porphyrins were utilized to create two series of homometallic and a series of heterometallic dimers; the choice of metallation states was both a consequence of their relatively long excited state lifetimes as well as their emitting properties, which allow detection and discrimination of their relaxation pathways. Two series of monomer models (free-base and Zn metallated) were also synthesized and characterized and their spectroscopic properties investigated in order to provide the background knowledge for the description of the novel porphyrin systems.

In all cases, the introduction of conjugated β-substituents resulted in a bathochromic shift of both absorption and emission bands of the examined porphyrins and in a broadening of the Soret band; increasing the conjugation (i.e. longer conjugated substituents) resulted in more pronounced modifications. Red-shifting and broadening of the absorption bands is consistent with a large delocalization of the porphyrin orbitals onto the conjugated substituent, resulting in lower energy electronic

transitions. These results suggest that phenylene-vinylene β-substituents can be considered useful interporphyrin linkers in the design of multiporphyrinic arrays with enhanced electronic communication. Early experiments involving the heterometallic Zn/free-base dyads showed that the electronic interaction is sufficient to allow efficient intramolecular energy/electron transfer according to the Dexter (through bond) mechanism, making such systems very interesting for photovoltaic/photosynthetic application, as well as for optical and electronic devices.

4.10. Experimental procedures

General

Commercially available solvents and chemicals were purchased from different sources, as analytical (AR) grade unless otherwise specified. Solvents for column chromatography (dichloromethane, hexane, methanol and toluene) were distilled lab grade. Water was purified by reverse osmosis. Dry THF and benzene were obtained by passing commercially available argon degassed solvent through an activated alumina column. 1,2-Dichloroethane, pyridine and *N,N*-dimethylformamide were dried and purified according to standard lab procedures.[106] Flash chromatography was used for compound purification. Column chromatography employed silica gel (0.032-0.063 mm, Merck Kieselgel 60) or equivalent. Thin layer chromatography (TLC) was performed using pre-coated silica gel plates (Merck Kieselgel $60F_{254}$). All reagents were used as purchased.

UV-vis experiments were performed on a Shimadzu UV-3101PC scanning spectrophotometer. High resolution FAB mass spectra were recorded on a VG-70SE instrument at the University of Auckland and on a VG ZAB 2 SEQ VG-Micromass at the Australian National University. MALDI-TOF mass spectra were carried out by the author and were performed on a Micromass ProteomWorks M@LDI-Reflectron mass spectrometer. ^{1}H-NMR spectrometry experiments were performed using 400 and 500 MHz Bruker Avance instruments running TOPSPIN 1.3 software. Proton chemical shifts in $CDCl_3$ are relative to TMS. Chemical shifts in other solvents are relative to residual protons (tetrahydrofurane-d_8, 3.58 ppm, dioxane-d_8, 3.53 ppm,

dichloromethane-d_2, 5.32). Data are expressed as position (in ppm), multiplicity (s = singlet, d = doublet, t = triplet, q = quartet, m = multiplet, br = broad, app = apparent), relative integral, coupling constant (J_P indicating ^1H-^{31}P coupling) and assignment. Coupling constants were not reported when smaller than 1Hz.

Precursor syntheses.

Porphyrin aldehydes **M-5** (M = 2H, Zn), **M-14** (M = 2H, Zn) and phosphonium salt **11** were prepared as previously reported.[75]

Zn metallations.

A general procedure (according to the acetate method)[97] was used for all Zn insertion into free-base porphyrins. The porphyrin was dissolved in dichloromethane (AR grade) and 1.2 equivalents of $Zn(OAc)_2 \cdot H_2O$, dissolved in the same amount of MeOH/water (10/1), were added. The mixture was stirred for 2 hours, then washed with water and the porphyrin precipitated with MeOH. The solid collected was the pure desired Zn porphyrin. Yields were always higher than 95%.

Zn demetallations.

A general procedure was used for the removal of Zn to give free-base porphyrins. The porphyrin was dissolved in dichloromethane (lab grade) and the same volume of 3M HCl, was added. The mixture was stirred for 20 min after which the organic layer was separated, washed twice with 3M HCl and then neutralized by bicarbonate solution and water. The product was finally precipitated (generally using MeOH, or water when methanol soluble) affording yields always higher than 90%.

TPP-ext-COOMe, 39.

3-*trans*-(2'-(5',10',15',20'-tetraphenylporphyrin)yl)methylpropenoate.

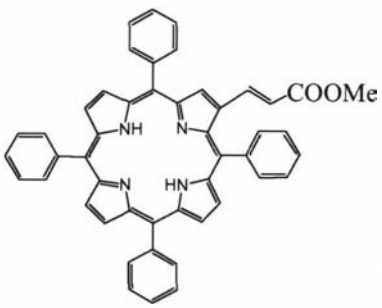

$C_{48}H_{34}N_4O_2$
Exact Mass: 698.27
Mol. Wt.: 698.81

The synthesis of this compound was realized according to the procedure developed in our laboratories.[60]

2 g (3.11 mmol) of aldehyde **5** and excess of methyl (triphenylphosphoranylylidene)acetate (Ph_3P=CH-COOMe, 4 g, 12 mmol) were dissolved in 250 mL of dry toluene under argon. The solution was refluxed for 18 hours after which the products were separated by column chromatography on silica gel, using toluene as solvent. Interestingly, the first fraction was isolated and characterized as TPP-CH=CH_2; the yield of this compound was less than 1%. The major band was collected after this and characterized as *cis/trans* mixture of the desired product. Isomerization to pure *trans* configuration was achieved by treating a dichloromethane solution (200 mL) of the porphyrin with 250 mg of I_2 for 30 hours. After this, the solution was washed three times with a saturated solution of $Na_2S_2O_3$ and water and then precipitated with methanol to afford 2.1 g of **39** (97%). ^{1}H-NMR (500 MHz, $CDCl_3$): δ 8.96 (s, 1H, $H_{\beta\text{-pyrrolic}}$), 8.85-8.77 (m, 6H, $H_{\beta\text{-pyrrolic}}$), 8.22-8.18 (m, 6H, $H_{o\text{-Ph}}$), 8.13-8.10 (m, 2H, $H_{o\text{-Ph}}$), 7.86-7.72 (m, 12H, $H_{m,p\text{-Ph}}$), 7.40 (d, J = 15.6 Hz, 1H, H_{alkene}), 6.56 (d, J = 15.6 Hz, 1H, H_{alkene}), 3.77 (s, 3H, H_{CH3}), -2.61 (s, 2H, $H_{N\text{-pyrrolic}}$). UV-vis (CH_2Cl_2): λ_{max} [nm] (ε x 10^{-3}) 429 (258), 523 (17), 563 (7), 601 (6), 659 (4).

TPP-ext-CH_2OH, 40.

3-*trans*-(2'-(5',10',15',20'-tetraphenylporphyrin)yl)propenol.

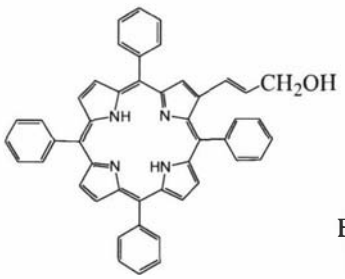

$C_{47}H_{34}N_4O$
Exact Mass: 670.27
Mol. Wt.: 670.80

The synthesis of this compound was realized according to the procedure developed in our laboratories.[60]

2 g (3 mmol) of ester **39** were dissolved in 250 mL of dry toluene under argon. 6 mL of 1.5M DIBAL in toluene were added at 0 °C and the stirred solution was left at this temperature for 30 min. After removal of the ice bath, stirring continued for further 30 min at room temperature. The temperature was then brought back to 0 °C and the excess DIBAL was hydrolyzed by addition of 15 mL of methanol followed by 100

mL of 10% NaOH. The solution was extracted with DCM and the organic phase brought to dryness and separated through column chromatography (silica gel, DCM/Et_2O = 99/1). After elution of side-products, the major band was collected and recrystallized from DCM/MeOH to give 1.1 g (55%) of pure **40** as purple crystals. ^{1}H-NMR (500 MHz, $CDCl_3$): δ 8.85-8.72 (m, 7H, $H_{\beta\text{-pyrrolic}}$), 8.24-8.18 (m, 6H, $H_{o\text{-Ph}}$), 8.13-8.08 (m, 2H, $H_{o\text{-Ph}}$), 7.84-7.70 (m, 12H, $H_{m,p\text{-Ph}}$), 6.53-6.44 (m, 1H, $H_{=CH\text{-}CH2}$), 6.29 (d, J = 15.6 Hz, 1H, $H_{porph\text{-}CH=}$), 4.13 (app t, J = 5.7 Hz, 2H, H_{CH2}), 1.07 (t, J = 6.3 Hz, 1H, H_{OH}), -2.69 (s, 2H, $H_{N\text{-pyrrolic}}$). UV-vis (CH_2Cl_2): λ_{max} [nm] (ε x 10^{-3}) 423 (240), 519 (17), 557 (6), 595 (5), 650 (2.6).

TPP-ext-CHO, 41.

3-*trans*-(2'-(5',10',15',20'-tetraphenylporphyrin)yl)propenaldehyde.

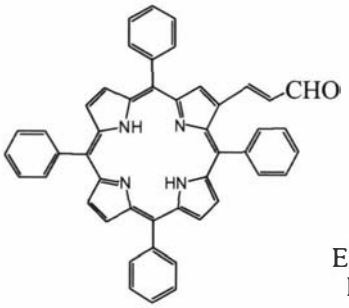

$C_{47}H_{32}N_4O$
Exact Mass: 668.26
Mol. Wt.: 668.78

The syntheses of porphyrin aldehydes **41** and **Zn-41** were realized according to the procedure developed in our laboratories.[60]

450 mg (671 μmol) of porphyrin alcohol **40** were dissolved (under argon) in 25 mL of dry chloroform with 2.5 g of activated MnO_2. The solution was refluxed for 3 h and quickly filtered through a few cm of celite (to remove inorganic materials). Precipitation by methanol addition afforded 430 mg (96%) of pure aldehyde **41** as purple-green crystals. ^{1}H-NMR (400 MHz, $CDCl_3$): δ 9.21 (d, J = 8 Hz, 1H, $H_{aldehyde}$), 9.00 (s, 1H, $H_{\beta\text{-pyrrolic}}$), 8.86-8.78 (m, 6H, $H_{\beta\text{-pyrrolic}}$), 8.21-8.18 (m, 6H, $H_{o\text{-Ph}}$), 8.13-8.10 (m, 2H, $H_{o\text{-Ph}}$), 7.85-7.71 (m, 12H, $H_{m,p\text{-Ph}}$), 7.00 (d, J_{trans} = 15.3 Hz, 1H, H_{alkene}), 6.86 (dd, J_{trans} = 15.3 Hz, $J_{CH\text{-}CHO}$ = 8 Hz, 1H_{alkene}), -2.59 (s, 2H, $H_{N\text{-pyrrolic}}$). UV-vis (CH_2Cl_2): λ_{max} [nm] (ε x 10^{-3}) 434 (210), 525 (21), 567 (8.5), 604 (7), 661 (5).

ZnTPP-ext-CHO, Zn-41.

3-*trans*-(2'-(5',10',15',20'-tetraphenylporphyrinato zinc(II))yl)propenaldehyde.

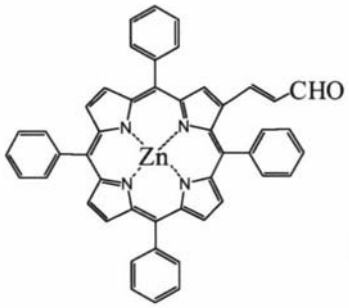

$C_{47}H_{30}N_4OZn$
Exact Mass: 730.17
Mol. Wt.: 732.16

Porphyrin aldehyde **Zn-41** was obtained by metallation of the already described free-base porphyrin **41**. 300 mg (448 μmol) of **41** gave 304 mg (93%) of desired **Zn-41.** ^{1}H-NMR (400 MHz, $CDCl_3$): δ 9.13 (br s, 2H, $1H_{aldehyde}$ + $1H_{\beta\text{-pyrrolic}}$), 8.95-8.87 (m, 6H, $H_{\beta\text{-pyrrolic}}$), 8.22-8.16 (m, 6H, $H_{o\text{-Ph}}$), 8.12 (d, J = 7.4 Hz, 2H, $H_{o\text{-Ph}}$), 7.86-7.71 (m, 12H, $H_{m,p\text{-Ph}}$), 7.06 (d, J_{trans} = 15 Hz, 1H, H_{alkene}), 6.81 (dd, J_{trans} = 15 Hz, $J_{CH\text{-}CHO}$ = 7.8 Hz, $1H_{alkene}$). UV-vis (toluene): λ_{max} [nm] (ε x 10^{-3}) 425 (393), 552 (22), 590 (4). *Assignments aided by variable concentration and COSY spectra.* FAB-HRMS for MH^+ ($C_{47}H_{31}N_4OZn$): 731.1786, calculated: 731.1789.

TPP-ext-CH_2Cl, 42.

trans-2-(2'-(5',10',15',20'-tetraphenylporphyrin)yl)-chloromethylethene.

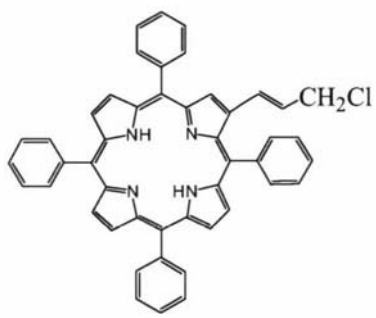

$C_{47}H_{33}ClN_4$
Exact Mass: 688.24
Mol. Wt.: 689.24

The synthesis of this compound was realized according to the procedure developed in our laboratories.[143]

650 mg (969 μmol) of porphyrin alcohol **40** were dissolved/suspended in 130 mL of dry Et_2O and 550 μl of pyridine, under argon. The temperature was brought to 0 °C before 270 μl of $SOCl_2$ were added and the stirred solution was kept at 0 °C for 10 min. After removal of the ice-bath, stirring continued at room temperature for further two hours (50 mL of dry DCM were added to facilitate dissolution of residual solid). The solution was then diluted with DCM, washed with water and bicarbonate solution

and dried over $MgSO_4$. ^{1}H-NMR showed good purity therefore the crude product was used for successive reaction without further purification. ^{1}H-NMR (500 MHz, $CDCl_3$): δ 8.85-8.75 (m, 7H, $H_{\beta\text{-pyrrolic}}$), 8.23-8.17 (m, 6H, $H_{o\text{-Ph}}$), 8.10-8.06 (m, 2H, $H_{o\text{-Ph}}$), 7.84-7.68 (m, 12H, $H_{m,p\text{-Ph}}$), 6.48-6.38 (m, 1H, $H_{=CH\text{-}CH_2}$), 6.24 (d, J = 15.3 Hz, 1H, $H_{porph\text{-}CH=}$), 4.07 (d, J = 7.3 Hz, 2H, H_{CH_2}), -2.70 (s, 2H, $H_{N\text{-pyrrolic}}$). UV-vis (CH_2Cl_2): λ_{max} [nm] (ε x 10^{-3}) 423 (299), 519 (18.4), 557 (7.1), 595 (6), 652 (3.2). FAB-HRMS for $(M\text{-}Cl)^+$ ($C_{47}H_{35}N_4$): 653.2706, calculated: 653.2705.

TPP-ext-ps, 43.

trans-2-(2'-(5',10',15',20'-tetraphenylporphyrin)yl),
1-methyltriphenylphosphoniumchloride)ethene.

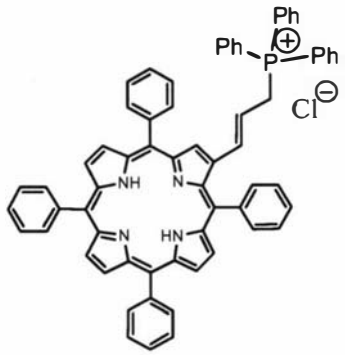

$C_{65}H_{48}ClN_4P$
Exact Mass: 950.33
Mol. Wt.: 951.53

The synthesis of this compound was realized according to the procedure developed in our laboratories.[143]

The crude product of the described synthesis of **42** (approximately 660 mg, 959 μmol) and 4 g (15.2 mmol) of triphenylphosphine were dissolved in 50 mL of chloroform under argon and the solution was brought to reflux. After 2.5 hours the solution was quickly filtered through few cm of silica gel to remove the low polar products (DCM was used as eluent). The desired product was then eluted with DCM/MeOH = 10/1 and recrystallized from DCM/hexane to afford 844 mg of pure **43**. Yield was 91% from the alcohol **40**. ^{1}H-NMR (500 MHz, $CDCl_3$): δ 8.86-8.76 (m, 5H, $H_{\beta\text{-pyrrolic}}$), 8.71 (d, J = 4.8 Hz, 1H, $H_{\beta\text{-pyrrolic}}$), 8.59 (s, 1H, $H_{\beta\text{-pyrrolic}}$), 8.24-8.16 (m, 6H, $H_{o\text{-Ph}}$), 7.97-7.93 (m, 2H, $H_{o\text{-Ph}}$), 7.88-7.72 (m, 19H, $12H_{m,p\text{-Ph}}$ + $7H_{Ph(ps)}$), 7.69-7.60 (m, 8H, $H_{Ph(ps)}$), 6.24-6.13 (m, 1H, $H_{=CH\text{-}CH_2}$), 5.95 (dd, J_{trans} = 15.6 Hz, J_P = 5.8 Hz 1H, $H_{porph\text{-}CH=}$), 4.79 (dd, J_P = 14.8 Hz, J = 7.3 Hz, 2H, H_{CH_2}), -2.73 (s, 2H, $H_{N\text{-pyrrolic}}$). UV-vis (CH_2Cl_2): λ_{max} [nm] (ε x 10^{-3}) 425 (347), 520 (20.4), 558 (6.8), 597 (6.2), 653 (4). FAB-HRMS for $(M\text{-}Cl)^+$ ($C_{65}H_{48}N_4P$): 915.3614, calculated: 915.3617.

1,4-xylenebis(diethylphosphonate), 44.

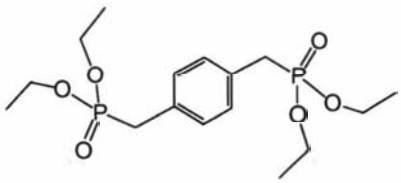

$C_{16}H_{28}O_6P_2$
Exact Mass: 378.14
Mol. Wt.: 378.34

Diphosphonate **35** was prepared according to the general method of Michaelis and Kaehne.[102,107]

1.45 g of commercial *p*-dibromoxylene were dissolved in 15 mL of commercial triethylphosphite under argon atmosphere. The solution was refluxed for 20 hours after which the excess phosphite and co-product EtBr were distilled off, yielding 2.06 g (99%) of pure **44** as pale yellow-green solid. ^{1}H-NMR (400 MHz, $CDCl_3$): δ 7.25 (br s, 4H, H_{Ph}), 4.06-3.95 (m, 8H, $H_{CH2\text{-}ethyl}$), 3.13 (d, J= 20.2 Hz, 4H, $H_{CH2\text{-}P}$), 1.24 (t, J = 7 Hz, 12H, $H_{CH3\text{-}ethyl}$). The ^{1}H-NMR spectrum is in agreement with the literature.[156]

ZnTPP-Ph-pep, Zn-45.

4-(*trans*-2'-(2"-(5",10",15",20"-tetraphenylporphyrinato zinc(II))yl)ethen-1'-yl)methyl(diethylphosphonate)benzene.

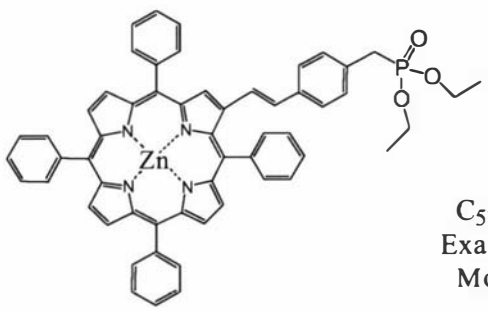

$C_{57}H_{45}N_4O_3PZn$
Exact Mass: 928.25
Mol. Wt.: 930.36

1 g (1.43 mmol) of **Zn-5** and 715 mg (1.89 mmol) of 1,4-xylenebis(diethylphosphonate) **44** were dissolved in 100 mL of dry THF, under argon atmosphere. To the stirred solution, 225 mg (2 mmol) of solid ^{t}BuOK were added at three intervals in 30min during which the product began precipitating. After a further 10 min, the solution was evaporated to dryness and the crude was purified using flash chromatography on silica gel: disubstituted co-product **Zn-46** and side-products were eluted with DCM after which the desired product **Zn-45** was eluted with DCM/MeOH = 100/1. This solution was then evaporated to dryness, redissolved in DCM/THF and precipitated by adding MeOH. 620 mg (47%) of pure **Zn-45** were obtained by recrystallization from DCM/MeOH as purple crystals. ^{1}H-NMR (500 MHz, THF-d_8,):

δ 9.03 (s, 1H, $H_{\beta\text{-pyrrolic}}$), 8.84-8.73 (m, 5H, $H_{\beta\text{-pyrrolic}}$), 8.70 (d, J = 4.5 Hz , 1H, $H_{\beta\text{-pyrrolic}}$), 8.28-8.14 (m, 8H, $H_{o\text{-Ph}}$), 7.93-7.69 (m, 12H, $H_{m,p\text{-Ph}}$), 7.30-7.18 (m, 5H, $4H_{Ph}$ + $1H_{alkene}$), 7.03 (d, J = 16.1 Hz, 1H, H_{alkene}), 4.03-3.95 (m, 4H, $H_{CH2\text{-ethyl}}$), 3.13 (d, J_P = 21.8 Hz, 2H, $H_{CH2\text{-P}}$), 1.23 (t, J = 7 Hz, 6H, $H_{CH3\text{-ethyl}}$). *Assignments aided by COSY spectra.* UV-vis (DCM): λ_{max} [nm] (ε x 10^{-3}) 428 (152), 559 (16), 593 (8). FAB-HRMS for M^- ($C_{57}H_{45}N_4PO_3Zn$): 928.2486, calculated: 928.2521.

ZnTPP-Ph-ZnTPP, Zn-46.

1,4-(*trans*-2'-(2"-(5",10",15",20"-tetraphenylporphyrinato zinc(II))yl)ethen-1'-yl) benzene.

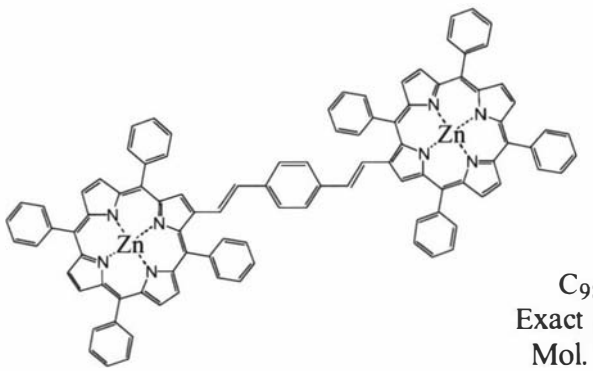

$C_{98}H_{62}N_8Zn_2$
Exact Mass: 1478.37
Mol. Wt.: 1482.37

Dimer **Zn-46** was obtained as a co-product in the course of the just described preparation of **Zn-45**. Yield in the disubstituted product was 180 mg (17%); this yield could be improved by using reagent amounts more appropriate for double substitution (e.g. excess of **Zn-5**). ^{1}H-NMR (500 MHz, dioxane-d_8): δ 9.05 (s, 2H, $H_{\beta\text{-pyrrolic}}$), 8.83-8.77 (m, 10H, $H_{\beta\text{-pyrrolic}}$), 8.75 (d, J = 4.7, 2H, $H_{\beta\text{-pyrrolic}}$), 8.28-8.17 (m, 16H, $H_{o\text{-Ph}}$), 8.04-7.70 (m, 24H, $H_{m,p\text{-Ph}}$), 7.29 (d, J = 16.1 Hz, 2H, H_{alkene}), 7.26 (s, 4H, $H_{Ph'}$), 7.06 (d, J = 16.1 Hz, 1H, H_{alkene}). *Assignments aided by COSY spectra.* UV-vis (toluene): λ_{max} [nm] (ε x 10^{-3}) 434 (336), 498 (sh 74), 568 (49), 607 (37). FAB-HRMS for MH^+ ($C_{98}H_{63}N_8Zn_2$): 1479.3756, calculated: 1479.3759.

TPP-Ph-TPP, 46.

1,4-(*trans*-2'-(2"-(5",10",15",20"-tetraphenylporphyrin)yl)ethen-1'-yl)benzene.

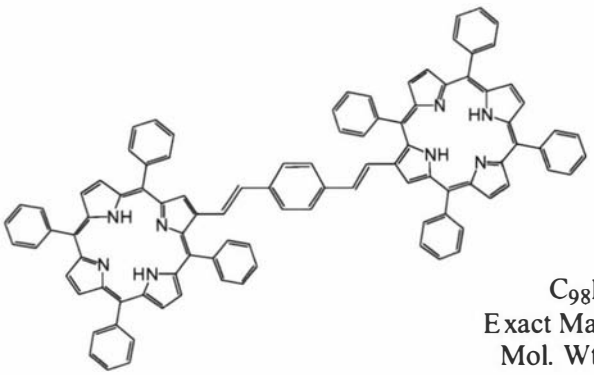

$C_{98}H_{66}N_8$
Exact Mass: 1354.54
Mol. Wt.: 1355.63

Free-base porphyrin **46** was prepared by demetallation of **Zn-46**, according to the described general procedure. 43 mg of pure **46** (94%) were obtained from 50 mg of the free base homologue. ^{1}H-NMR (500 MHz, $CDCl_3$): δ 9.04 (s, 2H, $H_{\beta\text{-pyrrolic}}$), 8.85-8.77 (m, 10H, $H_{\beta\text{-pyrrolic}}$), 8.74 (d, J = 4.6 Hz, 2H, $H_{\beta\text{-pyrrolic}}$), 8.29-8.18 (m, 16H, $H_{o\text{-Ph}}$), 7.98-7.70 (m, 24H, $H_{m,p\text{-Ph}}$), 7.34 (d, J = 16 Hz, 2H, $H_{\text{alkene}'}$), 7.25 (s, 4H, $H_{\text{Ph}'}$), 7.08 (d, J = 16 Hz, 1H, H_{alkene}), -2.56 (br s, 4H, $H_{N\text{-pyrrolic}}$). *Assignments aided by COSY spectra.* UV-vis (toluene): λ_{max} [nm] (ε x 10^{-3}) 427 (220), 484 (sh 57), 522 (40), 573 (29), 603 (19) 658 (5). FAB-HRMS for $(M+2H)^{2-}$ ($C_{98}H_{68}N_8$): 678.2778, calculated: 678.2784; for $(M+O_2+H)^-$ ($C_{98}H_{67}N_8O_2$): 1387.5370, calculated: 1387.5387.

ZnTPP-Ph-Ph-CHO, Zn-47.

4-(*trans*-2'-(4"-(*trans*-2"'-(2""-(5"",10"",15"",20""-tetraphenylporphyrinato zinc(II))yl) ethen-1"'-yl)phenyl)ethen-1'-yl)benzaldehyde.

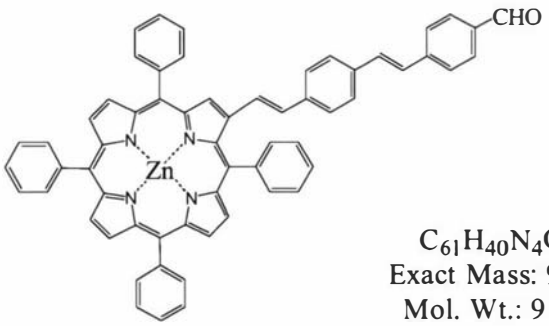

$C_{61}H_{40}N_4OZn$
Exact Mass: 908.25
Mol. Wt.: 910.39

170 mg (183 μmol) of phosphonate **Zn-45** and 35 mg (261 μmol) of terephthaldicarboxaldehyde **13** were dissolved in 30 mL of dry THF, under argon. To the stirred solution 30 mg (260 μmol) of solid ^{t}BuOK were added in three portions over 1 h. After a further 10 min, the solution was evaporated to dryness and the product mixture separated through flash chromatography (silica gel, DCM/hexane =

3/1). The first band contained the disubstituted by-product, followed by the desired **Zn-45** which was collected and precipitated, by hexane addition as purple-red crystals. Yield was 113 mg (68%). ^{1}H-NMR (500 MHz, $CDCl_3$): δ 9.96 (s, 1H, $H_{aldehyde}$), 9.11 (s, 1H, $H_{\beta\text{-pyrrolic}}$), 8.96-8.88 (m, 5H, $H_{\beta\text{-pyrrolic}}$), 8.82 (d, J = 4.7 Hz , 1H, $H_{\beta\text{-pyrrolic}}$), 8.28-8.18 (m, 8H, $H_{o\text{-Ph}}$), 7.87-7.72 (m, 14H, $12H_{m,p\text{-Ph}}$ + $2H_{Ph'}$), 7.64 (d, J = 8 Hz, 2H, $H_{Ph'}$), 7.51 (d, J = 8 Hz, 2H, $H_{Ph'}$), 7.28-7.22 (m, 4H, $2H_{Ph''}$ + $1H_{alkene}$ + $1H_{alkene'}$), 7.17 (d, J = 16.3 Hz, 1H, H_{alkene}), 7.03 (d, J = 16.1 Hz, 1H, $H_{alkene'}$). *Assignments aided by COSY spectra.* UV-vis (toluene): λ_{max} [nm] (ε x 10^{-3}) 437 (189), 558 (26), 596 (15). FAB-HRMS for M^- ($C_{61}H_{40}N_4OZn$): 908.2479, calculated: 908.2494.

TPP-CH=CH$_2$, 48.

2'-(5',10',15',20'-tetraphenylporphyrin)yl)ethene.

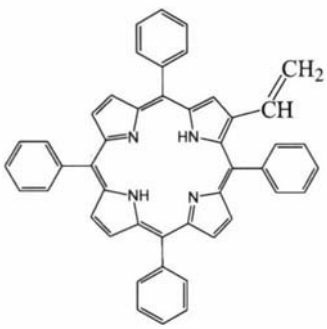

$C_{46}H_{32}N_4$
Exact Mass: 640.26
Mol. Wt.: 640.77

43.3 mg (67 μmol) of aldehyde **5** and 70 mg (194 μmol) of methyltriphenlphosphoniumbromide (Me-ps) were dissolved/suspended in 25 mL of dry toluene, under argon. The solution was heated to reflux and excess of DBU (50 mg, 329 μmol) was added. After 20 hours, TLC (DCM/hexane = 1/1) showed the reagent as the main component with a less polar product. More DBU was added (40 mg, 263 μmol) and the reflux continued for further 24 hours. The solution was then evaporated to dryness and separated through flash chromatography (silica gel, DCM/hexane = 1/1). The first band was collected and recrystallized from DCM/acetonitrile to yield 11 mg (26%) of pure **48** as purple crystals. ^{1}H-NMR (500 MHz, $CDCl_3$): δ 8.88 (s, 1H, $H_{\beta\text{-pyrrolic}}$), 8.85-8.74 (m, 5H, $H_{\beta\text{-pyrrolic}}$), 8.69 (d, J = 4.7 Hz , 1H, $H_{\beta\text{-pyrrolic}}$), 8.25-8.17 (m, 6H, $H_{o\text{-Ph}}$), 8.07 (app d, J = 7.5 Hz, 2H, $H_{o\text{-Ph}}$), 7.81-7.67 (m, 12H, $H_{m,p\text{-Ph}}$), 6.43 (dd, J_{trans} = 17 Hz, J_{cis} = 10.7 Hz , 1H, H_{alkene}), 5.89 (dd, J_{trans} = 17 Hz, $J_{geminal}$ = 1.4 Hz, 1H, H_{alkene}), 5.15 (dd, J_{cis} = 10.7 Hz, $J_{geminal}$ = 1.4 Hz, 1H, H_{alkene}), -2.68 (s, 2H, $H_{N\text{-pyrrolic}}$). *Assignments aided by COSY spectra.* UV-vis

(toluene): λ_{max} [nm] (ε x 10^{-3}) 424 (369), 519 (22), 554 (8), 596 (6), 653 (3). FAB-HRMS for M^+ ($C_{46}H_{32}N_4$): 640.2647, calculated: 640.2627.

ZnTPP-CH=CH$_2$, Zn-48.

2'-(5',10',15',20'-tetraphenylporphyrinato zinc(II))yl)ethene.

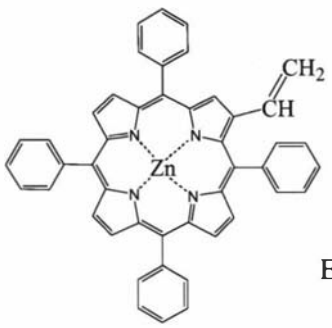

$C_{46}H_{30}N_4Zn$
Exact Mass: 702.18
Mol. Wt.: 704.15

10 mg (15.6 μmol) of **48** were metallated as described in the general procedures, providing 10.5 mg (96%) of **Zn-48**. ^{1}H-NMR (500 MHz, $CDCl_3$): δ 8.98 (s, 1H, $H_{\beta\text{-pyrrolic}}$), 8.96-8.87 (m, 5H, $H_{\beta\text{-pyrrolic}}$), 8.81 (d, J = 4.6 Hz , 1H, $H_{\beta\text{-pyrrolic}}$), 8.23-8.17 (m, 6H, $H_{o\text{-Ph}}$), 8.07 (app d, J = 7.5 Hz, 2H, $H_{o\text{-Ph}}$), 7.81-7.67 (m, 12H, $H_{m,p\text{-Ph}}$), 6.44 (dd, J_{trans} = 17 Hz, J_{cis} = 10 Hz , 1H, H_{alkene}), 5.85 (dd, J_{trans} = 17 Hz, $J_{geminal}$ = 1.8 Hz, 1H, H_{alkene}), 5.11 (dd, J_{cis} = 10 Hz, $J_{geminal}$ = 1.8 Hz, 1H, H_{alkene}). UV-vis (toluene): λ_{max} [nm] (ε x 10^{-3}) 425 (393), 552 (22), 590 (4). FAB-HRMS for M^+ ($C_{46}H_{30}N_4Zn$): 702.1756, calculated: 702.1762.

ZnTPP-ext-CH=CH$_2$, Zn-49.

1-*trans,trans*-(2'-(5',10',15',20'-tetraphenylporphyrinato zinc(II))yl)butadiene.

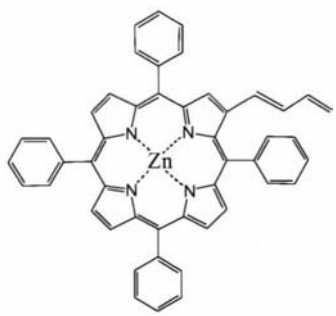

$C_{48}H_{32}N_4Zn$
Exact Mass: 728.19
Mol. Wt.: 730.18

64 mg (88 μmol) of aldehyde **Zn-41** and 48 mg (133 μmol) of Me-ps (methyltriphenlphosphoniumbromide) were dissolved/suspended in 30 mL of dry toluene, under argon. The solution was heated to reflux and excess of DBU (120 mg, 0.8 mmol) was added. After 24 hours the solution was evaporated to dryness and separated through flash chromatography (silica gel, DCM/hexane = 1/1). The first

band was collected and evaporated to dryness to give 18 mg (28%) of pure **Zn-49** as purple crystals. ^{1}H-NMR (500 MHz, $CDCl_3$): δ 8.96 (s, 1H, $H_{\beta\text{-pyrrolic}}$), 8.90-8.82 (m, 5H, $H_{\beta\text{-pyrrolic}}$), 8.80 (d, J = 4.7 Hz , 1H, $H_{\beta\text{-pyrrolic}}$), 8.27-8.14 (m, 6H, $H_{o\text{-Ph}}$), 8.19 (d, J = 7 Hz, 2H, $H_{o\text{-Ph}}$), 7.81-7.68 (m, 12H, $H_{m,p\text{-Ph}}$), 6.91 (dd, J_{trans} = 15.2 Hz, J_{cis} = 10.4 Hz , 1H, $H_{alkene'}$), 6.23-6.13 (m, 2H, $1H_{alkene}$+ $1H_{alkene'}$), 5.32 (d, J_{trans} = 17 Hz, 1H, H_{alkene}), 5.10 (d, J_{cis} = 10.4 Hz, 1H, $H_{alkene'}$). *Assignments aided by COSY spectra.* - UV-vis (toluene): λ_{max} [nm] (ε x 10^{-3}) 430 (216), 556 (18), 554 (5). FAB-HRMS for MH^+ ($C_{48}H_{33}N_4Zn$): 729.1990, calculated: 729.1997.

TPP-ext-CH=CH$_2$, 49.

1-*trans,trans*-(2'-(5',10',15',20'-tetraphenylporphyrin)yl)butadiene.

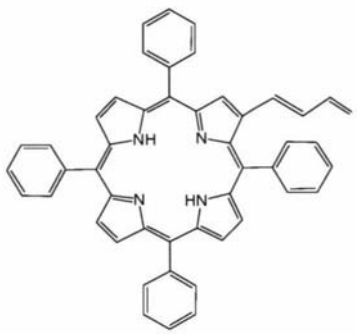

$C_{48}H_{34}N_4$
Exact Mass: 666.28
Mol. Wt.: 666.81

Free-base porphyrin **49** was obtained by demetallation of **Zn-49** according to the described general procedure. 8.7 mg (95%) of pure product **49** were obtained from 10 mg (13.7 μmol) of the Zn homologue. ^{1}H-NMR (500 MHz, $CDCl_3$): δ 8.88 (s, 1H, $H_{\beta\text{-pyrrolic}}$), 8.84-8.72 (m, 6H, $H_{\beta\text{-pyrrolic}}$), 8.24-8.18 (m, 6H, $H_{o\text{-Ph}}$), 8.10 (app d, J = 7.4 Hz, 2H, $H_{o\text{-Ph}}$), 7.83-7.67 (m, 12H, $H_{m,p\text{-Ph}}$), 6.96 (dd, J_{trans} = 15.2 Hz, J_{cis} = 10.6 Hz , 1H, $H_{alkene'}$), 6.23-6.13 (m, 2H, $1H_{alkene}$+ $1H_{alkene'}$), 5.35 (d, J_{trans} = 17 Hz, 1H, H_{alkene}), 5.14 (d, J_{cis} = 10.6 Hz, 1H, $H_{alkene'}$), -2.64 (s, 2H, $H_{N\text{-pyrrolic}}$). UV-vis (toluene): λ_{max} [nm] (ε x 10^{-3}) 426 (257), 522 (21), 560 (9), 600 (7), 659 (2). FAB-HRMS for M^+ ($C_{48}H_{34}N_4$): 666.2807, calculated: 666.2783.

ZnTPP-Ph-CH=CH$_2$, Zn-50.

4-(*trans*-2'-(2"-(5",10",15",20"-tetraphenylporphyrinato zinc(II))yl)ethen-1'-yl)styrene.

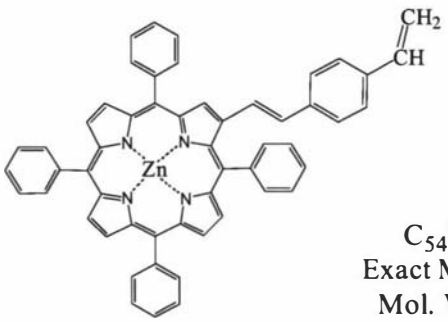

$C_{54}H_{36}N_4Zn$
Exact Mass: 804.22
Mol. Wt.: 806.28

45 mg (56 μmol) of **Zn-14** and 60 mg (166 μmol) of Me-ps were dissolved/suspended in 30 mL of dry toluene, under argon. The solution was heated to reflux and excess of DBU (60 mg, 0.4 mmol) was added. After 24 hours, the solution was evaporated to dryness and the products separated through flash chromatography (silica gel, DCM/hexane = 1/1). The first band was collected, evaporated to dryness and recrystallized from DCM/acetonitrile yielding 29 mg (64%) of pure **Zn-50** as purple crystals. ^{1}H-NMR (500 MHz, $CDCl_3$): δ 9.11 (s, 1H, $H_{\beta\text{-pyrrolic}}$), 8.97-8.88 (m, 5H, $H_{\beta\text{-pyrrolic}}$), 8.82 (d, J = 4.7 Hz , 1H, $H_{\beta\text{-pyrrolic}}$), 8.32-8.20 (m, 8H, $H_{o\text{-Ph}}$), 7.92-7.70 (m, 12H, $H_{m,p\text{-Ph}}$), 7.38 (d, J = 8 Hz, 2H, $H_{Ph'}$), 7.27-7.19 (m, 3H, $2H_{Ph'}$ + $1H_{alkene}$), 7.03 (d, J = 16 Hz, 1H, H_{alkene}), 6.75 (dd, J_{trans} = 17.6 Hz, J_{cis} = 10.8 Hz, 1H, $H_{alkene'}$), 5.80 (d, J_{trans} = 17.6 Hz, 1H, $H_{alkene'}$), 5.26 (d, J_{cis} = 10 Hz, 1H, $H_{alkene'}$). UV-vis (toluene): λ_{max} [nm] ($\varepsilon \times 10^{-3}$) 433 (218), 559 (23), 594 (11). FAB-HRMS for MH^+ ($C_{54}H_{37}N_4Zn$): 805.2270, calculated: 805.2310.

TPP-Ph-CH=CH$_2$, 50.

4-(*trans*-2'-(2"-(5",10",15",20"-tetraphenylporphyrin)yl)ethen-1'-yl)styrene.

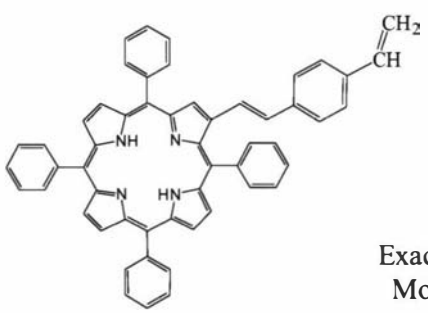

$C_{54}H_{38}N_4$
Exact Mass: 742.31
Mol. Wt.: 742.91

Free-base porphyrin **50** was obtained by demetallation of **Zn-50** using the described general procedure. 12.5 mg (90%) of pure product **50** were obtained from 15 mg (18.6

μmol) of the Zn homologue. ^{1}H-NMR (500 MHz, $CDCl_3$): δ 8.99 (s, 1H, $H_{\beta\text{-pyrrolic}}$), 8.84-8.74 (m, 5H, $H_{\beta\text{-pyrrolic}}$), 8.71 (d, J = 4.7 Hz , 1H, $H_{\beta\text{-pyrrolic}}$), 8.26-8.18 (m, 8H, $H_{o\text{-Ph}}$), 7.86-7.72 (m, 12H, $H_{m,p\text{-Ph}}$), 7.39 (d, J = 8 Hz, 2H, H_{Ph}), 7.28 (d, J = 16 Hz, H, H_{alkene}), 7.22 (d, J = 8 Hz, 2H, H_{Ph}), 6.99 (d, J = 16 Hz, H, H_{alkene}), 6.75 (dd, J_{trans} = 17.6 Hz, J_{cis} = 10.9 Hz , 1H, $H_{alkene'}$), 5.81 (d, J_{trans} = 17.6 Hz, 1H, $H_{alkene'}$), 5.28 (d, J_{cis} = 10 Hz, 1H, $H_{alkene'}$) -2.59 (s, 2H, $H_{N\text{-pyrrolic}}$). UV-vis (toluene): λ_{max} [nm] (ε x 10^{-3}) 427 (167), 524 (17), 564 (10), 602 (6), 659 (1). FAB-HRMS for M^- ($C_{54}H_{38}N_4$): 742.3113, calculated: 742.3097.

ZnTPP-Ph-Ph-CH=CH$_2$, Zn-51

4-(*trans*-2'-(4''-(*trans*-2'''-(2''''-(5'''',10'''',15'''',20''''-tetraphenylporphyrinato zinc(II))yl)ethen-1'''-yl)phenyl)ethen-1'-yl)styrene.

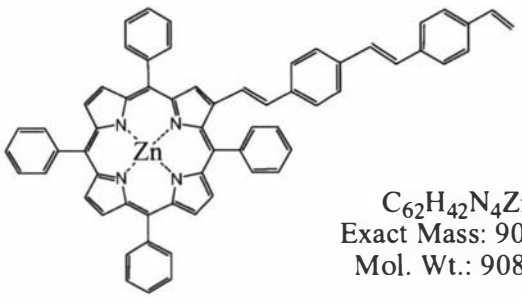

$C_{62}H_{42}N_4Zn$
Exact Mass: 906.27
Mol. Wt.: 908.41

35 mg (38.5 μmol) of aldehyde **Zn-47** and 40 mg (111 μmol) of Me-ps were dissolved/suspended in 25mL of dry toluene, under argon. The solution was heated to reflux and excess of DBU (70 mg, 0.46 mmol) was added. After 24 hours, the solution was evaporated to dryness and the mixture separated through flash chromatography (silica gel, DCM/hexane = 1/1). The first band was collected, evaporated to dryness and recrystallized from DCM/methanol, yielding 27.6 mg (79%) of pure **Zn-51** as purple crystals. ^{1}H-NMR (500 MHz, $CDCl_3$): δ 9.11 (s, 1H, $H_{\beta\text{-pyrrolic}}$), 8.96-8.87 (m, 5H, $H_{\beta\text{-pyrrolic}}$), 8.83 (d, J = 4.7 Hz , 1H, $H_{\beta\text{-pyrrolic}}$), 8.27-8.18 (m, 8H, $H_{o\text{-Ph}}$), 7.88-7.71 (m, 12H, $H_{m,p\text{-Ph}}$), 7.45 (m, 4H, $2H_{Ph'}$ +2 $H_{Ph''}$), 7.40 (d, J = 8 Hz, 2H, $H_{Ph'}$), 7.28-7.22 (m, 3H, $2H_{Ph''}$ + $1H_{alkene}$), 7.12 (br s, 2H, $H_{alkene'}$), 7.03 (d, J = 15.9 Hz, 1H, H_{alkene}), 6.72 (dd, J_{trans} = 17.5 Hz, J_{cis} = 10 Hz, 1H, $H_{alkene''}$), 5.78 (d, J_{trans} = 17.5 Hz, 1H, $H_{alkene''}$), 5.25 (d, J_{cis} = 10 Hz, 1H, $H_{alkene''}$). *Assignments aided by COSY spectra.* UV-vis (toluene): λ_{max} [nm] (ε x 10^{-3}) 433 (196), 560 (24), 597 (14). FAB-HRMS for M^- ($C_{62}H_{42}N_4Zn$): 906.2694, calculated: 906.2700.

TPP-Ph-Ph-CH=CH$_2$, 51.

4-(*trans*-2'-(4"-(*trans*-2'"-(2""-(5"",10"",15"",20""-tetraphenylporphyrin)yl)ethen-1'"-yl)phenyl)ethen-1'-yl)styrene.

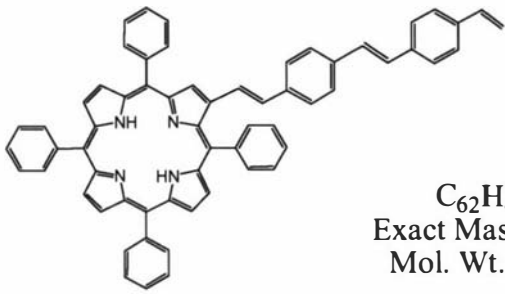

$C_{62}H_{44}N_4$
Exact Mass: 844.36
Mol. Wt.: 845.04

Free-base porphyrin **51** was obtained by demetallation of **Zn-51** using the described general procedure. 7.8 mg (98%) of pure product **51** were obtained from 8.5 mg (9.4 μmol) of the Zn homologue. ^{1}H-NMR (500 MHz, $CDCl_3$): δ 9.13-8.70 (m, 7H, $H_{\beta\text{-pyrrolic}}$), 8.28-8.17 (m, 8H, $H_{o\text{-Ph}}$), 7.88-7.72 (m, 12H, $H_{m,p\text{-Ph}}$), 7.55-7.48 (m, 4H, $2H_{Ph'}$ +$2H_{Ph''}$), 7.44 (d, J = 8 Hz, 2H, $H_{Ph'}$), 7.28-7.22 (m, 3H, $2H_{Ph''}$+H_{alkene}), 7.16-7.14 (m, 2H, $2H_{alkene'}$), 7.04 (d, J = 17 Hz, 1H, H_{alkene}), 6.72 (dd, J_{trans} = 17.5 Hz, J_{cis} = 10.8 Hz , 1H, H_{alkene}), 5.78 (d, J_{trans} = 17.5 Hz, 1H, H_{alkene}), 5.25 (d, J_{cis} = 10.8 Hz, 1H, H_{alkene}), -2.58 (s, 2H, $H_{N\text{-pyrrolic}}$). UV-vis (toluene): λ_{max} [nm] (ε x 10^{-3}) 428 (159), 524 (18), 568 (13), 602 (7), 659 (2). FAB-HRMS for MH^+ ($C_{62}H_{45}N_4$): 845.3660, calculated: 845.3644.

***trans*-4-stilbenecarboxaldehyde, 52.**

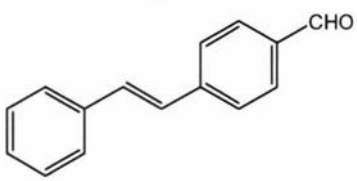

$C_{15}H_{12}O$
Exact Mass: 208.09
Mol. Wt.: 208.26

138 mg (539 μmol) of benzene phosphonate **37** and 283 mg (2 mmol) of terephthaldicarboxaldehyde **13** were dissolved in 15 mL of dry THF, under argon. To the stirred solution 70 mg (624 μmol) of solid ^{t}BuOK were added in two portions over 1h. After a further 10 min, the solution was evaporated to dryness and the mixture separated by flash chromatography (silica gel, DCM/hexane = 1/1). The first band afforded 84 mg (75%) of pure *trans* **52** as a colourless solid. ^{1}H-NMR (400 MHz, $CDCl_3$): δ 10.0 (s, 1H, $H_{aldehyde}$), 7.88 (d, J = 8.1 Hz, 2H, $H_{Ph\text{-}CHO}$), 7.66 (d, J = 8.1 Hz, 2H, $H_{Ph\text{-}CHO}$), 7.55 (d, J = 7.8 Hz, 2H, H_{Ph}), 7.39 (app t, J = 7.5 Hz, 2H, H_{Ph}), 7.32 (d,

J = 7.2 Hz, 1H, H_{Ph}), 7.27 (d, J = 16.4 Hz, 1H, H_{alkene}), 7.15 (d, J = 16.4 Hz, 1H, H_{alkene}). *Assignments aided by COSY spectra.*

trans-4-vinylstilbene, 53.

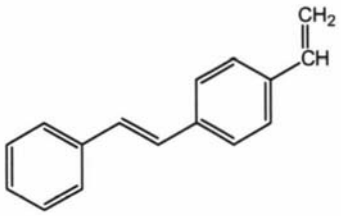

$C_{16}H_{14}$
Exact Mass: 206.11
Mol. Wt.: 206.28

20 mg (96 μmol) of aldehyde **52** and 100 mg (279 μmol) of Me-ps were dissolved/suspended in 25mL of dry toluene under argon. The solution was heated to reflux and an excess of DBU (80 mg, 0.5mmol) was added. After 18 hours, the solution was evaporated to dryness and the product isolated through flash chromatography (silica gel, DCM/hexane = 1/3). The first band was collected, evaporated to dryness and recrystallized from DCM/methanol, yielding 14.5 mg (73%) of pure **53** as pink-white crystals. ^{1}H-NMR (400 MHz, $CDCl_3$): δ 7.52 (d, J = 7.6 Hz, 2H, H_{Ph}), 7.48 (d, J = 8 Hz, 2H, $H_{stylbene}$), 7.41 (d, J = 8 Hz, 2H, $H_{stylbene}$), 7.36 (app t, J = 7.6 Hz, 2H, H_{Ph}), 7.26 (m, 1H, H_{Ph}), 7.11 (s, 2H, H_{alkene}), 6.72 (dd, J_{trans} = 17.6 Hz, J_{cis} = 10.8 Hz , 1H, $H_{alkene'}$), 5.77 (d, J_{trans} = 17.6 Hz, 1H, $H_{alkene'}$), 5.25 (d, J_{cis} = 10.8 Hz, 1H, $H_{alkene'}$). *Assignments aided by COSY spectra.* FAB-HRMS for $M^{+\cdot}$ ($C_{16}H_{14}$): 206.1103, calculated: 206.1096. The ^{1}H-NMR spectrum is in agreement with the literature.[145]

$(TPP)_2$, 54.

1,4-*trans,trans*-(2'-(5',10',15',20'-tetraphenylporphyrin)yl)butadiene.

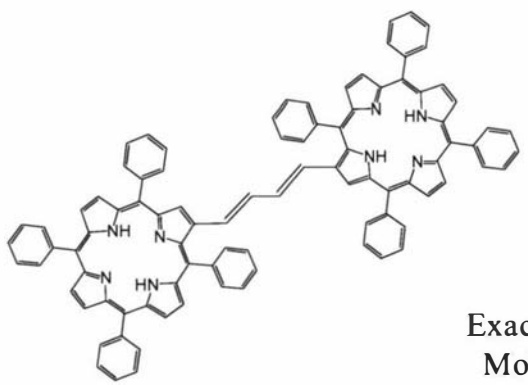

$C_{92}H_{62}N_8$
Exact Mass: 1278.51
Mol. Wt.: 1279.53

The synthesis of this dimer was performed according to the procedures described by Bonfantini and Officer.[146]

45 mg (67.3 μmol) of aldehyde **41** and 100 mg (108 μmol) of phosphonium salt **11** were dissolved in 15 mL of dichloromethane. The excess of phosphonium salt was needed because of its expected reactivity versus hydrolysis. To the stirred solution, 10 mL of 40% $NaOH_{(aq)}$ were added and reaction went on for 2 hours after which the organic phase was separated, washed with water and dried over $MgSO_4$. The crude was first purified through flash chromatography on silica gel (DCM/toluene = 1/1), which eliminated most of the low polar co-products (mainly TPP-CH_3). 29 mg (34%) of pure product **54** were obtained after two recrystallizations from DCM/MeOH. The ^{1}H-NMR spectrum showed pure *trans* configurations; it is probable that *cis* isomers were formed but removed in the purification process. ^{1}H-NMR (500 MHz, $CDCl_3$): δ 8.93 (s, 2H, $H_{\beta\text{-pyrrolic}}$), 8.87-8.77 (m, 12H, $H_{\beta\text{-pyrrolic}}$), 8.34 (d, J = 7 Hz, 4H, $H_{o\text{-Ph}}$), 8.26-8.11 (m, 12H, $H_{o\text{-Ph}}$), 8.01-7.91 (m, 6H, $H_{m,p\text{-Ph}}$), 7.82-7.66 (m, 18H, $H_{m,p\text{-Ph}}$), 6.82-6.76 (m, 2H, H_{alkene}), 6.26-6.20 (m, 2H, H_{alkene}), -2.55 (br s, 4H, $H_{N\text{-pyrrolic}}$). *Assignments aided by COSY spectra.* UV-vis (toluene): λ_{max} [nm] (ε x 10^{-3}) 422 (219), 483 (sh, 55), 522 (45), 581 (23), 607 (24), 661 (sh 5). FAB-HRMS for MH^+ ($C_{92}H_{63}N_8$): 1279.5165, calculated: 1279.5176.

$(ZnTPP)_2$, Zn-54.

1,4-*trans,trans*-(2'-(5',10',15',20'-tetraphenylporphyrinato zinc(II))yl)butadiene.

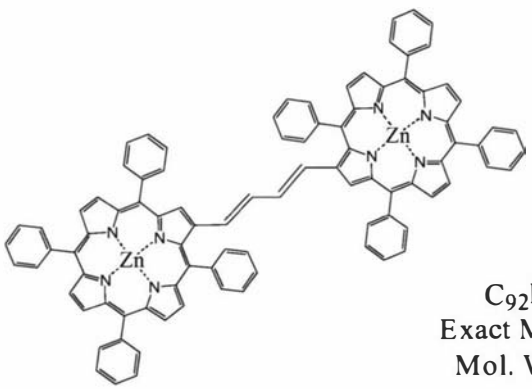

$C_{92}H_{58}N_8Zn_2$
Exact Mass: 1402.34
Mol. Wt.: 1406.28

10 mg (7.8 μmol) of **54** were metallated as described in the general procedures, yielding 10.5 mg (96%) of **Zn-54.** ^{1}H-NMR (500 MHz, $CDCl_3$): δ 9.04 (s, 2H, $H_{\beta\text{-pyrrolic}}$), 8.98-8.88 (m, 12H, $H_{\beta\text{-pyrrolic}}$), 8.35 (d, J = 7 Hz , 4H, $H_{o\text{-Ph}}$), 8.26-8.11 (m, 12H, $H_{o\text{-Ph}}$), 8.02-7.91 (m, 6H, $H_{m,p\text{-Ph}}$), 7.82-7.70 (m, 18H, $H_{m,p\text{-Ph}}$), 6.81-6.75 (m, 2H, H_{alkene}), 6.26-6.20 (m, 2H, H_{alkene}). *Assignments aided by COSY spectra.* UV-vis (toluene): λ_{max} [nm] (ε x 10^{-3}) 427 (319), 505 (sh 75), 566 (49), 614 (40). FAB-HRMS for MH^+ ($C_{92}H_{59}N_8Zn_2$): 1403.3431, calculated: 1403.3446.

TPP-ZnTPP, Zn/fb-55.

1-*trans*-(2'-(5',10',15',20'-tetraphenylporphyrinato zinc(II))yl),4-*trans*-(2'-(5',10',15',20'-tetraphenylporphyrin)yl)butadiene.

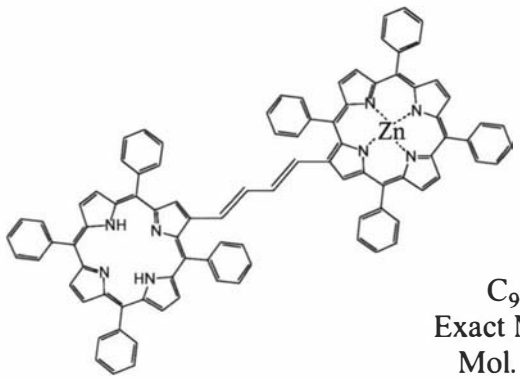

$C_{92}H_{60}N_8Zn$
Exact Mass: 1340.42
Mol. Wt.: 1342.9

The synthesis of this dimer was performed according to the procedures described by Bonfantini and Officer.[146]

100 mg (137 μmol) of aldehyde **Zn-41** and 183 mg (198 μmol) of phosphonium salt **11** were dissolved in 15 mL of dichloromethane. The excess of phosphonium salt was needed because of its expected reactivity versus hydrolysis. To the stirred solution, 15 mL of 32% $NaOH_{(aq)}$ were added and reaction went on for 2 hours after which the organic phase was separated, washed with water and dried over $MgSO_4$. The crude was first purified through flash chromatography on silica gel (chloroform as eluent), which eliminated most of the low polar co-products (mainly TPP-CH_3). The pure product was obtained by recrystallization involving a mixture of THF, DCM and hexane. 68 mg (37%) of pure **Zn/fb-55** were obtained. The ^{1}H-NMR spectrum showed pure *trans* configurations; it is probable that *cis* isomers were formed but removed in the purification process. ^{1}H-NMR (500 MHz, $CDCl_3$): δ 9.06-8.75 (m, 14H, $H_{\beta\text{-pyrrolic}}$), 8.41-8.10 (m, 16H, $H_{o\text{-Ph}}$), 8.03-7.90 (m, 6H, $H_{m,p\text{-Ph}}$), 7.77 (br s, 18H, $H_{m,p\text{-Ph}}$), 6.85-6.73 (m, 2H, H_{alkene}), 6.23 (app t, J = 14.7 Hz, 2H, H_{alkene}), -2.55 (br s, 2H, $H_{N\text{-pyrrolic}}$). UV-vis (toluene): λ_{max} [nm] (ε x 10^{-3}) 424 (253), 493 (sh 70), 522 (sh 50), 566 (36), 609 (35), 661 (sh 4). FAB-HRMS for MH^+ ($C_{92}H_{61}N_8Zn$): 1341.4369, calculated: 1341.4311.

TPP-Ph-ZnTPP, Zn/fb-56.

1-(*trans*-2'-(2"-(5",10",15",20"-tetraphenylporphyrinato zinc(II))yl),4-(*trans*-2'-(2"-(5",10",15",20"-tetraphenylporphyrin)yl)ethen-1'-yl)benzene.

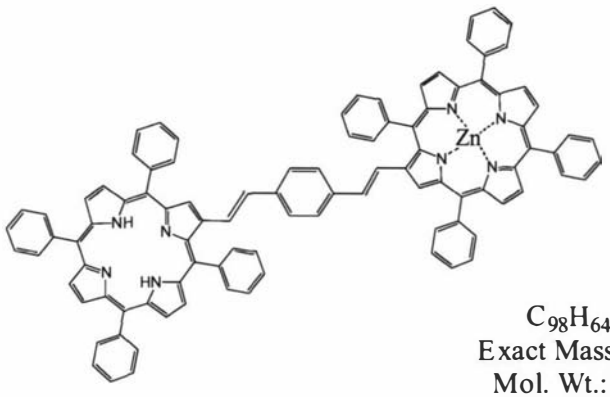

$C_{98}H_{64}N_8Zn$
Exact Mass: 1416.45
Mol. Wt.: 1419.00

75 mg (93 μmol) of aldehyde **Zn-14** and 90 mg (97.5 μmol) of phosphonium salt **11** were dissolved in 25 mL of dichloromethane under argon. To the stirred solution, 40 mg (263 μmol) of DBU were added and reaction went on for 30 minutes after which the crude was precipitated by MeOH addition. This poorly soluble solid was then redissolved in THF/hexane = 1/1 and filtered through few cm of silica gel and brought to dryness. The resulting solid was then dissolved in 50 mL of chloroform and 100 mg of I_2 were added. After 40 hours the solution was washed three times with a saturated solution of $Na_2S_2O_3$ and water and then precipitated with methanol. The pure product was obtained by further recrystallization from chloroform/hexane to yield 76.5 mg (58%) of **Zn/fb-56** as purple crystals. The ^{1}H-NMR spectrum showed pure *trans* configurations. ^{1}H-NMR (500 MHz, dioxane-d_8): δ 9.06 (s, 1H, $H_{\beta\text{-pyrrolic}}$), 9.03 (s, 1H, $H_{\beta\text{-pyrrolic}}$), 8.83-8.68 (m, 12H, $H_{\beta\text{-pyrrolic}}$), 8.32-8.18 (m, 16H, $H_{o\text{-Ph}}$), 8.05-7.98 (m, 2H, $H_{m,p\text{-Ph}}$), 7.96-7.90 (m, 4H, $H_{m,p\text{-Ph}}$), 7.86-7.73 (m, 18H, $H_{m,p\text{-Ph}}$), 7.36 (d, J = 15.4 Hz, 1H, H_{alkene}), 7.29 (d, J = 15.9 Hz, 1H, H_{alkene}), 7.25 (br s, 4H, $H_{\text{Ph'}}$), 7.10 (d, J = 15.9 Hz, 1H, H_{alkene}), 7.08 (d, J = 15.4 Hz, 1H, H_{alkene}), -2.53 (br s, 2H, $H_{N\text{-pyrrolic}}$). *Assignments aided by COSY spectra.* UV-vis (toluene): λ_{max} [nm] (ε x 10^{-3}) 429 (292), 492 (sh 65), 523 (sh 37), 566 (37), 601 (30), 659 (2). FAB-HRMS for MH^+ ($C_{98}H_{65}N_8Zn$): 1417.4574, calculated: 1417.4624

TPP-ext-Ph-ZnTPP, Zn/fb-57.

1-(*trans*-2'-(2"-(5",10",15",20"-tetraphenylporphyrinato zinc(II))yl)ethen-1'-yl),4-(*trans* -4'-(2"-(5',10"',15",20"-tetraphenylporphyrin)yl)butadien-*trans*-1'-yl)benzene.

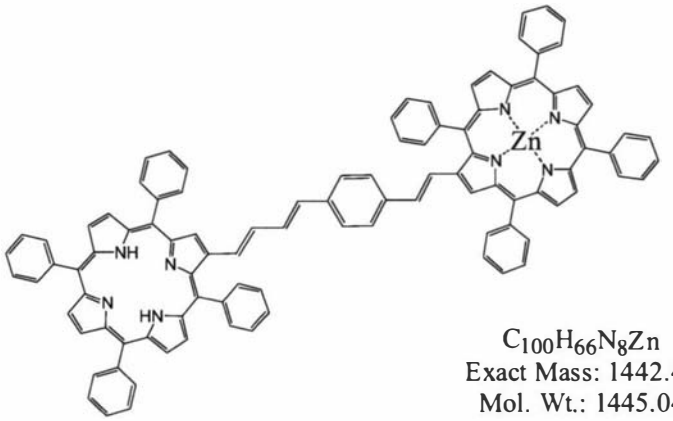

$C_{100}H_{66}N_8Zn$
Exact Mass: 1442.47
Mol. Wt.: 1445.04

93 mg (115 μmol) of aldehyde **Zn-14** and 124 mg (134 μmol) of phosphonium salt **43** were dissolved in 40 mL of dichloromethane under argon. To the stirred solution, 60 mg of DBU were added and reaction went on for 60 minutes. The solution/suspension was then brought to dryness, the solid dissolved in DCM/hexane = 2/1 and filtered through few cm of silica gel. 51 mg (31% yield) of the pure **Zn/fb-57** were obtained through two recrystallizations from chloroform/methanol and chloroform/hexane. The ^{1}H-NMR spectrum showed pure *trans* configurations; it is probable that *cis* isomers were formed but removed in the purification process. ^{1}H-NMR (500 MHz, $CDCl_3$): δ 9.13 (s, 1H, $H_{\beta\text{-pyrrolic}}$), 8.97-8.89 (m, 6H, $H_{\beta\text{-pyrrolic}}$), 8.86-8.74 (m, 7H, $H_{\beta\text{-pyrrolic}}$), 8.30-8.15 (m, 14H, $H_{o\text{-Ph}}$), 7.95-7.70 (m, 24H, $H_{m,p\text{-Ph}}$), 7.44-7.37 (m, 3H, $2H_{Ph'}$ + H_{alkene}), 7.29 (d, J = 8 Hz, 2H, $H_{Ph'}$), 7.22-7.15 (m 1H, H_{alkene}), 7.06 (d, J = 15.2 Hz, 1H, H_{alkene}), 6.75 (d, J = 15.5 Hz, 1H, H_{alkene}), 6.70-6.64 (m, 1H, H_{alkene}), 6.32 (d, J = 15.2 Hz, 1H, H_{alkene}), -2.57 (br s, 2H, $H_{N\text{-pyrrolic}}$). *Assignments aided by COSY spectra.* UV-vis (toluene): λ_{max} [nm] (ε x 10^{-3}) 430 (252), 518 (sh 42), 566 (33), 602 (27), 659 (3). FAB-HRMS for MH^- ($C_{100}H_{67}N_8Zn$): 1443.4783, calculated: 1443.4780.

ZnTPP-ext-Ph-ZnTPP, Zn-58.

1-(*trans*-2'-(2"-(5",10",15",20"-tetraphenylporphyrinato zinc(II))yl)ethen-1'-yl),4-(*trans,trans*-4'-(2"-(5',10"',15",20"-tetraphenylporphyrinato zinc(II))yl)butadien-1'-yl)benzene.

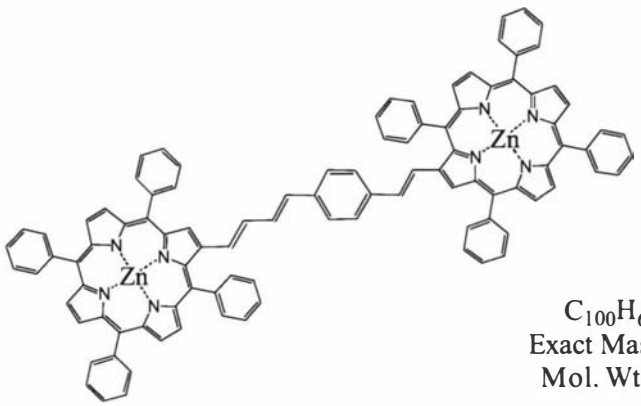

$C_{100}H_{64}N_8Zn_2$
Exact Mass: 1504.38
Mol. Wt.: 1508.41

61 mg (83.6 μmol) of aldehyde **Zn-41** and 78 mg (84 μmol) of phosphonate **Zn-45** were dissolved in 25 mL of dry THF, under argon atmosphere. To the stirred solution, 15 mg (133 μmol) of solid ^{t}BuOK were added in two portions in 30 min. After further 30 min, the solution was evaporated to dryness, dissolved in DCM purified through flash chromatography on silica gel (DCM). The fractions containing the desired product were collected and recrystallized from DCM/hexane to afford 45 mg (36%) of pure **Zn-58** as purple crystals. ^{1}H-NMR (500 MHz, $CDCl_3$): δ 9.13 (s, H, $H_{\beta\text{-pyrrolic}}$), 9.06 (s, H, $H_{\beta\text{-pyrrolic}}$), 8.97-8.82 (m, 12H, $H_{\beta\text{-pyrrolic}}$), 8.32-8.19 (m, 14H, $H_{o\text{-Ph}}$), 8.16 (d, J = 8 Hz, $H_{o\text{-Ph}}$), 7.95-7.72 (m, 24H, $H_{m,p\text{-Ph}}$), 7.41 (d, J = 8 Hz, 2H, $H_{Ph'}$), 7.32 (d, J = 16 Hz, 1H, H_{alkene}), 7.27 (d, J = 8 Hz, 2H, $H_{Ph'}$), 7.17 (dd, J_1 = 15 Hz, J_2 = 9.6 Hz, 1H, H_{alkene}), 7.08-7.03 (m, 2H, $1H_{alkene} + 1H_{alkene'}$), 6.76-6.65 (m, 2H, H_{alkene}), 6.33 (d, J = 15 Hz, 1H, H_{alkene}). *Assignments aided by COSY spectra.* UV-vis (toluene): λ_{max} [nm] ($\varepsilon \times 10^{-3}$) 434 (359), 498 (sh 96), 568 (57), 607 (47). FAB-HRMS for $(M+O_2+H)^+$ ($C_{100}H_{65}N_8Zn_2$): 1537.3843, calculated: 1537.3813.

TPP-ext-Ph-TPP, 58.

1-(*trans*-2'-(2"-(5",10",15",20"-tetraphenylporphyrin)yl)ethen-1'-yl),4-(*trans,trans*-4'-(2"-(5',10"',15",20"-tetraphenylporphyrin)yl)butadien-1'-yl)benzene.

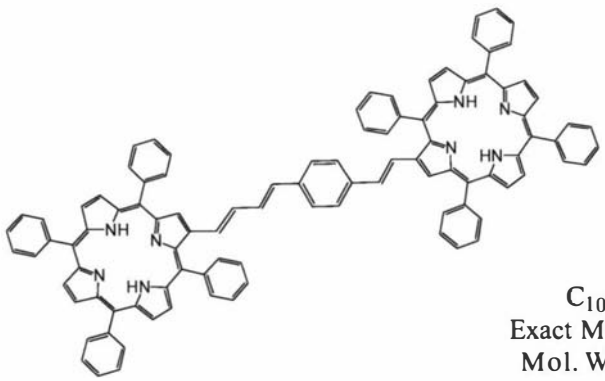

$C_{100}H_{68}N_8$
Exact Mass: 1380.56
Mol. Wt.: 1381.66

Free-base porphyrin **58** was prepared by demetallation of **Zn-58** according to the described general procedure. In this case, the low solubility of the product required a further recrystallization step (DCM/hexane) to obtain the desired purity. 16 mg (87% yield) of pure **58** were obtained from 20 mg (13.3 μmol) of the Zn homologue. ^{1}H-NMR (500 MHz, $CDCl_3$): δ 9.03 (s, H, $H_{\beta\text{-pyrrolic}}$), 8.96 (s, H, $H_{\beta\text{-pyrrolic}}$), 8.85-8.72 (m, 12H, $H_{\beta\text{-pyrrolic}}$), 8.29-8.19 (m, 14H, $H_{o\text{-Ph}}$), 8.17 (d, J = 8 Hz, 2H, $H_{o\text{-Ph}}$), 7.95-7.69 (m, 24H, $H_{m,p\text{-Ph}}$), 7.41 (d, J = 8.2 Hz, 2H, $H_{Ph'}$), 7.32 (d, J = 16 Hz, 1H, H_{alkene}), 7.28 (d, J = 8.2 Hz, 2H, $H_{Ph'}$), 7.16 (dd, J_1 = 15 Hz, J_2 = 9 Hz, 1H, H_{diene}), 7.08 (d, J = 16 Hz, 1H, H_{alkene}), 6.75-6.63 (m, 2H, H_{diene}), 6.31 (d, J = 15 Hz, 1H, $H_{diene\text{-Ph}}$), -2.56 (br s, 4H, $H_{N\text{-pyrrolic}}$). *Assignments aided by COSY spectra.* UV-vis (toluene): λ_{max} [nm] ($\varepsilon \times 10^{-3}$) 429 (221), 519 (sh 43), 574 (31), 605 (22) 660 (3). FAB-HRMS for $(M+2H)^{2+}$ ($C_{100}H_{70}N_8$): 691.2832, calculated: 691.2856; for $(M+O_2+2H)^{2+}$ ($C_{100}H_{70}N_8O_2$): 707.2774, calculated: 707.2805; for $(M+O_2+H)^+$ ($C_{100}H_{69}N_8O_2$): 1413.5651, calculated: 1413.5543.

TPP-Ph-Ph-ZnTPP, Zn/fb-59.

trans-1-(4'-(*trans*-2"-(2"'-(5"',10"',15"',20"'-tetraphenylporphyrinato zinc(II))yl)ethen-1"-yl)phenyl),2-(4'-(*trans*-2"-(2"'-(5"',10"',15"',20"'-tetraphenylporphyrin)yl)ethen-1"-yl)phenyl)ethene.

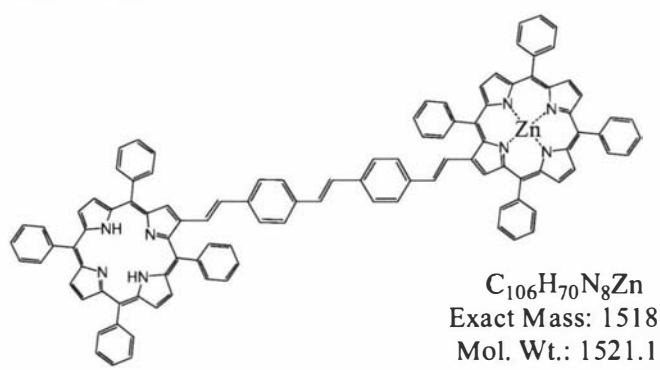

$C_{106}H_{70}N_8Zn$
Exact Mass: 1518.5
Mol. Wt.: 1521.13

80 mg (87.9 μmol) of aldehyde **Zn-47** and 100 mg (108 μmol) of phosphonium salt **11** were dissolved in 30 mL of dichloromethane under argon. To the stirred solution, 40 mg of DBU were added and reaction went on for 40 minutes. The solution/suspension was then brought to dryness, the solid dissolved in DCM and filtered twice through few cm of silica gel. The fractions containing the desired product were collected and 56 mg (42%) of pure **Zn/fb-59** were obtained through a series of recrystallizations from THF/DCM/hexane. The ^{1}H-NMR spectrum did not show the presence of any *cis* configuration, therefore no isomerization step was performed. ^{1}H-NMR (500 MHz, $CDCl_3$): δ 9.09 (s, 1H, $H_{\beta\text{-pyrrolic}}$), 9.07 (s, 1H, $H_{\beta\text{-pyrrolic}}$), 8.84-8.68 (m, 12H, $H_{\beta\text{-pyrrolic}}$), 8.28-8.16 (m, 16H, $H_{o\text{-Ph}}$), 7.95-7.70 (m, 24H, $H_{m,p\text{-Ph}}$), 7.60-7.55 (m, 4H, $2H_{Ph'(Zn)} + 2H_{Ph'(fb)}$), 7.38 (d, J = 16 Hz, 1H, H_{alkene}), 7.33-7.26 (m, 7H, $2H_{Ph'(Zn)} + 2H_{Ph'(fb)} + 3H_{alkene}$), 7.11 (app t, J = 15.8 Hz, 2H, $1H_{alkene} + 1H_{alkene}$), -2.48 (br s, 2H, $H_{N\text{-pyrrolic}}$). FAB-HRMS for MH^+ ($C_{106}H_{71}N_8Zn$): 1519.5075, calculated: 1519.5093. UV-vis (toluene): λ_{max} [nm] (ε x 10^{-3}) 432 (246), 525 (sh 29), 569 (36), 603 (21), 659 (2).

ZnTPP-Ph-Ph-ZnTPP, Zn-60.

trans-1,2-bis(4'-(*trans*-2"-(2"'-(5"',10"',15"',20"'-tetraphenylporphyrinato zinc(II))yl)ethen-1"-yl)phenyl)ethene.

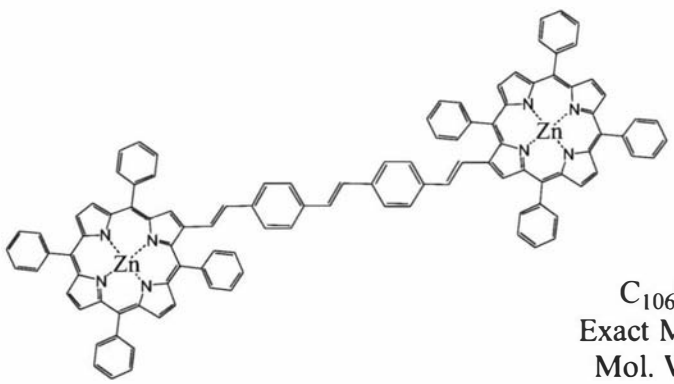

$C_{106}H_{68}N_8Zn_2$
Exact Mass: 1580.41
Mol. Wt.: 1584.51

24 mg (25.9 μmol) of aldehyde **Zn-14** and 25 mg (26.9 μmol) of phosphonate **Zn-45** were dissolved in 15 mL of dry THF, under argon atmosphere. To the stirred solution, 5 mg (44 μmol) of solid ^{t}BuOK were added. After 30 min, the solution was evaporated to dryness and purified through flash chromatography on silica gel (DCM/toluene = 2/1). The fractions containing the desired product were collected and recrystallized from DCM/MeOH and then from a mixture DCM/THF/hexane, affording 16 mg (39%) of pure **Zn-60** as purple crystals ^{1}H-NMR (500 MHz, CD_2Cl_2-

d_2/dioxane-d_8): δ 9.09 (s, 2H, $H_{\beta\text{-pyrrolic}}$), 8.87-8.79 (m, 10H, $H_{\beta\text{-pyrrolic}}$), 8.76 (d, J = 4.6, 2H, $H_{\beta\text{-pyrrolic}}$), 8.25-8.13 (m, 16H, $H_{o\text{-Ph}}$), 7.91-7.70 (m, 24H, $H_{m,p\text{-Ph}}$), 7.54 (d, J = 8 Hz, 4H, $H_{Ph'}$), 7.28 (d, J = 15.8 Hz, 1H, H_{alkene}), 7.27 (d, J = 8 Hz, 4H, $H_{Ph'}$), 7.21 (s, 2H, $H_{alkene'}$), 7.06 (d, J = 15.8 Hz, 1H, H_{alkene}). *Assignments aided by COSY spectra.* UV-vis (toluene): λ_{max} [nm] (ε x 10^{-3}) 435 (356), 495 (sh 89), 566 (52), 603 (34). FAB-HRMS for $(M+O_2+H)^+$ ($C_{106}H_{69}N_8Zn_2$): 1581.4323, calculated: 1581.4228.

TPP-Ph-Ph-TPP, 60.

trans-1,2-bis(4'-(*trans*-2"-(2"'-(5"',10"',15"',20"'-tetraphenylporphyrin)yl)ethen-1"-yl)phenyl)ethene.

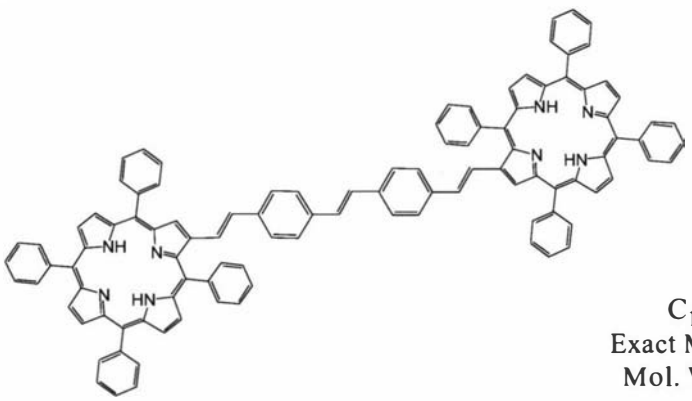

$C_{106}H_{72}N_8$
Exact Mass: 1456.59
Mol. Wt.: 1457.76

Free-base porphyrin **60** was prepared by demetallation of **Zn/fb-59**, according to the described general procedure. In this case, because of the lower solubility of the product, further recrystallization steps (THF/hexane and DCM/THF/hexane) were performed to obtain the desired purity. 16 mg (83%) of pure product **60** were obtained from 20 mg (13.1 μmol) of the metallated homologue. ^{1}H-NMR (500 MHz, $CDCl_3$): δ 9.02 (br s, 2H, $H_{\beta\text{-pyrrolic}}$), 8.85-8.71 (m, 12H, $H_{\beta\text{-pyrrolic}}$), 8.29-8.17 (m, 16H, $H_{o\text{-Ph}}$), 7.90-7.70 (m, 24H, $H_{m,p\text{-Ph}}$), 7.54 (d, J = 7.9 Hz, 4H, $H_{Ph'}$), 7.32 (d, J = 16.1 Hz, 2H, H_{alkene}), 7.29 (d, J = 7.9 Hz, 4H, $H_{Ph'}$), 7.21 (s, 2H, $H_{alkene'}$), 7.03 (d, J = 16.1 Hz, 2H, H_{alkene}), -2.57 (br s, 4H, $H_{N\text{-pyrrolic}}$). *Assignments aided by COSY spectra.* UV-vis (toluene): λ_{max} [nm] (ε x 10^{-3}) 428 (176), 526 (23), 571 (30), 606 (20), 665 (7). FAB-HRMS for MH^+ ($C_{106}H_{73}N_8$): 1457.5948, calculated: 1457.5958.

5. PORPHYRIN ARRAYS FOR MAQUETTE INCORPORATION

5.1. Porphyrins in biological systems

As seen in the Introduction, most of the work on synthetic porphyrins has been inspired by the extraordinary properties that natural porphyrins show in biological systems. Most of the processes involved in natural photosynthesis, as well as the mechanisms utilized in redox proteins containing metalloporphyrins, are still not fully understood in spite of enormous effort. However, the knowledge derived from such work has already made possible the application of synthetic porphyrins in biological processes. For example, the preferential accumulation of some porphyrins in tumour cells has permitted the creation of less invasive anti-cancer therapies.[11,37] There has also been interest in the possibility of incorporating porphyrins into nucleic acids for specific drug delivery and other biological activities; DNA intercalation has been achieved by electrostatic interaction between positively charged porphyrins and negatively charged DNA backbones.[164-167] Another interesting approach has been to synthesize porphyrin-containing oligonucleotides.[168]

A wider range of applications could potentially utilize porphyrin/protein systems. To date, most effort has been dedicated to the investigation of different kinds of natural protein/porphyrin bindings[204,205] and to the study of the effect of binding onto the protein and porphyrin activities.[206,207] Proteins are one of the most versatile classes of macromolecules, being involved in almost all biological processes and the coupling of the extraordinary properties of proteins and porphyrins could lead to completely new capabilities. The simplest way to obtain porphyrin/protein interactions is to bind metalloporphyrins to protein residues containing coordinating moieties such as amino, carboxy, phenolic or sulphhydryl/thioether groups;[169,170] The currently available synthetic methods allow the design of novel proteins and porphyrins so that their properties can be easily tuned to fit a variety of requirements. In this way it should be possible to make a large variety of porphyrin/protein-based functional materials.

5.2. Porphyrins and maquettes

Maquettes are synthetic proteins especially designed to allow the study of natural processes. Developed by Prof. Dutton's group at the University of Pennsylvania amongst others, maquettes typically consist of four α-helical bundles in which the sequences form domains that are similar to parts of more complicated natural proteins. These systems have been very useful in understanding biological processes, in particular those involving redox activities.[171] One of their major advantages is their variable physical properties. They can be designed to be hydrophilic[172] or amphiphilic[173,174] and their 3-dimensional structures can be tailored to bind different kind of molecules. In this way, maquettes can be used in various solvents, bound on solid supports,[175] inside membranes[176] or at the water/air interface[177] (Figure 5-1).

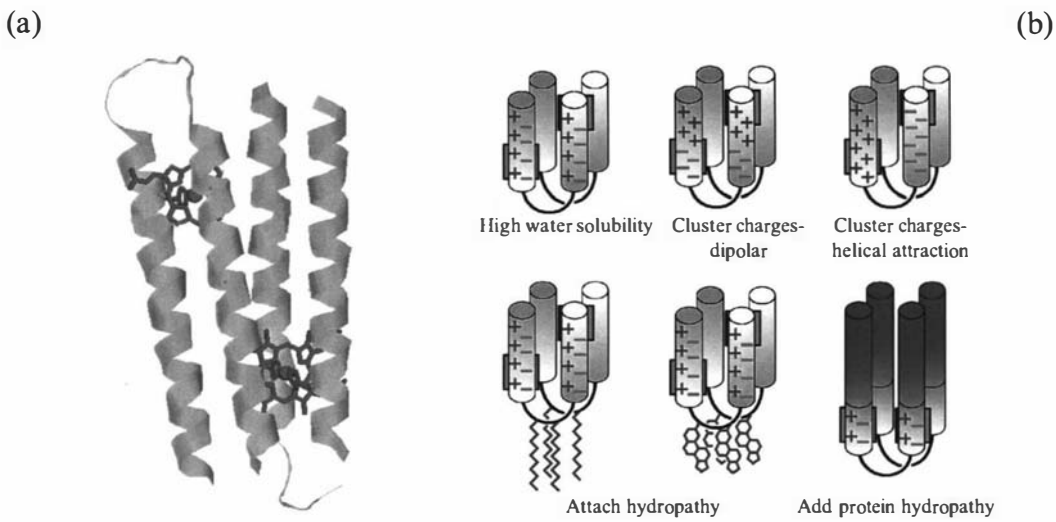

Figure 5-1 Maquettes: (a) porphyrin binding maquette; (b) chemical-physical ductility. By Dutton[175]

Our interest in those systems is connected to possible applications in new type of photovoltaic or photosynthetic devices. Maquettes could play an exceptional role in the charge separation of excited porphyrins by allowing the efficient transfer of the electrons from porphyrins to either an electrode (obtaining photocurrent) or an active centre (leading to reactions such as water splitting). The first application for our new porphyrin/maquette systems could be their incorporation into membranes to effect charge separation across a membrane, as schematized in Figure 5-2;[171,176] here, the porphyrin/maquette system can create an electron flow through the membrane that is

required by a coupled proton pump to generate charge separation across the membrane. This would create a 'membrane voltage' that can be exploited in many ways.

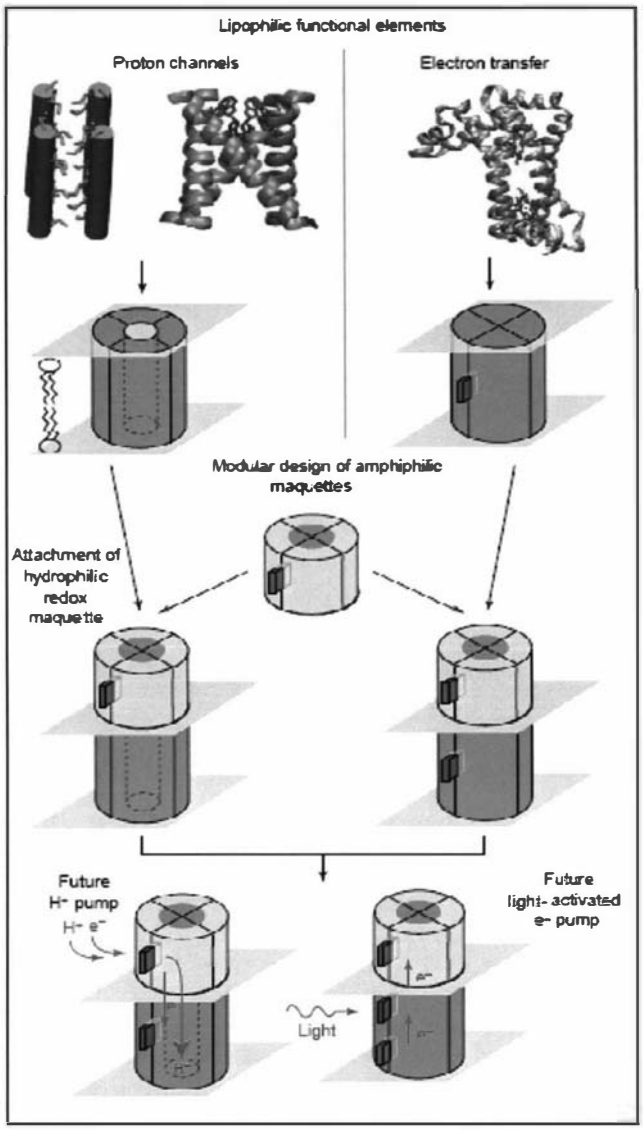

Figure 5-2 Maquette models for proton and electron pumps by Discher *et al.*[40]

In order to realize such systems, a series of new porphyrin arrays were designed and prepared to selectively bind inside the maquette proteins. By manipulating the amino acid sequence, it is possible to create maquettes which contain cavities large enough to host a molecule. Hystidine and cysteine residues in those cavities can bind Fe porphyrins;[169,178] selectivity over Zn porphyrin binding can be achieved both by using sulphhydryl/thioether groups as coordinating residues (which bind Zn porphyrin weakly) and by designing maquette cavities containing two facing imidazoles (Zn porphyrins usually coordinate only one N-ligand). Therefore, it is possible to make

porphyrin arrays containing a protein-binding Fe(III) porphyrin connected to a Zn porphyrin array antenna; the conjugated nature of our arrays should allow efficient electron transfer from the antenna to the maquette (Figure 5-3).

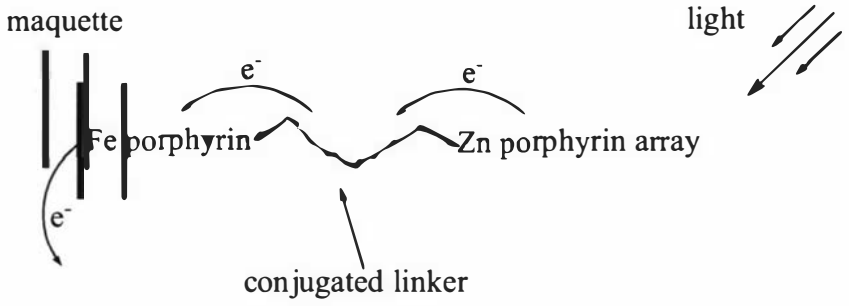

Figure 5-3 Model of a porphyrin array-maquette photoactive system

A series of Fe(III)/Zn TPP dyads, similar to the Zn/fb dyads described in Chapter 4, was prepared (Figure 5-4) in order to examine the influence of the conjugated bridge on the chemical-physical properties and on the binding ability. These molecules are hydrophobic and can potentially be utilized with amphiphilic maquettes in polar organic solvents (MeOH, DMSO, CH_3CN).

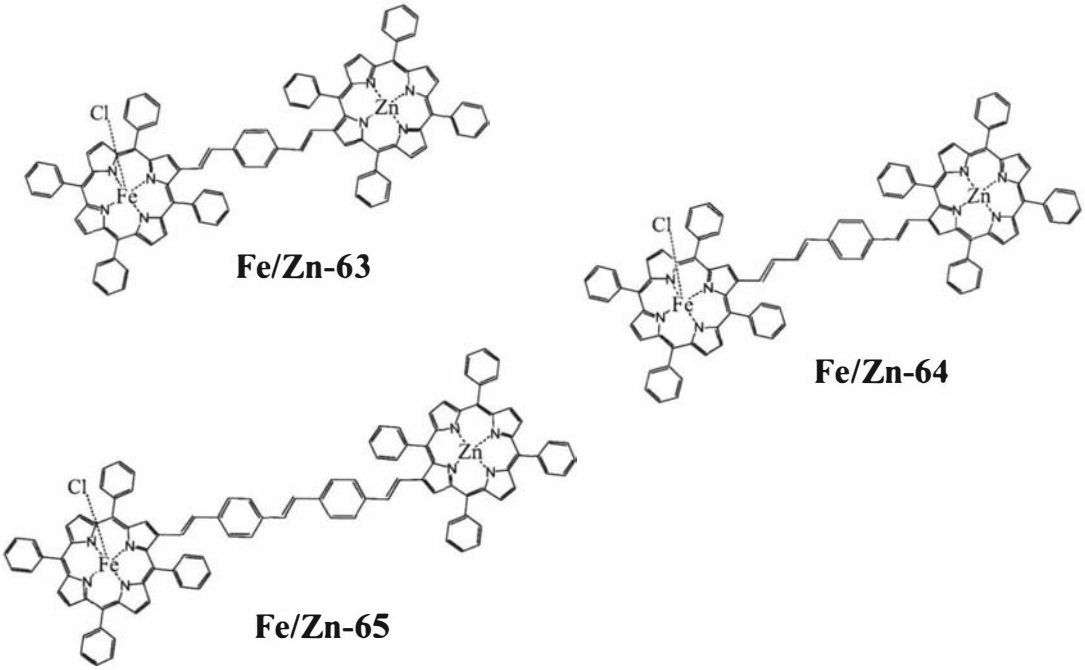

Figure 5-4 Fe/Zn porphyrin dyads for amphiphilic maquette binding

However, it was recognised that water-soluble porphyrin arrays would likely be required for incorporation into the hydrophilic class of maquettes, and so the synthesis of another series of Fe(III)/Zn dyads, in which the Zn porphyrin carries carboxylic groups, was investigated (Figure 5-5). The binding part of the array was still a hydrophobic Fe(III) porphyrin because the binding site of the hydrophilic proteins are hydrophobic. An unhindered monofunctionalized porphyrin was also prepared and used for array preparations in order to minimize the steric hindrance in the binding site.

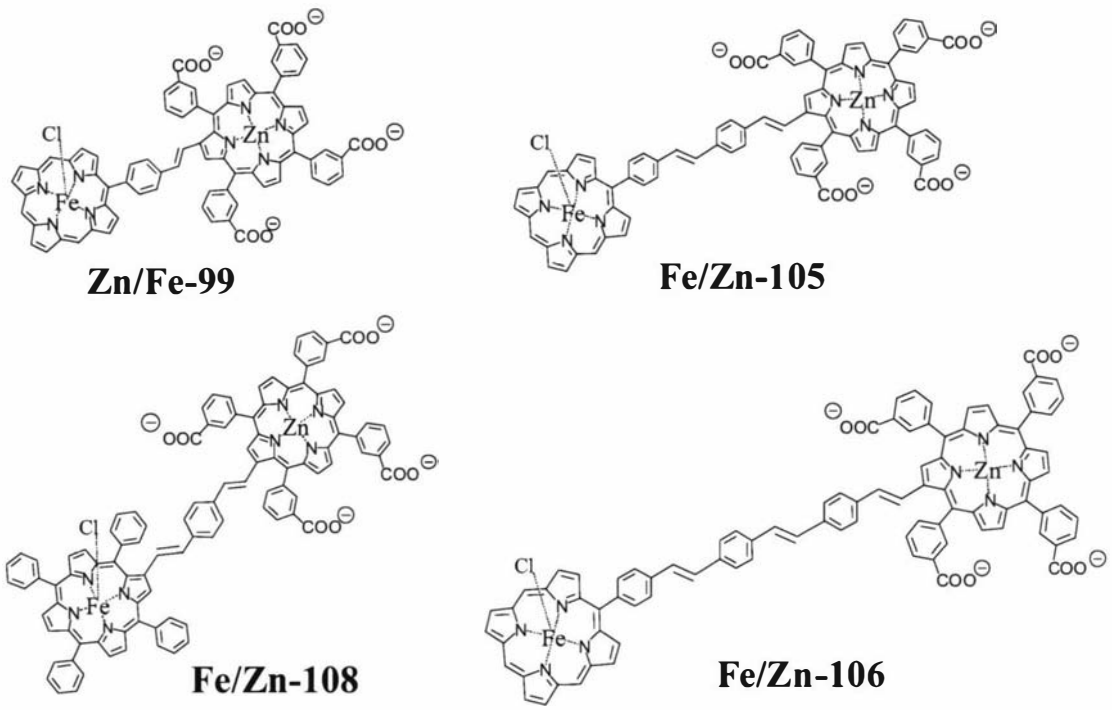

Figure 5-5 Fe/Zn porphyrin dyads for hydrophilic maquette binding

So far, only few works have been reported the synthesis of hydrophilic covalently linked porphyrin arrays;[179,180] to the best of our knowledge, this is the first example of a water-soluble array containing hydrophobic porphyrins. Both hydrophobic and hydrophilic dyads were prepared in order to investigate the porphyrin incorporation into the maquette and the efficiency of the conjugation in transferring electrons to the protein.

5.3. Fe(III) porphyrins

Fe(III) porphyrins are generally prepared by reaction of the free-base porphyrin with $FeCl_2$ in various solvents (solvent and temperature are critical). The resulting Fe(II) porphyrin is easily oxidized to a (Cl)Fe(III) porphyrin. In the course of this thesis, the best results were obtained using slight variations from the procedure described by Burns *et al.* (Scheme 5-1):[181] 10-20 equivalents of $FeCl_2 \cdot 4H_2O$ were dissolved in refluxing degassed acetonitrile after which the porphyrin, in degassed chloroform, was added. Reaction times were 3 to 5 hours, followed by overnight oxidation to Fe(III) by air at room temperature. Reactions have been successful also with substituted TPPs carrying either aldehyde or phosphonium salt groups. The yields were 75-90%.

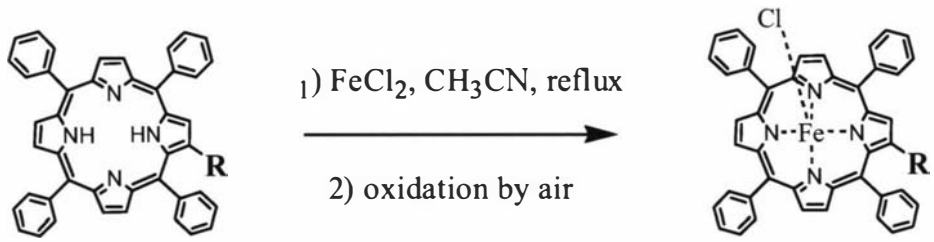

Product	Fe-5	Fe-14	Fe-11	Fe-43
		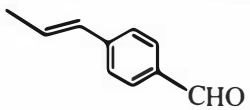	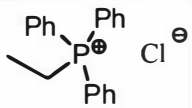	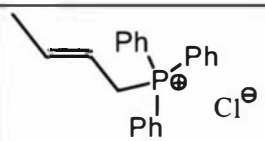

Scheme 5-1 Iron insertion in free-base porphyrins

Typically these iron insertion reactions did not go to completion but Fe(III) porphyrins were easily separated from the unreacted free-base porphyrin by chromatography, due to their higher polarity resulting from the ionic nature of these metalloporphyrins. The paramagnetism of the d^5 configuration of the Fe(III) centre made it impossible to use NMR spectrometry for analysis. Therefore, compounds were repeatedly purified (by recrystallization and column chromatography) until the TLC gave a single spot and the mass spectrum (usually MALDI spectrometry) did not show any unexpected high molecular weight peaks.

Fe(III) porphyrins typically undergo a rapid dimerization under non-acidic conditions forming μ-(O)-dimers, which are covalently bonded; the strength of this bond is typically enough to produce molecular peaks by MALDI spectrometry. The inverse reaction can be easily achieved by treating an organic solution of the porphyrin with 1-3M hydrochloric acid (Scheme 5-2). μ-(O)-Dimer formation can be detected by their characteristic Raman ($\nu_{Fe\text{-}O\text{-}Fe\ symm}$ = 360-420 cm^{-1})[185] and IR ($\nu_{Fe\text{-}O\text{-}Fe\ asymm}$ = 850-900 cm^{-1})[186,187] absorptions; UV-visible spectroscopy[186-190] and electrochemistry[185] have also been useful tools for characterizations of Fe porphyrins.

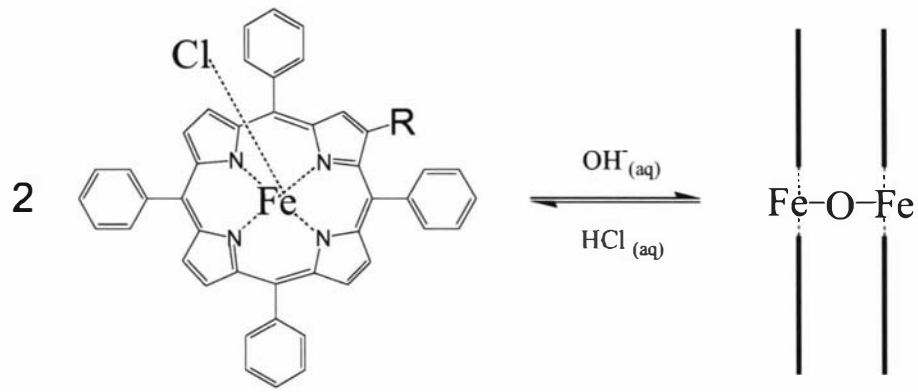

Scheme 5-2 Iron porphyrin dimerization equilibrium

μ-(O)-dimers are actually only one of the species present in equilibrium in basic conditions; the high affinity of Fe(III) ions for oxygen donors permits the formation of variously coordinated species, especially in the case of water soluble porphyrins (Scheme 5-3).[189-190]

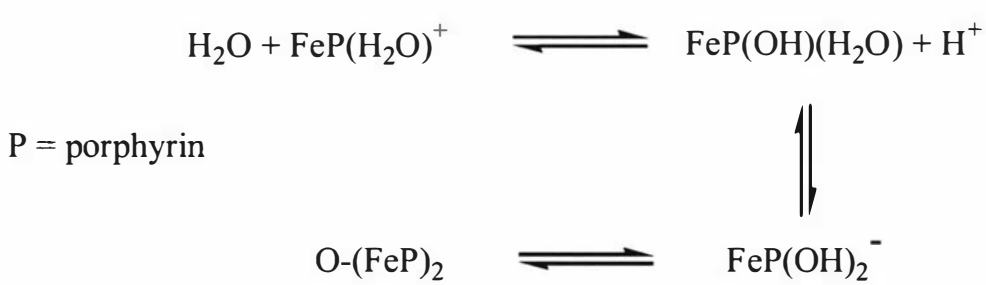

Scheme 5-3 Iron porphyrin equilibria in presence of basic water

The nature of the porphyrin substituents, as well as solvents and presence of salts, can have great influence on the dimerization equilibrium, either stabilizing different Fe-O species or sterically hindering the formation of dimers. For example, Manso *et al.*[188]

reported the formation of either mono-hydroxo (Fe-OH) or bis-hydroxo (HO-Fe-OH) species in place of μ-(O)-dimers when solution of hydrophobic porphyrins in 1,2-DCE were titrated with tetrabutylammonium hydroxide (TBAOH) in acetonitrile.

In all our cases (arrays included), dimerization equilibria occur, probably thanks to the planar conformation assumed by the conjugated substituents. For example, the MALDI spectrum of aldehyde **Fe-5**, after purification, shows two clusters with higher mass of 696 and 1408: the first number corresponds to the monomer ion $(M\text{-}Cl)^+$ while the higher number is the μ-(O)-dimer ion.

The presence of at least two species was confirmed by UV-visible spectroscopy, where reversibility between monomeric and μ-(O)-dimeric form was demonstrated. The spectrum of DCM solution of **Fe-5** was collected and it showed the absorption characteristic of the Fe-Cl bond (shoulder 360-380, absorptions at 670-690); after treatment with a saturated bicarbonate solution, the UV spectrum showed the disappearance of such characteristic bands with a blue shift of the Soret band (from 423 to 412 nm) and a new band at 610 nm, typical of μ-(O)-dimers. All this data are in agreement with the literature available for hydrophobic Fe porphyrins.[186] The treatment of the last sample with dilute HCl produced again the initial spectrum. Interestingly, the treatment of both the 'basic' and 'acid' solutions with excess imidazole brought to the same spectrum in which neither Fe-Cl or Fe-O characteristic bands were present and a red-shift of all the absorptions was registered; the formation of Fe-N complexes is therefore independent from the coordination around the Fe centre and is promising for the use of these molecules for protein binding, also in basic conditions. Similar complexation behaviour has already been described for water soluble Fe porphyrins.[191]

IR spectra were also taken and the strong absorption typical of the μ-(O)-dimer ($\nu_{Fe\text{-}O\text{-}Fe\ asymm}$) was found to be at 871 cm^{-1} in the μ-(O)-dimer form of **Fe-5**. Treatment of the same sample with dilute HCl resulted in the expected disappearance of this band.

Similar spectral information (MALDI, UV-visible and IR spectroscopy) was obtained for all the other porphyrins described in this section. All these Fe-porphyrins were

also characterized by HR-FAB mass spectrometry and the $(M-Cl)^+$ ion was always the highest peak.

5.4. Fe/Zn dyads syntheses

Array syntheses have been carried out using the same building block strategy utilized for all the other arrays in this work. As usual, Wittig reactions involving phosphonates were performed in THF, using potassium *tert*-butoxide as base while phosphonium salts were reacted in DCM or chloroform using DBU as base. An I_2 catalyzed isomerization step was used when phosphonium salts were involved.

The reaction of iron porphyrin phosphonium salts **Fe-11** and **Fe-43** with aldehyde **14** gave the mixed iron/free base dyads **Fe/fb-61** and **Fe/fb-62** according to Scheme 5-4. The result of these reactions was probably a mixture of *cis* and *trans* isomers (phosphonium salts usually give *trans*/*cis* ratio around 6/4) but the presence of the paramagnetic Fe(III) did not allow us to distinguish between the two isomers by NMR spectroscopy. The same isomerization step (treatment with I_2 in chloroform), which was successful with analogue Zn and free-base arrays, was also performed following all the Wittig reactions involving Fe phosphonium salts.

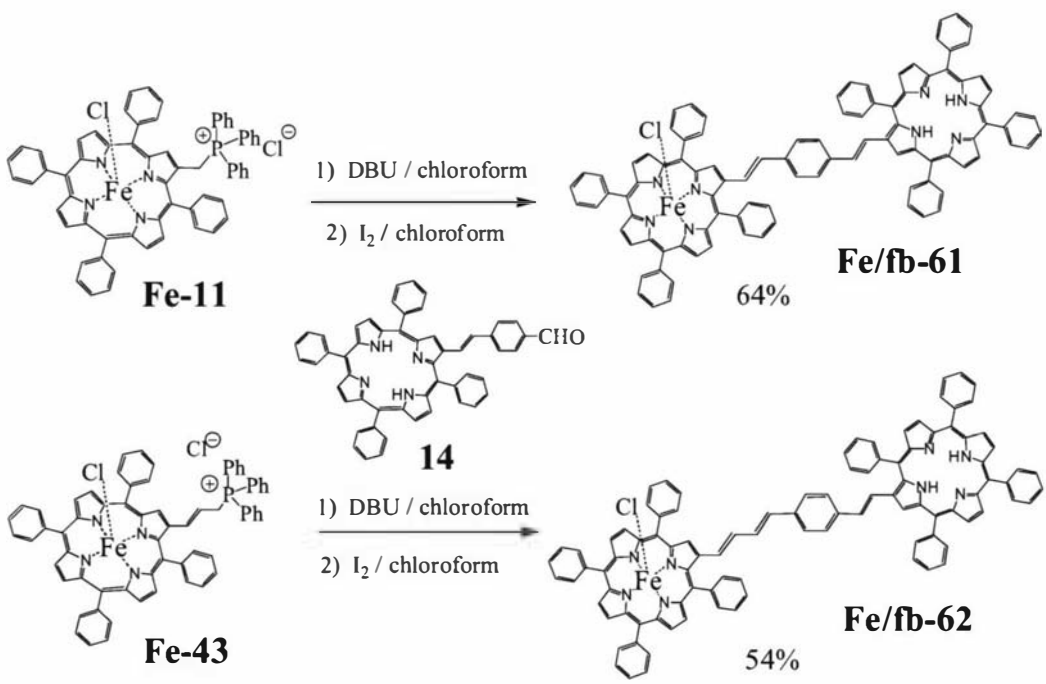

Scheme 5-4 Hydrophobic Fe/free base porphyrin dimer syntheses

Purifications were generally achieved by a first recrystallization from DCM/MeOH, followed by column chromatography and a second recrystallization of the fractions which contained the desired product. The main characterization tool was MALDI spectrometry, which was used for identification of the fractions, always providing the right mass and patterns for M^+, MH^+ or $(M\text{-}Cl)^+$ ions; high resolution FAB mass spectra were then obtained. An estimate of the purity of the porphyrin products was achieved using TLC and MALDI data. In order to reduce the number of species due to different Fe(III) coordination (e.g. μ-(O)-species) and different counter-ions, the solvents used in the purification process were slightly acidified by HCl addition.

The desired Fe/Zn dyads **Fe/Zn-63** and **Fe/Zn-64** were obtained from the just described Fe/free base dimers by standard Zn metallation with $Zn(OAc)_2$ in chloroform at room temperature (Scheme 5-5).

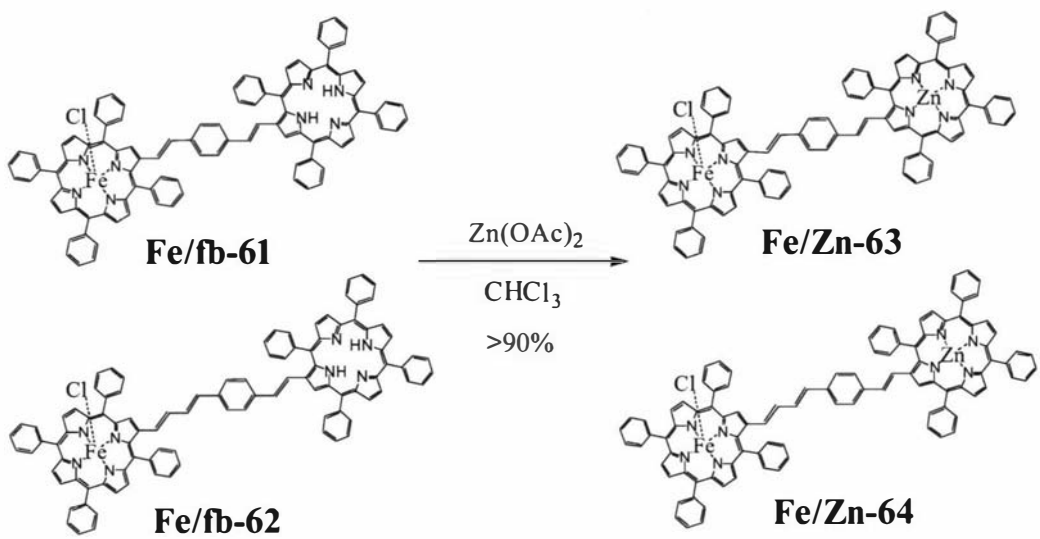

Scheme 5-5 Hydrophobic Fe/Zn porphyrin dimer syntheses

The dyads **Fe/Zn-63** and **Fe/Zn-64** could have also been prepared by reaction of the same Fe phosphonium salts with Zn aldehyde **Zn-14**; the choice to delay the Zn insertion step to the last moment was made to avoid undesired demetallations (Scheme 2-25) and because the isomerization with iodine seems to be less effective with Zn porphyrins. The mild conditions involved in Zn metallations do not cause transmetallation from Fe to Zn porphyrins. In contrast, the treatment of Zn porphyrins

with $FeCl_2$, under our typical conditions for Fe metallations, caused a certain degree of transmetallation (Scheme 5-6).

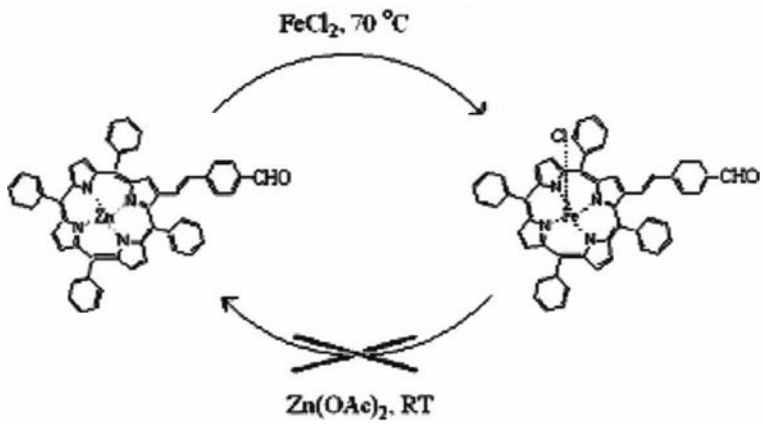

Scheme 5-6 Transmetallation between Zn and Fe porphyrins

One more dimer, **Fe/Zn-65**, with a longer distance between the two porphyrins, was synthesized by Wittig reaction between Fe porphyrin aldehyde **Fe-14** and the already described Zn porphyrin phosphonate **Zn-45** (Scheme 5-7). Because of the use of a phosphonate reagent, no isomerization step was performed in this case, as for similar reactions described in this work.

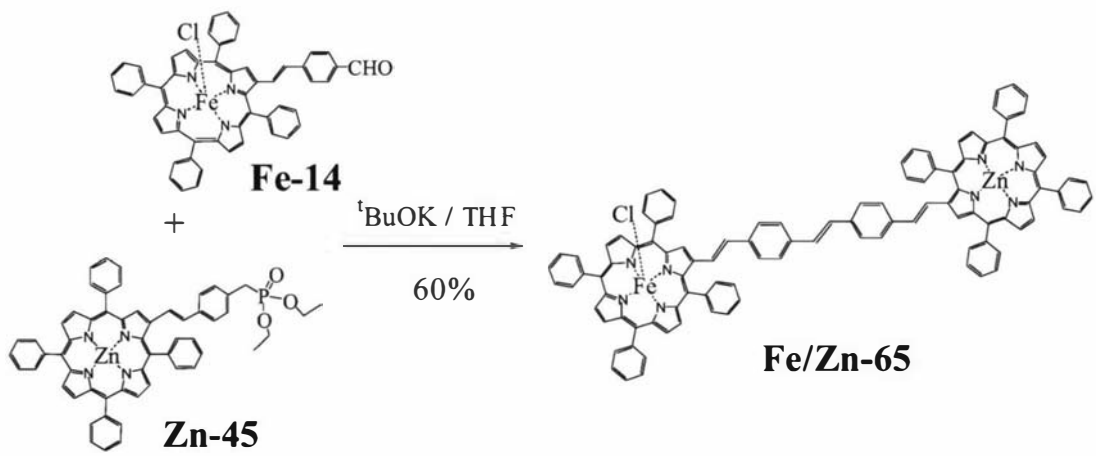

Scheme 5-7 Synthesis of a long chain hydrophobic dimer **Fe/Zn-65**

The purification of these products was carried out by 1-2 recrystallizations from DCM/MeOH. Characterization was again largely carried out by MALDI and HR-FAB mass spectrometry. UV-visible spectrometry was also used but it was not very useful for identification of the species. Spectra were taken using slightly acidified

solvents, so to reduce dimer formations; typical Fe-Cl bands/shoulders were registered in the 355-375 nm region for all the dyads presented in this chapter and very little differences (1-5 nm shifts of the absorptions) were registered both between longer or shorter conjugated bridges and Fe/Zn or Fe/fb dyads. As for the similar Zn/fb dyads described in Chapter 4, the delocalization of the excited states over the conjugated system results in broadening and red-shift of all the absorptions (compared to the single porphyrin units).

5.5. Water soluble porphyrins

In order to investigate the potential of the conjugated porphyrin arrays combined with hydrophilic redox maquettes,[172] the introduction of a hydrophilic porphyrin component was investigated. A number of water soluble porphyrins have already been described in the literature. For our purpose, both acid moieties and ionic groups appeared suitable, therefore three kinds of porphyrins were synthesized according to established procedures and their potential for covalently linked array formation was investigated.

The first possibility was to make derivatives of the tetraarylporphyrins so far described with acid functionalities on the phenyl rings. 5,10,15,20-Tetrakis(4-sulfonatophenyl)porphyrin (TSPP) **66** was prepared by treatment of CuTPP with concentrated sulphuric acid and showed very good solubility in water (Scheme 5-8). The reaction has been described for free base TPP[182] but it worked as well with the Cu derivative, demetallation occurring quantitatively.

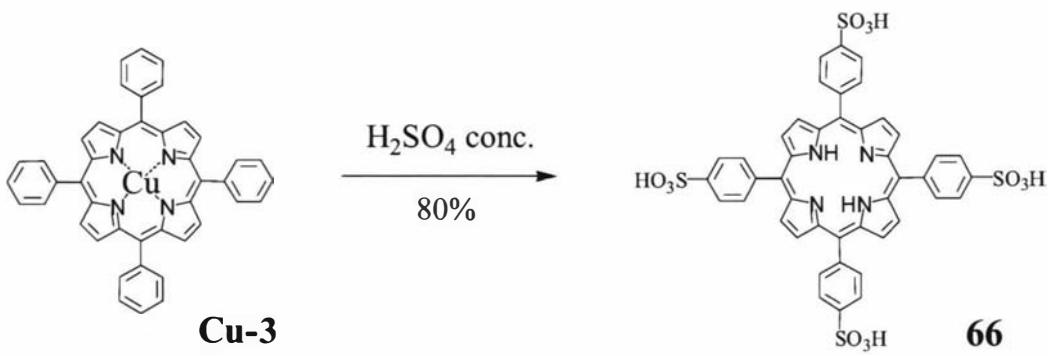

Cu-3 **66**

Scheme 5-8 Synthesis of TSPP **66**

A different approach to water soluble porphyrins was investigated by using TPyPs (tetrapyridylporphyrins). The synthesis of these molecules has already been described[192,193] and was obtained according to literature by condensation (under Adler conditions) of pyrrole with a pyridinecarboxaldehyde. Two isomers, respectively with the pyridine nitrogen in 4-position (**67**) and in 3-position (**68**), were prepared according to Scheme 5-9.

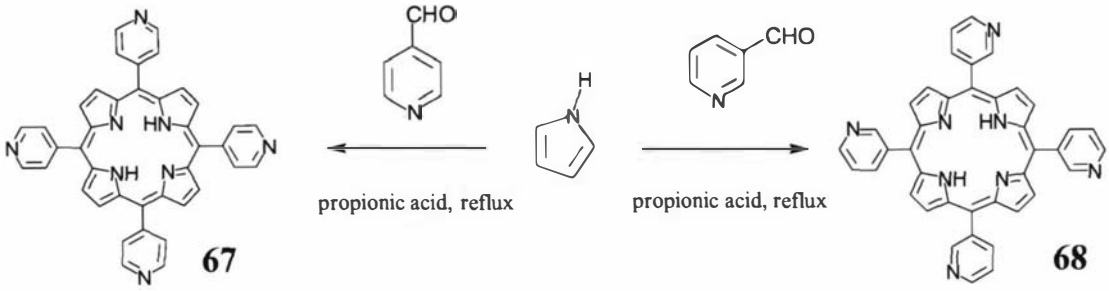

Scheme 5-9 Syntheses T4PyP **67** and T3PyP **68**

Tetrapyridylporphyrins are not soluble in water (except in very acid conditions) but the pyridyl nitrogen can be easily and quantitatively methylated, according to the procedure described by Hambright and Fleischer, to give the tetrapyridinium salts **69** and **70**, to Scheme 5-10.[46] The resulting ionic tetramethylpyridiniumporphyrins (TMPyPs) showed high solubility in water, independent of pH.

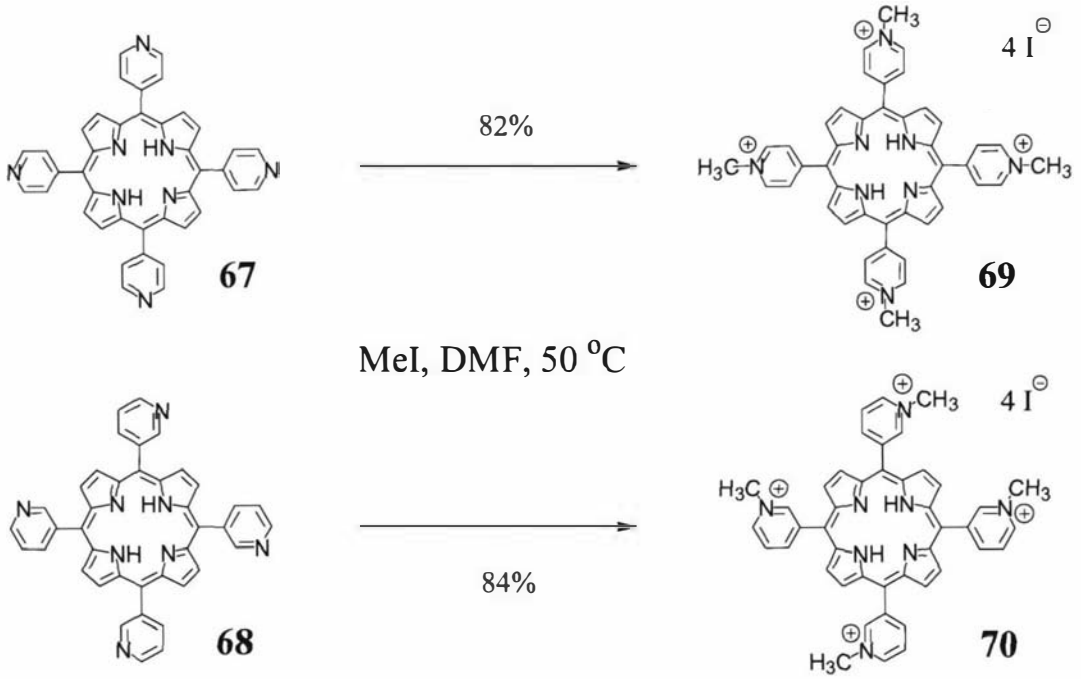

Scheme 5-10 Syntheses of water soluble T4MPyP **69** and T3MPyP **70**

In order to be used for making arrays, these porphyrins have to be functionalized. Given the insolubility of TSPP **66** and TMPyP **69** and **70** in organic solvents and the fact that water was not a suitable solvent for Vilsmeier reactions, the only way to effect the required functionalization was to carry it out before the introduction of the polar moieties (sulphonic acids or methyl pyridynium salts). The first attempts to achieve this involved the treatment of functionalized TPP with sulphuric acid (Scheme 5-11) and only led to decomposition of any porphyrin starting material or product; unfortunately, even employing lower temperatures and less concentrated acid compared to the reaction with TPP itself, no desired product was observed by MALDI and electrospray mass spectrometry.

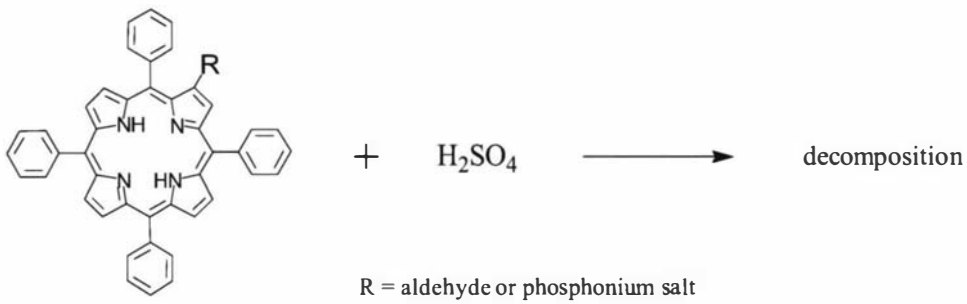

Scheme 5-11 Attempts to insert sulphonic groups in TPP derivatives

The functionalization of TPyP and subsequent methylation seemed a more viable way to pursue. The mild conditions involved in pyridine methylations should not be damaging to either the aldehyde or phosphonium salt/phosphonate groups. Vilsmeier formylation was attempted on both the tetrapyridylporphyrins **Cu-67** and **Cu-68**, after standard Cu metallation, but no aldehyde formation was detected (Scheme 5-12).

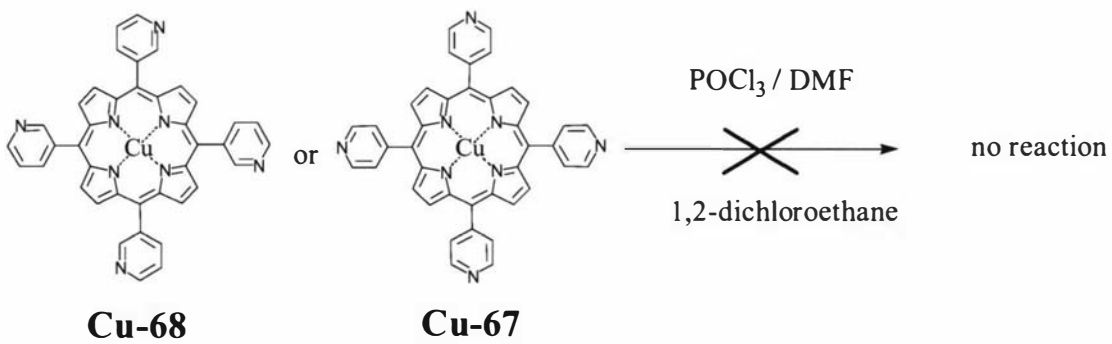

Scheme 5-12 Attempts of Vilsmeier formylation on TPyP **Cu-67** and **Cu-68**

The reason for the low reactivity of these porphyrins lies in the electron-withdrawing effect of the pyridyl groups, which deactivate the porphyrin ring towards electrophilic substitutions. To overcome this problem, two approaches were explored. One option was to activate the porphyrin ring by making the N-oxide of the pyridine substituent. The N-oxide formation is a classic way of activating pyridines towards electrophilic substitution[194] and can be achieved using a variety of oxidants; removal of the oxygen can then be readily achieved by treatment of the N-oxide with PCl_5, $RuCl_3$[195] or by using triphenylphosphine with Re catalysts (Scheme 5-13).[196]

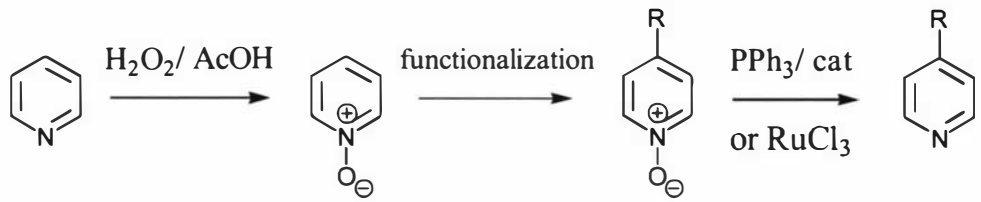

Scheme 5-13 Reversible activation of pyridines by N-oxide formation

Both the TPyP **67** and **68** were treated with H_2O_2 in acetic acid producing the same result; after 1-2 hours the colour of the solutions became less intense as solid started to precipitate. This solid, possibly the desired product or a mixture of partially N-oxidized pyridylporphyrins, turned out to be practically insoluble in any solvent, making characterization impossible and preventing further use in any of the required reactions.

The second idea for introducing an aldehyde group was to proceed through reactions that did not involve electrophilic substitutions. Radical bromination of porphyrins is a well known reaction[197] and, though difficult to control (polybrominated products always occur), it would allow functional group modifications to the desired aldehyde. Attempts involving both **67** and **Zn-67** are shown in Scheme 5-14. Formation of mono-, bis- and tris-brominated products was detected by MALDI spectrometry but this mixture proved difficult to separate (e.g. by column chromatography).

Scheme 5-14 Bromination of tetrapyridylporphyrins

Even though the products were not isolated, the reactivity of the variously brominated porphyrin mixtures was investigated. Okano *et al.*[198] showed that aldehyde formation can be obtained by CO insertion in aromatic bromides in presence of formate and Pd catalysts. Scheme 5-15 shows an attempt to react the brominated mixture **71** under these conditions; after 18 hours of CO bubbling, no product formation was detected by either TLC or MALDI spectrometry.

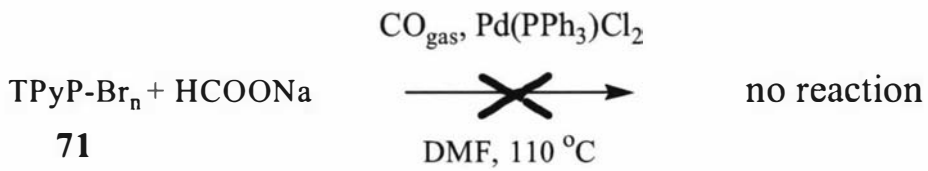

Scheme 5-15 Attempt of CO insertion in **71**

The last formylation reaction to be investigated was the attempted lithiation of the bromoporphyrin mixture followed by DMF addition; the use of this method in porphyrin chemistry has been reported, although not in the same positions.[199,200] Unfortunately, treatment of both polybrominated mixtures **67** and **Zn-67** with BuLi resulted in debromination (Scheme 5-16).

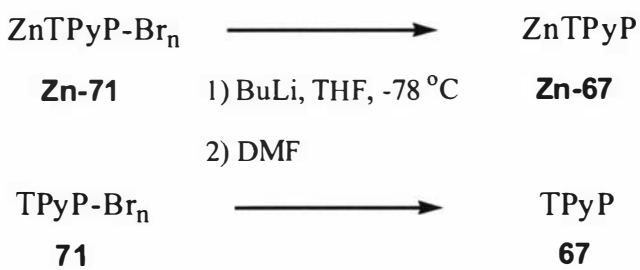

Scheme 5-16 Attempts to introduce formyl groups in **71** and **Zn-71**

The pursuit of water soluble functionalized porphyrins via pyridine/methyl pyridinium groups was abandoned at this point, partly because of the disappointment of the just described attempts but mostly because of constant solubility problems involved with the presence of pyridines, especially when Zn porphyrins were used (aggregation by Zn/pyridine coordination occurs).

An alternative option was represented by the use of carboxylic acids as the water solubilizing polar/ionic groups. The utilization of this route was initially rejected

because it was anticipated that the planned arrays would only be soluble at basic pH. Dr. W.M. Campbell, in the course of his Ph.D. thesis[63] in our laboratories, synthesized and functionalized the tetra(carboxymethyl)phenylporphyrin T3(M)EPP **76** as shown in Scheme 5-17. Interestingly, he also established that the equivalent porphyrin carrying the carboxylic groups in the para positions is not reactive towards Vilsmeier formylation. The synthesis of the precursor aldehydes **74** and **75** was also required and was performed according to the procedure optimized in our lab by Dr. S. Gambhir.

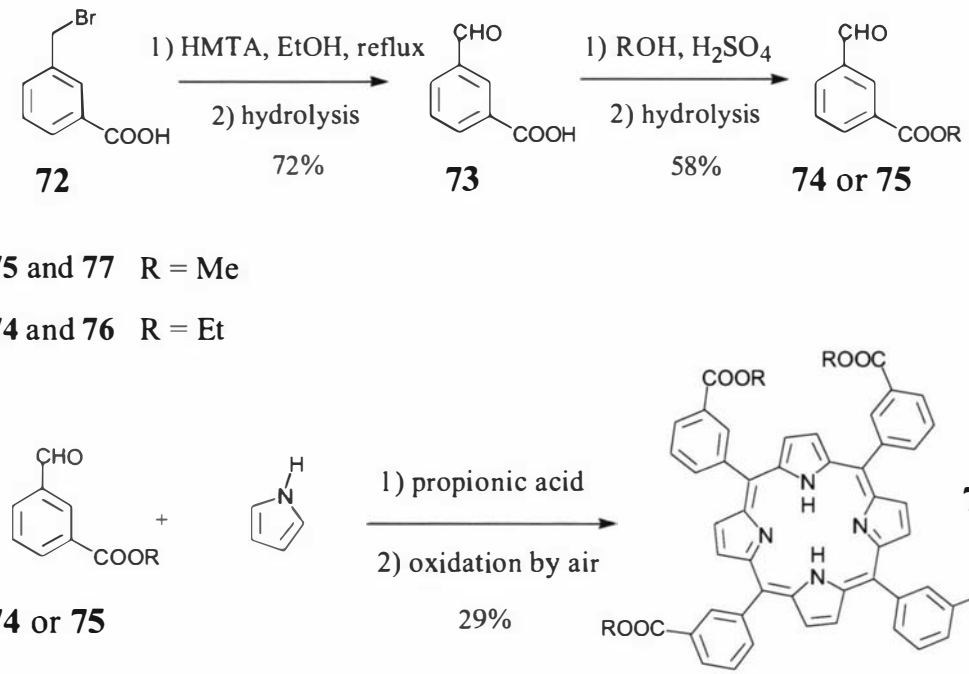

Scheme 5-17 Synthesis of T3(R)EPP **76** and **77**

The homologue porphyrin and derivatives carrying ethyl groups (T3(E)EPP) in place of methyl ones (T3(M)EPP) were synthesized, according to the same procedures, in our laboratory by A. Stephenson. During the course of this thesis, the carboxymethyl porphyrins were prepared by the author, while the carboxyethyl basic blocks **76** and **79** were prepared by A. Stephenson. The use of methyl or ethyl groups depended only on the most available material and did not result in any notable difference at any step in the course of this work. Functionalizations to provide aldehydes **76** and phosphonium salts **79** (Scheme 5-18) were performed according to the same procedures established in these laboratories for tetraarylporphrins and described in Chapter 2.

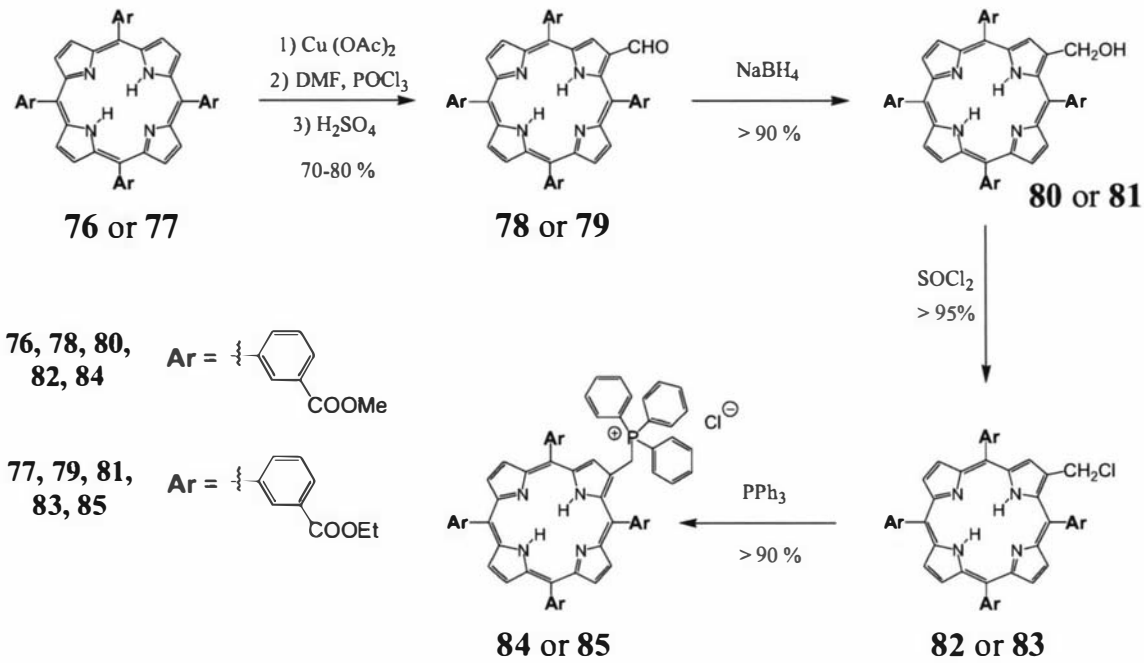

Scheme 5-18 Syntheses of T3EPP aldehyde and phosphonium salt

The resulting functionalized carboxyesterporphyrins can be dissolved in most organic solvents and used for array syntheses through Wittig chemistry under the same conditions described in previous chapters. Once the desired array was made, hydrophilicity could be achieved by the quantitative hydrolysis of the ester groups to acids. Dr. Campbell[63] had previously optimized the basic catalyzed hydrolysis for these substrates and this procedure was used for all similar reactions in the course of this thesis (Scheme 5-19).

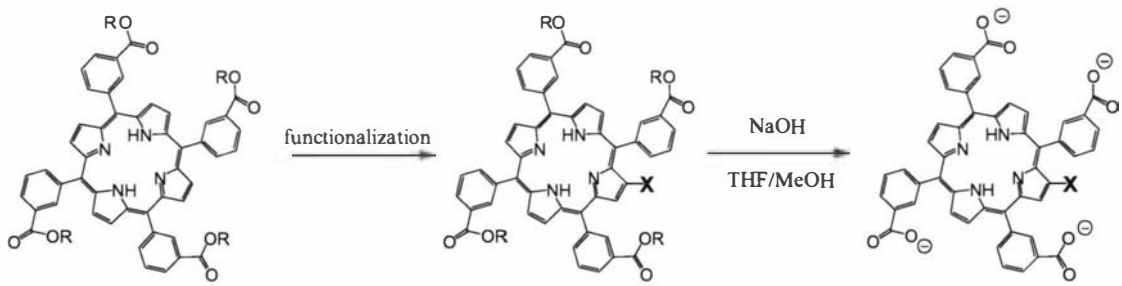

Scheme 5-19 Syntheses of functionalized hydrophilic porphyrins

5.6. Water soluble porphyrin dyads

Even though the purpose of this research is to make water soluble arrays, in order to obtain binding inside the protein we needed to 'localize' the hydrophilic component of the array at a good distance from the binding porphyrin. The reason is that hydrophilic (HP) type maquettes have a hydrophobic core and an external surface which is negatively charged. Our ideal target array required a binding hydrophobic porphyrin and a hydrophilic antenna separated by a conjugated bridge long enough to both reduce the electronic repulsion with the protein surface and allow electronic communication between the antenna and the binding porphyrin.

TPP may well be used as the hydrophobic component although early binding investigations in Professor Les Dutton's laboratory, University of Pennsylvania, showed lower binding constants than hemes. This can be attributed to the steric hindrance of the meso phenyl groups, therefore we explored the synthesis of unhindered functionalized porphyrins. The literature is particularly poor about the syntheses of such systems, which usually require long and low-yielding multi-step preparations. The only method for a simple synthesis of monosubstituted porphyrins has been described by Wiehe *et al.*[86] and was shown in Scheme 2-8a. By this route it should be possible to obtain, in one step, the synthesis of a monosubstituted porphyrin aldehyde (Scheme 5-20).

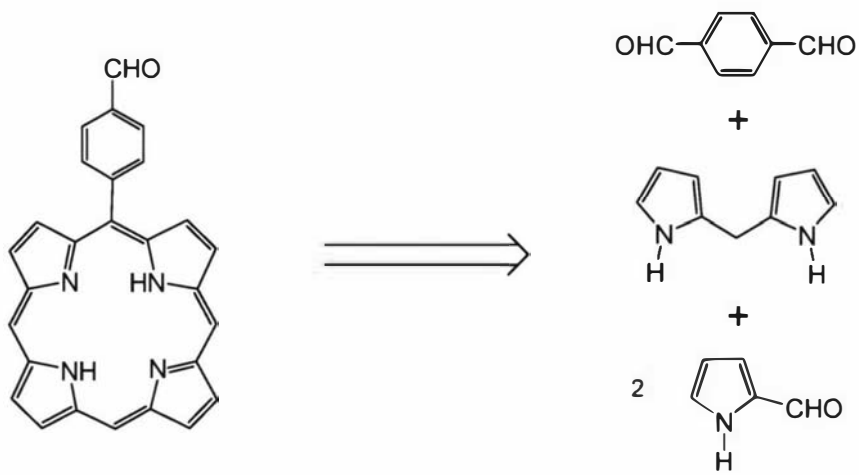

Scheme 5-20 Retrosynthetic scheme for monosubstituted porphyrin preparation according to the procedure described by Wiehe *et al.*[86]

Because of the expected low yield due to the statistical mixture of products obtained from this mixed condensation, a major improvement could be achieved by protecting one of the two aldehyde group of the terephthalaldehyde **13**. The preparation of the monoprotected dialdehyde **87** has already been described many times in the literature and in the course of this work it was achieved by way of a method developed by Dr P. Wagner in our laboratories (Scheme 5-21).

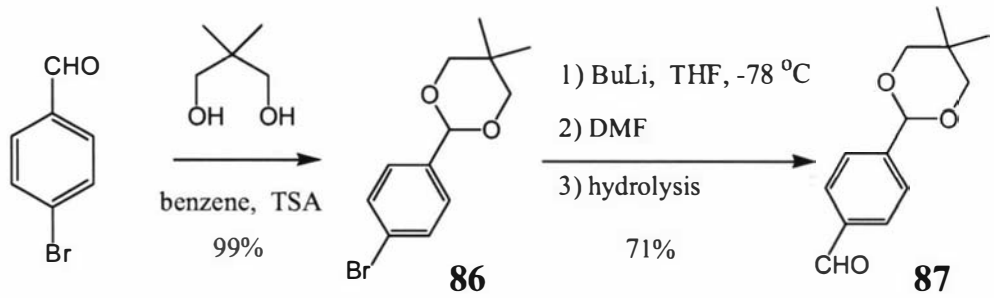

Scheme 5-21 Preparation of the monoprotected terephthalaldehyde **87**

The unsubstituted dipyrrylmethane **89** was also prepared by the author. Many synthetic approaches to **89** have already been published and, in the course of this work, the preparation of **89** was successfully obtained using two different methods (Scheme 5-22). The best yield was obtained via dipyrrylthione **90**, as described by Brückner *et al.*,[201,202] however, the alternative synthesis by Lin *et al.* was faster and did not require the use of toxic reagents (e.g. $CSCl_2$).[203] Both procedures were slightly modified but not optimized.

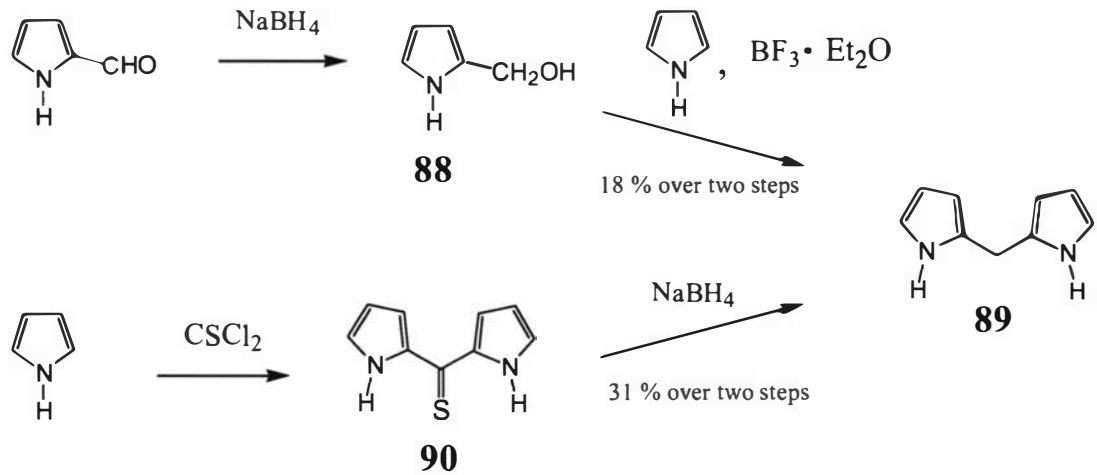

Scheme 5-22 Syntheses of dipyrrylmethane **89** by Lin *et al.*(via alcohol)[203] and Brückner *et al.* (via thione)[201]

The synthesis of the novel monoacetalporphyrin (MAP) **91** was achieved by mixed condensation with some modifications to the one step method described by Wiehe *et al.*[86] As implied by this kind of reaction, a small variation in catalyst nature and concentration, reaction time and temperature, and order of the reagent addition can all have a great influence on the statistical distribution of the products. First attempts showed that around 15% of the starting material produced porphyrins, usually as a mixture of 4-6 species with the desired monosubstituted porphyrin in the order of 2-3%. The major product was the para-diacetalporphyrin **92** and, interestingly, the unexpected porphine **93**, whose designed preparation is challenging, was also produced, although in less than 1%. The Lindsey group has closely investigated the nature and reactivity of the intermediates involved in this kind of porphyrin preparation.[84] By taking their findings into consideration, it was possible to slightly modify this procedure to maximize the production of the desired porphyrin. Scheme 5-23 shows that, by using a slight deficiency of monoprotected dialdehyde **87** and by delaying its addition, the yield of the desired porphyrin **91** was increased to 8.2%.

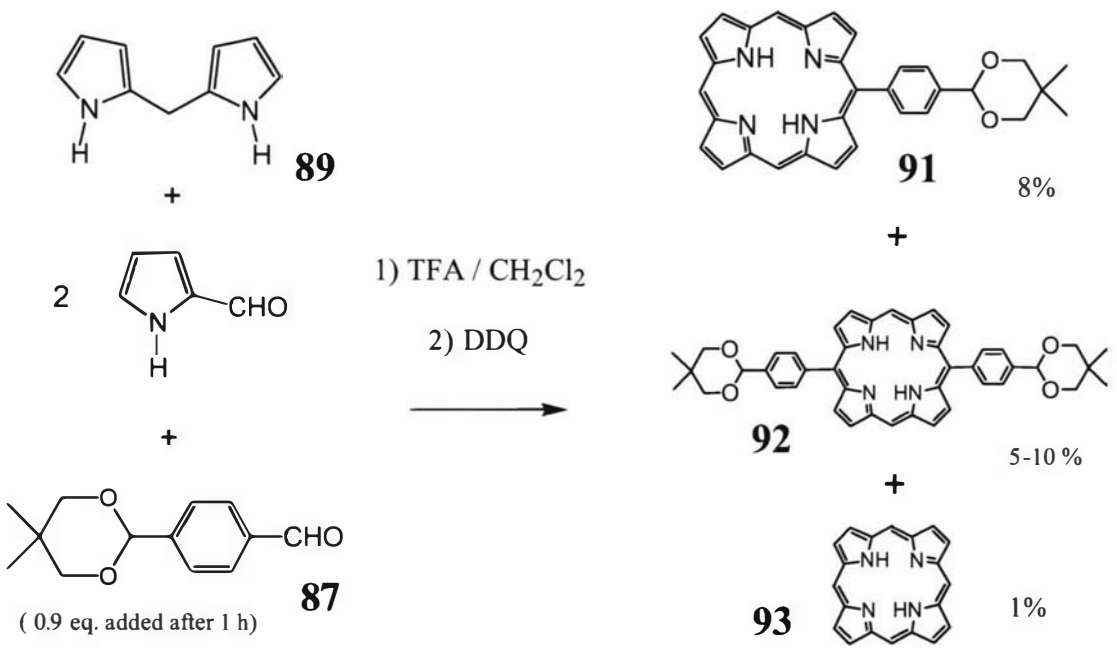

Scheme 5-23 Synthesis of MAP **91**

The desired MAP **91** was easily separated by chromatography and characterized by MALDI and HR-FAB mass spectrometry and ^{1}H-NMR spectrometry. The ^{1}H-NMR spectrum (Figure 5-6) shows two separate singlets for the three porphyrin meso protons (**a** and **b**), while the β-pyrrolic protons (**c**) produce a multiplet (4 protons) and

two doublets (2 + 2 protons), which are shifted by the presence of the aryl substituent; the aryl group (**d**) gives the two expected doublets (2 + 2 protons, J = 8 Hz) and the *N*-pyrrolic protons form the typical broad singlet at negative fields (**h**). The acetyl group produce a more complicated pattern due to the non-equivalent position of the protons of the CH_2 and CH_3 groups respect to the ring current from the aryl and the porphyrin ring-currents. In particular, the methyl groups (**g**) originate two well separated (> 0.5 ppm) singlets and the two CH_2 (**f**) result in two doublets.

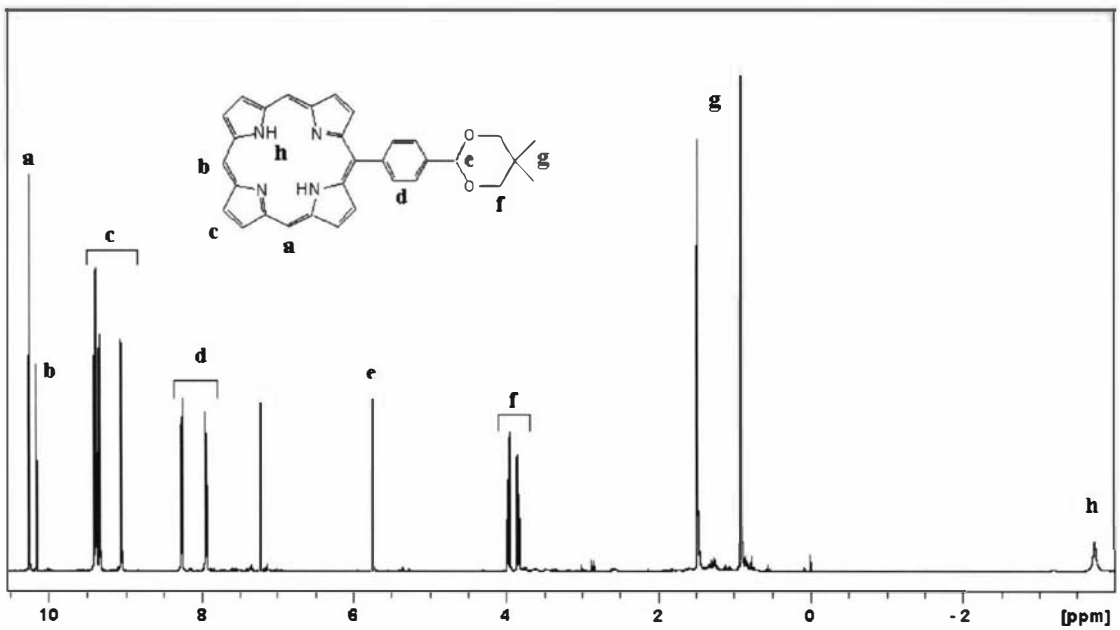

Figure 5-6 ^{1}H-NMR spectrum of MAP **91**

The free aldehyde monobenzylporphyrin (MBP) **94** was obtained by deprotection with TFA (Scheme 5-24). Iron insertion was successfully performed according to the same procedure described for TPP derivatives.

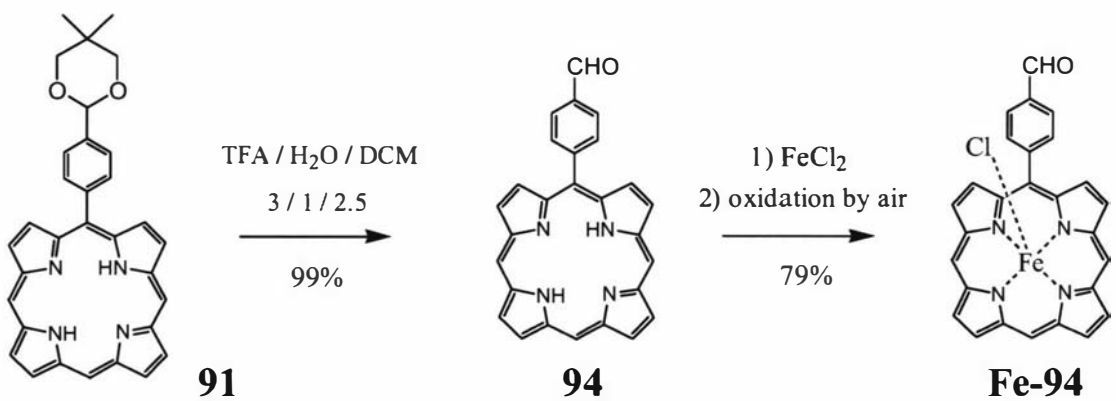

Scheme 5-24 Synthesis and Fe metallation of MBP **94**

As discussed previously, the paramagnetism of iron (III) makes it difficult to characterize the products; as a consequence, first attempts to make water soluble arrays involved the use of free-base porphyrins in place of the Fe(III) homologues. MBP **94** and TEPP-ps **76** were reacted in our standard Wittig conditions for phosphonium salts to give the dimer **95**. Hydrolysis of this product afforded an array which showed good water solubility at pH > 8.5 (Scheme 5-25).

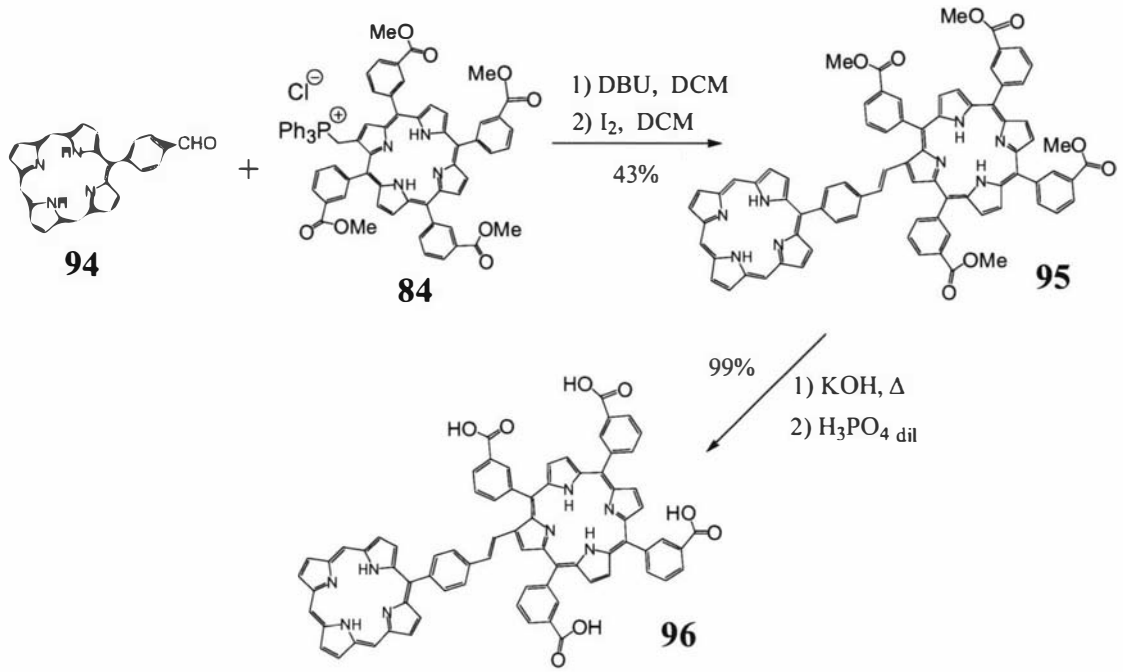

Scheme 5-25 Synthesis of water-soluble fb/fb porphyrin dimer **96**

The use of Zn porphyrin phosphonium salt in Wittig reaction has not been investigated therefore the same Wittig reaction utilized for the making of **96** was repeated using **Zn-84** in place of the free base homologue **84** (Scheme 5-26).

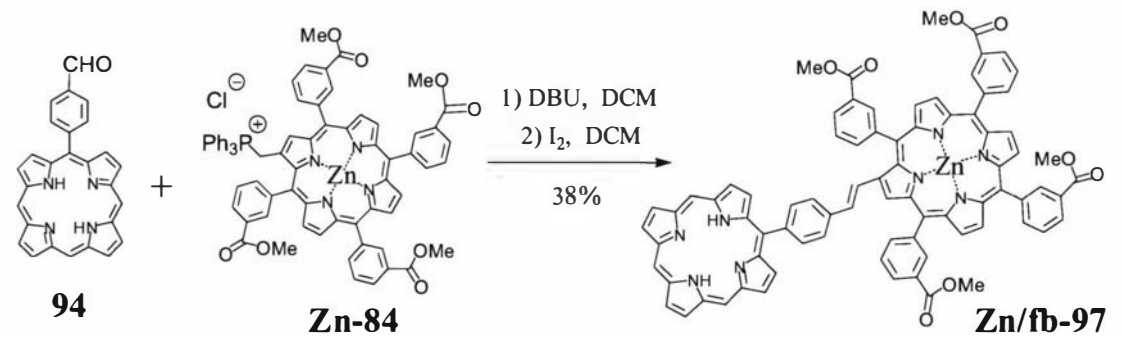

Scheme 5-26 Synthesis of water-soluble porphyrin dimer **Zn/fb-97**

The lower yield obtained in the case of the Zn equivalent has to be attributed to the higher tendency to hydrolysis of the metallated phosphonium salt (ZnTPP-CH_3 was the major product, as identified by MALDI).

The purification of the water soluble porphyrin arrays **96** and **Zn/fb-97** was achieved by ion-exchange flash column chromatography, using Source 15Q cationic resin. Products were dissolved in basic water and immobilized on the resin; separation and elution were obtained using water/methanol and methanol/HCl gradients.

The use of free-base porphyrins allowed the characterization of these arrays by ^{1}H-NMR spectroscopy. Figure 5-7 shows the spectrum of the mixed array **Zn/fb-97**. Groups of signals originating from protons in meso-porphyrin positions (**a**), β-pyrrolic positions (**b**), Zn porphyrin aryl positions (**c**), the phenylene bridge (**d**), carboxy-methyl groups (**e**) and *N*-pyrrolic position (**f**) are well recognizable and defined. The use of COSY spectrometry provided full assignment of the peaks. Unfortunately, NMR spectra of the water soluble porphyrins in D_2O and d^6-DMSO were not resolved as well as the spectra of their hydrophobic precursor.

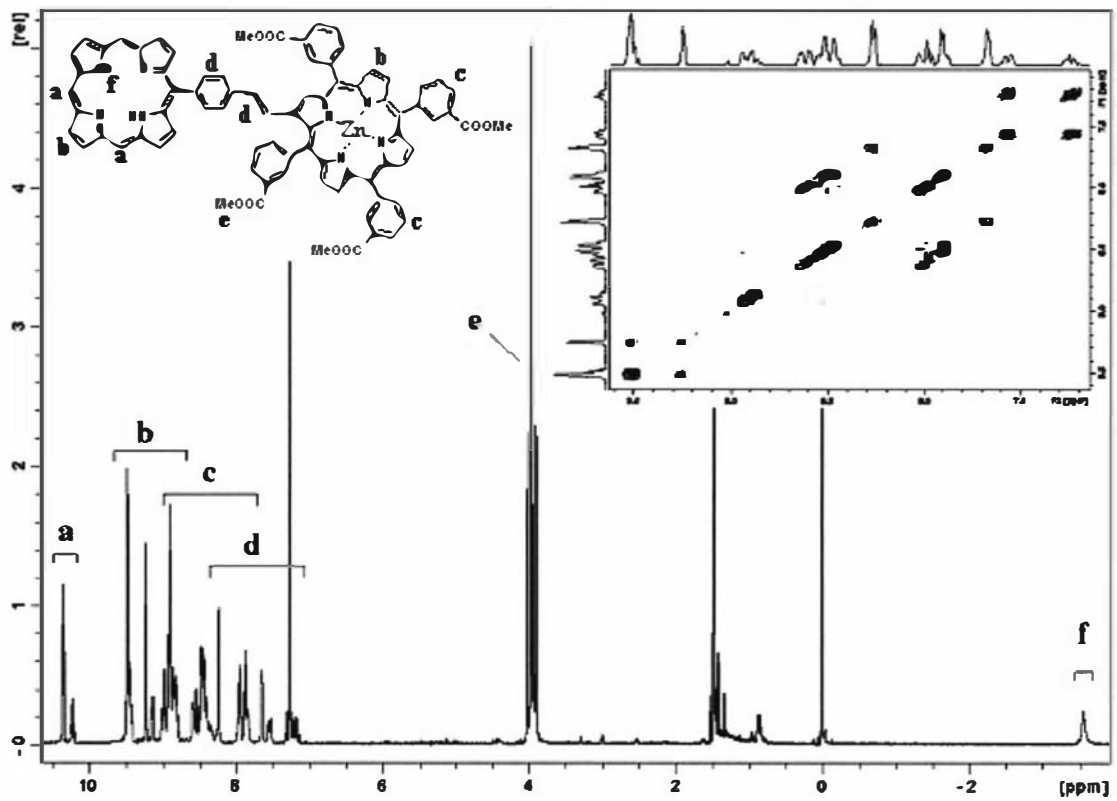

Figure 5-7 ^{1}H-NMR spectra of **Zn/fb-97**

5.7. Water soluble Fe/Zn dyads

Once it was established that all the porphyrin Wittig reagents were suitable for generating porphyrin arrays, the first Fe/Zn water soluble dyad was prepared from **Fe-94** and **Zn-84** according to Scheme 5-27.

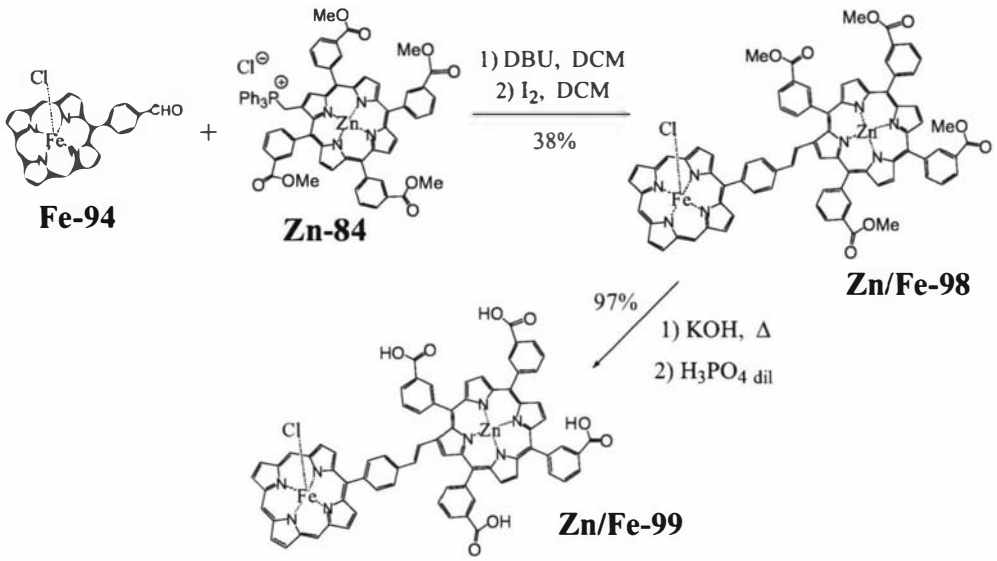

Scheme 5-27 Synthesis of water-soluble Zn/Fe(III) porphyrin dimer **Zn/Fe-99**

In order to study the effects of the distance between the binding Fe porphyrin and the Zn porphyrin antenna on the binding and the electronic communication properties, the preparation of two similar dyads, characterized by longer but similarly conjugated bridges, was carried out. The first step was the preparation of the TEPP equivalent of aldehyde **Zn-14**; TEPP phosphonium salt **85** was reacted with dialdehyde **13** and metallated with Zn (according to the standard procedures) to provide the porphyrin aldehyde **Zn-100,** as shown in Scheme 5-28.

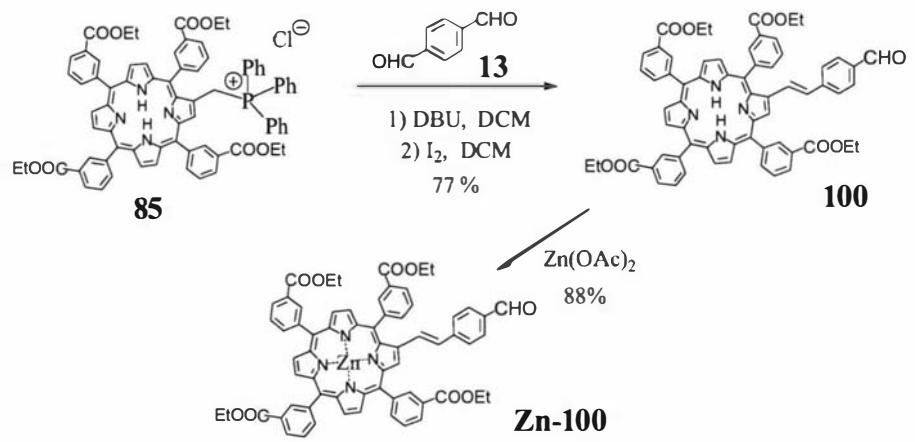

Scheme 5-28 Synthesis of porphyrin aldehyde **Zn-100**

The reaction of aldehydes **Zn-79** and **Zn-100** with excess diphosphonate **44** led to the novel porphyrin phosphonates **Zn-101** and **Zn-102** (Scheme 5-29).

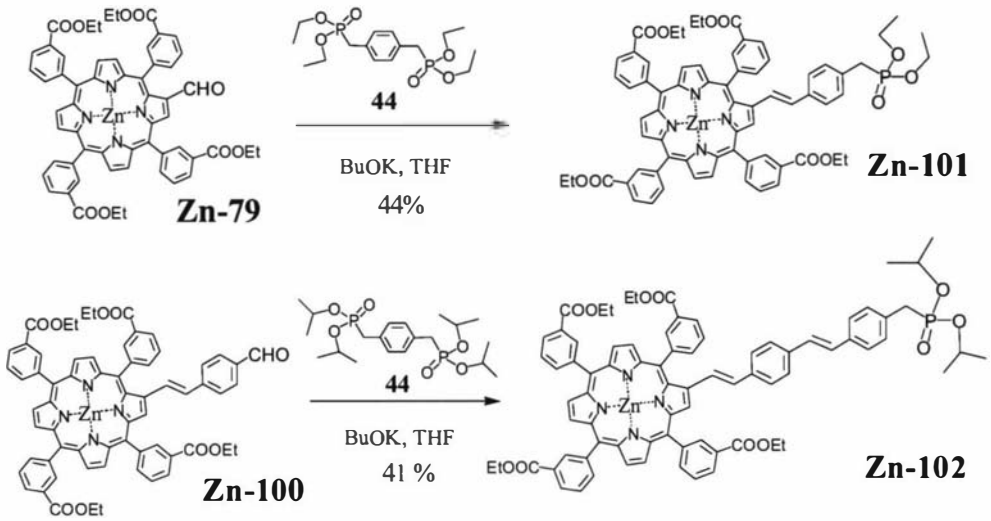

Scheme 5-29 Syntheses of Zn porphyrin phosphonates **Zn-101** and **Zn-102**

Phosphonate **Zn-101** and **Zn-102** were then employed in Horner-Emmons reactions with FeMBP **Fe-94** to give the dimers **Fe/Zn-103** and **Fe/Zn-104** (Scheme 5-30).

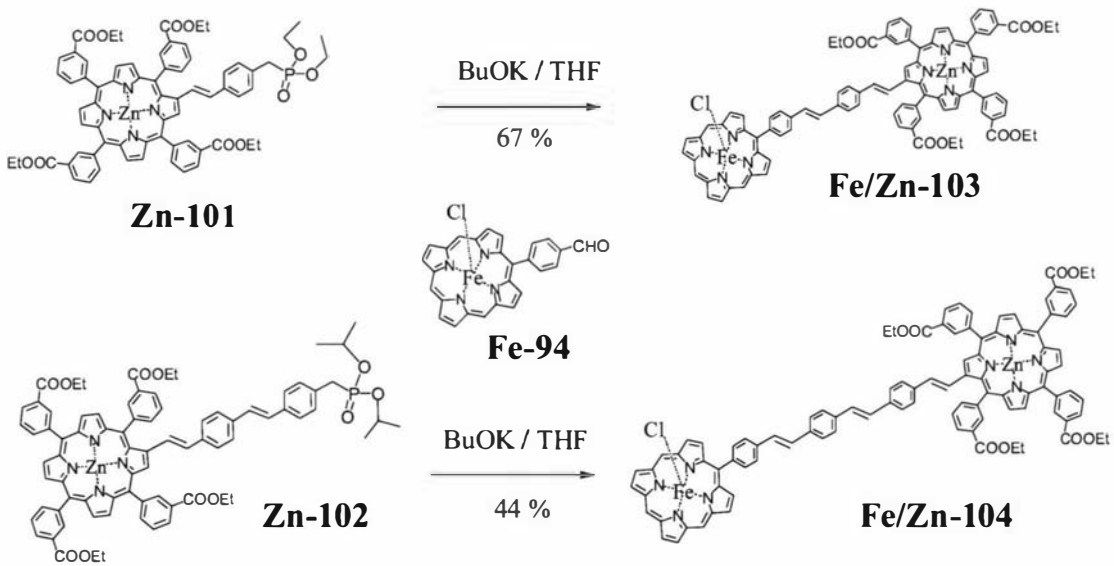

Scheme 5-30 Synthesis of long chain Zn/Fe(III) porphyrin dimers

Hydrolysis of these Fe/Zn dimers, performed according to the same base-catalyzed procedure described in the previous section, provided the two novel water soluble arrays **Fe/Zn-105** and **Fe/Zn-106** (Scheme 5-31).

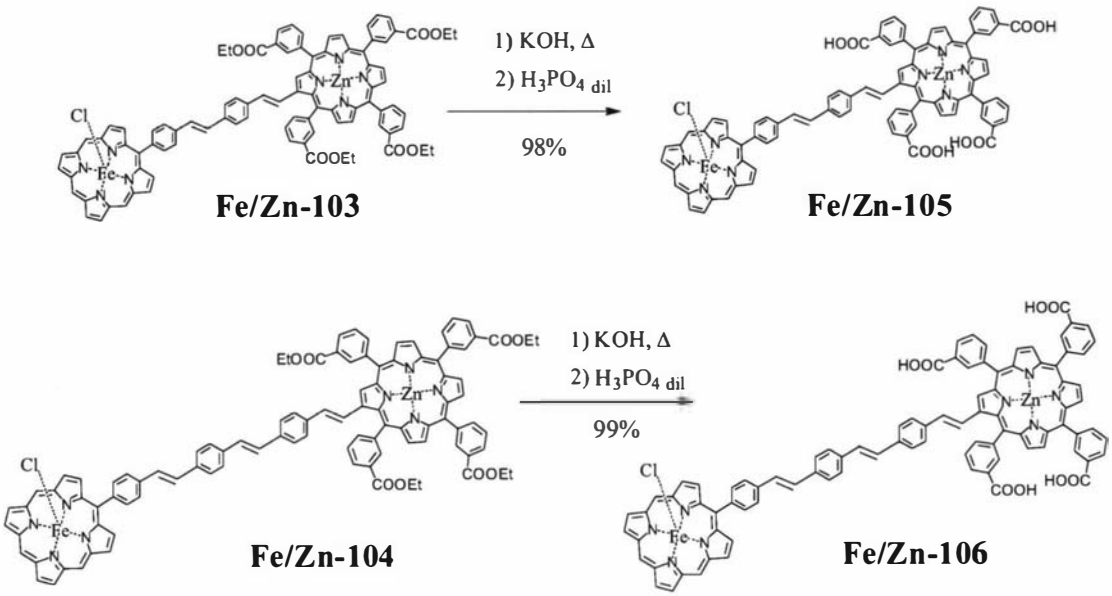

Scheme 5-31 Synthesis of long chain hydrophilic Zn/Fe(III) porphyrin dimers

Finally, in order to both establish if steric hindrance plays a major role in maquette binding and to examine the effect of the breakage of conjugation due to the use of MBP **94**, a similar dyad in which the iron porphyrin is a TPP was prepared from phosphonium salt **Fe-11** and aldehyde **Zn-100** (Scheme 5-32). The reactions were performed according to the standard procedures described for the other Fe/Zn dimers in this chapter, as was the characterization.

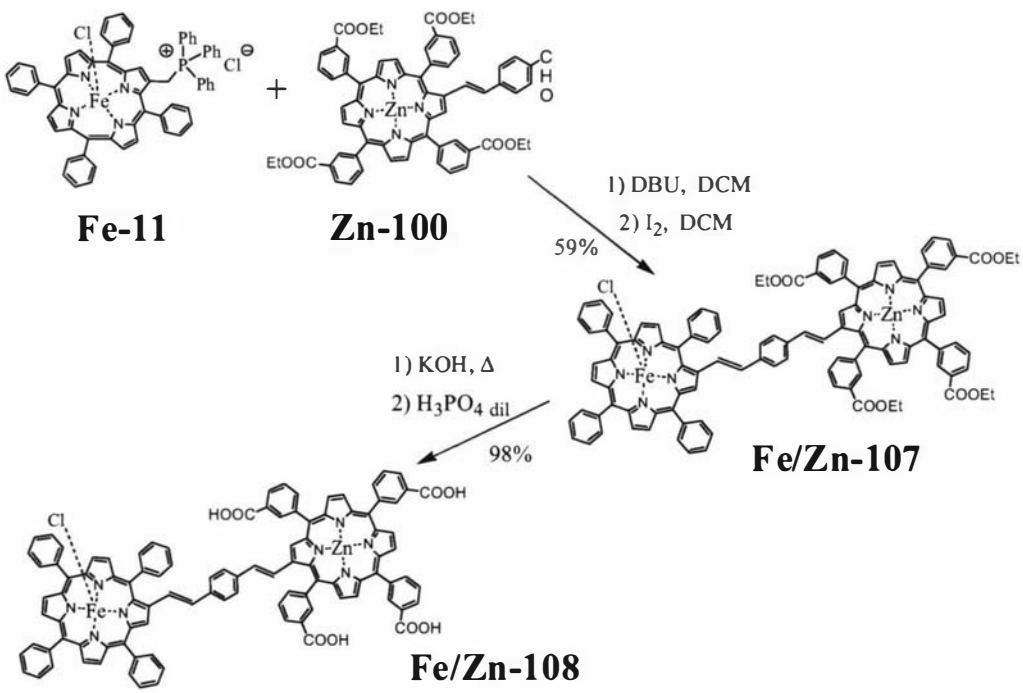

Scheme 5-32 Synthesis of TPP containing water-soluble dyad **Fe/Zn-108**

5.8. Fe(III) porphyrin array characterizations

The characterization of arrays containing paramagnetic Fe porphyrins is not straightforward. As introduced in the previous sections about hydrophobic Fe/Zn porphyrins, the most powerful and fast technique is without any doubt MALDI mass spectrometry. All compounds described in this section produced the ion corresponding to the loss of the chloride $(M\text{-}Cl)^+$. Moreover, by controlling the power of the laser source, it is generally possible to detect the μ-(O)-dimer species. Occasionally, ions like $(M)^+$ or $(M\text{-}Cl+O_2)^+$ have been also found, always with a lower intensity compared to $(M\text{-}Cl)^+$. HR-FAB spectra were obtained for all the compounds, except for **Fe/Zn-106**, which contains the longest linker among the water-soluble arrays; in all cases, the spectra of the hydrophobic ester homologues were better resolved and accurate than the spectra of the water-soluble acid derivatives, because of the difficulties to find proper solvents/matrix for the ionization of those samples under HR-FAB conditions.

UV-visible absorption spectra of the series of Fe/Zn dyads were not very useful, being almost identical. Only small shifts (1-5 nm) were registered passing from one member of a series to another. Furthermore, there was no clear trend in the shifts, although the increasing length of the conjugated linker always resulted in the increasing broadening of the bands. It is possible that the collected spectra were the result of absorption of more species (monomer, μ-(O)-dimer, other oxo-ligands, counter-ions other than Cl), making interpretation of the data difficult. However, UV-visible spectroscopy is a good tool for detecting changes in the coordination of the metal centre and was utilized for the initial maquette/porphyrin binding investigations (section 5.9).

Electrochemistry techniques have proved popular for Fe porphyrin characterization.[185,187,189] However, while they allow the discrimination of the differently coordinated Fe centre, they do not help to identify other parts of the molecule, such as the porphyrin substituents. Moreover, great care has to be taken in such experiments in order to avoid the simultaneous presence of different Fe-O species; reproducibility of the data requires the complete absence of O_2 traces and, for

hydrophobic porphyrins and arrays, complete absence of water dissolved in the solvents. Slightly acidic solvents were also employed, as for UV-visible absorption experiments, in order to move the μ-(O)-dimer equilibrium towards the monomeric form (Scheme 5.2). Our first attempts to employ electrochemical techniques were not particularly successful. Characteristic half-wave potentials for the first reduction of the Fe(III) centre (-0.3 V for Fe-Cl monomers, -0.55 V for μ-(O)-dimers)[187] were obtained for most of the samples but the cyclic voltammograms were ill defined and varied from cycle to cycle, particularly under acidic/monomeric conditions where reductions appear to be less reversible; in addition, reductive waves characteristic of μ-(O)-dimers usually appeared after a few scans.

5.9. Preliminary investigation into porphyrin/maquette binding

Early porphyrin/maquette binding investigations have been realized, producing some interesting information as well as some problems. Titrations have been followed by UV-visible spectroscopy and the interpretation of the data is not straightforward because of the difficulty in the identification of characteristic absorption of all the species involved. Binding constants in the order of 10^7-10^8 M^{-1} have been obtained for the first binding, both with water soluble porphyrin/maquettes and with hydrophobic systems (methanol was used as solvent). Much lower constants have been supposed for the second binding (maquettes typically have two equivalent binding sites), probably because of a structural reorganization involved with the first porphyrin binding. The use of the unhindered porphyrin **Fe-94** as binding porphyrin seems to increase the binding constant by a factor two. These values are similar to what has been previously determined for maquettes binding single porphyrins like hemes.[173,176]

5.10. Conclusions

The work presented in this chapter is part of a project towards the development of new artificial photosynthetic systems, in which porphyrin arrays would be used as

light harvesters bound to proteins that are able to efficiently utilize the energy from the photoexcitation. Porphyrin dyads composed of Fe(III) and Zn porphyrin were designed and prepared in order to obtain efficient electron transfer from the Zn porphyrin to the Fe porphyrin, which can bind into the protein. Two series of dimers were synthesized in order to obtain incorporation in both the classes of hydrophobic and hydrophilic proteins; these two series were composed of porphyrins connected by linkers of various lengths, so as to determine the influence of the bridge on the binding and the photophysical properties. TPPs were used for the making of the hydrophobic dyads while hydrophilicity was achieved by employing tetraester porphyrin derivatives, which were quantitatively hydrolyzed to afford the correspondent water soluble acids. A new monosubstituted porphyrin (**94**) was also synthesized and incorporated in the arrays to minimize steric hindrance inside the protein binding sites. First porphyrin dyads/protein binding investigations indicated that incorporation is always achieved with similar binding constant ($K = 10^7$-$10^8\ M^{-1}$) with little dependence from the distance between the two porphyrins; the use of an unhindered Fe(III) porphyrin seems to improve the binding abilities.

5.11. Experimental procedures

General

Commercially available solvents and chemicals were purchased from different sources, as AR grade unless otherwise specified. Solvents for column chromatography (dichloromethane, hexane, methanol and toluene) were distilled lab grade. Water was purified by reverse osmosis. Dry THF and benzene were obtained by passing commercially available argon degassed solvent through an activated alumina column. Ion-exchange chromatography was performed on Source 15Q cationic resin (polystyrene-divinylbenzene, trimethylammonium functionalized).

UV-vis experiments were performed on a Shimadzu UV-3101PC scanning spectrophotometer. In the cases with Fe porphyrins, solvents were slightly acidified with HCl 3M (one drop in 100 mL of solvent) to reduce formation of μ-oxo dimers. High resolution FAB mass spectra were recorded on a VG-70SE instrument at the

University of Auckland and on a VG ZAB 2 SEQ VG-Micromass at the Australian National University. MALDI-TOF mass spectra were carried out by the author and were performed on a Micromass ProteomWorks M@LDI-Reflectron mass spectrometer. ^{1}H-NMR spectrometry experiments were performed using 400 and 500 MHz Bruker Avance instruments running TOPSPIN 1.3 software. Proton chemical shifts in $CDCl_3$ are relative to TMS. Chemical shifts in other solvents are relative to residual protons (tetrahydrofurane-d_8, 3.58 ppm; dioxane-d_8, 3.53 ppm, dichloromethane-d_2, 5.32 ppm, DMSO-d_6, 2.49 ppm). Data are expressed as position (in ppm), multiplicity (s = singlet, d = doublet, t = triplet, q = quartet, m = multiplet, br = broad, app = apparent), relative integral, coupling constant and assignment. Coupling constants were not reported when smaller than 1 Hz.

Precursor syntheses.

Porphyrins aldehydes **M-5** (M = 2H, Zn), **M-14** (M = 2H, Zn), and phosphonium salts **11** and **43** were prepared as previously published by our group.[75,143]

Fe metallations.

All Fe(III) porphyrin monomers were prepared by Fe(II) insertion into the equivalent free-base porphyrin employing a general procedure. Spectroscopic grade acetonitrile was refluxed under argon for two hours to remove dissolved oxygen. Temperature was lowered to 70 °C and 10-20 eq. of $FeCl_2 \cdot 4H_2O$ were added in one portion. The free-base porphyrin was dissolved in a small amount of chloroform and added from a dropping funnel in 5 minutes. The temperature was raised back up and reflux was continued for 3 hours after which heating was turned off and the solution stirred overnight in open air, allowing oxidation to Fe(III) by oxygen. The solution was concentrated and inorganic salts were filtered off. This solution was diluted with DCM and washed many times with 0.1 M HCl to remove the remaining inorganic salts and obtain the Fe-porphyrin in monomeric form. The organic solution was then dried over $CaCl_2$ and the desired Fe(III) porphyrin was purified by chromatography on silica gel employing gradient of DCM/MeOH as solvents. In cases when the high polarity of the product required the use of high percentage of MeOH (e.g. phosphonium salts), a further step was necessary to remove dissolved silica from the chromatography. The solid was dissolved in the minimal amount of DCM and filtered through paper. Yields varied in the 70-90% range.

Fe(III)TPP-CHO, Fe-5.

(2-(5,10,15,20-tetraphenylporphyrinato iron(III))yl)carboxaldehyde chloride.

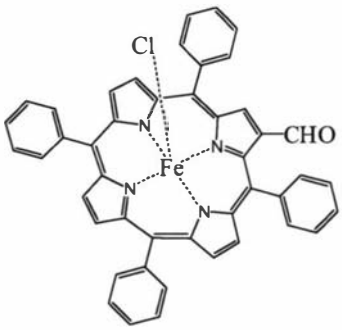

$C_{45}H_{28}ClFeN_4O$
Exact Mass: 731.13
Mol. Wt.: 732.03

50 mg (78 μmol) of TPP-CHO **5** were metallated with 150 mg (761 μmol) of $FeCl_2 \cdot 4H_2O$ according to the described general procedure. The product was isolated through flash chromatography using DCM/methanol = 15/1 as eluent. Yield was 49 mg (86%) of **Fe-5** as purple crystals. UV-vis (CH_3CN): λ_{max} [nm] ($\varepsilon \times 10^{-3}$) 423 (101), 583 (8), 650 (6). FAB-HRMS for $(M\text{-}Cl)^+$ ($C_{45}H_{28}N_4OFe$): 696.1619, calculated: 696.1612.

Fe(III)TPP-Ph-CHO, Fe-14.

4-(2'-(5',10',15',20'-tetraphenylporphyrinato iron(III))yl)benzaldehyde chloride.

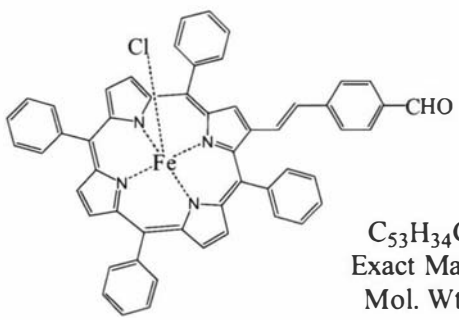

$C_{53}H_{34}ClFeN_4O$
Exact Mass: 833.18
Mol. Wt.: 834.16

75 mg (101 μmol) of porphyrin aldehyde **14** were metallated with 300 mg (1.52 mmol) of $FeCl_2 \cdot 4H_2O$ according to the described general procedure. The product was isolated through flash chromatography using DCM/methanol = 15/1 as eluent. Yield was 76 mg (91%) of **Fe-14** as purple crystals. UV-vis (CH_2Cl_2): λ_{max} [nm] ($\varepsilon \times 10^{-3}$) 372 (sh 22.5), 429 (51), 513 (7.9), 579 (sh 2.9), 686 (1.5). FAB-HRMS for $(M\text{-}Cl)^+$ ($C_{53}H_{34}N_4OFe$): 798.2088, calculated: 798.2082.

Fe(III)TPP-ps, Fe-11.

(2'-(5',10',15',20'-tetraphenylporphyrinato iron(III))yl)methyltriphenylphosphonium bischloride.

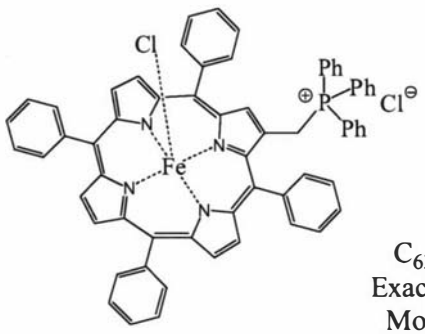

$C_{63}H_{44}Cl_2FeN_4P$
Exact Mass: 1013.20
Mol. Wt.: 1014.77

100 mg (108 μmol) of porphyrin phosphonium salt **11** were metallated with 325 mg (1.65 mmol) of $FeCl_2 \cdot 4H_2O$ according to the described general procedure. The product was isolated through flash chromatography using DCM/methanol = 10/1 as eluent. Yield was 84 mg (77%) of **Fe-11** as purple crystals. UV-vis (CH_2Cl_2): λ_{max} [nm] ($\varepsilon \times 10^{-3}$) 379 (34), 420.5 (79), 513 (8.4), 581 (2.5), 698.5 (1.7). FAB-HRMS for $(M\text{-}Cl)^+$ ($C_{63}H_{44}N_4FeCl$): 978.2357, calculated: 978.2342.

Fe(III)TPP-ext-ps, Fe-43.

(*trans*-2'-(2"-(5",10",15",20"-tetraphenylporphyrinato iron(III))yl)ethen-1'-yl) methyltriphenylphosphonium bischloride.

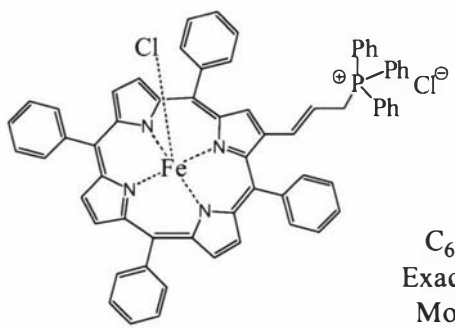

$C_{65}H_{46}Cl_2FeN_4P$
Exact Mass: 1039.22
Mol. Wt.: 1040.81

50 mg (51.4 μmol) of phosphonium salt **43** were metallated with 125 mg (635 mmol) of $FeCl_2 \cdot 4H_2O$ according to the described general procedure. The product was isolated through flash chromatography using DCM/methanol = 10/1 as eluent. Yield was 40 mg (75%) of **Fe-43** as purple crystals. UV-vis (CH_2Cl_2): λ_{max} [nm] ($\varepsilon \times 10^{-3}$) 382.5 (36), 423 (70), 513 (9), 582.5 (3.3), 687 (2). FAB-HRMS for $(M\text{-}Cl)^+$ ($C_{65}H_{46}N_4PFeCl$): 1004.2547, calculated: 1004.2498.

Fe(III)TPP-Ph-TPP, Fe/fb-61.

1-(*trans*-2'-(2"-(5",10",15",20"-tetraphenylporphyrinato iron(III))yl),4-(*trans*-2'-(2"-(5",10",15",20"-tetraphenylporphyrin)yl)ethen-1'-yl)benzene chloride.

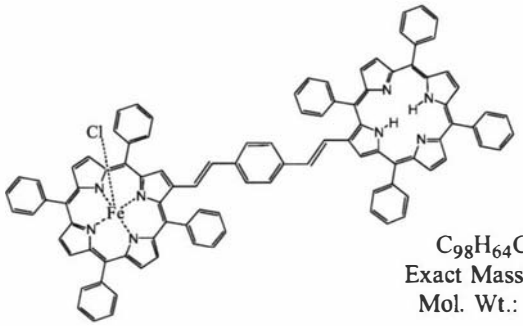

$C_{98}H_{64}ClFeN_8$
Exact Mass: 1443.43
Mol. Wt.: 1444.91

150 mg (201 μmol) of porphyrin aldehyde **14** and 198 mg (195 μmol) of phosphonium salt **Fe-11** were dissolved in 40 mL of chloroform under argon. To the stirred solution, 100 mg of DBU were added and reaction went on for 60 minutes. The solution was washed twice with 0.1M HCl, the organic phase was dried over $MgSO_4$ and brought to dryness. The solid was separated through flash chromatography using DCM/methanol = 33/1 as eluent and the fractions containing the desired **Fe/fb-61** (as characterized by MALDI) were concentrated under vacuum and precipitated by methanol. This product was isomerized to the *trans* form by I_2 treatment. The solid was dissolved in 25 mL of dichloromethane and 50 mg of I_2 were added. After 40 hours the solution was washed three times with a saturated solution of $Na_2S_2O_3$ and water and then precipitated with methanol. The yield was 180 mg (64%) of **Fe/fb-61** as purple crystals. UV-vis (CH_2Cl_2): λ_{max} [nm] (ε x 10^{-3}) 372 (63), 424.5 (sh 116), 447 (149), 627 (14), 678 (26.6). FAB-HRMS for $(M\text{-}Cl)^+$ ($C_{98}H_{64}N_8Fe$): 1408.4646, calculated: 1408.4603.

Fe(III)TPP-Ph-ZnTPP, Fe/Zn-63.

1-(*trans*-2'-(2"-(5",10",15",20"-tetraphenylporphyrinato zinc(II))yl),4-(*trans*-2'-(2"-(5",10",15",20"-tetraphenylporphyrinato iron(III))yl)ethen-1'-yl)benzene chloride.

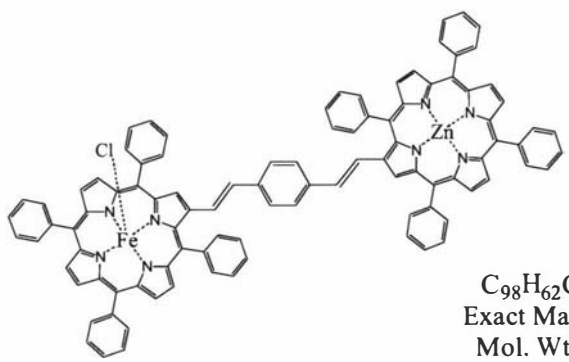

$C_{98}H_{62}ClFeN_8Zn$
Exact Mass: 1505.34
Mol. Wt.: 1508.28

The Fe/Zn dimer **Fe/Zn-63** was obtained by its Zn/free base homologue **Fe/fb-61** by standard Zn metallation (described in Chapter 2). 100 mg (69 μmol) of **Fe/fb-61** were dissolved in chloroform and 18 mg (1.2 equivalents) of $Zn(OAc)_2 \cdot H_2O$, dissolved in the same amount of MeOH/water:10/1, was added. The mixture was stirred for 2 hours and then washed with water and precipitate with MeOH. 97 mg (93%) of solid **Fe/Zn-63** were collected. TLC (silica gel, DCM/MeOH = 50/1) and MALDI showed absence of non-metallated impurities. UV-vis (CH_2Cl_2): λ_{max} [nm] ($\varepsilon \times 10^{-3}$) 373 (55), 424 (sh 113), 445 (163), 509 (sh 31.7), 629.5 (16.6), 679 (sh 26.4). FAB-HRMS for $(M-Cl)^+$ ($C_{98}H_{62}N_8FeZn$): 1470.3728, calculated: 1470.3738.

Fe(III)TPP-ext-Ph-ZnTPP, Fe/Zn-64.

1-(*trans*-2'-(2"-(5",10",15",20"-tetraphenylporphyrinato zinc(II))yl)ethen-1'-yl),4-(*trans-trans*-4'-(2"-(5',10"',15",20"-tetraphenylporphyrinato iron(III))yl)butadien-1'-yl)benzene chloride.

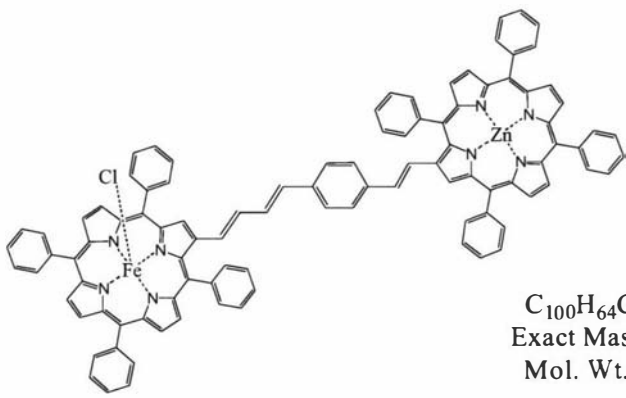

$C_{100}H_{64}ClFeN_8Zn$
Exact Mass: 1531.36
Mol. Wt.: 1534.32

The synthesis of the Fe/Zn dimer **Fe/Zn-64** was obtained by its Zn/free base homologue **Fe/fb-62** by standard Zn metallation, as for **Fe/Zn-63**. 37 mg (49.7 μmol) of porphyrin aldehyde **14** and 60 mg (57.6 μmol) of phosphonium salt **Fe-43** were dissolved in 40 mL of chloroform under argon. To the stirred solution, 25 mg of DBU were added and reaction went on for 60 minutes. The solution was washed twice with 0.1M HCl, the organic phase was dried over $MgSO_4$ and brought to dryness. The solid was separated through flash chromatography using DCM/methanol = 33/1 as eluent. Isomerization to the *trans* isomer was achieved by I_2 treatment; the solid was dissolved in 20 mL of dichloromethane and 50 mg of I_2 were added. After 40 hours the solution was washed three times with a saturated solution of $Na_2S_2O_3$ and water and then precipitated with methanol. Purity of the product **Fe/fb-62** was controlled by TLC (silica gel, DCM/MeOH = 50/1) and MALDI. 50 mg of the Fe/free-base dimer

Fe/fb-62 were metallated with 18 mg of $Zn(OAc)_2 \cdot H_2O$ according the described general procedure affording 51 mg of **Fe/Zn-64**. The yield of the three steps (Wittig, isomerization and metallation) was 38 mg (50%). UV-vis (CH_2Cl_2): λ_{max} [nm] (ε x 10^{-3}) 366 (52.6), 425 (sh 111), 447 (174), 512 (sh 32), 627.5 (17.4), 677.5 (sh 27). FAB-HRMS for $(M\text{-}Cl)^+$ ($C_{100}H_{64}N_8FeZn$): 1496.3880, calculated: 1496.3895.

Fe(III)TPP-Ph-Ph-ZnTPP, Fe/Zn-65.

trans-1-(4'-(*trans*-2"-(2"'-(5"',10"',15"',20"'-tetraphenylporphyrinato zinc(II))yl)ethen-1"-yl)phenyl),2-(4'-(*trans*-2"-(2"'-(5"',10"',15"',20"'-tetraphenylporphyrinato iron(III))yl)ethen-1"-yl)phenyl)ethene chloride.

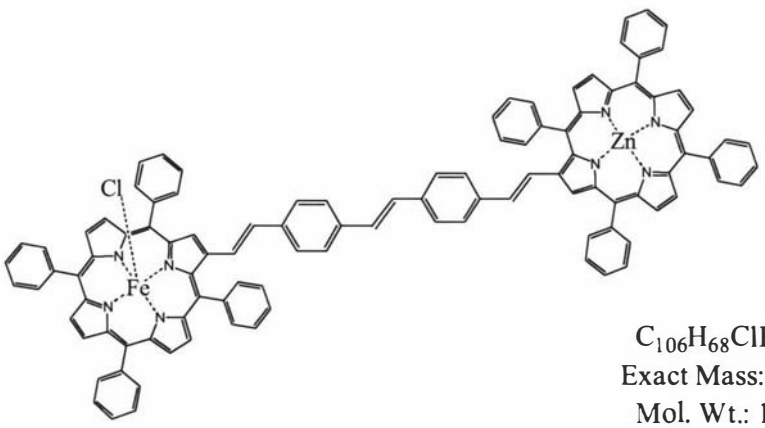

$C_{106}H_{68}ClFeN_8Zn$
Exact Mass: 1607.39
Mol. Wt.: 1610.42

78 mg (93.5 μmol) of aldehyde **Fe-14** and 90 mg (97 μmol) of phosphonate **Zn-45** were dissolved in 50 mL of dry THF, under argon atmosphere. To the stirred solution, 20 mg (178 μmol) of solid ^{t}BuOK were added in two portions over 30 min. After further 15 min, the solution was evaporated to dryness and purified through flash chromatography on silica gel (DCM/MeOH = 50/1). The fractions containing the desired product were collected and recrystallized from DCM/MeOH affording 90 mg (60%) of pure **Fe/Zn-65** as purple crystals. UV-vis (CH_2Cl_2): λ_{max} [nm] (ε x 10^{-3}) 426.5 (154), 558 (19.8), 594.5 (13), 677 (sh 1.9). FAB-HRMS for $(M\text{-}Cl)^+$ ($C_{106}H_{68}N_8FeZn$): 1572.4206, calculated: 1572.4208.

TSPP, 66.

5,10,15,20-tetra(4'-sulphonyl)phenyl porphyrin.

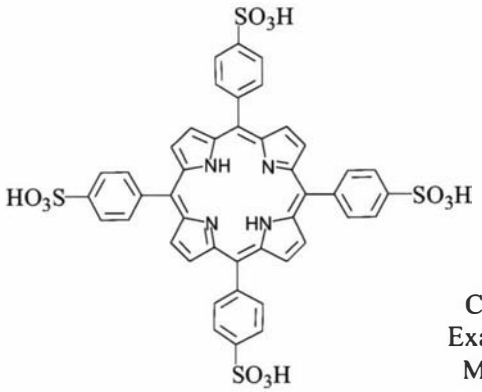

$C_{44}H_{30}N_4O_{12}S_4$
Exact Mass: 934.07
Mol. Wt.: 934.99

The synthesis has already been reported many times with a variety of little variations, particularly on the purification methods involved.[182] In this work further modifications were utilized. 200 mg of CuTPP **Cu-3** (296 μmol) were dissolved in 5 mL of concentrated sulphuric acid and stirred at 100 °C for 4 h. The solution slowly was diluted to 20 mL and filtered through glass filter. A sludge of CaO, suspended in water, was used to neutralize the acid solution (until the colour turned from green to red) and the solution was filtered off. The remaining solid was washed repeatedly with water and MeOH and this solution was added to the first one. To the aqueous phase Na_2CO_3 and EtOH were added to precipitate Ca ions as $CaCO_3$ after which the solution was filtered off and concentrated at the rotovapor. The pure TSPP **66** was precipitated by 3M HCl addition as purple-red crystals, yielding 105 mg (38%). ^{1}H-NMR (400 MHz, DMSO-d_6): δ 8.84 (s, 8H, $H_{\beta\text{-pyrrolic}}$), 8.17 (d, J = 8.1 Hz, 8H, H_{phenyl}), 8.03 (d, J_1 = 8.1 Hz, 8H, H_{phenyl}), -2.96 (br s, 2H, $H_{N\text{-pyrrolic}}$). The ^{1}H-NMR spectrum is consistent with the literature.[182]

T4PyP, 67.

5,10,15,20-tetra(4'-pyridinyl)porphyrin.

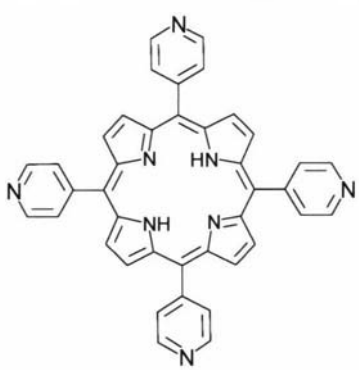

$C_{40}H_{26}N_8$
Exact Mass: 618.23
Mol. Wt.: 618.69

The synthesis of tetra(4)pyridylporphyrin **67** was performed as adaptation of the Adler method.[1] 0.7 mL (10 mmol) of pyrrole and 1.1 mL (10 mmol) of 4-carboxaldehyde-pyridine (both commercial reagents) were refluxed in 120 mL of propionic acid for 35 min. The solution was poured in water and neutralized by adding solid NaOH to the stirred solution (kept cold through an ice bath). Addition continued until solid start to precipitate. The solid was filtered off, washed with water and MeOH and dried under high vacuum to afford 252 mg (16.3%) of pure **67** as purple crystals. ^{1}H-NMR (400 MHz, $CDCl_3$): δ 9.07 (dd, J_1 = 4.2 Hz, J_2 = 1.6 Hz, 8H, $H_{pyridine}$), 8.88 (s, 8H, $H_{\beta\text{-pyrrolic}}$), 8.17 (dd, J_1 = 4.2 Hz, J_2 = 1.6 Hz, 8H, $H_{pyridine}$), -2.93 (br s, 2H, $H_{N\text{-pyrrolic}}$). MALDI-LRMS for M^+ ($C_{40}H_{24}N_8Zn$): cluster 618.2-621.2 (max 619.2), calculated: cluster 618.2-621.2 (max 618.2). The shifted maximum is probably due to the sum of signal coming from M^+ and MH^+ ions. The ^{1}H-NMR spectrum is consistent with the literature.[192]

CuT4PyP, Cu-67.

5,10,15,20-tetra(4'-pyridinyl)porphyrinato copper(II).

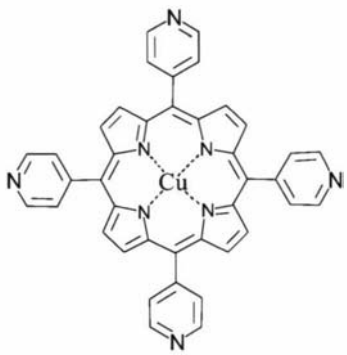

$C_{40}H_{24}CuN_8$
Exact Mass: 679.15
Mol. Wt.: 680.22

200 mg (323 μmol) of free base porphyrin **67** were dissolved in 30 mL of chloroform and the solution was brought to reflux. 130 mg (650 μmol) of $Cu(OAc)_2 \cdot H_2O$ were dissolved in 8 mL of MeOH/water = 10/1 and added to the porphyrin solution. The reflux continued for 2 h after which the solution was repeatedly washed with water and precipitated by methanol, providing 200 mg (91%) of **Cu-67.**

ZnT4PyP, Zn-67

5,10,15,20-tetra(4'-pyridinyl)porphyrinato zinc(II).

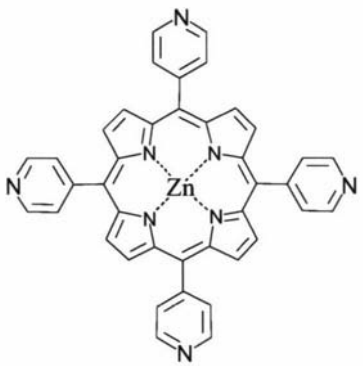

$C_{40}H_{24}N_8Zn$
Exact Mass: 680.14
Mol. Wt.: 682.06

320 mg (517 μmol) of **67** were metallated with 140 mg of $Zn(OAc)_2 \cdot H_2O$ (as described in the general procedures in Chapter 2) providing 290 mg (82%) of **Zn-67.** The relatively low yield was due to low solubility of the product. DCM containing 5-20% of methanol was found to be the only suitable choice. ^{1}H-NMR (400 MHz, $CDCl_3$ + CD_3OD): δ 8.15 (br s, 16H, $H_{pyridine}$), 7.88 (br s, 8H, $H_{\beta\text{-pyrrolic}}$). MALDI-LRMS for M^+ ($C_{40}H_{24}N_8Zn$): cluster 680.4-686.5 (max 680.4), calculated: cluster 680.1-686.1 (max 680.1).

T3PyP, 68.

5,10,15,20-tetra(3'-pyridinyl)porphyrin

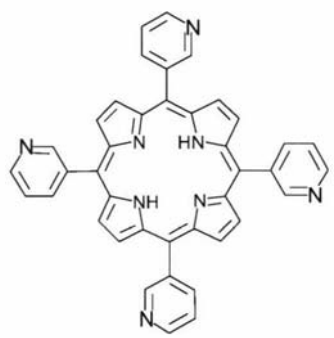

$C_{40}H_{26}N_8$
Exact Mass: 618.23
Mol. Wt.: 618.69

The synthesis of tetra(3)pyridylporphyrin **68** was performed as adaptation of the Adler method.[1] as for the homologue **67**. 0.7 mL (10 mmol) of pyrrole and 1.1 mL (10 mmol) of 4-carboxaldehyde-pyridine were refluxed in 120 mL of propionic acid for 30 min. The solution was poured in water and neutralized by adding solid NaOH to the stirred solution (kept cold through an ice bath). Addition continued until solid start to precipitate. The solid was filtered off, washed with water and MeOH and dried under high vacuum to afford 240 mg (15.5%) of pure **68** as purple crystals. ^{1}H-NMR (400 MHz, $CDCl_3$): δ 9.47 (s, 4H, $H_{pyridine}$), 9.09 (dd, J_1 = 5 Hz, J_2 = 1.6 Hz, 4H,

$H_{pyridine}$), 8.86 (s, 8H, $H_{\beta\text{-pyrrolic}}$), 8.61-8.54 (m, 4H, $H_{pyridine}$), 7.85-7.79 (m, 4H, $H_{pyridine}$), -2.85 (br s, 2H, $H_{N\text{-pyrrolic}}$).

CuT3PyP, Cu-68.

5,10,15,20-tetra(3'-pyridinyl)porphyrinato copper(II).

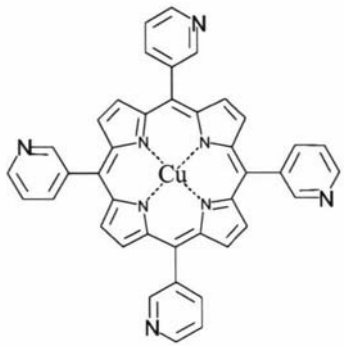

$C_{40}H_{24}CuN_8$
Exact Mass: 679.14
Mol. Wt.: 680.22

160 mg (259 μmol) of free base porphyrin **68** were dissolved in 30 mL of chloroform and the solution was brought to reflux. 110 mg (550 μmol) of $Cu(OAc)_2 \cdot H_2O$ were dissolved in 5 mL of MeOH/water = 10/1 and added to the porphyrin solution. Reflux continued for 2 h after which the solution was repeatedly washed with water and precipitated by methanol, providing 162 mg (92%) of **Cu-68.**

T4MPyP, 69.

5,10,15,20-tetra(4'-methylpyridinium iodide)porphyrin.

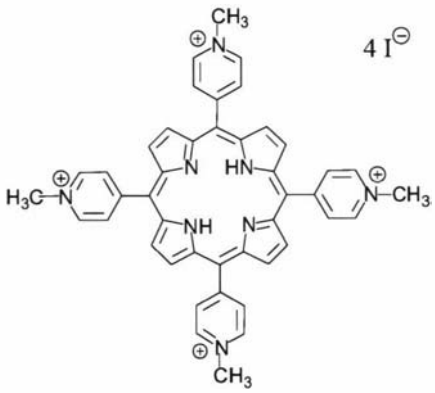

$C_{44}H_{38}I_4N_8$
Exact Mass: 1185.94
Mol. Wt.: 1186.44

200 mg (323 μmol) of T4PyP **67** were dissolved, under argon, in dry DMF. Excess methyl iodide (400 μL, 3 mmol) was added and the solution was stirred at 50 °C for 60 hours. The product was then precipitated by dichloromethane addition and washed with dichloromethane and methanol to afford 314 mg (82%) of pure T4MPyP **69** as purple crystals. ^{1}H-NMR (400 MHz, DMSO-d_6): δ 9.46 (d, J = 6.1 Hz, 8H, $H_{pyridine}$), 9.18 (s, 8H, $H_{\beta\text{-pyrrolic}}$), 8.98 (d, J_1 = 6.1 Hz, 8H, $H_{pyridine}$), 4.71 (s, 12H, H_{CH3}), -3.13

(br s, 2H, $H_{N\text{-pyrrolic}}$). Electrospray-LRMS for $(M\text{-}4I)^{4+}$ ($C_{44}H_{38}N_8$): 169.8, calculated: 169.7

T3MPyP, 70.

5,10,15,20-tetra(3'-methylpyridinium iodide)porphyrin.

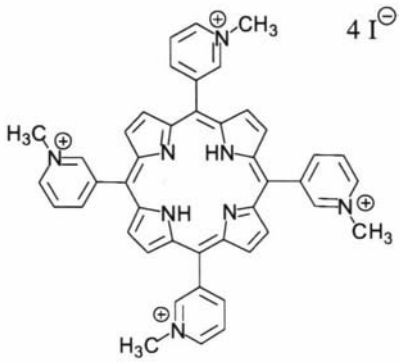

$C_{44}H_{38}I_4N_8$
Exact Mass: 1185.94
Mol. Wt.: 1186.44

160 mg (259 μmol) of T3PyP **68** were dissolved, under argon, in dry DMF. Excess methyl iodide (400 μL, 3 mmol) was added and the solution was stirred at 50 °C for 60 hours. The product was then precipitated by dichloromethane addition and washed with dichloromethane and methanol to afford 258 mg (84%) of pure T3MPyP **70** as purple crystals. ^{1}H-NMR (400 MHz, DMSO-d_6): δ 10.01 (s, 4H, $H_{pyridine}$), 9.57 (d, J = 6.2 Hz, 4H, $H_{pyridine}$), 9.36-9.22 (m, 12H, $8H_{\beta\text{-pyrrolic}}$+ $4H_{pyridine}$), 8.64 (app t, J = 7.2 Hz, 4H, $H_{pyridine}$), 4.69 (s, 12H, H_{CH3}), -3.15 (br s, 2H, $H_{N\text{-pyrrolic}}$). Electrospray-LRMS for $(M\text{-}4I)^{4+}$ ($C_{44}H_{38}N_8$): 169.8, calculated: 169.7.

3-carboxaldehyde-benzoic acid, 73.

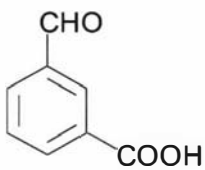

$C_8H_6O_3$
Exact Mass: 150.03
Mol. Wt.: 150.13

The synthesis of this compound was performed according to the procedure optimized in our lab by Dr. S. Gambhir.

28 g (130 mmol) of commercial 3-bromomethyl benzoic acid **72** were dissolved in 70 mL of EtOH at 60 °C. 23 g (164 mmol) of commercial HMTA (hexamethylenetetramine) were dissolved in 40 mL of water and the solution added to the first one. The mixture was refluxed for 1 h after which temperature was brought at 0 °C with an ice bath. 200 mL of HCl 5M were added and hydrolysis continued for 30 min at room temperature. The organic part was extracted with DCM, dried over

Mg_2SO_4 and brought to dryness to afford 14 g (72%) of the desired carboxaldehyde benzoic acid **73**. This material was used for the next reaction as it was. ^{1}H-NMR (400 MHz, DMSO): δ 10.12 (s, 1H, $H_{aldehyde}$), 8.47 (s, 1H, H_{Ph}), 8.27 (d, J = 8 Hz, 1H, H_{Ph}), 8.16 (d, J = 8 Hz, 1H, H_{Ph}), 7.75 (app t, J = 8 Hz, 1H, H_{Ph}).

3-carboxaldehyde-ethylbenzoate, 75.

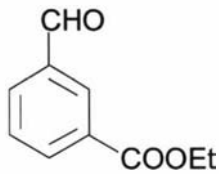

$C_{10}H_{10}O_3$
Exact Mass: 178.06
Mol. Wt.: 178.18

The synthesis of this compound was performed according to the procedure optimized in our lab by Dr. S. Gambhir.

13 g (86.7 μmol) of benzoic acid **73** were dissolved in 70 mL of hot EtOH and 2 mL of concentrated sulphuric acid were added. The mixture was refluxed for 6 hours after which the organic part was extracted with DCM. The organic phase was washed with saturated bicarbonate solution to remove unreacted benzoic acid and then dried over Mg_2SO_4. After removal of the solvent, the crude was purified by flash chromatography (silica gel, DCM as eluent) to afford a mixture of the desired product and the homologue acetal EtOOC-Ph-CH$(OEt)_2$. This mixture was dissolved in 30 mL of chloroform and this solution was stirred with 15 mL of TFA/water = 1/1 for 30 min at RT, after which it was poured in water and extracted with DCM. The organic phase was dried over Mg_2SO_4 and removal of the solvent afforded 8.9 g (58%) of the desired carboxaldehyde benzoate **75**. ^{1}H-NMR (400 MHz, $CDCl_3$): δ 10.10 (s, 1H, $H_{aldehyde}$), 8.55 (s, 1H, H_{Ph}), 8.33 (d, J = 8 Hz, 1H, H_{Ph}), 8.09 (d, J = 8 Hz, 1H, H_{Ph}), 7.64 (app t, J = 8 Hz, 1H, H_{Ph}), 4.42 (q, J = 7 Hz, 2H, H_{CH2}), 1.41 (t, J = 7 Hz, 3H, H_{CH3}).

T3(E)EPP, 77.

5,10,15,20-tetra(3'-(ethylcarboxylate)phenyl)porphyrin.

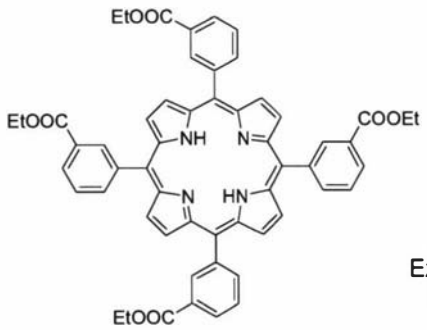

$C_{56}H_{46}N_4O_8$
Exact Mass: 902.33
Mol. Wt.: 902.99

The preparation and characterization of this compound were realized by A. Stephenson.

To a solution of ethyl 3-formylbenzoate (3.80 g, 21.3 mmol) and pyrrole (1.48 ml, 21.3 mmol) in dry degassed CH_2Cl_2 (2130 mL) under Ar at RT was added $BF_3{\cdot}OEt_2$ (225 μL, 2.13 mmol, 0.1 eq). After stirring for 2.5 h, *p*-chloranil (3.93 g, 0.75 eq) was added and the solution heated at reflux for 2 h. Excess Et_3N (9.0 mL) was added and the reaction cooled to RT overnight. The solution was column chromatographed (silica, 70 mm_{dia} x 95 mm, CH_2Cl_2:Et_2O (49:1)) collecting a red band. Recrystallisation from CH_2Cl_2/MeOH gave the title compound **77** (1.40 g, 29%) as a purple powder. ^{1}H NMR (400 MHz, $CDCl_3$, TMS): δ -2.795 (s, 2H, NH), 1.396 (t, 12H, ^3J = 7.1 Hz, $CO_2CH_2CH_3$), 4.463 (q, 8H, ^3J = 7.1 Hz, $CO_2CH_2CH_3$), 7.856 (t, 4H, ^3J = 7.7 Hz, $H_{5'}$), 8.400 (d, 4H, ^3J = 6.9 Hz, $H_{4' \text{ or } 6'}$), 8.499 (dt, 4H, ^3J = 7.9 Hz, ^4J = 1.2 Hz, $H_{6' \text{ or } 4'}$), 8.806 (s, 8H, $H_{\beta\text{-pyrrolic}}$), 8.893 (app t, 4H, $H_{2'}$). UV-vis (CH_2Cl_2): λ_{max} [nm] (ε x 10^{-3}) 418.5 (466.7), 446 (38.2), 514.5 (19.3), 548.5 (7.0), 589.5 (6.1), 647 (5.9). FAB-LRMS: *m/z* (%, assignment) cluster at 902-904, 902 (86, M^-). HRMS: Calcd for M^+ ($C_{52}H_{36}N_4O_8$): 902.3317, found: 902.3336.

CuT3(E)EPP, Cu-77.

5,10,15,20-tetra(3'-(ethylcarboxylate)phenyl)porphyrinato copper(II).

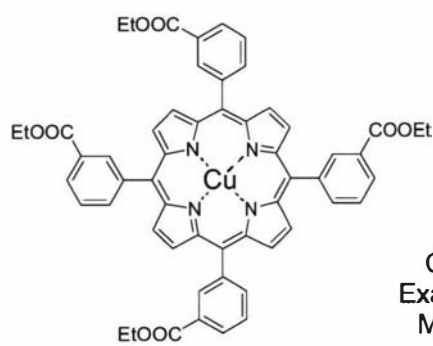

$C_{56}H_{44}CuN_4O_8$
Exact Mass: 963.26
Mol. Wt.: 964.52

The preparation and characterization of this compound were realized by A. Stephenson.

A solution of $Cu(OAc)_2 \cdot H_2O$ (341 mg, 1.71 mmol, 1.1 eq) in MeOH (40 mL) was added to a refluxing solution of T3EEP **77** (1.40 mg, 1.55 mmol) in $CHCl_3$ (200 mL). The reaction was adjudged complete by TLC after 1 h. On cooling to RT, the volume was reduced *in vacuo*. Recrystallisation from $CHCl_3$/MeOH gave the title compound **Cu-77** (828 mg, 100%) as a red powder. UV-vis (CH_2Cl_2): λ_{max} [nm] ($\varepsilon \times 10^{-3}$) 416 (636), 539 (26.3). FAB-LRMS: *m/z* (%, assignment) cluster at 962-968, 964 (100, M+1). HRMS: Calcd for M+1 ($C_{52}H_{36}N_4O_8Cu$): 964.2503, found: 964.2533.

T3(E)EPP-CHO, 79.

(2-(5,10,15,20-tetra(3'-(methylcarboxylate)phenyl)porphyrin)yl)carboxaldehyde.

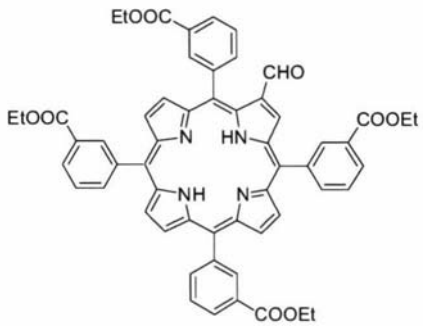

$C_{57}H_{46}N_4O_9$
Exact Mass: 930.33
Mol. Wt.: 931.00

The preparation and characterization of this compound were realized by A. Stephenson.

Vilsmeier complex was prepared by adding $POCl_3$ (10.45 mL) slowly to dry DMF (13.08 mL) at 0 °C under argon. After 25 min a solution of Cu-T3EEP **Cu-77** (1.47g, 1.55 mmol) in dry 1,2-DCE (125 ml) was added and the reaction heated at 93 °C for 22 h. On cooling to RT, conc. H_2SO_4 (21.0 mL) was added to the vigorously stirred mixture and the reaction stirred vigorously for 15 min exactly, following the reaction mixture was poured into ice cold RO water (2 L) and extracted into CH_2Cl_2 (2 x 1 L). The aqueous layer was decanted off and the organic layer washed with H_2O (3 x 1 L) then sat. aq. $NaHCO_3$ (1 L). The organic layer was separated, dried ($MgSO_4$), filtered and the solvent removed *in vacuo*. The residue was column chromatographed (silica, 70 mm_{dia} x 100 mm), first eluting with CH_2Cl_2:Et_2O (197:3) to give demetallated starting material (40 mg, 2.7%), then CH_2Cl_2:Et_2O (49:1) to give the title compound **79** (1.01 g, 70%, recrystallised from CH_2Cl_2/MeOH) as a purple powder. ^1H NMR (500 MHz, $CDCl_3$, TMS): δ -2.549 (br s, 2H, NH), 1.409 (t, 12H, ^3J = 6.9 Hz,

$CO_2CH_2CH_3$), 4.470 (q, 8H, ^3J = 7.0 Hz, $CO_2CH_2CH_3$), 7.85-7.88 (m, 4H, $H_{5'}$), 8.37-8.54 (m, 8H, $H_{4',6'}$), 8.72-8.73 (m, 2H, $H_{\beta\text{-pyrrolic}}$), 8.82-8.95 (m, 8H, $4H_{\beta\text{-pyrrolic}}$ + $4H_{2'}$), 9.334 (s, 1H, CHO [coupled to δ 188]), 9.353 (s, 1H, $H_{3,\beta\text{-pyrrolic}}$ [coupled to δ 138]). *Assignments aided by ^1H-^{13}C HMQC and COSY spectra* UV-vis (CH_2Cl_2): λ_{max} [nm] (ε x 10^{-3}) 431 (310), 525 (17.5), 567 (6.73), 604 (5.85), 663 (8.49). FAB-LRMS: *m/z* (%, assignment) cluster at 930-933, 931 (100, MH^+). HRMS: Calcd for MH^+ ($C_{57}H_{47}N_4O_9$): 931.3328, found: 931.3343.

T3(E)EPP-CH_2OH, 81.

(2-(5,10,15,20-tetra(3'-(ethylcarboxylate)phenyl)porphyrin)yl)methanol.

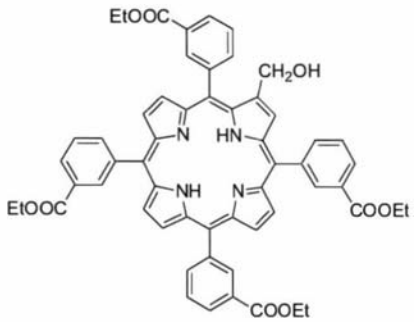

$C_{57}H_{48}N_4O_9$
Exact Mass: 932.34
Mol. Wt.: 933.01

The preparation and characterization of this compound were realized by A. Stephenson.

A mixture of porphyrin aldehyde **79** (750 mg, 805 μmol) and $NaBH_4$ (700 mg, 18.5 mmol, 23 eq) in THF (59 mL) and H_2O (1.19 mL) was stirred at RT. After 45 min TLC analysis indicated that the starting material had been consumed with the appearance of a new more polar red band. Excess H_2O (≈ 100 mL) was added and the aqueous layer extracted with CH_2Cl_2 (200 mL). The organic layer was washed with H_2O (150 mL), sat. aq. $NaHCO_3$ (150 mL), then separated and dried ($MgSO_4$) and the solvent removed *in vacuo*. The residue was column chromatographed (silica gel, 45 mm_{dia} x 170 mm, CH_2Cl_2:Et_2O (20:1)) until all more non polar material was eluted, then CH_2Cl_2:Et_2O (10:1). Recrystallisation from CH_2Cl_2/hexane gave the title compound **81** (660 mg, 88%) as a purple powder. ^1H NMR (500 MHz, $CDCl_3$, TMS): δ -2.785 (br s, 2H, NH), 1.386 (q, 12H, ^3J = 7.3 Hz, $CO_2CH_2CH_3$), 2.059 (t, 1H, ^3J = 6.9 Hz, CH_2OH), 4.41-4.48 (m, 12H, $CO_2CH_2CH_3$), 4.81-4.90 (m, 2H, CH_2OH), 7.81-7.86 (m, 4H, $H_{5'}$), 8.275 (br d, ^3J = 7.4 Hz, $H_{4' \text{ or } 6'}$, 1H), 8.36-8.39 (d, 3H, $H_{6' \text{ or } 4'}$), 8.48-8.52 (m, 4H, $H_{6' \text{ or } 4'}$), 8.557 (d, ^3J = 4.5 Hz, 1H, $H_{\beta\text{-pyrrolic}}$), 8.72-8.81 (m, 6H, , $H_{\beta\text{-pyrrolic}}$), 8.87-8.89 (m, 4H, $H_{2'}$). *Assignments aided by COSY spectra.* UV-vis

(CH_2Cl_2): λ_{max} [nm] (ε x 10^{-3}) 419 (420), 448 (40.15), 515 (20.5), 548 (6.09), 590 (5.75), 650 (5.01). FAB-LRMS: *m/z* (%, assignment) cluster at 930-937, 933 (100, M^-). HRMS: Calcd for M^- ($C_{57}H_{48}N_4O_9$): 932.3421, found: 932.3433.

T3(E)EPP-CH_2Cl, 83.

(2-(5,10,15,20-tetra(3'-(ethylcarboxylate)phenyl)porphyrin)yl)chloromethane.

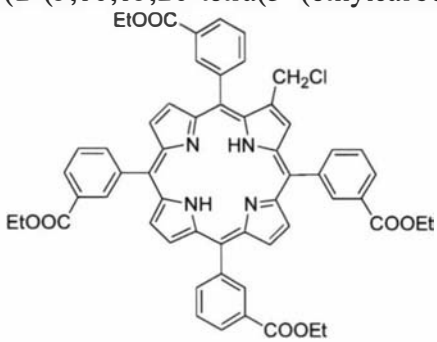

$C_{57}H_{47}ClN_4O_8$
Exact Mass: 950.31
Mol. Wt.: 951.46

The preparation and characterization of this compound were realized by A. Stephenson.

$SOCl_2$ (204 µL, 2.81 mmol) was added to a solution of porphyrin alcohol **81** (630 mg, 675 µmol) and dry pyridine (516 µL, 6.38 mmol) in dry CH_2Cl_2 (72 mL) at 0 °C under argon. After stirring at 0 °C for 15 min, the solution was warmed to RT. After 15 min no starting material remained by TLC and a new red band of lower polarity was evident. The reaction was poured into $CHCl_3$ (100 mL) and stirred for 15 min. The resulting green solution was washed with H_2O (5 x 70 mL) then sat. aq. $NaHCO_3$ (70 mL). The red-brown organic layer was separated and dried ($MgSO_4$) and precipitated from MeOH to give the title compound **83** (550 mg, 85%) as a purple solid. ^1H NMR (400 MHz, CDCl3, TMS): δ -2.758 (br s, 2H, NH), 1.37-1.42 (m, 12H, $CO_2CH_2CH_3$), 4.42-4.49 (m, 8H, $CO_2CH_2CH_3$), 4.70-4.83 (m, 2H, CH_2Cl), 7.82-7.88 (m, 4H, $H_{5'}$), 8.36-8.39 (m, 4H, $H_{4' \text{ or } 6'}$), 8.48-8.55 (m, 4H, $H_{6' \text{ or } 4'}$), 8.603 (d, 1H, ^3J = 4.8 Hz, $H_{\beta\text{-pyrrolic}}$), 8.747 (d, 1H, ^3J = 4.9 Hz, $H_{\beta\text{-pyrrolic}}$), 8.76-8.82 (m, 5H, $H_{\beta\text{-pyrrolic}}$), 8.87-9.89 (m, 4H, $4H_{2'}$). *Assignments aided by COSY spectra.* UV-vis (CH_2Cl_2): λ_{max} [nm] (ε x 10^{-3}) 420 (393), 450 (48.6), 516 (18.5), 550 (6.00), 593 (6.18), 652 (7.12). FAB-LRMS: *m/z* (%, assignment) cluster at 950-953, 894 (100, MH^-). HRMS: Calcd for MH^- ($C_{57}H_{38}Cl_1N_4O_8$): 951.3161, found: 951.3142.

T3(E)EPP-ps, 85.

(2-(5,10,15,20-tetra(3'-(ethylcarboxylate)phenyl)porphyrin)yl)methyltriphenyl-phosphonium chloride.

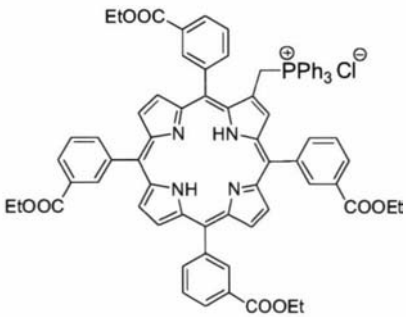

$C_{75}H_{62}ClN_4O_8P$
Exact Mass: 1212.40
Mol. Wt.: 1213.74

The preparation and characterization of this compound were realized by A. Stephenson.

Porphyrin chloride **83** (528 mg, 555 μmol) and PPh_3 (2.91 g, 11.10 mmol, 20 eq) in $CHCl_3$ (25 mL) were heated to reflux under argon. The reaction was adjudged to be complete by TLC after 7.5 h with the formation of a single spot of higher polarity than the starting material. The solvent was removed *in vacuo* and the residue column chromatographed (silica, 45 mm_{dia} x 60 mm, CH_2Cl_2:MeOH (20:1)) to give the title phosphonium salt **85** (610 mg, 90%) as a purple solid. ^1H NMR (500 MHz, $CDCl_3$, TMS): δ -2.798 (br s, 2H, NH), 1.38-1.47 (m, 12H, $CO_2CH_2CH_3$), 4.37-4.54 (m, 12H, $CO_2CH_2CH_3$ + CH_2), 7.18-8.89 (m, 40H). UV-vis (CH_2Cl_2): λ_{max} [nm] (ε x 10^{-3}) 425 (373), 452 (34.7), 520 (17.3), 555 (4.67) 596 (5.53), 653 (7.11). FAB-LRMS: *m/z* (%, assignment) 1177 (100, $[M - Cl]^+$), 915 (75, $[M - (P^+Ph_3Cl^-)]^+$). HRMS: Calcd for $[M - Cl]^+$ ($C_{75}H_{62}N_4O_8P_1$): 1177.4307, found: 1177.4305.

T3(M)EPPs

The syntheses of all T3(M)EPP derivatives (**76**, **78**, **80**, **82** and **84**) were performed as described by Dr. W.M. Campbell.[63] Procedures are identical to the one just described for the T3(E)EPP homologues.

Bromophenyl acetal, 86.

4-bromobenzaldehyde-2',2'-dimethyl-1',3'-propanediol acetal.

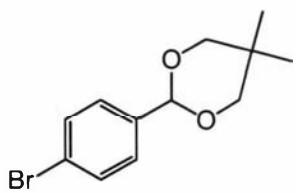

$C_{12}H_{15}BrO_2$
Exact Mass: 270.03
Mol. Wt.: 271.15

The synthesis of **86** was performed according to the procedure optimized in our laboratories by Dr. P. Wagner. 7.6 g (41 mmol) of *p*-bromobenzaldehyde and 8.6 g (97.6 mmol) of dimethylpropanediol were dissolved in 50 mL of benzene in a 100 mL flask equipped with a Dean-Starck apparatus (to remove the water formed during the course of the reaction). 5 mg (26 μmol) of *p*-toluensulphonic acid monohydrate were added and the solution was refluxed for 24 hours. After removal of the solvent at the rotovapor, the resulting slurry was dissolved in dichloromethane and filtrated through 5 cm of silica gel. Removal of the solvent provided 11.1 g (99%) of pure **86** as white crystals. ^{1}H-NMR (400 MHz, $CDCl_3$): δ 7.42-7.58 (m, 2H, H_{Ph}), 7.40-7.36 (m, 2H, H_{Ph}), 5.35 (s, 1H, H_{CH}), 3.76 (app d, J = 11 Hz, 2H, H_{CH2}), 3.64 (app d, J = 11 Hz, 2H, H_{CH2}), 1.28 (s, 3H, H_{CH3}), 0.80 (s, 3H, H_{CH3}).

Dialdehyde monoacetal, 87.

terephthalaldehyde-2,2-dimethyl-1,3-propanediol monoacetal

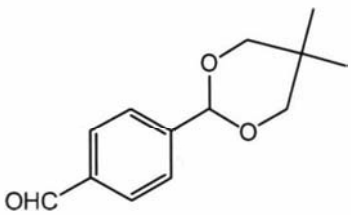

$C_{13}H_{16}O_3$
Exact Mass: 220.11
Mol. Wt.: 220.26

The synthesis of **87** was performed according to the procedure optimized in our laboratories by Dr. P. Wagner. 11 g (40.9 mmol) of bromophenyl acetal **86** were dissolved, under argon, in 130 mL of dry THF and the stirred solution was brought at -78 °C in acetone/liquid N_2 bath. 40 mL of 2.5M BuLi (100 mmol) in hexane were added through syringe/septum and the bath was removed to allow reaching room temperature. After this, the temperature was brought back to -78 °C, 7 mL of dry DMF were added and the bath was removed again. After further 20 min the solution was poured in 100 mL of 10% HCl solution at 0 °C (to hydrolyze the excess BuLi) and extracted with ether. The organic phase was dried over $MgSO_4$ and the solvent removed. Flash chromatography through silica gel (DCM/hexane = 2/1) afforded 6.4 g (71%) of pure **87** as white crystals. ^{1}H-NMR (400 MHz, $CDCl_3$): δ 10.03 (s, 1H, $H_{aldehyde}$), 7.92-7.88 (m, 2H, H_{Ph}), 7.71-7.66 (m, 2H, H_{Ph}), 5.45 (s, 1H, H_{CH}), 3.82-3.78 (m, 2H, H_{CH2}), 3.70-3.66 (m, 2H, H_{CH2}), 1.29 (s, 3H, H_{CH3}), 0.82 (s, 3H, H_{CH3}).

bis-2-pyrryl methane, 89.

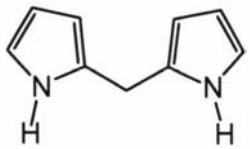

$C_9H_{10}N_2$
Exact Mass: 146.08
Mol. Wt.: 146.19

The synthesis of this dipyrrylmethane was achieved using two different and already described procedures. The two methods were slightly modified and provided the same pure product in comparable yields.

Method 1 (via alcohol):[116] 2 g (21 mmol) of commercial 2-pyrrolecarboxaldehyde were dissolved in 60 mL of water. 2.2 g (58 mmol) of $NaBH_4$ were dissolved/suspended in 30 mL and added dropwise over 10 min to the aldehyde solution. Stirring was continued for 1 h after which the solution was extracted with ether, washed with saturated bicarbonate solution and dried over $MgSO_4$. Removal of the solvent provided a pale orange oil. This oil was dissolved in 15 mL of pyrrole, the solution degassed by flushing argon for 10 min and 170 μL (1.2 μmol) of $BF_3 \cdot Et_2O$ were added through syringe/septum. Stirring continued for 16 hours after which the solution was diluted with DCM, washed with saturated bicarbonate solution and dried over $MgSO_4$. Removal of the solvents gave a brown oil which was repeatedly extracted with hexane at 50 °C. Removal of solvents (pyrrole and hexane) under high vacuum afforded 550 mg (3.76 mmol, 18% from pyrrolcarboxaldehyde) of pure dipyrrylmethane **89** as pale yellow crystals.

Method 2 (via thione):[117,127] The synthesis of bis-2-pyrryl thione 90 was realized according to Clezy and Smithe.[117] 12.5 g (186 mmol) of pyrrole were dissolved in 125 mL of dry diethyl ether and added dropwise (over 10 min) to 10.5 g (91 mmol) of $CSCl_2$ dissolved in 250 mL of dry benzene, at 0 °C. The resulting solution was poured into 300 mL of MeOH/water = 4/1 and stirred for 30 min at room temperature. After removal of solvents and low boiling co-products (rotovapor, 65 °C in fumehood), the resulting oil was separated through flash chromatography (silica gel, DCM/hexane = 2/1) and the fractions containing the desired product were recrystallized form MeOH/water to provide 7.1 g (40.3 mmol, 43.4% from pyrrole) of pure bis-2-pyrryl thione **90** as red crystals. 1.4 g of KOH were dissolved in 100 mL of 95% ethanol after which 7 g (18.2 mmol) of $NaBH_4$ were added. This solution was used for the reduction of 6 g (34 mmol) of the thione **90** which were dissolved in 200 mL of 95% ethanol: the two solutions were added and refluxed for 3 h after which argon was bubbled through the solution to remove H_2S. The solution was allowed to reach RT

and 30 mL of acetone were added to neutralize the excess hydride. The solution was filtered off and the remaining inorganic solid washed with methanol. After removal of these solvents, a further dissolution in DCM and filtration was required to remove inorganic salts. Flash chromatography on silica gel (DCM/hexane = 5/1) provided 4.3 g (29.4 mmol, 31% from pyrrole) of pure bis-2-pyrryl methane **89** as pale yellow crystals. ^{1}H-NMR (400 MHz, $CDCl_3$): δ 7.89 (br s, 2H, $H_{N\text{-pyrrolic}}$), 6.68-6.65 (m, 2H, $H_{pyrrolic}$), 6.15 (dd, J_1 = 5.8 Hz, J_2 = 2.8 Hz, 2H, $H_{pyrrolic}$), 6.06-6.02 (m, 2H, $H_{pyrrolic}$), 3.98 (s, 2H, H_{CH2}).

MAP, 91.

4-(1'-porphyrinyl)benzaldehyde-2',2'-dimethyl-1',3'-propanediol acetal.

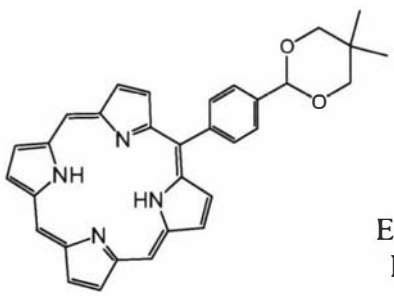

$C_{32}H_{28}N_4O_2$
Exact Mass: 500.22
Mol. Wt.: 500.59

304 mg (2.08 mmol) of dipyrrylmethane **89** and 396 mg (4.12 mmol) of commercial 2-pyrrolecarboxaldehyde were dissolved in 1 L of dry DCM under argon. 100 μL of TFA were added and the solution was stirred at room temperature for 1 h. 417 mg (1.89 mmol) of monoprotected dialdehyde **87**, dissolved in 50 mL of dry DCM, were then added dropwise and the stirring continued for 5 h. 1.3 g (5.73 mmol) of DDQ were added and stirring continued for a further hour after which 1 mL of triethylamine was added and the solvent removed at the rotovapor. The resulting solid was separated through flash column chromatography on silica gel (dichloromethane as eluent) to provide traces of porphine **93** followed by the desired product **91** and then by other co-products. Recrystallization from DCM/hexane afforded 85.5 mg (8.2 % from dipyrrylmethane) of pure **91** as purple-red crystals. ^{1}H-NMR (500 MHz, $CDCl_3$): δ 10.24 (s, 2H, H_{meso}), 10.15 (s, 1H, H_{meso}), 9.39 (app dd, J_1 = 11.2 Hz, J_2 = 4.5 Hz, 4H, $H_{\beta\text{-pyrrolic}}$), 9.34 (d, J = 4.6 Hz, 2H, $H_{\beta\text{-pyrrolic}}$), 9.06 (d, J = 4.6 Hz, 2H, $H_{\beta\text{-pyrrolic}}$), 8.26 (d, J = 8 Hz, 2H, H_{Ph}), 7.94 (d, J = 8 Hz, 2H, H_{Ph}), 5.75 (s, 1H, H_{CH}), 3.97 (app d, J = 10.8 Hz, 2H, H_{CH2}), 3.84 (app d, J = 10.8 Hz, 2H, H_{CH2}), 1.48 (s, 3H, H_{CH3}), 0.90 (s, 3H, H_{CH3}), -3.73 (br s, 2H, $H_{N\text{-pyrrolic}}$). UV-vis (CH_2Cl_2): λ_{max} [nm]

(ε x 10^{-3}) 399 (505), 495 (26), 526.5 (3.6), 569 (8), 622 (0.8). FAB-HRMS for M^+ ($C_{32}H_{28}N_4O_2$): 500.2219, calculated: 500.2212.

MBP, 94.

4-(1'-porphyrinyl)benzaldehyde.

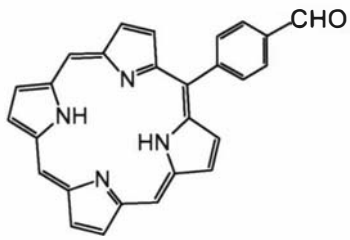

$C_{27}H_{18}N_4O$
Exact Mass: 414.15
Mol. Wt.: 414.46

The synthesis of monobenzylporphyrin **94** was obtained by deprotection of the aldehyde group of **91**. 97 mg (194 μmol) of **91** were dissolved in 25 mL of DCM. 40 mL of TFA/water = 3/1 was added and stirring continued for 2 h after which the solution was neutralized with saturated bicarbonate solution and the organic phase was separated and dried over $MgSO_4$. The solid obtained was recrystallized from DCM/MeOH to provide 80 mg (99%) of pure **93** as purple crystals. ^{1}H-NMR (500 MHz, $CDCl_3$): δ 10.43 (s, 1H, $H_{aldehyde}$), 10.37 (s, 2H, H_{meso}), 10.31 (s, 1H, H_{meso}), 9.51 (dd, J_1 = 9.6 Hz, J_2 = 4.5 Hz, 4H, $H_{\beta\text{-pyrrolic}}$), 9.45 (d, J = 4.5 Hz, 2H, $H_{\beta\text{-pyrrolic}}$), 8.46 (d, J = 7.8 Hz, 2H, H_{Ph}), 8.34 (d, J = 7.8 Hz, 2H, H_{Ph}), -3.59 (br s, 2H, $H_{N\text{-pyrrolic}}$). FAB-HRMS for MH^+ ($C_{27}H_{19}N_4O$): 415.1560, calculated: 415.1559.

Fe(III)MBP, Fe-94.

4-(1'-(porphyrinato iron(III))yl)benzaldehyde chloride.

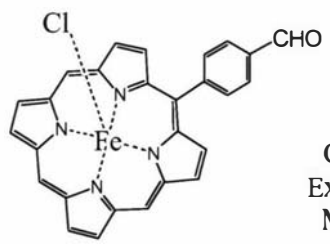

$C_{27}H_{16}ClFeN_4O$
Exact Mass: 503.04
Mol. Wt.: 503.74

74 mg (178 μmol) of MBP **94** were metallated with 330 mg (1.68 mmol) of $FeCl_2 \cdot 4H_2O$ according to the described general procedure. The product was isolated through flash chromatography using DCM/methanol = 20/1 as eluent. Yield was 71 mg (79%) of **Fe-94** as dark purple crystals. UV-vis (CH_2Cl_2): λ_{max} [nm] (ε x 10^{-3}) 398.5 (212), 494.5 (24), 561 (12), 626.5 (7). FAB-HRMS for $(M\text{-}Cl)^+$ ($C_{27}H_{16}N_4OFe$): 468.0676, calculated: 468.0674.

ZnT3(M)EPP-ps,, Zn-84

(2-(5,10,15,20-tetra(3'-(methylcarboxylate)phenyl)porphyrinato zinc(II))yl)methyltriphenylphosphonium chloride.

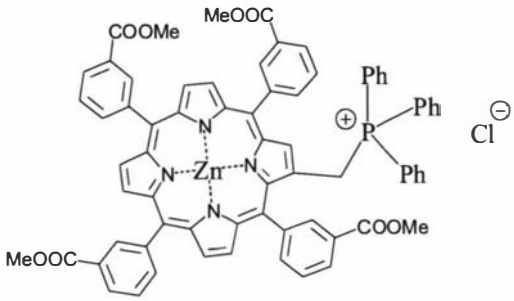

$C_{71}H_{52}ClN_4O_8PZn$
Exact Mass: 1218.25
Mol. Wt.: 1221.01

Phosphonium salt **Zn-84** was prepared from its free-base homologue **84** by standard Zn insertion. 670 mg (577 μmol) of **84** were metallated with 155 mg (705 μmol) of $Zn(OAc)_2 \cdot H_2O$ to give 680 mg (96%) of **Zn-84** as purple crystals. ^{1}H-NMR (500 MHz, $CDCl_3$): δ 8.89-8.56 (m, 7H, $H_{\beta\text{-pyrrolic}}$), 8.53-8.02 (m, 12H, $8H_{o\text{-Ph}}$ + $4H_{p\text{-Ph}}$), 7.85-7.58 (m, 4H, $4H_{m\text{-Ph}}$), 7.49 (br s, 3H, $H_{p\text{-Ph'}}$), 7.19 (br s, 6H, $H_{m\text{-Ph'}}$), 6.81 (br s, 6H, $H_{m\text{-Ph'}}$), 4.02-3.56 (m, 12H, H_{CH3}), 2.43 (m, 2H, H_{CH2}). *Assignments aided by COSY spectra.* UV-vis (CH_2Cl_2): λ_{max} [nm] (ε x 10^{-3}) 424.5 (254), 553 (11), 582.5 (2.8). MALDI-LRMS for M^+($C_{71}H_{52}N_4O_8PZn$): cluster 1182.9-1190.3 (max 1182.9), calculated: cluster 1183.3-1190.3 (max 1183.3).

ZnT3(E)EPP-CHO, Zn-79.

(2-(5,10,15,20-tetra(3'-(ethylcarboxylate)phenyl)porphyrinato zinc(II))yl) carboxaldehyde.

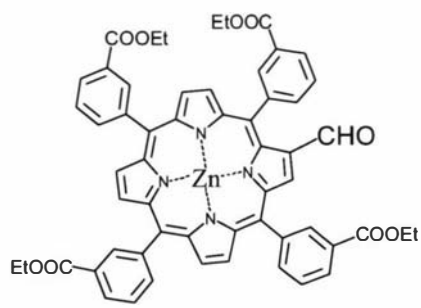

$C_{57}H_{44}N_4O_9Zn$
Exact Mass: 992.24
Mol. Wt.: 994.37

Zn porphyrin aldehyde **Zn-79** was prepared from its free base homologue by standard Zn insertion. 190 mg (203 μmol) of **79** were metallated with 68 mg (309 μmol) of $Zn(OAc)_2 \cdot H_2O$ to give 198 mg (96%) of **Zn-79** as purple crystals. ^{1}H-NMR (500 MHz, $CDCl_3$): δ 9.32-9.23 (m, 1H, $H_{\beta\text{-pyrrolic}}$), 9.15-8.96 (m, 1H, $H_{\beta\text{-pyrrolic}}$), 8.82 (s, 1H, $H_{aldehyde}$), 8.84-8.67 (m, 9H, $5H_{\beta\text{-pyrrolic}}$ + $4H_{o\text{-Ph}}$), 8.48-8.28 (m, 8H, + $4H_{o\text{-Ph}}$ +

$4H_{p\text{-}Ph}$), 7.87-7.68 (m, 4H, $H_{m\text{-}Ph}$), 4.46-4.25 (m, 8H, H_{CH2}), 1.45-1.30 (m, 12H, H_{CH3}). *Assignments aided by COSY spectra.* UV-vis (CH_2Cl_2): λ_{max} [nm] ($\varepsilon \times 10^{-3}$) 433.5 (310), 599 (17.7), 601.5 (12), 671.5 (2.9). FAB-HRMS for M^+ ($C_{57}H_{44}N_4O_9Zn$): 992.2379, calculated: 992.2400.

MBP-T3EPP, 95.

1-(1'-porphyrinyl),4-(*trans*-2'-(2"-(5",10",15",20"-tetra(3"'-(methylcarboxylate) phenyl)porphyrin)yl)ethen-1'-yl)benzene.

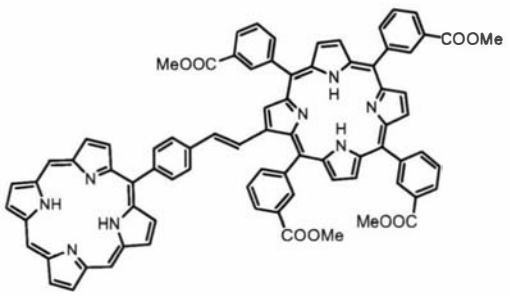

$C_{80}H_{56}N_8O_8$
Exact Mass: 1256.42
Mol. Wt.: 1257.35

40 mg (96.5 μmol) of porphyrin aldehyde **94** and 142 mg (116 μmol) of of phosphonium salt **84** were dissolved in 50 mL of chloroform under argon. To the stirred solution, 200 mg of DBU were added and reaction went on for 60 minutes. The solution was washed twice with 0.1M HCl, the organic phase was dried over $MgSO_4$ and brought to dryness. The solid was separated through flash chromatography using DCM/methanol 50/1 as eluent. The product was probably a mixture of *cis* and *trans* isomers which was isomerized to the *trans* form by I_2 treatment. The solid was dissolved in 20 mL of dichloromethane and 80 mg of I_2 were added. After 42 hours the solution was washed three times with a saturated solution of $Na_2S_2O_3$ and water and then precipitated with methanol. The yield was 52 mg (43%) of pure **95** as purple-red crystals. ^{1}H-NMR (500 MHz, $CDCl_3$): δ 10.38 (br s, 2H, H_{meso}), 10.30 (br s, 1H, H_{meso}), 9.55-9.47 (m, 6H, $H_{\beta\text{-pyrrolic}}$), 9.22 (d, J = 4.5 Hz, 2H, $H_{\beta\text{-pyrrolic}}$), 9.08-9.00 (m, 4H, $6H_{\beta\text{-pyrrolic}}$), 8.93 (br s, 3H, $H_{\beta\text{-pyrrolic}}$), 8.83-8.75 (m, 4H, $H_{o\text{-Ph}}$), 8.65-8.35 (m, 8H, $4H_{o\text{-Ph}}$ + $4H_{p\text{-Ph}}$), 8.25 (d, J = 7.7 Hz, 2H), 8.05-7.82 (m, 4H, $H_{m\text{-Ph}}$), 7.65 (d, J = 7.7 Hz, 2H, $H_{Ph'}$), 7.59 (d, J = 15.7 Hz, 1H, H_{alkene}), 7.22 (d, J = 15.7 Hz, 1H, H_{alkene}), 4.08-3.93 (m, 12H, H_{CH3}), -2.54 (br s, 2H, $H_{N\text{-pyrrolic}}$), -3.51 (br s, 2H, $H_{N\text{-pyrrolic}}$). FAB-HRMS for MH^+ ($C_{80}H_{56}N_8O_8$): 1257.4308, calculated: 1257.4299.

MBP-T3CPP, 96.

1-(1'-porphyrinyl),4-(*trans*-2'-(2"-(5",10",15",20"-tetra(3'"-carboxyphenyl)porphyrin) yl)ethen-1'-yl)benzene.

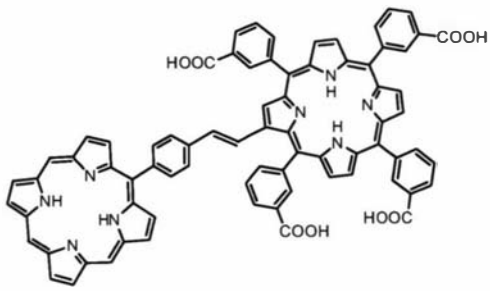

$C_{76}H_{48}N_8O_8$
Exact Mass: 1200.36
Mol. Wt.: 1201.24

The synthesis of the water-soluble dimer **96** was obtained from the homologue **95** by hydrolysis of the ester groups. 10 mg (8 μmol) of **95** were dissolved in 5 mL of THF and 35 mg of KOH were dissolved in 5 mL of MeOH/water = 10/1. The two solutions were mixed and the resulting mixture was brought to reflux. After 24 hours, the solution was then concentrated at the rotovapor (to remove THF) and washed with dichloromethane. The water phase was slowly neutralized with dilute phosphoric acid until precipitation of the desired product. Purification was obtained through ion-exchange chromatography. The solid was dissolved in basic water and immobilized on the Source 15Q resin packed in a small column (10 mm_{dia} x 20 mm); water, dilute HCl and water/methanol = 1/1 solutions were passed through the column before elution of the product was achieved with methanol with HCl 10^{-5}M. Evaporation of the solvents provided 9.5 mg (99%) of the desired dyad **96** were collected as purple-red crystals. ^{1}H-NMR (500 MHz) in DMSO-d_6 and D_2O were poorly resolved. FAB-HRMS for MH^+ ($C_{76}H_{49}N_8O_8$): 1201.3631, calculated: 1201.3673.

MBP-ZnT3EPP, Zn/fb-97.

1-(1'-porphyrinyl),4-(*trans*-2'-(2"-(5",10",15",20"-tetra(3'"-(methylcarboxylate) phenyl)porphyrinato zinc(II))yl)ethen-1'-yl)benzene.

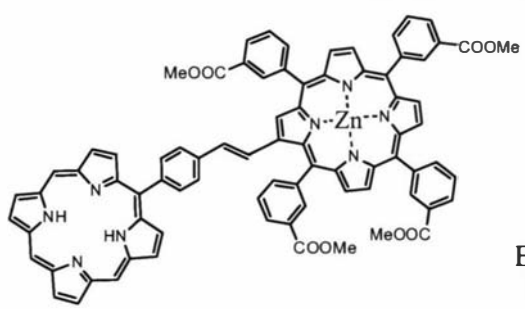

$C_{80}H_{54}N_8O_8Zn$
Exact Mass: 1318.34
Mol. Wt.: 1320.72

10 mg (24 μmol) of MBP **94** and 34 mg (28 μmol) of phosphonium salt **Zn-84** were dissolved in 20 mL of dichloromethane under argon. To the stirred solution, 50 mg of DBU were added and reaction went on for 50 minutes. The solution was washed twice with 0.1M HCl, the organic phase was dried over $MgSO_4$ and brought to dryness. The solid was separated through flash chromatography using DCM/methanol 100/1 as eluent. The product was probably a mixture of *cis* and *trans* isomers which was isomerized to the *trans* form by I_2 treatment. The solid was dissolved in 20 mL of dichloromethane and 30 mg of I_2 were added. After 39 hours the solution was washed three times with a saturated solution of $Na_2S_2O_3$ and water and then precipitated with hexane. The yield was 12 mg (38%) of pure **Zn/fb-97** as purple crystals. ^{1}H-NMR (500 MHz, $CDCl_3$): δ 10.37 (br s, 2H, H_{meso}), 10.26 (br s, 1H, H_{meso}), 9.55-9.45 (m, 6H, $H_{\beta\text{-pyrrolic}}$), 9.23 (d, J = 4.5 Hz, 2H, $H_{\beta\text{-pyrrolic}}$), 9.14 (m, 1H, $H_{\beta\text{-pyrrolic}}$), 9.05-8.81 (m, 10H, $6H_{\beta\text{-pyrrolic}} + 4H_{o\text{-Ph}}$), 8.65-8.40 (m, 8H, $4H_{o\text{-Ph}} + 4H_{p\text{-Ph}}$), 8.25 (d, J = 7.7 Hz, 2H, $H_{Ph'}$), 8.05-7.83 (m, 4H, $4H_{m\text{-Ph}}$), 7.65 (d, J = 7.7 Hz, 2H, $H_{Ph'}$), 7.54 (br d, J = 16 Hz, 1H, H_{alkene}), 7.21 (br d, J = 16 Hz, 1H, H_{alkene}), 4.08-3.90 (m, 12H, H_{CH3}), -3.53 (br s, 2H, $H_{N\text{-pyrrolic}}$). *Assignments aided by COSY spectra.* FAB-HRMS for MH^+ ($C_{80}H_{55}N_8O_8Zn$): 1319.3472, calculated: 1319.3434.

Fe(III)MBP-ZnT3EPP, Fe/Zn-98.

1-(1'-porphyrinato iron(III)),4-(*trans*-2'-(2"-(5",10",15",20"-tetra (3"'-(methylcarboxylate)phenyl)porphyrinato zinc(II))yl)ethen-1'-yl)benzene chloride.

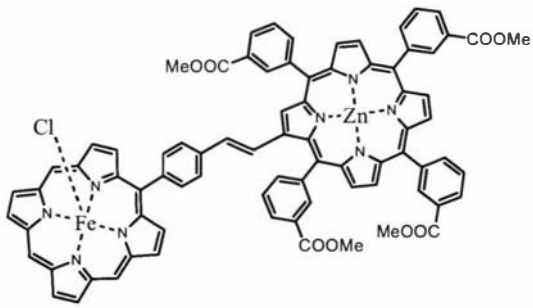

$C_{80}H_{52}ClFeN_8O_8Zn$
Exact Mass: 1407.22
Mol. Wt.: 1410.01

20 mg (39.7 μmol) FeMBP **Fe-94** and 70 mg (57.3 μmol) of phosphonium salt **Zn-84** were dissolved in 25 mL of chloroform under argon. To the stirred solution, 80 mg of DBU were added and reaction went on for 70 minutes. The solution was washed twice with 0.1M HCl, the organic phase was dried over $CaCl_2$ and brought to dryness. The solid was separated through flash chromatography using DCM/methanol 20/1 as eluent. The product was probably a mixture of *cis* and *trans* isomers which was

isomerized to the *trans* form by I_2 treatment. The solid was dissolved in 20 mL of dichloromethane and 50 mg of I_2 were added. After 40 hours the solution was washed three times with a saturated solution of $Na_2S_2O_3$ and water and then precipitated with methanol. The yield was 12 mg (38%) of **Fe/Zn-98** as dark purple crystals.

Fe(III)MBP-ZnT3CPP, Fe/Zn-99.

1-(1'-porphyrinato iron(III)),4-(*trans*-2'-(2"-(5",10",15",20"-tetra (3'"-carboxyphenyl)porphyrinato zinc(II))yl)ethen-1'-yl)benzene chloride.

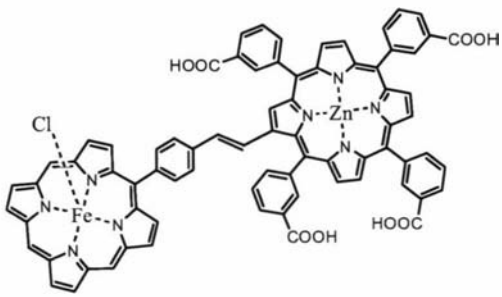

$C_{76}H_{44}ClFeN_8O_8Zn$
Exact Mass: 1351.16
Mol. Wt.: 1353.9

The synthesis of the water soluble dimer **Fe/Zn-99** was obtained from the homologue **Fe/Zn-98** by hydrolysis of the ester groups. 10 mg (7.1 mmol) of **Fe/Zn-98** were dissolved in 10 mL of THF to which 70 mg of KOH, dissolved in 10 mL of MeOH/water = 10/1, were added and the mixture was refluxed for 22 h. The solution was then concentrated at the rotovapor (to remove THF) and washed with dichloromethane. The water phase was slowly neutralized with 0.1M HCl until precipitation of the desired product. The solid was dissolved in basic water and immobilized on the Source 15Q resin packed in a small column (10 mm_{dia} x 20 mm); water, dilute HCl and water/methanol = 1/1 solutions were passed through the column before elution of the product was achieved with HCl 10^{-5}M in methanol. Evaporation of the solvents provided 9.3 mg (97%) of **Fe/Zn-99**. UV-vis (CH_2Cl_2): λ_{max} [nm] 400 (sh), 428, 559, 596. FAB-HRMS for $(M\text{-}Cl)^+$ ($C_{76}H_{44}N_8O_8FeZn$): 1316.1563, calculated: 1316.1923.

T3(E)EPP-Ph-CHO, 100.

4-(2'-(2"-(5",10",15",20"-tetra(3"'-(ethylcarboxylate)phenyl)porphyrin)yl)ethen-1'-yl)benzaldehyde.

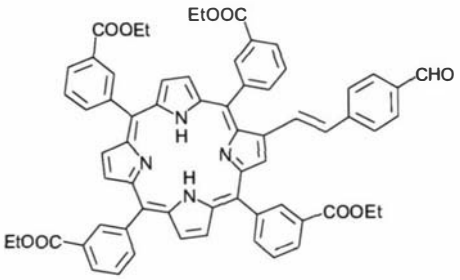

$C_{65}H_{52}N_4O_9$
Exact Mass: 1032.37
Mol. Wt.: 1033.13

570 mg (470 μmol) of phosphonium salt **85** and 120 mg (895 μmol) of terephthaldicarboxaldehyde **13** were dissolved in 120 mL of DCM, under argon. To the stirred solution 100 mg (660 μmol) of DBU were added. After 45 min, the solution was evaporated to dryness and the product mixture separated through flash chromatography (silica gel, DCM/ether = 33/1). The fractions containing the product were brought to dryness and the resulting solid was then dissolved in 150 mL of chloroform and 300 mg of I_2 were added. After 40 hours the solution was washed three times with a saturated solution of $Na_2S_2O_3$ and water and then precipitated with methanol. The pure product was obtained by further recrystallization from chloroform/hexane to yield 373 mg (77%) of **100** as purple crystals. The ^{1}H-NMR spectrum showed pure *trans* configurations. ^{1}H-NMR (500 MHz, $CDCl_3$): δ 10.02 (s, 1H, $H_{aldehyde}$), 8.93-8.86 (m, 5H, $1H_{\beta\text{-pyrrolic}} + 4H_{o\text{-Ph}}$), 8.78 (br s, 3H, $H_{\beta\text{-pyrrolic}}$), 8.75 (d, J = 4.7 Hz, 2H, $H_{\beta\text{-pyrrolic}}$), 8.70 (d, J = 4.7 Hz, 1H, $H_{\beta\text{-pyrrolic}}$), 8.59 (d, J = 8 Hz, 1H, $H_{o\text{-Ph}}$), 8.50 (d, J = 8 Hz, 3H, $H_{o\text{-Ph}}$), 8.45-8.34 (m, 4H, $4H_{p\text{-Ph}}$), 7.92-7.82 (m, 6H, $4H_{,\text{-Ph}} + 2H_{Ph'}$), 7.33 (d, J = 8.1 Hz, 2H, $H_{Ph'}$), 7.27 (d, J = 16 Hz, 1H, H_{alkene}), 7.04 (d, J = 16 Hz, 1H, H_{alkene}), 4.51-4.42 (m, 6H, H_{CH2}), 4.36 (q, J = 7 Hz, 2H, H_{CH2}), 1.44-1.37 (m, 9H, H_{CH3}), 1.32 (t, J = 7 Hz, 2H, H_{CH3}), -2.61 (br s, 2H, $H_{N\text{-pyrrolic}}$). *Assignments aided by COSY spectra.*

ZnT3(E)EPP-Ph-CHO, Zn-100.

4-(2'-(2"-(5",10",15",20"-tetra(3'"-(ethylcarboxylate)phenyl)porphyrinato zinc(II))yl) ethen-1'-yl)benzaldehyde.

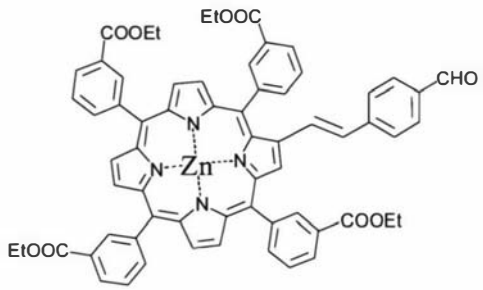

$C_{65}H_{50}N_4O_9Zn$
Exact Mass: 1094.29
Mol. Wt.: 1096.50

Zn porphyrin aldehyde **Zn-100** was prepared from its free base homologue by standard Zn insertion. 363 mg (352 μmol) of **100** were metallated with 93 mg (423 μmol) of $Zn(OAc)_2 \cdot H_2O$ to give 340 mg (88%) of **Zn-100** as purple crystals. ^{1}H-NMR (500 MHz, $CDCl_3$): δ 9.93 (s, 1H, $H_{aldehyde}$), 8.98 (d, J = 3.4 Hz, 1H, $H_{\beta\text{-pyrrolic}}$), 8.87-8.75 (m, 10H, $6H_{\beta\text{-pyrrolic}} + 4H_{o\text{-Ph}}$), 8.45-8.32 (m, 8H, $4H_{o\text{-Ph}} + 4H_{p\text{-Ph}}$), 7.87-7.73 (m, 6H, $4H_{m\text{-Ph}} + 2H_{Ph'}$), 7.27-7.21 (m, 2H, $H_{Ph'}$), 7.21-7.14 (m, 1H, H_{alkene}), 7.05-6.95 (m, 1H, H_{alkene}), 4.40-4.21 (m, 8H, H_{CH2}), 1.39-1.30 (m, 12H, H_{CH3}). *Assignments aided by COSY spectra.* UV-vis (CH_2Cl_2): λ_{max} [nm] ($\varepsilon \times 10^{-3}$) 432.5 (177), 557 (16), 593.5 (6.2). FAB-HRMS for M^+ ($C_{65}H_{50}N_4O_9Zn$): 1094.2844, calculated: 1094.2869.

Fe(III)MBP-Ph-ZnT3(E)EPP, Fe/Zn-103.

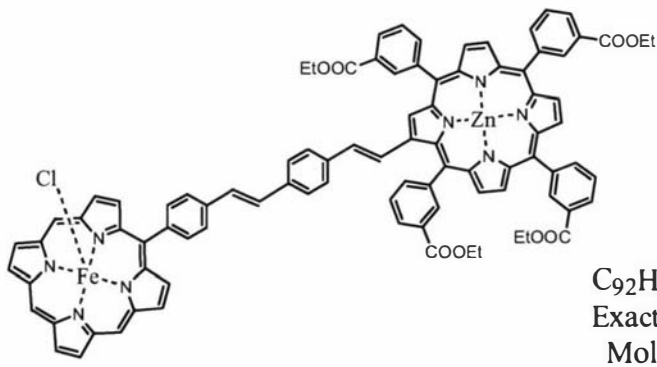

$C_{92}H_{66}ClFeN_8O_8Zn$
Exact Mass: 1565.33
Mol. Wt.: 1568.25

15 mg (29.7 μmol) of FeMBP **Fe-94** and 40 mg (32.8 μmol) of phosphonate **Zn-101** were dissolved in 20 mL of dry THF, under argon atmosphere. To the stirred solution, 5 mg (44 μmol) of solid ^{t}BuOK were added. After 60 min, the solution was evaporated to dryness and purified through flash chromatography on silica gel (DCM/methanol = 15/1). The fractions containing the desired product were collected and recrystallized from DCM/MeOH, affording 25 mg (67%) of pure **Fe/Zn-103** as

dark-purple crystals. UV-vis (CH_2Cl_2): λ_{max} [nm] 405 (sh), 432, 563, 600. FAB-HRMS for $(M\text{-}Cl)^+$ ($C_{92}H_{66}N_8O_8FeZn$): 1530.3692, calculated: 1530.3644.

Fe(III)MBP-Ph-Ph-ZnT3(E)EPP, Fe/Zn-104.

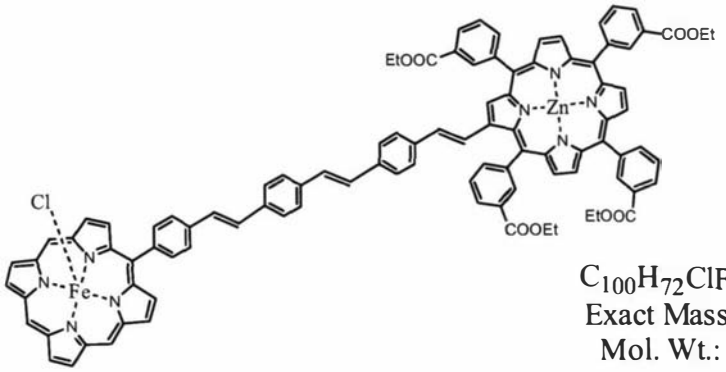

$C_{100}H_{72}ClFeN_8O_8Zn$
Exact Mass: 1667.38
Mol. Wt.: 1670.38

15 mg (29.7 μmol) of FeMBP **Fe-94** and 42 mg (31.1 μmol) of phosphonate **Zn-102** were dissolved in 20 mL of dry THF, under argon atmosphere. To the stirred solution, 5 mg (44 μmol) of solid ^{t}BuOK were added. After 60 min, the solution was evaporated to dryness and purified through flash chromatography on silica gel (DCM/methanol = 15/1). The fractions containing the desired product were collected and recrystallized from DCM/MeOH, affording 22 mg (44%) of **Fe/Zn-104** as dark-purple crystals. UV-vis (CH_2Cl_2): λ_{max} [nm] 403 (sh), 433, 567, 605. FAB-HRMS for $(M\text{-}Cl)^+$ ($C_{100}H_{72}N_8O_8FeZn$): 1632.4035, calculated: 1632.4114.

Fe(III)MBP-Ph-ZnT3CPP, Fe/Zn-105.

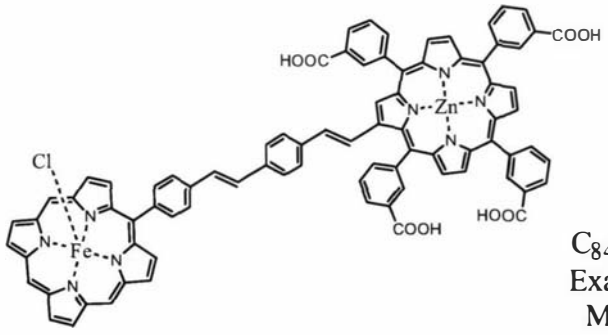

$C_{84}H_{50}ClFeN_8O_8Zn$
Exact Mass: 1453.21
Mol. Wt.: 1456.03

The synthesis of water soluble dimer **Fe/Zn-105** was obtained from the homologue **Fe/Zn-103** by hydrolysis of the ester groups. 20 mg (12.7 μmol) of **Fe/Zn-103** were dissolved in 10 mL of THF. 100 mg of KOH were dissolved in 10 mL of MeOH/water = 10/1, added to the porphyrin solution and the mixture was refluxed for 28 h. The solution was then concentrated at the rotovapor (to remove THF) and washed with dichloromethane. The water phase was slowly neutralized with 0.1M

HCl until precipitation of the desired product. The solid was dissolved in basic water and immobilized on the Source 15Q resin packed in a small column (10 mm_{dia} x 20 mm); water, dilute HCl and water/methanol = 1/1 solutions were passed through the column before elution of the product was achieved with HCl 10^{-5}M in methanol. Evaporation of the solvents provided 18.2 mg (98%). UV-vis (water): λ_{max} [nm] 397 (sh), 430.5, 567, 608. FAB-HRMS for $(M\text{-}Cl)^+$ ($C_{84}H_{50}N_8O_8FeZn$): 1418.2354, calculated: 1418.2392.

Fe(III)MBP-Ph-Ph-ZnT3CPP, Fe/Zn-106.

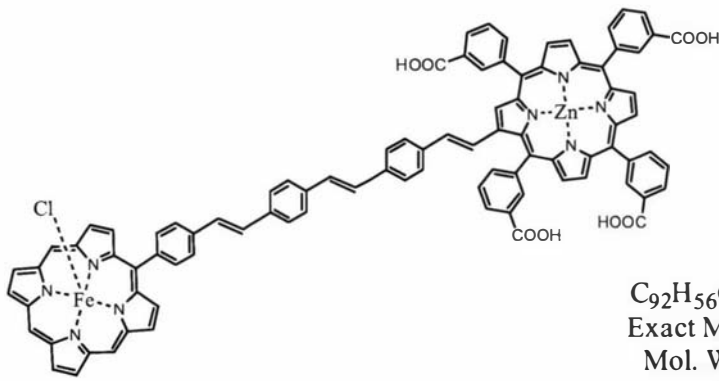

$C_{92}H_{56}ClFeN_8O_8Zn$
Exact Mass: 1555.26
Mol. Wt.: 1558.17

The synthesis of water soluble dimer **Fe/Zn-106** was obtained from the homologue **Fe/Zn-104** by hydrolysis of the ester groups. 20 mg of **Fe/Zn-104** were dissolved in 10 mL of THF. 100 mg of KOH were dissolved in 10 mL of MeOH/water = 10/1, added to the porphyrin solution and the mixture was refluxed for 28 h. The solution was then concentrated at the rotovapor (to remove THF) and washed with dichloromethane. The water phase was slowly neutralized with 0.1M HCl until precipitation of the desired product. The solid was dissolved in basic water and immobilized on the Source 15Q resin packed in a small column (10 mm_{dia} x 20 mm); water, dilute HCl and water/methanol = 1/1 solutions were passed through the column before elution of the product was achieved with HCl 10^{-5}M in methanol. Evaporation of the solvents provided 18.5 mg (99%). UV-vis (water): λ_{max} [nm] 433, 569.5, 609. MALDI-LRMS for M^+ ($C_{92}H_{56}N_8O_8FeZnCl$): cluster 1555.5-1563.5 (max 1557.5), calculated: cluster 1555.3-1563.3 (max 1557.3); for $(M\text{-}Cl)^+$ ($C_{92}H_{56}N_8O_8FeZn$): cluster 1519.5-1527.4 (max 1522.4), calculated: cluster 1519.3-1527.3 (max 1522.3).

Fe(III)TPP-Ph-ZnT3(E)EPP, Fe/Zn-107.

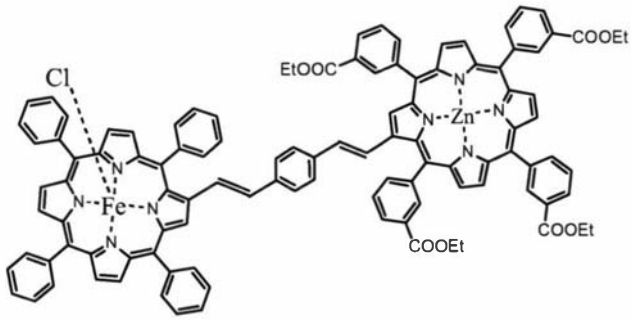

$C_{110}H_{78}ClFeN_8O_8Zn$
Exact Mass: 1793.43
Mol. Wt.: 1796.53

30 mg (27.3 μmol) of aldehyde **Zn-100** and 34 mg (33.5 μmol) of phosphonium salt **Fe-11** were dissolved in 15 mL of dichloromethane under argon. To the stirred solution, 40 mg of DBU were added and reaction went on for 60 minutes. The solution was washed twice with 0.1M HCl, the organic phase was dried over $CaCl_2$ and brought to dryness. The solid was separated through flash chromatography using DCM/methanol (gradient from 100/1 to 20/1) as eluent. The product was probably a mixture of *cis* and *trans* isomers which was isomerized to the *trans* form by I_2 treatment. The solid was dissolved in 20 mL of dichloromethane and 30 mg of I_2 were added. After 40 hours the solution was washed three times with a saturated solution of $Na_2S_2O_3$ and water and then precipitated with methanol. The yield was 29 mg (59%) of pure **Fe/Zn-107** as dark-purple crystals. FAB-HRMS for $(M\text{-}Cl)^+$ FAB-HRMS for $(M\text{-}Cl)^+$ ($C_{110}H_{78}N_8O_8FeZn$): 1758.4579, calculated: 1758.4583.

Fe(III)TPP-Ph-ZnT3CPP, Fe/Zn-108.

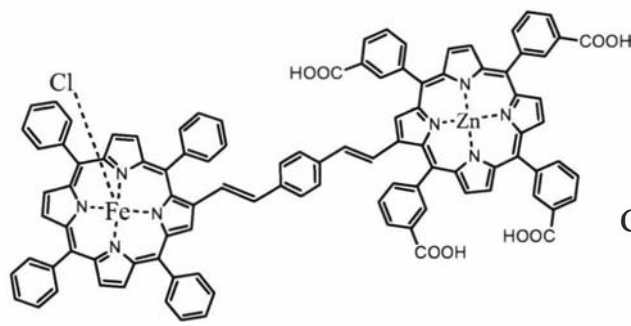

$C_{102}H_{62}ClFeN_8O_8Zn$
Exact Mass: 1681.3
Mol. Wt.: 1684.32

The synthesis of water soluble dimer **Fe/Zn-108** was obtained from the homologue **Fe/Zn-107** by hydrolysis of the ester groups. 20 mg (11.1 μmol) of **Fe/Zn-107** were dissolved in 10 mL of THF. 100 mg of KOH were dissolved in 10 mL of MeOH/water = 10/1, added to the porphyrin solution and the mixture was refluxed for 22 h. The solution was then concentrated at the rotovapor (to remove THF) and washed with dichloromethane. The water phase was slowly neutralized with 0.1M

HCl until precipitation of the desired product. The solid was dissolved in basic water and immobilized on the Source 15Q resin packed in a small column (10 mm_{dia} x 20 mm); water, dilute HCl and water/methanol = 1/1 solutions were passed through the column before elution of the product was achieved with HCl 10^{-5}M in methanol. Evaporation of the solvents provided 18.3 mg (98%). UV-vis (water): λ_{max} [nm] 433.5, 567, 610.5. FAB-HRMS for $(M\text{-}Cl)^+$ ($C_{102}H_{62}N_8O_8ZnFe$): 1646.3331, calculated: 1646.4640.

6. REFERENCES

(1) Sanders, J. K. M., Bampos, N., Clyde-Watson, Z., Darling, S. L., Hawley, J. C., Kim, H-J., Mak, C. C. and Webb, S. J. Axial coordination chemistry of metalloporphyrins. In *The Porphyrin Handbook*, Kadish, K. M., Smith, K. M. and Guilard, R., Ed., Academic Press: San Diego, 2000, Volume 3, Chapter 15.

(2) Krygowski, T. M. and Cyranski. M. K *Phys. Chem. Chem. Phys.,* 2004, 6, 249-255.

(3) Lazzeretti, P. *Phys. Chem. Chem. Phys.,* 2004, 6, 217-223.

(4) Cyrañski, M. K., Krygowski, T. M., Wisiorowski, M., van Eikema /Hommes, N. J. R. and von Rague' Schleyer, P. *Angew. Chem. Int. Ed.,* 1998, 37, 177-180.

(5) Namslauer, A. and Brzezinski, P. *FEBS Lett.* 2004, 567, 103-110.

(6) McMahon, B. H., Fabian, M., Tomson, F., Causgrove, T. P., Biley, J. A., Rein, F. N., Dyer, R. B., Palmer, G., Gennis, R. B. and Woodruff, W. H. *Biochim. Biophys. Acta,* 2004, 1655, 321-331.

(7) Fromme, P., Melkozernov, A., Jordan, P. and Krauss, N. *FEBS Lett.,* 2003, 555, 40-44.

(8) Perlinger, J. A., Bushmann, J., Angst, W. and Schwarzenbach, R. P. *Envir. Sci. Technol.* 1998, 32, 2431-2437.

(9) Sheldon, R. A. *Metalloporphyrinsin Catalytic Oxidation*, Marcel Dekker Inc.: New York, 1994.

(10) Sheng, H., Spasojevic, I., Warner, D. S. and Batinic-Haberle, I. *Neurosci. Lett.,* 2004, 366, 220-225.

(11) Stylli, S. S., Howes, M., MacGregor, L., Rajendra, P. and Kaye, A. H. *J. Clinical Neurosci.,* 2004, 11, 584-598.

(12) Fukuzawa, N. *U. S. Pat. Appl.* 20040142138, 22/7/2004.

(13) Lammi, R. K., Ambroise, A., Wagner, R. W., Diers, J. R., Bocian, D. F., Holten, D. and Lindsey, J. S. *Chem. Phys. Lett,*, 2001, 341, 35-44.

(14) Kim, D. and Osuka, A. *J. Phys. Chem. A*, 2003, 107, 8791-8816.

(15) Splan, K. E., Keefe, M. H., Massari, A. M., Walters, K. and Hupp, J. T. *Inorg. Chem.,* 2002, 41, 619-621.

(16) Hsiao, J.-S., Krueger, B. P., Wagner, R. W., Johnson, T. E., Delaney, J. K., Mauzerall, D. C., Fleming, G. R., Lindsey, J. S., Bocian, D. F. and Donohoe, R. J. *J. Am. Chem. Soc.,* 1996, 118, 11181-11193.

(17) Sadamoto, R., Tomioka, N. and Aida, T. *J. Am. Chem. Soc.,* 1996, 118, 3978-3979.

(18) Perlinger, J. A., Buschmann, W. A. and Schwarzenbach, R. P. *Environ. Sci. Technol.,* 1998, 32, 2431-2437.

(19) Ahn, T. K., Kim, D. Y., Noh, S. B., Aratani, N., Ikeda, C., Osuka, A. and Kim, D. *J. Am. Chem. Soc.,* 2006, 128, 1700-1704.

(20) Fletcher, J. T. and Therien, M. J. *Inorg. Chem.,* 2002, 41, 331-341.

(21) Choi, M. S., Aida, T., Yamazaki T. and Yamazaki, I. *Chem.-Eur. J.,* 2002, 8, 2668-2678.

(22) Tsuda, A. and Osuka, A. *Science*, 2001, 293, 79-82.

(23) Collman, J. P., Bencosme, C. S., Durand, R. R., Kreh, R. P. and Anson, F. C. *J. Am. Chem. Soc.,* 1983, 105, 2699-2703.

(24) Fletcher, J. T. and Therien, M. J. *J. Am. Chem. Soc.,* 2002, 124, 4298-4311.

(25) Sanders, J. K. M. Coordination chemistry of oligoporphyrins. In *The Porphyrin Handbook*, Kadish, K. M., Smith, K. M. and Guilard, R., Ed., Academic Press: San Diego, 2000, Volume 3, Chapter 22.

(26) Ogawa, K. and Kobuke, Y. *Angew. Chem. Int. Ed.,* 2000, 39, 4070-4073.

(27) Fleischer, E. B. and Shachter, A. M. *Inorg. Chem.,* 1991, 30, 3763-3769.

(28) Okumura, A., Funatsu, K., Sasaki, Y. and Imamura, T. *Chem. Lett.,* 1999, 779.

(29) Burrell, A. K., Officer, D. L., Plieger, P. G. and Reid, D. C. W. *Chem. Rev.,* 2001, 101, 2751-2796.

(30) Plieger, P. G., Burrell, A. K., Hall, S, B. and Officer, D. L. *J. Inclusion Phenom. Macro. Chem.* 2005, 53, 143-148.

(31) Inorganic, organometallic and coordination chemistry. In *The Porphyrin Handbook*, Kadish, K. M., Smith, K. M. and Guilard, R., Ed., Academic Press: San Diego, 2000, Volume 3.

(32) Nardo, J. V. and Dawson, J. H. *Inorg. Chim. Acta,* 1986, 123, 9-13.

(33) Mak, C. C., Pomeranc, D., Montalti, M., Prodi, L. and Sanders, J. K. M. *Chem. Comm.* 1999, 1083.

(34) Slagt, V. F., Kamer, P. C. J., van Leeuwen, P. W. N. M. and Reek, J. N. H. *J. Am. Chem. Soc.,* 2004, 126, 1526-1536.

(35) Mak, C. C., Bampos, W. and Sanders, J. K. M. *Chem. Comm.,* 1999, 1085.

(36) Osuka, A. and Shimidzu, H. *Angew. Chem. Int. Ed.,* 1997, 36, 135-137.

(37) Jori, G. *NATO ASI Series, Ser. A: Life Sciences*, 1985, 85, 381-39.

(38) Umemura, K., Nishigaki, R. and Yumita, N. *Jpn. Kokai Tok. Koho.* JP 87-305317.

(39) Chang, C. J., Chng, L. L. and Nocera, D. G. *J. Am. Chem. Soc.,* 2003, 125, 1866-1876.

(40) Yang, J. and Breslow, R. *Tetrahedron Lett.*, 2000, 41, 8063-8067.

(41) Simonnaux, G. and Le Maux, P. *Coord. Chem. Rev.,* 2002, 228, 43-60

(42) Che, C. M. and Huang, J. S. *Coord. Chem. Rev.,* 2002, 231, 151-164.

(43) Ferrand, Y., Le Maux, P. and Simonneaux, G. *Tetrahedron: Asymmetry*, 2005, 16, 3829-3836.

(44) Ono, N., Aramaki, S., Sakai, Y. and Yoshiyama, R., *Jpn. Kokai Tok. Koho. JP 2004-224312.*

(45) Li, B., Xu, X., Sun, M., Fu, Y., Yu, G., Liu, Y. and Bo, Z. *Macromolecules*, 2006, 39, 456-461.

(46) Hambright, P. and Fleischer, E. B. *Inorg. Chem.*, 1970, 9, 1757.

(47) Ventura, B., Flamigni, L., Marconi, G., Lodato, F. and D. Officer. *New J. Chem.*, 2006, submitted for publication.

(48) Aramaki, S. *Jpn. Kokai Tok. Koho.* JP 2003-148946.

(49) Kuhr, W. G. and Gallo, A. R. *PCT. Int. Appl.* WO 2005-US3133.

(50) Schweikart, K.-H., Malinovskii, V. L., Diers, J. R., Yasseri, A. A., Bocian, D. F., Kuhr, W. G. and Lindsey, J. S. *J. Mater. Chem.*, 2002, 12, 808-828.

(51) Susumu, K., Duncan, T. V. and Therien, M. J. *J. Am. Chem. Soc.*, 2005, 127, 5186-5195.

(52) Holten, D., Bocian, D. F. and Lindsey, J. S. *Acc. Chem. Res.*, 2002, 35, 57-69.

(53) Aratani, N. and Osuka, A. *Acc. Bull. Chem. Soc. Jpn.,* 2001, 74, 1361-1379.

(54) Nakano, A., Yamazaki, T., Nishimura, Y., Yamaaki, I. and Osuka, A. *Chem.-Eur. J.,* 2000, 6, 3254-3271.

(55) Cramer, W. A., Zhang, H., Yan, J., Kurisu, G. and Smith, J. L. *Biochemistry,* 2004, 43, 5921-5929.

(56) Pullerits, T. and Sundtröm, V. *Acc. Chem. Res.*, 1996, 9, 381-389.

(57) Imahori, H., Kimura, M., Hosomizu, K. and Fukuzumi, S. *J. Photochem. Photobiol. A,* 2004, 166, 57-62.

(58) Miyatani, R. and Amao, Y. *Photochem. Photobiol. Sci.,* 2004, 3, 681-683.

(59) Saiki, Y. and Amao, Y. *Biotechnol. Bionengineer.,* 2003, 82, 710-714.

(60) Wang, Q., Campbell, W. M., Bonfantini, E. E., Jolley, K. W., Officer, D. L., Walsh, P. J., Gordon, K., Humphry-Baker, R., Nazeeruddin, M. K. and Grätzel, M. *J. Phys. Chem. B*, 2005, 109, 15397-15409.

(61) Grätzel, M. *Inorg. Chem.*, 2005, 44, 6841-6851.

(62) Hagfeldt, A. and Grätzel, M. *Acc. Chem. Res.*, 2000, 33, 269-277.

(63) Campbell, W. M. *Porphyrins for surface modifications*, 2001, PhD Thesis, IFS Chemistry, Massey University, Palmerston North, New Zealand.

(64) Borgström, M., Blart, E., Boschloo, G., Mukhtar, E., Hagfeldt, A., Hammarström, L. and Odobel, F. *J. Phys. Chem. B,* 2005, 109, 22928-22934.

(65) Peter, K., Wietasch, H., Peng, B. and Thelakkat, M. *Appl. Phys. A*, 2004, 79, 65-71.

(66) Park, T., Haque, S. A., Potter, R. J., Holmes, A. B. and Durrant, J. R. *Chem. Comm.*, 2003, 23, 2878-2879.

(67) Geary, E. A. M., Hirata, N., Clifford, J., Durrant, J. R., Parsons, S., Dawson, A., Yellowlees, L. J. and Robertson, N. *Dalton Trans.*, 2003, 3757-3762.

(69) Kakkassery, J. J., Fermin, D. J. and Girault, H. H. *Chem. Comm.*, 2002, 1240-1241.

(70) Hasobe, T., Kamat, P. V., Troiani, V., Solladie', N., Ahn, T. K., Kim, S. K., Kim, D., Kongkanand, A., Kuvubata, S. and Fukuzumi, S. *J. Phys. Chem. B Lett*, 2005, 109, 19-23.

(71) Liddell, P. A., Kodis, G., de la Garza, L., Moore, A. L., Moore, T. A. and Gust, D. *J. Phys. Chem. B*, 2004, 108, 10256-10265.

(72) Kodis, G., Liddell, P. A., de la Garza, L., Clausen, P. C., Lindsey, J. S., Moore, A. L., Moore, T. A. and Gust, D. *J. Phys. Chem. A*, 2002, 106, 2036-2048.

(73) Amao, Y. and Okura, I. *J. Mol. Cat. B: Enzymatic*, 2002, 17, 9-21.

(74) Anderson, J. M. *Aust. J. Plant Physiol.* 1999, 26, 625-639.

(75) Burrell, A. K. and Officer, D. L. *Synlett,* 1998, (12), 1297-1307.

(76) Annoni, E., Pizzotti, M., Ugo, R., Quici, S., Morotti, T., Bruschi, M. and Mussini, P. *Eur. J. Inorg. Chem.*, 2005, 3857-3874.

(77) Lin, V. S.-Y., DiMagno, S. G. and Therien, M. J. *Science*, 1994, 264, 1105-1111.

(78) Osuka, A., Tanabe, N., Kawabata, S., Yamazaki, I. and Nishimura, Y. *J. Org. Chem.*, 1995, 60, 7177-7185.

(79) Nagata, T., Osuka, A. and Maruyama, K. *J. Am. Chem. Soc.,* 1990, 112, 3054-3059.

(80) Anton, J. A., Kwong, J. and Loach, P. A. *J. Heterocycl. Chem.* 1976, 13, 717-725.

(81) Prathapan, S., Johnson, T. A. and Lindsey, J. S. *J. Am. Chem. Soc.,* 1993, 115, 7519-7520.

(82) Park, M., Cho, S., Aratani, N., Osuka, A. and Kim, D. *J. Am. Chem. Soc.,* 2005, 127, 15201-15206.

(83) Shanmugathasan, S., Edwards, C. and Boyle, R. W. *Tetrahedron,* 2000, 1025-1046.

(84) Geier, G. R. III and Lindsay, J. S. *J. Chem. Soc., Perkin Trans. II,* 2001, 677-700.

(85) Lindsay, J. S., Schreiman, I. C.,Hsu, H. C., Kearney, P. C. and Marguettaz, A. M. *J. Org. Chem.,* 1987, 52, 827-836.

(86) Wiehe, A., Ryppa, C and Senge, M. O. *Org. Lett.,* 2002, 3807-3809.

(87) Kadish, K. M., Guo, N., Van Caemelbecke, E., Froiio, A., Paolesse, R., Monti, D., Tagliatesta, P., Boschi, T., Prodi, L., Bolletta, F. and Zaccheroni, N. *Inorg. Chem.*, 1998, 37, 2358-2365.

(88) Vicente, M. G. H. Reactivity and functionalization of β-substituted porphyrins and chlorines. In *The porphyrin handbook,* Kadish, K. M., Smith, K. M. and Guilard, R. Eds., Academic Press: San Diego, 2000, Volume 1, Chapter 4.

(89) Jaquinod, L. Functionalization of 5,10,15,20-tetrasubstituted porphyrins. In *The porphyrin handbook,* Kadish, K. M., Smith, K. M. and Guilard, R. Eds., Academic Press: San Diego, 2000, Volume 1, Chapter 5.

(90) Inhoffen, H. H., Fuhrhop, J. H., Voigt, H. and Brockmann, H. Jr. *Justus Liebigs Ann. Chemie*, 1966, 695, 133-143.

(91) Momenteau, M., Loock, B. and Bisagni, E. *Can. J. Chem.,* 1979, 57, 1804-1813.

(92) Freeman, A. W. and Fréchet, J. M. J. *Org. Lett.*, 1999, 1, 685-687.

(93) Zeng, F. and Zimmerman, S. C. *J. Am. Chem. Soc.,* 1996, 118, 5326-5327.

(94) Diez-Barra, E., Garcia-Martinez, J. C., Merino, S., del Rey, R., Rodriguez-Lopez, J., Sanchez-Verdú, P. and Tejeda, J. *J. Org. Chem.*, 2001, 66, 5664-5670.

(95) Vigneswaran, M. and Officer, D. L. Unpublished results.

(96) Adler, A. D., Longo, F. R., Finarelli, J. D., Goldmacher, J., Assour, J. and Korsakoff, L. *J. Org. Chem.,* 1967, 32, 476.

(97) Buchler, J. W. In *Porphyrins and Metalloporphyrins*, 2nd ed.; K.M. Smith Ed.; Elsevier: Amsterdam, 1975, Chapter 5.

(98) Storck, W. and Manecke, G. *Makromolecular Chemie,* 1975, 176, 97-124.

(99) Beltcher, W., unpublished results.

(100) Diez-Barra, E., Garcia-Martinez, J. C. and Rodriguz-Lopez, J. *Tetrahedron Lett.,* 1999, 40, 8181-8184.

(101) Boutagy, J. and Thomas, R., *Chem. Rev.,* 1974, 74, 87-99.

(102) Michaelis, A. and Kaehne, R. *Chem. Ber.,* 1898, 31, 1048.

(103) Campbell, W. M., Burrell, A. K., Officer, D. L. and Jolley, K. W. *Coord. Chem. Rev.,* 2004, 248, 1363-1379.

(104) Meyers, A. I., Tomioka, K., Roland, D. M. and Comins, D. *Tetrahedron Lett.,* 1978, 16, 1375-1378.

(105) Siddall, T. H. III and Prohaska, C. A. *J. Am. Chem. Soc.*, 1962, 84, 3467-3473.

(106) Perrin, D. D. and Armarego, W. L. F. *Purification of Laboratory Chemicals*; 3rd ed.; Pergamon Press: Great Britain, 1993.

(107) Lee, J.-K., Schrock, R. R., Baigent, D. R. and Friend, R. H. *Macromolecules*, 1995, 28, 1966-1971.

(108) Mitchell, R. H., *Chem Rev.*, 2001, 101, 1301-1315.

(109) Choi, C. H. and Kertesz, M. *J. Chem. Phys.,* 1998, 108, 6681-6688.

(110) Cross, K. J. and Crossley, M. J. *Aust. J. Chem.,* 1992, 45, 991-1004.

(111) Riche, C., Gouedard, M. and Gaudemer, A. *J. Chem. Res., Synop.*, 1978, 34-35.

(112) Bonfantini, E. E., Burrell, A. K., Officer, D. L., Reid, D. C. W., McDonald, M. R., Cocks, P. A. and Gordon, K. C. *Inorg. Chem.*, 1997, 36, 6270-6278.

(113) Mao, J.-G., Wang, Z. and Clearfield, A. *Inorg. Chem.,* 2002, 41, 2334-2340.

(114) Ogawa, K. and Kobuke, Y. *Angew. Chem. Int. Ed.,* 2000, 39, 4070-4073.

(115) Nardo, J. V. amd Dawson, J. H. *Inorg. Chim. Acta,* 1986, 123, 9-13.

(116) Song, H. and Scheidt, W. R. *Inorg. Chim. Acta,* 1990, 173, 37-41.

(117) Williamson, M. M., Prosser-McCartha, C. M., Mukundan, Jr., S. and Hill. C. L. *Inorg. Chem.,* 1988, 7, 1061-1068.

(118) Kroleva, T. A., Koifman, O. I. and Berezin, B. D. *Koord. Khim.,* 1981, 7, 1642.

(119) Gutowsky, H. S. and Holm, C. H. *J. Chem. Phys.,* 1956, 25, 1228-1234.

(120) Kroleva, T. A., Koifman, O. I. and Berezin, B. D. *Koord. Khim.,* 1981, 7, 1642.

(121) Song, H. and Scheidt, W. R. *Inorg. Chim. Acta,* 1990, 173, 37-41.

(122) Williamson, M. M., Prosser-McCartha, C. M., Mukundan, Jr., S. and Hill. C. L. *Inorg. Chem.,* 1988, 7, 1061-1068.

(123) Jelle, C.-P. and Bettermann, H. *J. Mol. Struct.*, 2005, 744-747, 121-125.

(124) Officer, D. L., Lodato, F. and Jolley, K.W. *Inorg. Chem. Comm.*, 2006, submitted for publication.

(125) Seybold, P. G. and Gouterman, M. *J. Mol. Spectrosc.*, 1969, 31, 1-13.

(126) Krasnovsky, Jr., A. A., Bashtanov, M. E., Drozdova, N. N., Liddell, P. A., Moore, A. L., Moore, T. A. and Gust, D. *J. Photochem. Photobiol. A*, 1997, 102, 157-161.

(127) Nyarko, E., Hanada, N., Habib, A. and Tabata, M. *Inorg. Chim. Acta*, 2004, 357, 739-745.

(128) Piet, J. J., Taylor, P. N., Wegewijs, B. R., Anderson, H. L., Osuka, A. and Warman, J.M. *J. Phys. Chem. B*, 2001, 105, 97-104.

(129) Arnold, D. P. *Synlett*, 2000, 3, 296-305.

(130) Binstead, R. A., Crossley, M. J., Maxwell, J. and Hush, N. S. *Inorg. Chem.*, 1991, 30, 1259-1264.

(131) Shelnutt, J. A. and Ortiz, V. *J. Phys. Chem.*, 1985, 89, 4733-4739.

(132) Chen, C.-T., Yeh, H.-C., Zhang, X. and Yu, J. *Org. Lett.*, 1999, 1, 1767-1770.

(133) Gust, D. and Moore, T. A. Intramolecular photoinduced electron-transfer reactions of porphyrins. In *The Porphyrin Handbook*, Kadish, K. M., Smith, K. M. and Guilard, R., Ed., Academic Press: San Diego, 2000, Volume 8, Chapter 57.

(134) Fukuzumi, S. Electron transfer chemistry of porphyrins and metalloporphyrins. In *The Porphyrin Handbook*, Kadish, K. M., Smith, K. M.

and Guilard, R., Ed., Academic Press: San Diego, 2000, Volume 8, Chapter 56.

(135) Schuster, D. I., MacMahon, S., Guldi, D. M., Echegoyen, L. and Braslavsky, S. E. *Tetrahedron*, 2006, 62, 1928-1936.

(136) Tomizaki, K., Loewe, R. S., Kirmaier, C., Schwartz, J. K., Retsek, J. L., Bocian, D. F., Holten, D. and Lindsey, J. S. *J. Org. Chem.*, 2002, 67, 6519-6534.

(137) Monnereau, C., Gomez, J., Blart, E. and Odobel, F. *Inorg. Chem.*, 2005, 44. 4806-4817.

(138) Fukuzumi, S., Ohkubo, K., E, W., Ou, Z., Shao, J., Kadish, K. M., Hutchinson, J. A., Ghiggino, K. P., Sitic, P. J. and Crossley, M. J. *J. Am. Chem. Soc.*, 2003, 125, 14984-14985.

(139) Knör, G. *Coord. Chem. Rev.*, 1998, 171, 61-70 and references cited therein.

(140) Helms, A., Heiler, D. and McLendon, G. *J. Am. Chem. Soc.,* 1992, 114, 6227-6238.

(141) Fujita, I., Netzel, T. L., Chang, C. K. and Wang, C.-B. *Proc. Natl. Acad. Sci., Biophysics*, 1982, 79, 413-417.

(142) Okuma, K., Sakai, O. and Shioji, K. *Bull. Chem. Soc. Japan*, 2003, 76, 1675-1676.

(143) Campbell, W. M., Personal communication, 2003.

(144) Callot, H. J. *Tetrahedron* , 1973, 29, 899-901.

(145) Hesemann, P. and Greiner, A. *Polym. Adv. Technol.*, 1996, 8, 23-29.

(146) Bonfantini, E. E. and Officer, D. L. *Tetrahedron Lett.*, 1993, 34, 8531-8534.

(147) Angiolillo, P. J., Lin, V. S.-Y., Vanderkooi, J. M. and Therien, M. J. *J. Am. Chem. Soc.,* 1995, 117, 12514-12527.

(148) Plater, M. J. and Jackson, T. *Tetrahedron*, 2003, 59, 4673-4685.

(149) Renard, P.-Y., Vayron, P., Leclerc, E., Valleix, A. and Mioskowski, C. *Angew. Chem. Int. Ed.,* 2003, 42, 2389-239.

(150) Meyers, A. I., Tomioka, K., Roland, D. M. and Comins, D. *Tetrahedron Lett.*, 1978, 16, 1375-1378.

(151) Hutchinson, D. K. and Fuchs, P. L. *J. Am. Chem. Soc.,* 1987, 109, 4755-4756.

(152) Cheng, B. and Scheidt, W. R. *Inorg. Chim. Acta*, 1995, 237, 5-11.

(153) Golder, A. J., Povey, D. C., Silver, J. and Jassim, Q. A. A. *Acta Cryst.*, 1990, C46, 1210-1212.

(154) Fleisher, E. B., Miller, C. K. and Webb, L. E. *J. Am. Chem. Soc.*, 1964, 86, 2342-2347.

(155) Schauer, C. K., Anderson, O. P., Eaton, S. S. and Eaton, G. R. *Inorg. Chem.*, 1985, 24, 4082-4086.

(156) Tajima, K., Li, L. and Stupp, S. I. *J. Am. Chem. Soc.,* 2006, 128, 5488-5495.

(158) Kuciauskas, D., Lin, S., Seely, G. R., Moore, A. L., Moore, T. A., Gust, D., Drovetskaya, T., Reed, C. A. and Boyd, P. D. W. *J. Phys. Chem.*, 1996, 100, 15926-15932.

(159) Lin, V. S.-Y., Di Magno, S. G. and Therien, M. J. *Science*, 1994, 264, 1105-1111.

(160) Angiolillo, P. J., Lin, V. S.-Y. and Therien, M. J. *J. Am. Chem. Soc.,* 1995, 117, 12514-12527.

(161) Fletcher, J. T. and Therien, M. J. *J. Am. Chem. Soc.,* 2002, 124, 4298-4311.

(162) Walsh, P. J., Gordon, K. C., Officer, D. L. and Campbell, W. M. *J. Mol. Struct.: Theochem*, 2006, 759, 17-24.

(163) Jellen, C.-P. and Bettermann, H. *J. Mol. Struct.*, 2005, 744-747, 121-125.

(164) Pasternack, R. F., Gibbs, E. J. and Villafranca, J. J. *Biochemistry*, 1983, 22, 2406-2414.

(165) Pasternack, R. F., Giannetto, A., Pagano, P. and Gibbs, E. J. *J. Am. Chem. Soc.,* 1991, 113, 7799-7800.

(166) Chirvony, V. S., Galievsky, V. A., Terekhov, S. N., Dzhagarov, B. M., Ermolenkov, V. V. and Turpin, P.-Y. *Biospectroscopy*, 1999, 5, 302-312.

(167) Strickland, J. A., Marzilli, L. G., Gay, K. M. and Wilson, W. D. *Biochemistry*, 1988, 27, 8870-8878.

(168) Balaz, M., Steinkruger, J. D., Ellestad, G. A. and Berova, N. *Org. Lett.*, 2005, 7, 5613-5616.

(169) Adachi, S., Nagano, S., Ishimori, K., Watanabe, Y. and Morishima, I. *Biochemistry,* 1993, 32, 241-252.

(170) Mashiko, T., Reed, C. A., Haller, K. J., Kastner, M. E. and Scheidt, W. R. *J. Am. Chem. Soc.*, 1981, 103, 5758-5767.

(171) Discher, B. M., Koder, R. L., Moser, C. C. and Dutton, P. L. *Curr. Opin. Chem. Biol.,* 2003, 7, 741-748.

(172) Huang, S. S., Koder, R. L., Lewis, M., Wand, A. J. and Dutton, P. L. *Proc. Natl. Acad. Sci.*, 2004, 101, 5536-5541.

(173) Discher, B. M., Noy, D., Strzalka, J., Ye, S., Moser, C. C., Lear, J. L., Blasie, J. K. and Dutton, P. L. *Biochemistry*, 2005, 44, 12329-12343

(174) Noy, D., Discher, B. M., Rubtsov, I. V., Hochstrasser, R. M. and Dutton, P. L. *Biochemistry*, 2005, 44, 12344-12354.

(175) Topoglidis, E., Discher, B. M., Moser, C. C., Dutton, P. L. and Durrant, J. R. *ChemBioChem*, 2003, 4, 1332-1339.

(176) Ye, S., Discher, B. M., Strzalka, J., Xu, T., Wu, S. P., Noy, D., Kuzmenko, I., Gog, T., Therien, M. J., Dutton, P. L. and Blasie, J. K. *Nano Lett.*, 2005, 5, 1658-1667.

(177) Ye, S., Strzalka, J., Chen, X., Moser, C. C., Dutton, P. L. and Blasie, J. K. *Langmuir,* 2003, 19, 1515-1521.

(178) Sharp, R. E., Diers, J. R., Bocian, D. F. and Dutton, P. L. *J. Am. Chem. Soc.,* 1998, 120, 7103-7104.

(179) Karaman, R. and Bruice, T. C. *J. Org. Chem.*, 1991, 56, 3470-3472.

(180) Ye, B.-H. and Naruta, Y. *Tetrahedron*, 2003, 59, 3593-3601.

(181) Burns, D. H., Lai, J. J. and Smith, K. M. *J. Chem. Soc., Perkin Trans. I,* 1988, 3119-3131

(182) Srivastava, T. S. and Tsutsui M. *J. Org. Chem.*, 1973, 38, 2103.

(183) Kilså, K., Kajanus, J., Larsson, S., Macpherson, A. N., Mårtensson, J. and Albinsson, B. *Chem. Eur. J.*, 2001, 7, 2122-2133.

(184) Pettersson, K., Kilså, K., Mårtensson, J. and Albinsson, B. *J. Am. Chem. Soc.,* 2004, 126, 6710-6719.

(185) Rywkin, S., Hosten, C. M., Lombardi, J. R. and Birke, R. L. *Langmuir*, 2002, 18, 5869-580.

(186) Fleisher, E. B., Palmer, J. M., Srivastava, T. S. and Chatterjee, A. *J. Am. Chem. Soc.,* 1971, 93, 3162-3167.

(187) Chen, S.-P., Qiao, Z., Udeochu, U., Fletcher, M., Jimerson, T. and Hosten, C. M. *J. Electroanal. Chem.*, 2006, 590, 66-75.

(188) Manso, C. M. C. P., Neri, C. R., Vidoto, E. A., Sacco, H. C., Ciuffi, K. J., Iwamoto, L. S., Iamamoto, Y., Nascimento, O. R. and Serra, O. A. *J. Inorg. Biochem.*, 1999, 73, 85-92.

(189) Koval, C. A., Drew, S. M., Noble, R. D. and Yu, J. *Inorg. Chem.*, 1990, 29, 4708-4714.

(190) Pasternack, R. F., Lee, H., Malek, P. and Spencer, C. *J. Inorg. Nucl. Chem.*, 1977, 39, 1865-1870.

(191) Weinraub, D., Peretz, P and Faraggi, M. *J. Phys. Chem.*, 1982, 86, 1839-1842.

(192) Fleisher, E. B. and Shachter, A. M. *Inorg. Chem.*, 1991, 30, 3763-3769.

(193) Kalyanasundaram, K. *Inorg Chem.*, 1984, 23, 2453-2459 and references cited therein.

(194) Campeau, L.-C., Rousseaux, S. and Fagnou, K. *J. Am. Chem. Soc.*, 2005, 127, 18020-18021.

(195) Kumar, S., Saini, A. and Sandhu, J. S. *Tetrahedron Lett.*, 2005, 46, 8737-8739.

(196) Wang, Y. and Espenson, J. H. *Org. Lett.*, 2000, 22, 3525-3526.

(197) Callot, H. J. *Tetrahedron Lett.*, 1973, 50, 4987-4990.

(198) Okano, T., Harada, N. and Kiji, J. *Bull. Chem. Soc. Jpn.*, 1994, 67, 2329-2332.

(199) Wennerstroem, O., Ericsson, H., Raston, I., Svensson, S. and Pimlott, W. *Tetrahedron Lett.*, 1989, 30, 1129-1132.

(200) Cosmo, R., Kautz, C., Meerholz, K., Heinze, J. and Muellen, K. *Angew. Chem.*, 1989, 101, 638-640.

(201) Brückner, C., Posakony, J. J., Johnson, C. K., Boyle, R. W., James, B. R. and Dolphin, D. *J. Porphyrins Phthalocyanines*, 1998, 2, 455-465.

(202) Clezy, P. S. and Smythe, G. A. *Aust. J. Chem.*, 1969, 22, 239-49.

(203) Lin, V. S.-Y., Iovine, P. M., DiMagno, S. G., Therien, M. J., Malinak, S. and Coucouvanis, D. *Inorg. Synth.*, 2002, 33, 55-61.

(204) Sutton, J. M., Clarke, O. J., Fernandez, N. and Boyle, R. W. *Bioconjugate Chem.*, 2002, 13, 249-263.

(205) Zhou, H., Baldini, L., Hong, J., Wilson, A. J. and Hamilton, A. D. *J. Am. Chem. Soc.*, 2006, 128, 2421-2425.

(206) Groves, K., Wilson, A. J. and Hamilton, A. D. *J. Am. Chem. Soc.*, 2004, 126, 12833-12842.

(207) Masinovský, Z., Lozovaya, G. I., Sivash, A. A. and Drašner, M. *BioSystems*, 1989, 22, 305-310.